1-1-2012

The Application of Geoarchaeological and Micromorphological Perspectives to Issues of Hominin Behavior in the Late Pleistocene

Vera Lúcia Dias Aldeias
University of Pennsylvania, veraldeias@gmail.com

The Application of Geoarchaeological and Micromorphological Perspectives to Issues of Hominin Behavior in the Late Pleistocene

Abstract
It is commonly accepted that several processes come into play in the formation of the archaeological record, and often the challenge of reconstructing past human behaviors and activities is dependent on the interpretation of the sedimentary context of the archaeological remains. In archaeological sites, in addition to geogenic and biogenic depositional and post-depositional processes commonly referred to in geology, humans play important roles as well as agents of sedimentation and transformation of the sedimentary record. This Ph.D. thesis takes a geoarchaeological perspective on the study of archaeological sediments and features using micromorphology, or the microscopic study of soils and sediments, to reconstruct formation processes at Contrebandiers Cave, Morocco (Chapter 2), and to study anthropogenic-derived sediments associated with fire use at early anatomical Modern humans occupations in Africa (at Contrebandiers Cave - Chapter 3) and Neanderthal populations in Europe (Roc de Marsal Cave - Chapter 4).

North Africa has several important, well-stratified archaeological sites that provide evidence for the understanding of early modern humans' adaptations and behavior. However, little is known on the formation processes and the degree of preservation of many of the archaeological assemblages there. In this thesis, the sedimentary history of Contrebandiers Cave is reconstructed taking into consideration the overall evolution of the cave's surroundings. The results show that gravity-driven and aeolian inputs contributed greatly for the fairly rapid fill of the cave during the last Interglacial (Marine Isotopic Stage 5). Since diagenesis played a minor role, the archaeological assemblages are mainly affected by mechanical disturbance related to bioturbation.

The micromorphology study of fire residues showed that the combustion features from Contrebandiers Cave are poorly preserved, with common mechanical disturbance by biological activity, and the presence of natural features that might be mistaken as fire evidence. The displacement of some of the fire residues is, in addition, attributed to human action of ranking out hearth deposits. On the other hand, micromorphology observations of fire derived sediments at Roc de Marsal attest to the well-preserved nature of the hearths in this site, which suffered little or no post-depositional displacement. Despite this almost `pristine' preservation, the developed study highlights the difficulty of tracing past human activities in association with each of the identified hearths. Such results suggest that is often impossible to access the degree of contemporaneity between different combustion events and, consequently, to distinguish between temporally separated prehistoric occupations at an archaeological site.

Degree Type
Dissertation

Degree Name
Doctor of Philosophy (PhD)

Graduate Group
Earth & Environmental Science

THE APPLICATION OF GEOARCHAEOLOGICAL AND MICROMORPHOLOGICAL PERSPECTIVES TO ISSUES OF HOMININ BEHAVIOR IN THE LATE PLEISTOCENE

Vera Aldeias

A DISSERTATION

in

Earth and Environmental Science

Presented to the Faculties of the University of Pennsylvania

in

Partial Fulfillment of the Requirements for the

Degree of Doctor of Philosophy

2012

Supervisor of Dissertation

Signature _____

Harold L. Dibble, Professor, Anthropology

Graduate Group Chairperson

*Signature*_____

Arthur H. Johnson, Professor, Earth and Environmental Science

Dissertation Committee

Paul Goldberg, Professor, Boston University

Hermann Pfefferkorn, Professor, Earth and Environmental Science

Frederick Scatena, Professor, Earth and Environmental Science

Arthur H. Johnson, Professor, Earth and Environmental Science

THE APPLICATION OF GEOARCHAEOLOGICAL AND MICROMORPHOLOGICAL PERSPECTIVES TO ISSUES OF HOMININ BEHAVIOR IN THE LATE PLEISTOCENE

DEDICATION

Para ti Mãe

ACKNOWLEDGEMENTS

This thesis represents the culmination of five years of research in a 'foreign land' and it is a pleasure to look back on this past journey and acknowledge all the support, advice and friendships that surrounded me along these years.

First and foremost I would like to thank my main advisers, Harold Dibble and Paul Goldberg. Harold provided an amazing support, motivation, friendship and yes, I have to thank him for his witty jokes that were a constant both during these years at UPenn and the many days of fieldwork. Harold definitely made this journey a fun and engaging one! The amount of knowledge that Harold shared is something that I will always look upon as an example for my future personal and academic career. Obrigada Harold!

This thesis would have not been possible without the support and teaching provided by Paul Goldberg. Paul is one of the great mentors I have ever come across with, and learning from him is a continuous and engaging pleasure. I owe Paul sincere thanks for helping me discover the wonders of the microscopic world and making sense of it. Thank you Paul for being such a supportive external adviser!

I would also like to thank all my committee members – Fred Scatena, Art Johnson, and Hermann Pfefferkorn– for all the good guidance and believing that someone with an archaeological background could embark in a geological-driven research. From Gieg I additionally learned that even a small-Moroccan-car can go anywhere! Special thanks are also due to Joan Buccilli and Arlene Mand for all the help skimming through the bureaucratic and academic paperwork that a PhD entails.

My colleagues and friends with whom I worked in the field and during my laboratory work were also an inspiration and have shared a considerable degree of knowledge with me, including: Dennis Sandgathe, Zenobia Jacobs, Shannon McPherron, Deborah Olszewski, Utsav Schurmans, and Francesco Berna.

Making the journeys between the departments of Earth and Environmental Science and Anthropology was a pleasure due to my classmates and friends: Natalie

Nahil, Candace Grand Pre – for the EES side, and Zeljko Rezek and Sam Lin for the Paleo group.

This work would have not been possible without the encouragement of my family and friends that chatted with me during endless Skype calls. So these words are for them – though I am aware that they will probably never be bored enough to actually read this thesis! Helena e Sofia: a nossa amizade sobrevive mesmo a uma distância de Oceanos e eu tenho uma sorte incrível de vos ter na minha vida. Mano: és e sempre foste uma inspiração para mim e ter-te por perto, mesmo quando longe, faz toda a diferença do mundo! Ana Estanqueiro, Alexandre, André, Filipe, Pai e Idalinda: obrigado por sempre me fazerem querer voltar a casa. Fernanda: a brazuca mais portuguesa que conheço, vou ter imensas saudades tuas. Godefroy Devevey made me love Philadelphia and our afternoon walks and conversations were essential for keeping my mental sanity in check!

This research was supported by grants from the National Science Foundation, Leakey Foundation and National Geographic. Work at the site of Contrebandiers Cave was made possible by Mohammed El-Hajraoui. Additional, and personally very relevant support, was given by the Penn summer stipend in Paleontology and the Greg and Susan Walker Foundation.

To all, my sincere: Obrigada.

ABSTRACT

THE APPLICATION OF GEOARCHAEOLOGICAL AND MICROMORPHOLOGICAL PERSPECTIVES TO ISSUES OF HOMININ BEHAVIOR IN THE LATE PLEISTOCENE

Vera Aldeias

Harold L. Dibble

It is commonly accepted that several processes come into play in the formation of the archaeological record, and often the challenge of reconstructing past human behaviors and activities is dependent on the interpretation of the sedimentary context of the archaeological remains. In archaeological sites, in addition to geogenic and biogenic depositional and post-depositional processes commonly referred to in geology, humans play important roles as well as agents of sedimentation and transformation of the sedimentary record. This Ph.D. thesis takes a geoarchaeological perspective on the study of archaeological sediments and features using micromorphology, or the microscopic study of soils and sediments, to reconstruct formation processes at Contrebandiers Cave, Morocco (Chapter 2), and to study anthropogenic-derived sediments associated with fire use at early anatomical Modern humans occupations in Africa (at Contrebandiers Cave – Chapter 3) and Neanderthal populations in Europe (Roc de Marsal Cave – Chapter 4).

North Africa has several important, well-stratified archaeological sites that provide evidence for the understanding of early modern humans' adaptations and behavior. However, little is known on the formation processes and the degree of

preservation of many of the archaeological assemblages there. In this thesis, the sedimentary history of Contrebandiers Cave is reconstructed taking into consideration the overall evolution of the cave's surroundings. The results show that gravity-driven and aeolian inputs contributed greatly for the fairly rapid fill of the cave during the last Interglacial (Marine Isotopic Stage 5). Since diagenesis played a minor role, the archaeological assemblages are mainly affected by mechanical disturbance related to bioturbation.

The micromorphology study of fire residues showed that the combustion features from Contrebandiers Cave are poorly preserved, with common mechanical disturbance by biological activity, and the presence of natural features that might be mistaken as fire evidence. The displacement of some of the fire residues is, in addition, attributed to human action of ranking out hearth deposits. On the other hand, micromorphology observations of fire derived sediments at Roc de Marsal attest to the well-preserved nature of the hearths in this site, which suffered little or no post-depositional displacement. Despite this almost 'pristine' preservation, the developed study highlights the difficulty of tracing past human activities in association with each of the identified hearths. Such results suggest that is often impossible to access the degree of contemporaneity between different combustion events and, consequently, to distinguish between temporally separated prehistoric occupations at an archaeological site.

TABLE OF CONTENTS

List of Tables

List of Figures

CHAPTER 1

CHAPTER 2

CHAPTER 3

CHAPTER 4

CHAPTER 1: Introduction

1.1 Context of study: geoarchaeological approaches

In the words of Renfrew: "(…) because archaeology recovers almost all its basic data by excavation, every archaeological problem starts as a problem in geoarchaeology" (Renfrew, 1976, p. 2)

The term geoarchaeology has been increasingly used in the scientific literature since the late 1970s, expressing a multi- and interdisciplinary area of research that situates itself between the traditional fields of Archaeology and Earth and Environmental Sciences (Butzer, 1982; Butzer, 1977; Butzer, 2008; Davidson and Shackley, 1976; Gladfelter, 1977; Goldberg and Macphail, 2006; Rapp, 1987; Waters, 1992). A broad definition states it as the application of geosciences methods and concepts to archaeological research during the geologic time span of human history (Butzer, 1982; Gladfelter, 1977; Rapp Jr and Hill, 1998). While there are several archaeological-driven questions that can be addressed through geoarchaeological research, one of the pervasive issues is the need to establish the contextual/sedimentary framework of cultural remains. Thus, reconstructing the sedimentary history of a site is of crucial relevance in order to understand the nature, integrity of the data, and the processes that ultimately lead to the formation of the archaeological record.

The relevance of reconstruction site formation processes is rooted in the fact that several processes directly affect the original occupational signatures since the moment former humans ceased their active occupation of a site yielding the information and the state of what is found today in the archaeological record. Such processes result from a constant interplay between geologically-driven mechanisms (geogenic), biological transformations (biogenic), and human inputs (anthropogenic). Each of these mechanisms may act as isolated factors or, more frequently, in combination with each other. Over time, archaeological artifacts, features, and constructions are embedded in essentially a geological matrix along with sedimentary particles that comprise the bulk of the stratigraphic record. As such, they are susceptible to burial, weathering, and transport.

Briefly, several examples and archaeological case studies can be described to better illustrate some of the implications of these processes in the formation, preservation, and alteration of the archaeological record.

Geogenic Processes:

The effect of specific geogenic processes is intrinsically dependent on the environmental setting under consideration. A rapid burial of the archeological evidence enhances its preservation through time in geological settings with high sedimentation rates. Low energy floodplain sedimentation – comprised mainly of overbank clays and silts – favored, for instance, the preservation of numerous hearth features and their associated artifacts close to, or at their original positions at the prehistoric site of Pincevent (France - Leroi-Gourhan, 1984; Leroi-Gourhan and Brezillon, 1972). An

analogous situation of optimal preservation environment is the rapid deposition by volcanic sediments, and, in this case, one of the best illustrative examples is the well-known site of Pompeii (Italy). Here, the unique time window into the behaviors of ancient Roman populations is possible due to the rapid rates of pyroclastic deposition of volcanic ashes and lapilli, which entirely covered the city within a time span of hours.

Such examples of optimal preservation in open-air sites are nonetheless rare and cave settings contexts are more widespread in the archaeological record. Cave sites act as sedimentary traps and, consequently, show a predisposition towards sedimentation over erosion. Overall, these geomorphological settings are characterized by an availability of accommodation space, and, hence, they act as repositories for a diversity of sediments, some of which originate from within the cave setting itself (autochthonous sediments), while others are derived from elsewhere (allochthonous sediments) (Farrand, 1985; Mylroie and Sasowsky, 2007). Consequently, such deposits are of special interest not only for understanding the geomorphological progression that lead to the formation and development of the cave deposits per se, but also as a body of data that can be used to infer the evolution and the paleoclimatic setting of the surrounding landscape (Courty and Vallverdú, 2001; Ellwood et al., 2001; Farrand, 1985; Woodward and Goldberg, 2001). The gathering of sediments in a natural cavity tends to be idiosyncratic (Farrand, 2001; Woodward and Goldberg, 2001), with the sedimentary characteristics depending on variables that are unique to each site, such as the geomorphological setting of the cave, its bedrock, structural arrangement, microenvironment, and the availability of source material to be deposited in the first place. The introduction of frequent human

occupations to these natural cavities (discussed below) adds to the complexity of the sedimentary record.

Although cave settings do enhance deposition, there are still important post-depositional processes that are capable of altering the deposits. For instance, reactivation of the karstic system (with enhanced water circulation) may lead to the erosion and slumping of previously deposited sediments; weathering processes (such as decalcification or phosphatization) can bring about significant transformations of the sediments and preferential weathering of organic archaeological components (Campy and Chaline, 1993; Farrand, 1985; Goldberg et al., 1993; Goldberg and Sherwood, 2006; Shahack-Gross et al., 2004; Weiner et al., 1993).

Similarly, other geogenic processes are prone to promote erosion and diagenesis. Dynamic high-energy settings (e.g., parts of fluvial environments), colluvial processes (e.g., debris flow, solifluction), or temperature-related factors (such as cryoturbation and ice lenses) can lead to significant alterations of the original sediments and associated archaeological evidence. In sites closer to active stream channels, for instance, cultural remains can easily be eroded and dispersed if the threshold for sediment motion is achieved, resulting in size sorting and washing out of the smaller, lighter components (Boggs, 2001; Shackley, 1974; Shackley, 1978). For example, the accumulation of stone tools in a thin stratigraphic layer at the Lower Paleolithic site of Cagny L'Epinette was first interpreted as representing a pristine occupation, in an undisturbed "living floor" context located on a terrace of the Avre River, in France (Tuffreau et al. 1986: Tuffreau et al. 1995). However, Dibble et al. (1997) have shown that high-energy fluvial dynamics

had actually impacted the deposits, and that the accumulation of stone tools was not due to human action, but a result of fluvial transport and redeposition of the materials by the paleostream. Conversely, erosional episodes can be less evident, promoting not the complete reworking of entire assemblages, but acting as discrete erosional events affecting certain strata within a stratigraphic sequence. In such cases, stratigraphic analyses have to take into account the presence of these stratigraphical unconformities, since the absence of anthropogenic material can be misleadingly interpreted as periods when there was no human occupation at a site (such as at Dust Cave: Goldberg and Sherwood, 1994).

Biogenic Processes:

Biogenic processes are related to the activity of flora and fauna, contributing to an accumulation of organic materials, which can favor further sedimentation or, more commonly, serve as agents of post-depositional disturbance. The effects of plants (e.g., rooting, tree throws - Evans et al., 1998; Goldberg and Macphail, 2006; Waters, 1992), and burrowing animals (e.g., insects, rodents or carnivores - Canti, 2003b; Feller et al., 2003; Nest, 2002) contribute to the mechanical reworking of previously deposited sediments with horizontal and vertical displacement of artifacts (Balek, 2002; Feller et al., 2003; McBrearty, 1990). These actions tend to encompass a mixing and homogenization of the sediments and potential obliteration of the original sedimentary structures (e.g., Morin, 2006). Moreover, biogenic inputs can also contribute to substantial chemical diagenetic alterations. The incorporation of organic matter and

phosphates can lead to considerable changes in the chemical composition of the deposits, impacting the preservation of organic remains and bones. The common presence of bat and bird guano in caves, for instance, has been proven to be a significant contributor to the preferential dissolution of bone fragments and alteration of combustion residues through decalcification (Albert et al., 2003; Berna et al., 2004; Karkanas et al., 2002; Schiegl et al., 1996; Shahack-Gross et al., 2004; Weiner et al., 2002)

Anthropogenic Processes:

The introduction of human inputs into the sedimentary record is seen not only in the discard of manufactured artifacts, but also as agents of deposition, formation, mobilization, and erosion of the sediments themselves. Anthropogenic processes can be related to the incorporation of materials such as food related resources (bones, shells, etc.), material for the construction of structures, fire related sediments, exogenous raw materials, or even the incorporation of fine-grained sediments, such as muds, introduced by people walking to and from a specific occupational site (Farrand, 1985; Goldberg, 2008). Humans can also extensively alter deposits by removing and modifying previously deposited strata, for instance, by the construction and infilling of storage/disposal pits or burial features in the underlying deposits. Examples of such features are ubiquitous in the archaeological record, and the sediments that were removed can be deposited elsewhere in the site. At the Upper Paleolithic site of Abri Pataud in France, for example, Farrand (2001) argued that human inhabitants of the site had removed considerable sediments associated with previous occupations in order to broaden their living space. These

excavated deposits were, subsequently, redeposited in other loci of the site, creating a situation of "reversed stratigraphy" – that is, with older sediments overlying younger deposits. Similarly, it is common to assume that frequent visits by humans communities to a site results in situations where previously discarded artifacts may be subject to reuse or recycling. As a result, even if a specific archaeological level is not significantly affected by geogenic or biogenic processes, it still often encompasses a diachronic view of several occupational events (which may be thousands of years apart) superimposed into a single stratigraphic surface (Bailey, 2007; Ferring, 1986; Schiffer, 1985; Schiffer, 1987).

This coarse temporal resolution of the archaeological evidence highlights the significance of identifying discrete anthropogenic features that reflect short-term events and activities. One of the most prevalent examples of anthropogenic sediments is their relation to the construction and use of fire features. Although combustion features (hearths) can assume different shapes and sizes, they typically tend to be somewhat circular with a microstratigraphic layering characteristically composed of whitish-beige ashy sediments underlain by a charcoal-rich layer and fire-reddened (rubefied) substrate (e.g., Goldberg et al., 2012; Goldberg et al., 2009; Meignen et al., 1989; Meignen et al., 2007). Although these microfacies of ash and charcoal can be easily lost (for instance by the mere presence of windblown disturbance or diagenetic alterations) thin rubefied sediments can be a compelling evidence of direct exposure to high temperatures, and high-resolution analytical techniques such as soil micromorphology (see below), paleomagnetic methods, or FTIR can be used to detect the presence of poorly-preserved

combustion-associated deposits (e.g., Carrancho et al., 2009; Goldberg and Berna, 2010; Schiegl et al., 1996; Schiegl et al., 2004; Sergant et al., 2006; Weiner, 2010). Experimental studies (e.g., March, 1992) have shown that even in good sedimentary preservation conditions, the presence of charcoal may intrinsically depend on the type of hearth being built (fires in shallow depressions, or open flat fires), related to their functions (e.g., indirect cooking) or to rainwater ceasing combustion, for instance. Charcoal represents incomplete combustion of wood, and studies conducted by March (1992) have shown that fires constructed in a *cuvette* (that is, in a depression in the underlying sediments) are susceptible of creating more charcoals due to lower temperatures of combustion, less exposure to wind, and the thermal control imposed by the surrounding sediments.

Where there is a better preservation of the deposits, the ash components can be quite substantial in an archaeological site (Goldberg et al., 2009; Karkanas and Goldberg, 2008; Schiegl et al., 1996). The bulk composition of ashes derived from the burning of plant residues is mainly calcite formed by the decomposition of unstable calcium cellular oxalate crystals present in many plants and usually concentrated in the leaves and cellular walls (Courty et al., 1989). The cellular minerals recrystallize into calcite ($CaCO_3$) after the ashes are exposed to enough moisture and CO_2 from the atmosphere (Canti, 2003a). After deposition, the ash components can be affected by substantial and complex diagenetic alterations, both mechanical and chemical. The reaction of calcitic ashes with phosphate-rich solutions will lead to dissolution and react alteration of calcite into several phosphate minerals (Karkanas, 2010; Karkanas et al., 2002; Schiegl et al., 1996).

In sum, a vast array of geogenic, biogenic and anthropogenic processes serve as both agents of formation and as post-depositional disturbances of cultural remains. The increased awareness that archaeological materials need to be understood within their stratigraphic context, has urged the application of geoarchaeological research to untangle the aspects that are natural (geological or biologically-driven), from those that can be directly linked to past human activities (Schiffer, 1987; Stein, 1993, 2001). In this thesis, geoarchaeological approaches are employed in the (1) characterization of the lithostratigraphic framework and site formation processes at the prehistoric site of Contrebandiers cave (Morocco); and (2) to characterize the nature and pyrotechnological traits of anthropogenic hearths (Contrebandiers Cave – Morocco and Roc de Marsal – France). The main analytical technique employed is the use of soil micromorphology to archaeological sediments and features.

1.2 Notes on Soil Micromorphology

Micromorphology is the study of soils and sediments through the analysis of petrographic thin sections, an analytical technique that originally is derived from pedological studies (Courty et al., 1989; e.g. Goldberg, 1983; Karkanas and Goldberg, 2008). Micromorphological samples are taken as blocks of oriented, undisturbed

sediments, allowing for the preservation of the contextual and spatial arrangement of the components that make up the deposits. The thin sections taken from this block can be analyzed under the microscope and the descriptive parameters of the deposits can follow soil-oriented approaches (Brewer, 1972; Stoops, 2003) or standardized nomenclature that reflects the application of this methodology to archaeological contexts and components (Courty et al., 1989).

These microscopic observations include shape, size, texture, fabric and geometric arrangement of the sampled material (Courty et al., 1989; Karkanas and Goldberg, 2007). Its application to archaeological contexts and sediments has proven to be an essential technique for deciphering formation processes (agents of depositional and post-depositional processes), as well as the nature of anthropogenic signatures (e.g., Angelucci, 2003; Courty et al., 1989; Donald et al., 1992; Goldberg, 1983, 2000, 2008; Goldberg and Berna, 2010; Karkanas, 2002; Karkanas and Goldberg, 2007; Karkanas and Goldberg, 2008; Weiner, 2010). Archaeological sediments can be fairly complex, often lacking macro sedimentary structures, and with many of the behaviorally relevant layers expressed only as millimeter thick strata (for example prepared habitation floors, or small-scale truncations of the sediments are difficult or even impossible to define macroscopically - Courty, 2001; Courty et al., 1989; Karkanas and Goldberg, 2008). Since micromorphological samples preserve the original context and arrangement of the stratigraphic components, it is possible to analyze the relationship between cultural remains and their surrounding matrix. Conversely, more traditional sedimentary analyses (grain size, XRD, etc.) typically take loose, bulk samples from a thickness that may

actually encompass several microstratigraphic layers, or include areas of bioturbation that are not discernible macroscopically. Despite the relevance of such sedimentological methods, the results have to be viewed as an average instead of clear identification of the nature and composition of each unit. Since cultural remains most often reflect occupations that are laterally variable and spatially distinct, such averaging of the results falls short if one wants to achieve high-scale resolutions and direct interpretation of cultural remains and/or occupational signatures. As a consequence, the microscopic scale of analysis given by micromorphology has been increasingly applied to a variety of geographical and temporal archaeological contexts, documenting not only the contextual position of the archaeological artifacts but also emerging as an indispensable tool for interpreting the archaeological record as a whole (e.g., Macphail et al., 2006 and citations within). The present research relies heavily in the application of micromorphology technique and scale of analysis.

1.3 Geological and geomorphological context of Rabat, Morocco

Since the majority of the research presented here is located in the Atlantic coast of Morocco around Rabat, an annotated overview of the main geological formations and paleoclimatic signatures is needed to better understand the evolution of the paleolandscape and its impact on human occupations and sedimentation at Contrebandiers Cave.

Overall, the study area focuses on the Moroccan Atlantic coast, south of the Moroccan capital of Rabat (Figure 1). Structurally, this area belongs to the flat plateau that constitutes the western Meseta. This geomorphological domain is bordered on the north by the Rift mountain chain, and separated from the Sahara regions in the south and east by the tectonically elevated Atlas mountain chains. The geodynamic evolution of the Meseta terrains has been associated with two main periods: a rifting phase followed by a collision period (Michard, et al 2008). The onset of the rifting episode is assigned to the Permo-Triassic period, and it eventually led to the opening of the Atlantic Ocean, which in turn separates the Moroccan terrains from those of the Canadian margin of Nova Scotia. During this extensional period, salt deposition and volcanism episodes are the most important geological events. In this area, the Triassic formations include sandstones and shales unconformably overlying Hercynian basement deposits. Subsequent to the syn-rift sequence, the beginning of drifting conditions in the central Atlantic led to the formation of shallow marine limestones and dolomites in near shore settings. Until the end of the Cretaceous, predominantly transgressive marine conditions prevailed along the Moroccan margin, namely during the Cenomanian-Turonian high sea level stand. Alternation of marine shales and carbonates characterize the stratigraphy. From the Late Cretaceous onwards, orogenic episodes of the Rift mountains start to develop due to the collision of the Eurasian and African plates (Ait Brahim et al., 2002). In the study area, the pre-Quaternary deposits are mainly exposed in the valleys of the main rivers, namely the Bouregreg valley near Rabat and the Yquem River, south of the city of Témara.

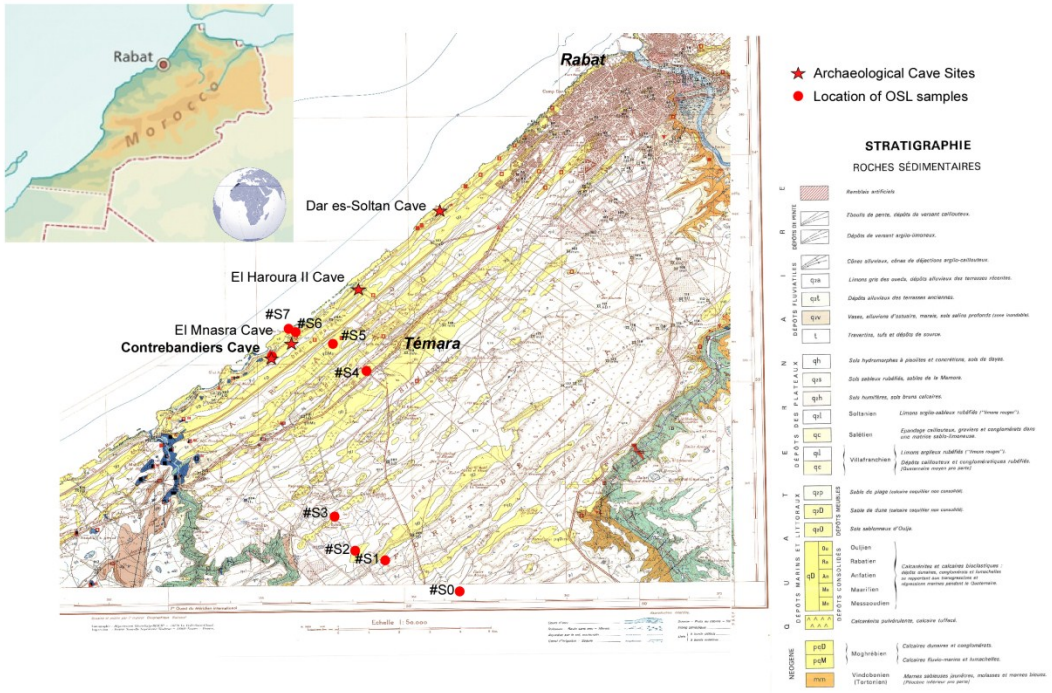

Figure 1: Geographical setting of Morocco (top, left) and position of Contrebandiers Cave in the geological map of the Témara area (bottom) – adapted from the Carte Geotéchnique de la Région de Rabat, scale 1: 50,000 – (Millies-Lacroix, 1874). The red stars show the location of the nearby archaeological sites, and the red circles correspond to the eight samples collected for Optically Stimulated Luminescence (OSL) dating

An extensive Pleistocene sedimentary cover is abundant around the Rabat and Casablanca regions. These formations consist mainly of bioclast-rich aeolianites and raised beach deposits that rise inland with successive elongated lithified belts oriented roughly parallel to the shoreline (Stearns, 1978). These coastal formations are interspersed with red loamy soils present in the slack depressions between the lithified ridges and as beds within the dune systems (Bronger and Bruhn-Lobin, 1997; Bronger and Sedov, 2003). The present shoreline is characterized by a lithified calcarenite ridge, currently being eroded by wave action, with remnants of indurated and karst-derived red

soils occasionally overlying the cemented dunes. Large boulders that unconformably overlying the calcarenite coastal ridge are interpreted as tsunami deposits and present along the coast (Mhammdi et al., 2008). The present shoreline is characterized by common embayments with modern shelly beach sands and coastal dunes with intertidal lagoons present along the modern coastal area. Overall, the entire sequence suggests relatively steady uplift, with no reversals of trends identified either in the Casablanca or the Rabat areas (Lefévre and Raynal, 2002; Stearns, 1978, 1981). A More or less uniform rate of uplift for the Moroccan Meseta was assumed by Stearns (1981), with a rate of 0.063 m / 1000 yr in the Casablanca sequence, and 0.053 m / 1000 yr for the Rabat area. As discussed below, there are several caveats to these estimations, and currently there is an increased need for improved chronometric dating techniques and better understanding of the depositional environment of these formations.

The Moroccan Pleistocene sequences have been extensively studied for some time (Aboumaria et al., 2006; Andre and Beaudet, 1981; Arboleya et al., 2008; Biberson, 1961; Brebion et al., 1986; Gigout, 1957; Lefévre and Raynal, 2002; Plaziat et al., 2006; Raynal et al., 1986; Stearns, 1978, 1981; Texier et al., 1985; Texier et al., 1992, 1994; Texier et al., 2002; Texier et al., 1985-1986; Weisrock et al., 1999). Early research was synthesized by Biberson (1961), who identified six primary marine stages (Messaodian, Maanfien, Anfatian, Harounien, Ouljien, and the youngest Mellahien), intercalated by continental stages (Moulouyen, Salétien, Amirien, Tensiftien, Pré-Soltanien, Soltanien and Rharbien). Though these chronostratigraphic units have been used in subsequent studies (cf. Nahid, 2001), the overall validity of the classical Moroccan stages has been

increasingly challenged, with new research showing a more complex picture of Quaternary fluctuations and deposition.

Much of the recent research has focused on the Casablanca area due to better exposures of outcrops in local quarries (Lefévre and Raynal, 2002; Texier et al., 2002). Conversely, though Quaternary-associated formations extend over 10 km inland around Rabat, the lack of extensive, well-exposed outcrops led the majority of researchers to focus on the coastal cliffs. Attesting to the more complex depositional environment during Pleistocene fluctuations, the profile from Sidi Moussa (North of Rabat) was extensively described by Aberkan (1986, 2000) and Plaziat (2006). These deposits show a succession with a lowermost unit of horizontally bedded calcarenite associated with MIS 7 interglacial high stand (TL age of 220 ± 30 ka, Aberkan 2000), followed by roughly 2 m thick mud-rich lagoon deposit located at +2 m above mean sea level (amsl). These deposits are capped by a calcarenitic dune complex which is then truncated by a subsequent paleo-cliff notch and entrenched coarser marine bed at +4/5 m amsl (Plaziat et al., 2006). An age within the last interglacial Marine Isotopic Stage 5e (MIS 5e) is inferred for the two raised marine units (i.e., lagoon-associated unit and the coarser deposits interpreted as a beach facies). In accordance to this evidence of superimposed marine and several dune systems from the Sidi Moussa profile, detailed reviews and lithostratigraphy from the Casablanca regions also show a more intricate picture with the presence of at least twenty successive formations, as reported by Texier et al. (2002) and Lefèvre and Raynal (2002), with common episodes of erosion and associated colluvium deposits. Recently, a correlation between the traditional marine "Moroccan stages" with

MIS chronology has been published by Plaziat et al. (2008), and chronometric dating based on OSL reported by Rhodes et al. (2006). Nevertheless, the limited knowledge on the sedimentary characteristics and specific depositional environments (aeolian, marine or colluvium) continues to hamper a clear understanding of the relationship between the coastal deposits with climatic and sea-level fluctuations during the Late Pleistocene. The majority of the sites lack controlled numerical age estimations and, consequently, the timing and nature of Pleistocene evolution and high stands remains unclear.

Considering the marine deposits, several oscillations in sea-level during the Pleistocene, coupled with the relative uplift of Moroccan coastal areas, enabled the preservation of raised beaches inland from the current coast. Based on stratigraphic and sedimentary evidence, Hearty et al. (2007) studied several worldwide sites with emergent marine deposits dated to the last interglacial. They conclude that several sea-level intervals can be defined within MIS 5e, with major high stand peaks in the intervals between 130 and ~125 ka. This was followed by brief fall of sea-level closer to present day values around 125 ka, and subsequent sea-level rise to levels between +6 to +9 m amsl at around 120 ka. Rapid initiations of regressive sea-level trends are seen after 119 ka (MIS 5d). In accordance with these arguments of multiple high stands within MIS 5e is the evidence from several sites worldwide, for examples at least two phases of higher sea-level stands bracketed within 6 – 8.5 m amsl are recorded at Cape Agulhas, South Africa (Carr et al., 2010), on the western Australian coast (O'Leary et al., 2008), and along the southern Iberian coast (Zazo et al., 1999). Similarly, data from fossil reefs in Barbados (Potter et al., 2004; Schellmann et al., 2004) show that sea-level high stands

were present between ~130 and 128 ka, with rapid sea-level fall to -11 m in the interval between 120-118 ka. A maximum of -20 m sea-level drop was estimated during MIS 5c (~105 ka). Closer to the Moroccan coasts, Bardaji et al. (2009) report on marked meteorological changes after 117 ka in western Mediterranean coastal formations associated with increase climatic instability and a shift to the deposition of reddish conglomeratic facies. Overall, after MIS 5, sea levels were always considerably lower than today, remaining at least -15 m below present values (e.g., Cuttler et al. 2003).

A similar pattern of rapid fluctuations and several high stand peaks is also emerging for the penultimate interglacial (MIS 7, c. 245 to 190 ka) with two to three main sea level high stands (MIS 7a, 7c and 7e - e.g., Andersen et al., 2010; Siddall et al., 2007). However, uncertainties in the ages, and consequent uplift corrections used, make accurate estimates of worldwide sea levels during MIS 7 difficult. Data from Barbados suggest an oscillation between -6 to +9 m, whereas from other raised coral reefs these values are estimated to be up to +10 m (Siddall et al., 2007). Conversely, during MIS 11 (420 to 360 ka) a high sea level stand seems to be associated with stable values during a 30 ka time span at ±10 m amsl, but with a maximum of +20 m amsl in records from the Bahamas (Hearty et al., 1999; Olson and Hearty, 2009; Siddall et al., 2007).

It follows from this evidence that at least the high stands associated with MIS 5e and potentially previous interglacial sea-level peaks (MIS 7 and MIS 11) should be preserved if the neotectonic model of relatively constant uplift holds up for the Moroccan Atlantic coasts. Though, as pointed out by Barton et al. (2009), there was probably not

enough time for the lithification and preservation of marine deposits during sea-level stages lower than -15 m amsl before subsequent transgressions take place.

Other data come from studies of archaeological cave sites in the Rabat region. At Contrebandiers Cave, marine sedimentary facies with an age of ~126 ka were identified roughly at 8 m above present sea level (Jacobs et al., 2011). The altimetric estimation for Contrebandiers Cave sequence was obtained by survey with a total station to an accurate geodesic datum within 0.02 m of accuracy in elevation. However, the present study from Contrebandiers (see Chapter 2) has shown that, to some extent, these sediments post-date the high sea-level peak seen from 130 to ~126 ka (Hearty et al., 2007), and precede the brief fall to sea level values close to or below present associated with interval around 125 ka. Neither the subsequent secondary rise to ~4 m high sea level stand, seen in the interval between 124 to 122 ka (Hearty et al., 2007) nor the high stand maximum around 120 ka (Hearty et al., 2007; Schellmann et al., 2004) are observed in the exposed outcrops at this site. It is possible that more extensive excavations towards the terrace area currently outside the cave's entrance could expose more complete marine deposits, although the values of sea-level above 8 m inferred for ~ 120 ka are not evidenced in the Contrebandiers sequence. In fact, during this time, the deposition in the cave was associated with terrestrial depositional environment, with common presence of human occupations of the site. For the nearby Dar es-Soltan I cave, Barton et al. (2009) report on similar marine deposits at the base of the sequence, interpreted as *in situ* raised beach deposits (though based solely on macro-scale observations). These deposits have been dated to around 125 ka and are located at roughly 4.07 m amsl – yet the altimetric

estimations by Barton et al. can reportedly have at least 1 m oscillations in accuracy. Subsequent to the basal "marine" deposits in the caves, continental sedimentary dynamics prevailed for the remaining sedimentary sequence (from MIS 5e onwards) at both Contrebandiers and Dar es-Soltan (Barton et al. 2009), as well as in nearby sites carved into approximately the same calcarenite ridge, including: El Mnasra and El Haroura II caves (El Hajraoui, 2004; Nespoulet et al., 2008b).

It follows from these observations that the marine-associated deposits encountered on the basal strata of the cave sites are mainly associated with high sea-levels stands during the initial transgressive peak associated with MIS 5e during ~130 and 125 ka and that subsequent sea-level rises, namely during the period from ~122 to 120 ka, did not exceed a maximum of +6 m amsl in this coastal area. The latter inference is in accordance with estimations from the Red Sea cores published by Murray-Wallace et al. (2002; 2003), and possibly with the sequence of raised beaches observed at Sidi Moussa (described above) located closer to the present shoreline than the archaeological cave sites. Furthermore, if the implicit constant uplift model is accepted, it should be possible, at least theoretically, to recognize marine deposits associated with prior sea level high stands along this coastal area, taking the maximum values of +10 (MIS 7) or even +20 (MIS 11). Nonetheless, the lack of accurate chronometric dating and well-resolved stratigraphy precludes such determinations for the Rabat area. Hence, the uplift rate is still largely unknown.

Turning our attention to the continental aeolian deposits, these formations are ubiquitous in the Rabat and Casablanca areas and have been commonly interpreted as

lithified coastal dune sands. The date at which this occurred is uncertain, though the dynamic processes of cementation have been synthetically studied. For example, Akil and Gayet (1984) have demonstrated several stages of lithification through the circulation of meteoric water into these formations rich in bioclastic material. The first stage encompasses localized dissolution of bioclastic materials (mainly marine shells and some terrestrial gastropods), followed by saturation of the water with calcium carbonate, and subsequent precipitation of calcitic cement (Akil and Gayet, 1984).

It is, however, somewhat more challenging to propose chronometric attributions for these formations due to the variety of climatic conditions in which dunes can form (Bateman et al., 2011; Brooke, 2001; McLaren, 2007). Though increased dune accumulations are commonly assumed within interglacial periods in concert with marine transgressions (Brooke, 2001), and several reports from the Casablanca sequence associate aeolian accumulations with major interglacial Late Pleistocene stages (Lefévre and Raynal, 2002; Texier et al., 2002), there is increased evidence that generalized dune activity can also occur during predominantly cold/arid stages (e.g., Bateman et al., 2004; Fornós et al., 2009; Nielsen et al., 2004). Besides the climatic glacial/interglacial association, another important constraint is the correct interpretation of the depositional environment when the main remobilized materials are bioclastic components – as in the Rabat coastal area. Frébourg et al. (2008) note that the diversity of the classical sedimentological criteria used for aeolian deposits (well-sorted fine grained sands) can be misleading in carbonate deposits since these particles present inherent variability in shapes and densities that can lead to lower critical shear velocity for initiation of

movement. As a consequence, carbonate aeolian accumulations can be potentially misinterpreted as low-energy shallow marine depositions (Frébourg et al., 2008).

Presently, the Rabat study area is characterized by a Mediterranean climate with precipitation between 300 and 500 mm in the period from October to April, with maximum precipitation during the months of November-December (Bouzouggar, 1997b). The dominant winds are normally oriented North – West (during the summer), and South – Southwest during the winter months. For North Africa climates, there is a clear correlation between the onset of high-latitude shift to glacial environments and a shift towards aridity and cooler temperatures in subtropical Africa (e.g., deMenocal, 1995). Climate of subtropical Africa reflects the seasonal shifts of the West African monsoon, controlled by the periodic variations in insolation derived from the 23 to 19 Ka cycles of Earth's orbital precession. This enhanced aridity during glacial 'stages' is visible in wind-borne (aeolian) dust present in maritime records, but can also be traced on terrestrial records, specifically from late Pleistocene lacustrine records. Currently, there are no continuous records in the Rabat area for the Late Pleistocene. Still, general paleoenvironmental inferences can be made using data from marine cores taken off the coast of Northwest Africa. These deposits record aeolian and fluvial sediment inputs from the Sahara/Sahel regions and inferences about the type or extent of vegetation cover can be estimated (Figure 2 - Castañeda et al., 2009; Tjallingii et al., 2008). Castañeda et al (2009) show predominantly arid conditions during the last 200 ka, with the Sahara and Sahel areas being dominated by C4 grasses. Main shifts to wetter conditions in association with relative abundance of C_3 vegetation are recorded at 120 – 110 ka (MIS

5d), 55-45 ka (MIS 3) and around 10 ka. The atmospheric-vegetation model produced by Tjallingii et al (2008) identified three increased humidity periods during 105 (MIS 5c), ~83 ka (MIS 5a) and 10 ka, alongside a more subtle peak with vegetation cover from 60 to 55 ka. Based on OSL ages obtained for the cave sites in the Témara area, Jacobs et al. (2012b), point out that the expansion of vegetation cover in the southern Sahara-Sahel regions roughly coincides with the major periods of human occupations in Contrebandiers, El Mnasra and El Haroura 2 caves, specifically during MIS 5d and 5c, and with occupations only in El Haroura 2 and El Mnasra around 73 ka (MIS 5a) - Figures 2 and 3. As discussed in Chapter 2 of this thesis, the lack of evidence of sediments/human occupations during MIS 5a in Contrebandiers Cave can be explained by post-depositional processes, namely localized erosion due to reconfiguration of the cave's roof. Conversely, the increased arid conditions identified by Tjallingii et al (2008) and Castañeda et al (2009) during MIS 4 seem to coincide with lack of deposition/erosion in all the archaeological cave sites and with lower sea-level stands of roughly -80 m during MIS 4 (Figure 2). The latter encompass increased distance of the caves to the shoreline (at least > ~ 10km) and change in the sedimentary dynamics in this area. However, the effects of increased aridity in the vegetation cover of the Rabat coastal area are still largely undetermined, and some researchers point out that Northwestern Africa coasts presented Mediterranean scrub vegetation even during the extreme arid conditions that characterized MIS 6 (Banks et al., 2006).

Overall, a clear need still exists for further in-depth stratigraphic studies (both macroscopic and in thin section) in association with accurate age determinations in order to better understand the environmental/depositional setting and chronology of the Quaternary deposits present in the Moroccan Atlantic coast around Rabat. Currently, research is being conducted along these lines by a research team from Bordeaux University (France) and I have also collected several samples for OSL dating (see Figure 1) and soil micromorphology that are currently being processed. It is then likely that more robust results will be obtained in a near future. In addition to the lithostratigraphic and dating of the Pleistocene formations, my future research in this topic will also involve creating a sea-level distance model similar to the one constructed for South Africa integrating off-shore bathymetry (Fisher et al., 2010), in a collaborative work with researchers from Arizona State University.

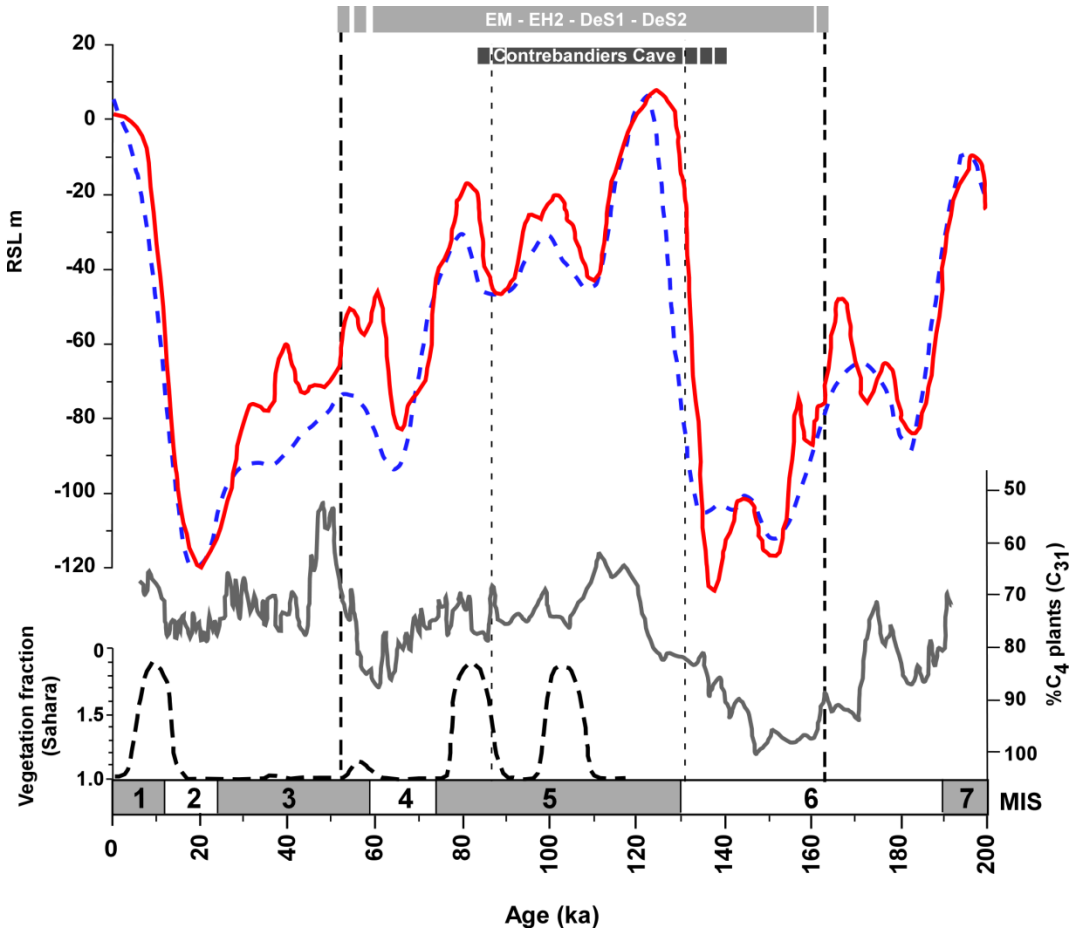

Figure 2: Compiled data from paleoenvironmental reconstructions from cores collected from off the northwest African coast, with sea-level records during the last 200 ka and OSL dates for archaeological cave sites in the Témara area. The left-hand dashed line corresponds to data from Tjallingii et al. (2008) on changes in grassland vegetation in the Sahara. The right-hand grey continuous trace corresponds to the relative abundance of C_4 (shrub-tress) and C_3 (grasses) vegetation deriving from the Sahara/Sahel region and recorded in marine sediment core offshore of northwest Africa (Castañeda et al., 2009). The above dashed and continuous lines correspond to sea-level curves published by Antonioli et al. (2004) based on $\delta^{18}O$ measurements: the dashed blue line represents the SPECMAP curve (Imbrie et al., 1984) and in red is the curve obtained by (Waelbroeck et al., 2002). The uppermost bars correspond to the OSL dates obtained for archaeological cave sediments in the Témara area by Jacobs et al. (Jacobs et al., 2011; Jacobs et al., 2012b): the first bar is the age of deposits from Contrebandiers Cave, and the second is the ages for the sites of El Mnasra (EM), El Haroura 2 (EL2), Dar es-Soltan 1 (DeS1) and Dar es-Soltan 2 (DeS2).

.

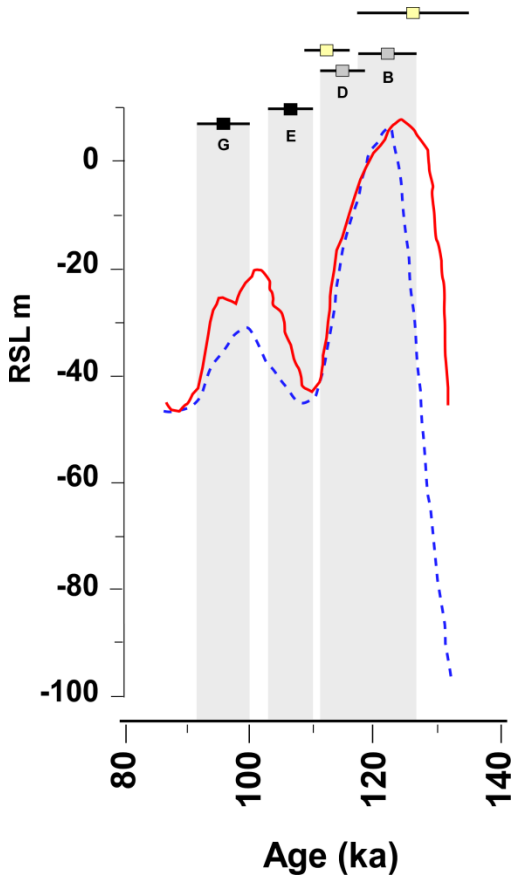

Figure 3: Detail of the sea-level curves for the time span of deposition in Contrebandiers Cave and ages for the lithostratigraphic units in the site obtained by single-grain OSL technique (see Chapters 2 of this thesis). The dashed and continuous lines correspond to sea-level curves published by Antonioli et al. (2004) based on $\delta^{18}O$ measurements: the dashed blue line represents the SPECMAP curve (Imbrie et al., 1984) and in red is the curve obtained by (Waelbroeck et al., 2002).

CHAPTER 2: Deciphering Site Formation Processes through Micromorphological Observations at Contrebandiers Cave, Morocco

2.1 Abstract

Contrebandiers Cave preserves a Late Pleistocene sequence containing Middle Stone Age (MSA) Mousterian and Aterian occupations, spanning from ~126 to 95 ka, followed by spatially restricted Iberomaurusian industries. Site formation processes were reconstructed using micromorphological techniques, complemented by Fourier transform infrared spectroscopy (FTIR) and fabric orientation analyses. The initial deposition at the site is characterized by locally reworked marine shelly sands dating to Marine Isotopic Stage 5e (MIS5e). The subsequent stratification yields sedimentary dynamics predominantly associated with gravity-driven inputs and contributions from weathering of the encasing bedrock, at the same time that anthropogenic sediments were being accumulated. The allochthonous components reflect soil degradation and vegetation changes in the cave's environs during the last interglacial. Human occupations seems to be somewhat ephemeral in nature, with some stratigraphic Units apparently lacking archaeological components, while in others human associated sediments (e.g., burned bones, charcoals and ashes) can be rather substantial. Ephemeral periods of interruption of sedimentation and/or erosion are mainly discernible microscopically by the presence of short-lived surfaces, with peaks of increased humidity and colonization by plants. More substantial erosion affects the stratigraphical uppermost Aterian strata, presumably due to localized reconfigurations of the cave's roof. The encountered Iberomaurusian

occupations are not in their primary position and are associated with well-sorted silts of aeolian origin. The stratigraphic sequence has been affected by only limited chemical diagenesis. On the other hand, physical bioturbation (e.g., wasps, rodents and earthworms) is more pervasive and leads to localized movement of the original sedimentary particles.

2.2 Introduction

Morocco has been emerging as one of the crucial areas for understanding the origins of anatomical modern humans and the emergence of cultural modernity in Africa (Balter, 2011; d'Errico et al., 2009; Hublin, 1992; Hublin, 1993; Hublin, 2001; McBrearty and Brooks, 2000). *Homo sapiens* remains are present in the archaeological record at least from 160 ka onwards (Hublin, 1992, 2001; Hublin and Tillier, 1981; Smith et al., 2007). In somewhat later contexts during Marine Isotopic Stage (MIS) 5, early modern human occupations have been commonly linked to the emergence of modern symbolic behavior through the use of perforated shell ornaments and ochre, as well as innovative tool types and bone tools (Bouzouggar et al., 2007; d'Errico et al., 2009; McBrearty and Brooks, 2000; Nami and Moser, 2010; Nespoulet et al., 2008b). The majority of sites known today in Morocco, however, have not been the target of high-resolution analyses that focus on the processes that led to the formation and preservation of the archaeological record. Consequently, the stratigraphical context and the integrity of the studied collections and assemblages are often imprecise or understudied. Applying

specific geoarchaeological-oriented approaches to such contexts is now being seen as a requirement for further developments in the refinement of archaeological interpretations.

Recent archaeological excavations have been geared to investigate stratified sequences that preserve evidence of Middle Stone Age (MSA) occupations in North Africa, and one of these sites is Contrebandiers Cave. Contrebandiers Cave is a Late Pleistocene site located near the village of Témara on the Atlantic coast of Morocco, approximately 17 km south of the city of Rabat. The cave is currently about 300 m from the shoreline, inland from the beach of Contrebandiers, in a geographical coastal area characterized by the presence of several archaeological sites, including Dar es-Soltan I and II, El Haroura I and II, and El Mnasra caves (Barton et al., 2009; Debénath, 1976, 2000; Debénath et al., 1986; El Hajraoui, 1993; El Hajraoui, 1994; El Hajraoui, 2004; Nespoulet et al., 2008a; Nespoulet et al., 2008b; Ruhlmann, 1951). The Northern African MSA is typically associated with Aterian and the so-called Mousterian industries, both presenting similarities in terms of their stone tool technology, which is largely characterized by a flake-based industry with some use of Levallois and low frequency of retouched tools. These industries have been traditionally distinguished on the basis of the presence of stemmed tools and bifacial foliates in Aterian assemblages. The sedimentary sequence associated with MSA occupations at Contrebandiers Cave spans from ca. 126 ka up to 95 ka, followed by yet undated Iberomaurusian and Neolithic occupations. The MSA succession is characterized by Mousterian and Aterian industries in association with the remains of *Homo sapiens*. Human remains have been uncovered from the Aterian layers (see Debénath, 2000; Ferembach, 1976, 1998; Hublin, 1993; Roche,

1976b) and recently in association with the underlying Mousterian strata (Balter, 2011). In addition to the *Nassarius sp*. shell beads reported from Aterian bearing layers (d'Errico et al., 2009), renewed research at the site has also shown the presence of these shells in the lower Mousterian strata dated to ca. 110 ka (Dibble et al., submitted; Jacobs et al., 2011 see Chapters 6 and 7 of this thesis). Finally, the stratigraphic sequence also bears evidence for the end of the MSA and advent of Upper Paleolithic/Epipaleolithic occupations associated with Iberomaurusian industries that are located in a spatially restricted area of the site (Olszewski et al., 2011; Roche, 1958-1959, 1963; Roche, 1976a).

This long stratigraphic record establishes Contrebandiers has one of the crucial sites for the study of the MSA in North Africa. Although some lithostratigraphic and chronological aspects of the sedimentary sequence have been previously described (Jacobs et al., 2011; Niftah et al., 2005; Roche, 1976b; Roche and Texier, 1976; Schwenninger et al., 2009), still to be fully understood are the mode of accumulation of the deposits, the primary or derived position of the archaeological content, or the degree and nature of post-depositional processes. Consequently, several geoarchaeological aspects pertaining to site formation processes remain unresolved, and their study constitutes the main framework of the present paper. Here we employ soil micromorphology techniques, complemented by some instrumental mineralogical analyses (FTIR and XRD) and fabric orientation, to investigate the sedimentary dynamics, post-depositional aspects and anthropogenic signatures at Contrebandiers cave.

2.3 Description and Formation of the Cave

Contrebandiers Cave is carved into a calcarenite (calcareous sandstone) cliff, with its top at roughly 14 m above present seal level (Figure 1). The site was discovered in 1955 and, according to the earlier excavator, Jean Roche, the cave entrance was originally obstructed by large blocks overlying the Neolithic layers (Figure 2). Such blocks were related to a main episode of roof collapse, and point to the possibility that the cave had a significantly different configuration during the Pleistocene and quite possibly even during the Neolithic.

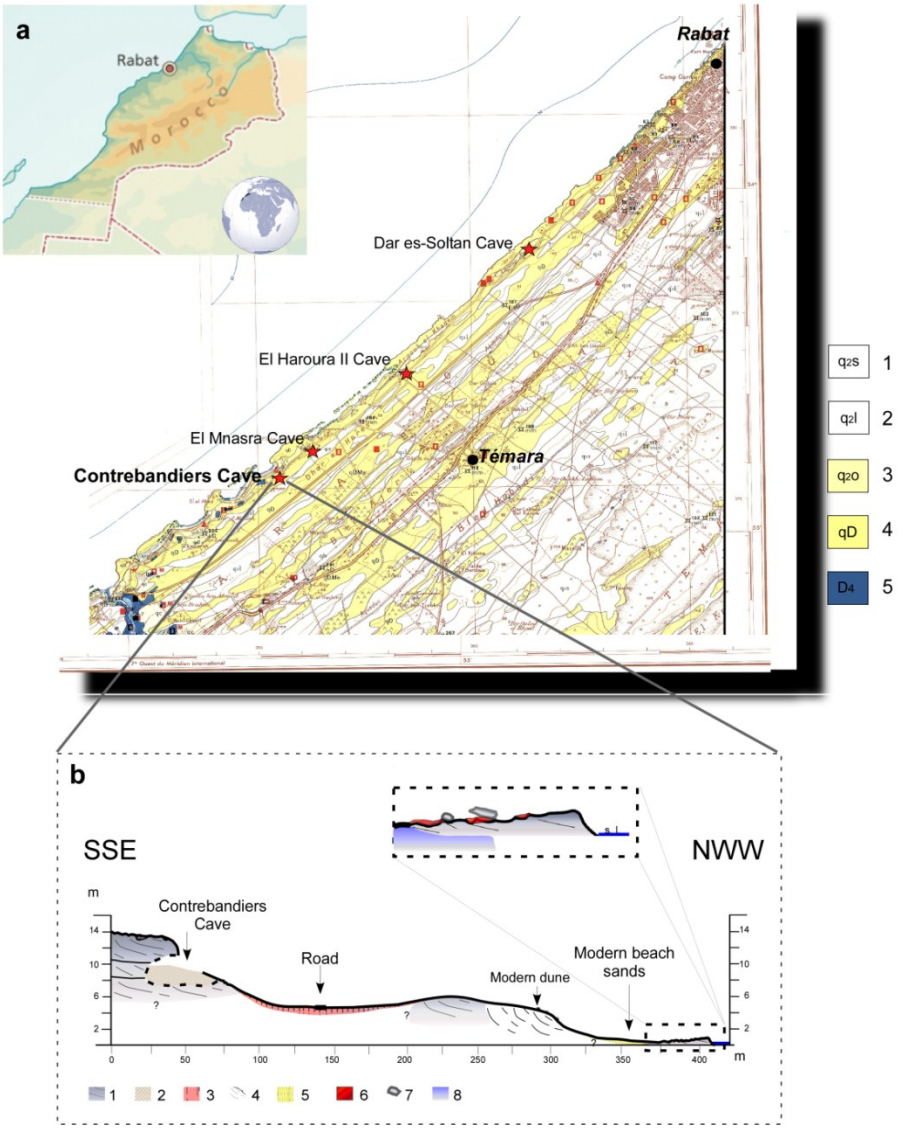

Figure 1: (**a**) Geographical setting of Morocco (top) and position of Contrebandiers Cave in the geological map of the Témara area (bottom), (– adapted from the Carte Geotéchnique de la Région de Rabat, scale 1: 50,000 Millies-Lacroix, 1874). The red stars point to the location of the nearby archaeological sites. 1-4 are Quaternary sedimentary deposits:1- Plateau deposits composed by sandy rubefied soils, sands of Mamora; 2- Plateau deposits composed by rubefied silts attributed to the Soltanian; 3- Marine and littoral deposits, sandy soils of Ouljas (local depressions); 4- Marine and littoral deposits, limestone and bioclastic limestone. 5- Massive limestones from the Devonian. (**b**) Synthetic sketched profile from Contrebandiers Cave to the shoreline. 1: calcarenite belts with karstic features; 2: cave's deposits; 3: sandy rubefied soils present in the Oulja depression; 4: modern dunes; 5: modern beach composed by quartz and bioclastic components; 6: patches of cemented remnants of rubefied soils that are karstified and eroded; 7: large calcarenite blocks associated with tsunami deposits (Mhammdi et al., 2008); 8: Devonian formation

limestone substrate. s.l. = present sea level. The enlarged area in the box corresponds to the active calcarenite cliff that is within the intertidal zone and underwater during high tides in this area of the coast.

Presently, the site is 30 m deep, and more than 11m wide, with an entrance width of ~28 m facing northwest (Figure 3). The cave constitutes a karstic gallery with its interior characterized by smooth roof with karstic dissolution features, including two visible chimneys, one of which was recently artificially covered and which connects directly to the plateau area above the site. It is possible that mechanical wave erosion played a role in the opening or enlargement of the cave entrance during MIS 5e high sea level stand (the Eemian, also locally known as the Ouljien). The basal deposits at Contrebandiers are, in effect, associated with marine deposition and a weighted mean OSL age of 126 ± 9 ka was obtained for these deposits (Jacobs et al., 2011). In accordance with this evidence, several of the cave sites in the vicinity are characterized by similar geomorphological settings, that is, the caves' entrances are more or less parallel to the current shoreline, and the basal layers tend to be shelly sands associated with a marine deposition in accordance with MIS 5e chronologies (Barton et al., 2009; Jacobs et al., 2012a; Nespoulet et al., 2008a).

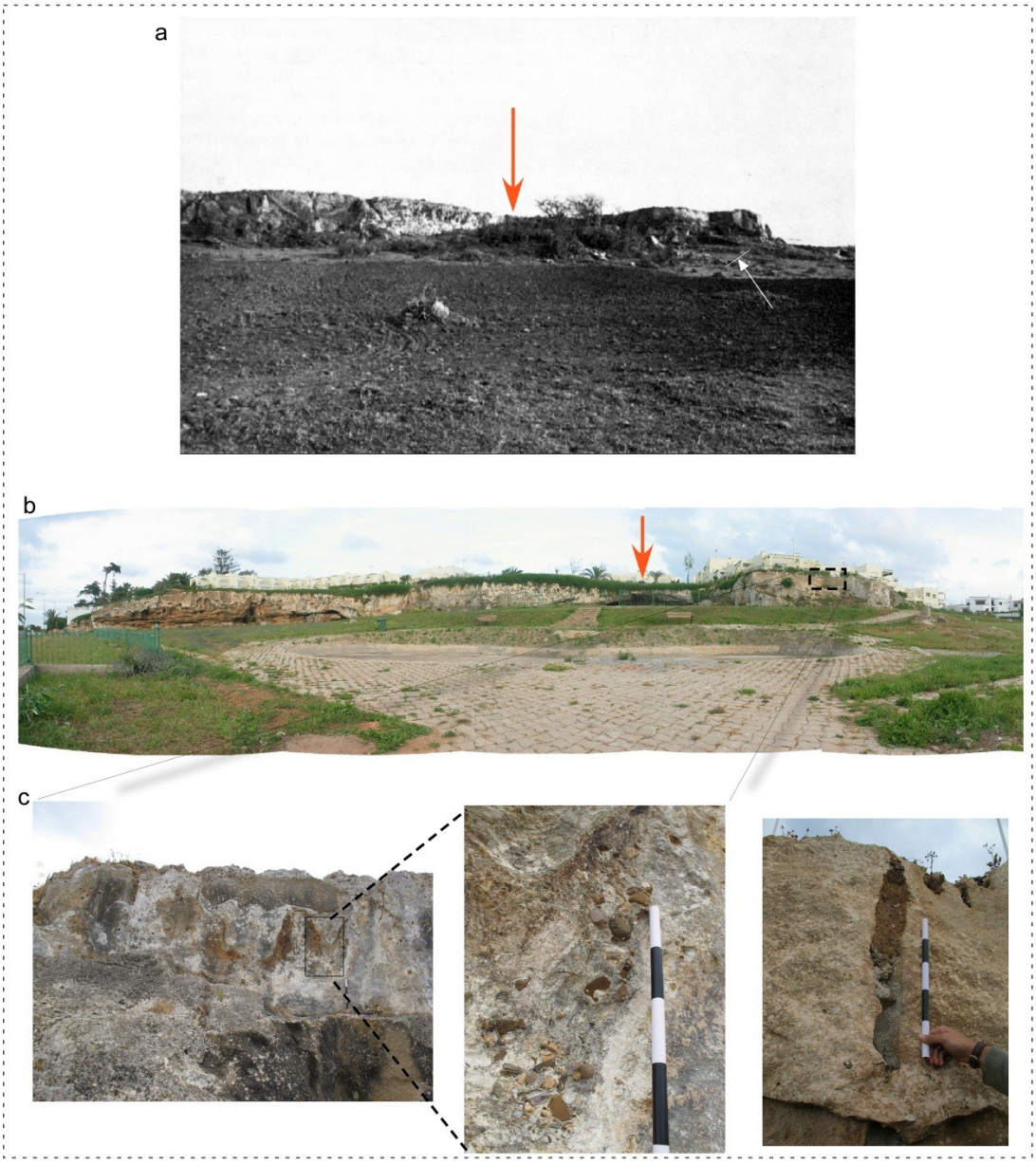

Figure 2: Contrebandiers Cave. (**a**) The site at the time of its discovery in a photograph from Jean Roche's archive presumably taken ~1955; the diagonal arrow (in white) indicates the slope deposits that existed in the site's surroundings. (**b**) The bottom photograph shows the site in 2006 (photograph by Roland Nespoulet). Note the degree of alteration of the original surroundings of the cave due to increased urbanization in this area. The vertical arrows (in red) point to the entrance of the cave in each photo. (**c**) Detail photographs of the area marked by a square in photograph (b) showing the karstified nature of the top of the bedrock and the presence of dissolution features that incorporate round pebbles (namely quartz and other lithologies), and smaller thinner dissolution features filled with relict clay sand red sediments. The scale bars are divided into 10 cm increments.

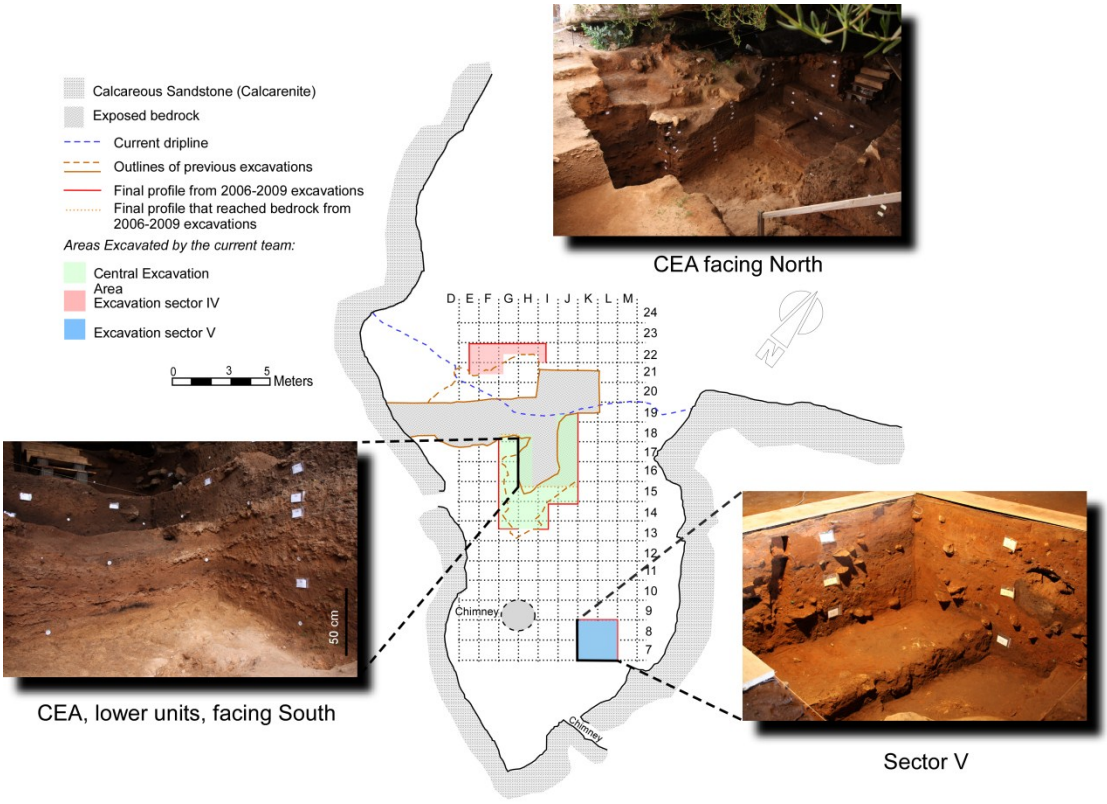

Figure 3: Map of Contrebandiers cave showing the excavation grid, the cave morphology, and location of the main areas of excavation. Photographs showing the main profiles at the site.

2.4 Geological and Geomorphological Context

Structurally, the Rabat coastal area belongs to the flat plateau of the Moroccan western Meseta. This geomorphological domain is bordered on the north by the Riftian chain, and separated from the Sahara regions in the south and east through the tectonic elevated Atlasic chains. The coastal area is characterized by a cover of Pliocene and Quaternary sedimentary formations that overlie Paleozoic substratum (Figure 1a). The latter are mainly exposed in the valleys of the Bouregreg River to the northeast, and the Yquem River, south of Témara (Piqué, 1979). Sea level oscillations, in concert with the

tectonic uplift of this area, allowed for the preservation of coastal deposits during Quaternary transgressions. The Quaternary formations are thus characterized by several belts roughly parallel to the shoreline that comprise lithified dune systems and paleo beach deposits, interspersed with the formation of red sandy terra rossa soils (‘*harmri’*) (Aberkan, 1986; Bronger and Bruhn-Lobin, 1997; Plaziat et al., 2008; Texier et al., 1985). This costal formations rise upwards inland in an overall configuration that assumes a staircase arrangement (Stearns, 1978). Swale lakes (locally named ‘*dayas’*) are occasionally present in the interdunal areas inland and associated with hydromorphic soils (‘*Hrach’*). The cave of Contrebandiers is carved into one of the calcarenite deposits that constitute an inactive cliff. The calcarenite is rich in shell fragments and quartz grains and its formation has been dated by OSL to the MIS 11, with an age of 421 ± 31 ka for the cave’s floor exposed in the excavation area, and a date of 341 ± 27 ka for the deposits that constitute the cave’s wall (Jacobs et al. 2011). The top of the calcarenite is karstified and characterized by the presence of several up to 1 m wide dissolution pockets that incorporate 2 to 7 cm rounded pebbles. As it is characteristic of many of the calcarenite outcrops in the Témara area, deep dissolution features filled with red sandy soils were also detected at Contrebandiers calcarenite formation (Figure 1c). A profile from the cave to the present shoreline shows that the cave faces an altimetric depression (locally named *Oulja*) filled with continental formations of *harmri*-type soils (Figure 3b). A second, presumably younger, calcarenite cliff is present near the shoreline and is currently being eroded by wave action.

2.5 The Stratigraphic and Archaeological Sequence

Since its discovery, several excavations have been undertaken at Contrebandiers Cave initially by Roche from 1955 to 1957, and from 1967 to 1975 in co-direction with Texier (Roche, 1969, 1976b; Roche and Texier, 1976). In 1994, small excavations were carried out by Bouzouggar (Bouzouggar, 1997a, b). These works exposed a sedimentary sequence with MSA occupations containing the so-called Mousterian overlain by Aterian industries, followed by sparse sediments associated with the Upper Paleolithic/Epipaleolithic Iberomaurusian and extensive Neolithic occupations. Renewed excavations at the site started in 2006 under the direction of Dibble and El Hajraoui (Dibble et al., submitted). From the geological side, some lithostratigraphic aspects of the deposits were examined by Niftah (Niftah, 2003; Niftah et al., 2005), and optically stimulated luminescence (OSL) dating of the sedimentary sequence has been recently published by Schwenninger et al. (2009) and Jacobs et al. (2011).

Figure 3 shows the three main sectors which were the focus of the recent excavations, specifically the Central Excavation Area (designated as CEA from here onwards), sector IV and sector V. A detailed description of the archaeological content and stratigraphic framework at Contrebandiers Cave is published in Dibble et al. (*submitted*), and the readers are referred to this source for more details. A summary description of the lithostratigraphic Units is available in Table 1 and illustrate in Figure 4. Only the most salient elements of the site stratigraphy and assemblages are discussed below and in association with the micromorphological observations.

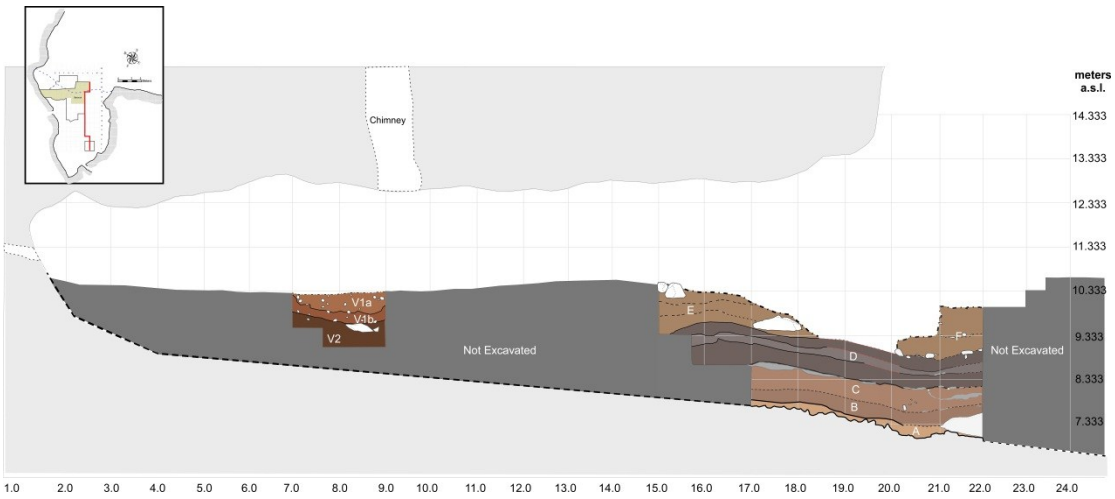

Figure 4: Schematic view of the stratigraphic deposits, illustrating the major stratigraphic units recognized by the recent excavations and their integration with Roche's excavation (in rows K/L). The location of the drawn profiles is marked by a red line in the site grid map in the upper left-hand corner. This synthetic view of the deposits shows their absolute altimetry (in meters above sea level – a.s.l.) and overall geometry of the deposits.

Briefly, the CEA is the only area where bedrock was reached. The roughly 3 m-thick deposits consist of sands and silts with common carbonated cemented areas, expressed as thin discontinuous indurated lenses or as localized cementation of the deposits. Major episodes of roof fall, with dm-size calcarenite blocks, are present in Unit E/F, specifically towards its lower limit throughout the CEA (Figure 4). Large blocks are also abundant in sector V and in association with the Upper Paleolithic Unit H in sector IV. The latter Unit rests unconformably with the underlying Unit G deposits in a cut/fill type of structure that was interpreted by Roche as intentionally dug pits (Roche, 1976a). Although only a small thickness of these deposits was actually targeted by the recent excavations in sector IV, it is possible to observe that the upper limit of Unit G is truncated and dips towards the interior of the cave.

In the CEA, the geometry of the deposits displays several dip directions, with a general inclination towards the cave entrance in squares J/K 19-16, and flattening in the area of K/L 20-22 (Figure 4). In squares H18-15 and G18-16, there is a dip in the opposite direction, roughly towards the back of the cave. The dips appear to be controlled by the presence of a swallow hole that was active in the area of squares G-H 15/13.

Unit [a]	Arch. Layer	Sector	Thickness	Color [b]	Field Description	Archaeological Industry
A	7	CEA	12 – 26 cm	Reddish brown (5YR 5/4) with brownish yellow mottles (10YR 6/6)	Shell-rich sands, with rare rounded cm-size clasts (<7cm) and the presence of interstitial red clays; massive or with discrete horizontal internal bedding; moderately sorted; the Unit varies from loose to strongly cemented towards its base.	Sterile
B	6c		~30 cm	Yellowish red (5YR 4/6) with reddish brown areas (5YR 3/4)	Sandy clay deposits with occasional stones (~7 to 15 cm), moderately loose with occasional concreted areas and domains where weakly developed bedding is apparent; indurated 1 cm thick lenses (specifically in squares J/I -18-16); anthropogenic inputs; gradual inferior limit.	Moroccan Mousterian
Subunit C1	6a/6b		45 to 60 cm	6a: Brown to light brown (7.5YR 5.5/4) 6b: dark yellowish brown (10YR 4/4)	Silty sands, with interfingering discontinuous lenses of darker sediments (=AL subdivision 6b); sediments are locally cemented to heavily cemented; lower limit with Unit B is diffuse.	Sterile ?
Subunit C2			5 to 10cm	Brown to light brown (7.5YR 5.5/4)	A heavily cemented and somewhat continuous indurated crust of variable thickness (typically 5 to 10 cm) that caps Unit C.	
Subunit D1	5c, and 5d		~45 cm	Dark brown (10 YR 4/3)	Somewhat organic sandy loam with abundant human inputs (charcoal, ashes, stone tools, shells, bones, etc.); locally cemented with rare, >10 cm-sized stones; its lower boundary with Unit C is sharp and	Moroccan Mousterian

					seemingly truncated in certain areas.	
Subunit D2	5b		~16 cm	Brown/dark brown (7.5YR 4/4)	Similar to subunit D1 in basic composition but with lighter brown coloration, rarer ash accumulations and smaller and scattered charcoal specks, with occasional cm-size concretions.	
Subunit D3	5a		~20 cm	Dark brown (7.5YR3/2)	Like subunit D1 both in color and composition, with rarer presence of ashy deposits, at least in the excavated areas. Overall, human inputs continue to be frequent.	
E	4		110 cm	Reddish yellow (7.5YR 6/6)	Silty sands, with a clayey component, occasional stones, usually within a 5cm range, and with mottled pockets of slightly darker brown sediments attributed to burrows; occurrence of dm-size roof spall near or at the base of this Unit, and towards its upper boundary in squares J-I 13-15. Variable cementation and presence of human inputs; lower boundary is sharp, truncating Unit D.	Aterian
F	-		~120 cm	Reddish yellow (7.5YR 6/6	Identified in Roche's trench (squares K/l22-21), composed by finer silty deposits moderately sorted, with a stone line, with clasts from 5 to 10 cm in diameter. Correlated with Unit E.	
G	IV-2	IV	Varies from 20 to ~80 cm	Light yellowish brown (10YR 6/4) to pale brown (10YR 6/3)	Crumbly pebbly silty sands laterally varying from almost clast-supported (with stones typically in the 3 to 15 cm range) and ubiquitous shells in its southern area, to extensively cemented matrix-supported deposits toward North. Anthropogenic inputs are common.	Aterian
H	IV-1a and IV-1b		~ 60 cm	yellowish brown (10YR 5/6 – in IV-1a) to orange-brown silty sands (Subunit H1, Layer IV-1b)	Unit unconformably overlies Unit G in a cut/fill type of structure. Correspond to silty sands, fairly loose and moderately sorted with extensive dm-size roof spall. Anthropogenic inputs in the form of lithics and bones.	Iberomaurusian

V-A	V-2	V	~ 70 cm	dark reddish brown (2.5YR 3/4) to dusky red (10R3/3)	Silty sands, with increased clay content, containing common charcoal specks; large dm-size roof spall blocks characterize the top of the Unit. Anthropogenic sediments are expressed by the presence of features rich in charcoal and ash.	Aterian
V-B	V-1a and V-1b		~30 cm to 60 cm	is reddish brown (2.5YR 4/4) to dark reddish brown (2.5YR 3/4)	Silty sand with abundant, ~15 cm darker brown mottles regularly distributed throughout the deposits, attributed to biogenic burrows frequent stone lines (the stones vary from 5 to 15 cm in diameter), and larger dm-sized blocks of roof spall that mark the Unit lower boundary. Anthropogenic inputs include stone tools and bone fragments. The upper part of the Unit is moderately sorted fine silty sand, fairly loose and with occasional stones (5 to 10 cm in diameter) with presence of irregular, roughly 1 cm thick, phosphatic and Fe-Mn indurated crusts that pinch out towards north.	Aterian

Table 1: Lithostratigraphic descriptions of strata from Contrebandiers Cave. a: From bottom to top; b: color was established on dry samples and based on Munsell soil color charts.

The bulk of the deposits in the CEA and in sector V are comprised of MSA industries, with assemblages containing stemmed pieces (traditionally associated with the Aterian) superimposing strata were this type of diagnostic tool is absent (the so-called Moroccan). Albeit the fact that the interpretation of Mousterian and Aterian as separate entities or as simple variants within the same archaeological complex is still controversial (see Dibble et al. in prep.), in this paper we maintain this distinction just as a descriptive parameter to express the archaeological content of the stratigraphic Units at Contrebandiers Cave.

The first human occupation is expressed in Unit B, which consists of sandy clay with anthropogenic inputs, (e.g., discrete combustion areas - charcoal, ashes, and

combusted remains). The density of lithic artifacts in Unit B is, however, extremely low – an average of 86 blanks (proximal or complete flakes) per cubic meter of excavated sediment. This Unit is overlain by the brown deposits of Unit C, which seem to lack archaeological content, at least in the excavated areas. Relatively more extensive human occupations are present in the somewhat more organic Unit D, which is associated with Mousterian assemblages. Aterian occupation, (*stricto sensu*: assemblages associated with diagnostic stemmed pieces), have been excavated in Units E and G, as well as in the deposits excavated thus far in sector V (see Table 1). The faunal assemblages are still being studied, but we can note the abundance of *Gazella* species in all the levels; carnivores – characterized mainly by the presence of hyenas in the Units associated with so-called Mousterian Units – and Rüppel's fox (*vulpes rueppelli*) are mostly present in Aterian levels.

Roche's extensive excavations removed an unknown thickness of the Aterian, and possibly Iberomaurusian and Neolithic deposits. Sediments associated with the Neolithic are present only in the form of pits dug into the underneath sediments or as remnants preserved along the cave walls. The Iberomaurusian occupations are, as it was mention before, located only in excavated sector IV and do not extent to the rest of the excavated areas. This seems to be in accordance with Roche's reports, which state that the Iberomaurusian at Contrebandiers was only present in a restricted area and absent inside the cavity (Roche, 1958-1959; Roche, 1969, 1976a). The Iberomaurusian assemblages are characterized by the production of small flakes with nongeometric microliths being

the most abundant tool type, alongside with sidescrapers and *pièces ésquillées* (Dibble et al., submitted; Olszewski et al., 2011).

2.6 Methods

Samples for soil micromorphology were systematically collected across the site in order to access the overall nature of the deposits, including lateral variability in sedimentation, anthropogenic inputs, and post-depositional processes (see Table S1 and Figures S1-3 in Supplementary Materials). Forty-three samples were collected from the new and old profiles in the CEA where the deepest deposits are currently exposed. Additionally, five samples were collected from sector IV, seven from sector V and four from the sparse remnants of more organic sediments attributed to the Neolithic. The samples from the Neolithic strata are not discussed here since the present paper focuses mainly on the Paleolithic Units at Contrebandiers; in addition, the present-day exposures of Neolithic deposits are very sparse.

The soil micromorphology samples were collected as undisturbed, oriented blocks that were cut out of the profile and wrapped in soft paper and packaging tape; for poorly consolidated samples plaster bandages were used (see Goldberg and Macphail, 2006; and Goldberg and Macphail, 2003 for further description of approaches to remove undisturbed samples). The sampled blocks were then oven-dried for several days (at ~60^{o}C) and impregnated with a mixture of unpromoted polyester resin and styrene at a ratio of 7:3; 1 L of this mixture was catalyzed with 7 mL of Methyl ethyl ketone peroxide

(MEKP). The indurated blocks were trimmed and prepared into 30 μm thick, 5 x 7.5 cm thin sections by Spectrum Petrographics (Vancouver, WA, USA). The final thin sections were studied with a petrographic microscope under magnifications ranging from 2x to 40x, and described following standardized micromorphological nomenclature (Courty et al., 1989; Stoops, 2003).

The archaeological samples processed in thin section were analyzed by FTIR microspectroscopy using a Nicolet Spectra Tech Continuum™ IR microscope attached to a Nicolet Nexus 460 spectrometer. Spectra of particles with diameters near 150 μm were collected in transmission and total reflectance mode between 4000 and 450 cm–1 at 8 cm–1 resolution using a Reflectocromat 15× objective. FTIR spectroscopy is a molecular analytical technique well suited to identify heat-related transformation in materials of different nature such as clay minerals (e.g., Berna et al., 2007 and refs. therein) and bone (Berna, 2010). Common carbonates, phosphates, sulfate and organic compounds (charcoal and collagen) can be positively identified by FTIR (Weiner, 2010).

2.7 Results

Since the relative degree of homogeneity observed in the field is also expressed in the thin sections, some micromorphological characteristics of the deposits will be presented as a whole, including main coarse composition, microstructure, and a number of physical post-depositional processes of the observed samples. The most prominent

micromorphological aspects of each Unit will be discussed below in stratigraphic order within each of the excavation sectors. In order to keep track of the micromorphological details, these descriptions are supplemented by specific interpretations, with a more systematic summary of interpretations being presented in the Discussion.

Independent of the lithostratigraphic Unit or location in the cave, the coarse fraction in thin section shows ubiquitous silt- and sand-sized grains of subrounded to rounded monocrystalline quartz grains. Silt-size rounded opaque mafic minerals are also commonly present and scattered throughout the deposits. Feldspar grains (some weathered), and mm size rounded quartzite pebbles are generally scarce. Carbonate components consist of grains of subangular to subrounded fragments of shelly calcareous sandstone (representing roof spall) and very rare travertine fragments (e.g., sample 09-5a from Unit E). Bioclasts from bedrock (non-descriptive fragmented shells and sea urchins) are scattered throughout the sampled Units.

Anthropogenic, but mainly biogenic components are common, primarily in the form of bones, marine mollusks, land snails, and phosphatic coprolite grains. Rare fish bones were also observed in Units B and D. Bone fragments, exhibiting various degrees of burning, are usually angular in shape, although subrounded to rounded sand size bones were occasionally observed. Charred fragments (charcoal and plant remains) are commonly observed in Units D and V-A, and calcitic ashes in the form of lenticular accumulations or cm-size massive accumulations are present; the latter typically in Unit D.

Overall, the deposits at Contrebandiers Cave display a low variability with the majority of the samples exhibiting a poorly developed microstructure. The porosity tends to be high in the observed slides, represented by voids linked to biological activity – mainly channels and chambers-, with packing voids being more relevant in the deposits from Unit A). The coarse/fine (c/f) related distribution is, on the other hand, more heterogeneous and will be discussed below. The groundmass is mainly crystallitic due to the presence of dispersed micrite in the groundmass, with the exception of the Unit D deposits in the axis of the cave (in squares H/I 16/15) and layer V-A in the rear of the cave where the deposits are being decalcified. Common to almost all the observed thin sections is the presence of bioturbation, although the degree and agents of this biological activity may change depending on the lithostratigraphic Unit and/or location within the site (see below).

2.7.1 Micromorphological observations from the Central Excavation Area (CEA)

Unit-based micromorphological results are presented in stratigraphic order from the bottom to the top of the sequence.

Unit A (AL 7, samples CB09-34b, Cb09-34c, CB09-41b, CB09-41c, CB10-13b - see Table 1 in supplementary material for sample location):

This Unit is composed mainly of geogenic bioclastic sands that currently are exposed only in the CEA, squares F/K 21-17. Under the microscope, the deposits are composed of monic, well-sorted, rounded, sand-sized shell fragments (typically around 500 μm), with compound packing voids and low frequency of rounded calcarenite fragments; almost no fine matrix is present (Figure 4a). In samples from squares G/J 17-16, there is a gradual contact to stringers of opaque grains, probably manganese. Weak bedding is occasionally observed and expressed by sub horizontal thin lenses of oriented coarse components. The geogenic nature of these deposits changes upwards with an increase of biogenic terrestrial inputs, namely bones, coprolites, and soil aggregates (Figure 5b-e). There is a gradual contact to the overlying Unit.

Traditionally, these basal sands have been associated with marine incursion during the last interglacial, MIS5e (Eemian). The age obtained for this Unit (weighted mean of 126.4 ± 9.1 ka) seems to concur with this initial interpretation (see Jacobs et al. 2011). However, as seen in thin section, the incorporation of terrestrial elements shows that these deposits have been remobilized in certain areas and have incorporated terrestrial inputs due to the occupation of the site by animals. It seems likely that such reworking occurred inside the cave after the sea's retreat, and the original bedding of the coarse components is still locally preserved. The inherent dip of the unit follows the cave's floor (i.e., seawards towards NNW) and can be attributed to some degree of post-depositional subsidence.

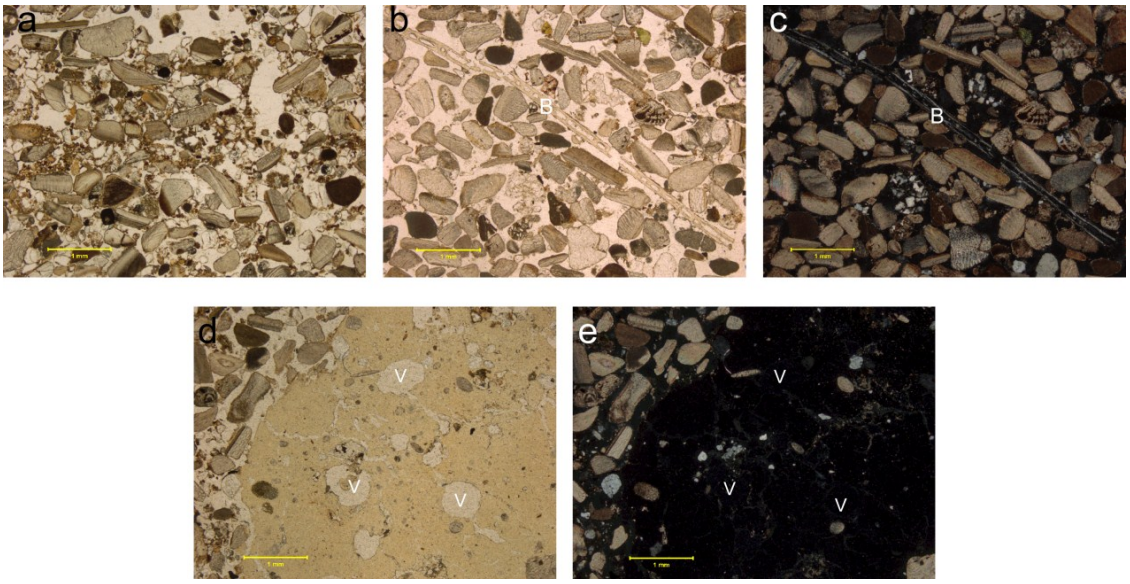

Figure 5: Sample CB10-13 from Unit A. (**a**) Photomicrograph of sediments from Unit A showing the ubiquity of well-rounded shells and the loose nature of the deposits with common packing voids and channels; Plane-polarized light (PPL). (**b**) Photomicrograph showing the presence of an elongated bone (B) within Unit A; PPL. (**c**) Same as (b) but in cross-polarized light (XPL). (**d**) Detail of yellow isotropic coprolite grain with common vesicles (V); PPL. (**e**) Same as (d) in XPL. Note the isotropic nature of the phosphatic grain

Unit B (AL 6c, samples CB08-1, CB09-5, CB09-21, CB09-24a, CB9-24b, CB09-25, CB9-27, CB10-2a, CB10-2b, CB09-41, CB10-9, CB10-10, CB10-13a - see Table 1 in supplementary material for sample location):

Although the contact with the underlying Unit A is gradual and somewhat diffuse, Unit B deposits are recognizable in the field by darker yellowish-red to brown-red sediments that incorporate anthropogenic inputs. In the microscope, it is possible to see that this coloration is related to a higher percentage of the clay fraction, both in the groundmass and as clay coatings on voids (Figure 6i-j). Clay is present in the groundmass in the form of mm-size reddish silty-clay rounded to subrounded pellets, as soil

aggregates that incorporate quartz sand- and silt-sized grains and, very rarely, as limpid strong red clay papules (see CB 08-1a). Rarer mm-thick, discontinuous lenses of clay are also visible but very rare in frequency in the analyzed samples. The presence of dusty clay and silt coating on voids is linked to clay illuviation. Anthropogenic and biogenic inputs are expressed in the form of charcoal fragments, lenses of calcitic ashes, coprolites, and common angular bone fragments, the latter exhibiting a variety of thermal alterations. Horizontally disposed stringers of organic matter are locally present, particularly in square K20 and, unlike in other areas, these do not seem to be charred but representing somewhat humified plant remains (Figure 6c). The incorporation of rounded shell fragments is common and reflects the upward movement of reworked deposits from Unit A. Unit B deposits also expresses the presence of phosphates in the form of pale yellow domains in the groundmass and as discontinuous tabular-shaped weathering crusts (Figure 6b). The latter are interpreted as ephemeral episodes of stabilization of the surface, with guano-derived phosphates accumulating on the exposed sediments. Indurated cm-thick black lenses are seen in several localized areas in the field and are expressed in the microscope as stringers of manganese and/or coating quartz grains and altered shell fragments. Intense syn- and post-depositional biological activity is supported by the presence of channels, fecal pellets (some clearly due earthworm activity), and rare plant roots.

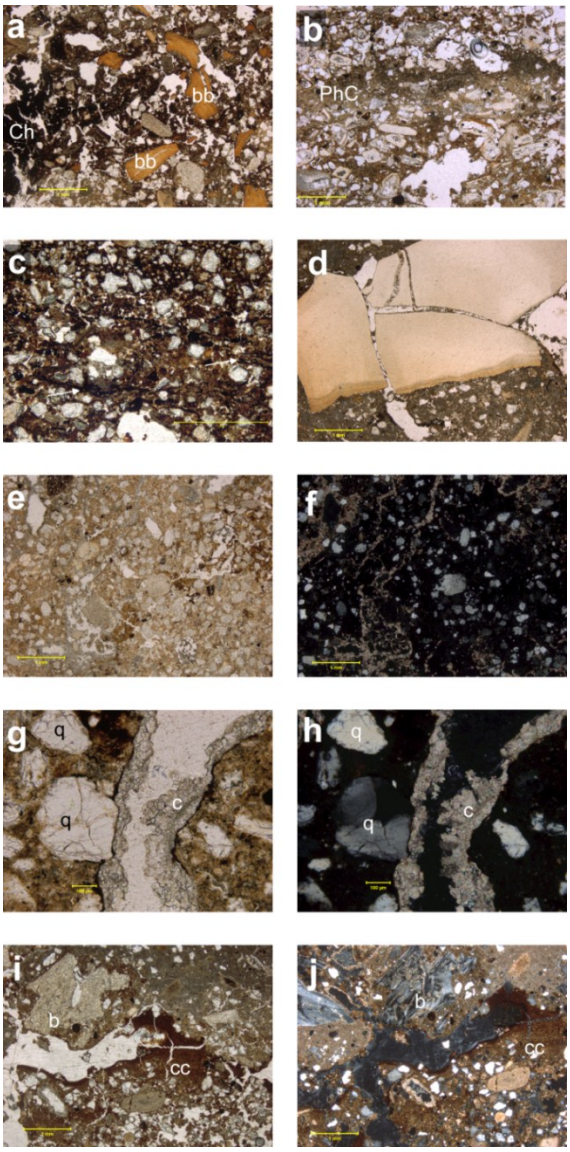

Figure 6: Photomicrographs from Unit B. (**a**) Sample CB10-2a with burned bones (bb) and interspersed stringers of charcoal (ch), PPL. (**b**) Sample CB09-41a with lenticular phosphatic weathering crust (PhC), PPL. (**c**) Sample CB09-27b dispersed isotropic stringers of organic matter (arrows) that do not seem to be charred, PPL. (**d**) Tooth fragments in place fractured within one of the ash accumulations in sample CB10-2a, possibly due to trampling, PPL. (**e**) Detail of the matrix in sample CB10-2b where it is possible to observe the phosphatized domains, PPL. (**f**) Same as (e) but in XPL. Note the isotropic nature of phosphatic domains in the groundmass and the present of calcitic infillings, which are presently being decalcified. (**g**) Detail of a calcitic sparitic coating (cl) of a channel in sample CB10-2b. Note the rounded to subrounded ubiquitous quartz grains (q) and the yellowish brown color of the matrix in PPL. (**h**) Same as (g) but in XPL. Note the birefringence of the calcitic coating versus the black nature of the phosphatic groundmass. (**i**) Example of dusty laminated silty clay coatings on voids (cc) and bone fragments (b) in sample CB 10-2a, PPL. (**j**) Same area as in (i) showing the deposits in XPL. Note the calcitic nature of the sediment in the upper part of the image.

Unit C1 (AL 6a/b, samples 08-2, 08-3, 08-4a-b, 09-4, 10-19, 10-23 - see figure S3 in supplementary material for sample location):

In the field the deposits show interfingering darker lenses (from 5 to 10 cm thick) that are both laterally and vertically discontinuous, pinching out along the profile. In thin section, these areas often contain dahllite (confirmed by FTIR analyzes) expressed in the form of amorphous yellow fluffy masses in the matrix (Figure 7b-c), and occasionally in association with stringers of manganese within reddish groundmass (Figure 7d). In addition, red-brownish isotropic nodules of authigenic minerals appear to be precipitated in the silty sand matrix (Figure 7e-f). FTIR analyzes have shown that these authigenic minerals do not correspond with phosphates, but unfortunately, their mineralogical nature has not been possible to attest either by petrographic or FTIR characteristics.

The calcareous nature of the deposits is still evident in several domains of the analyzed samples. The presence of rare calcitic voids coatings is rare; although overall they are being decalcified. Despite localized decalcification, bone fragments are still present, although not abundant, and are somewhat bedded in sample CB10-19 (Figure 7a).

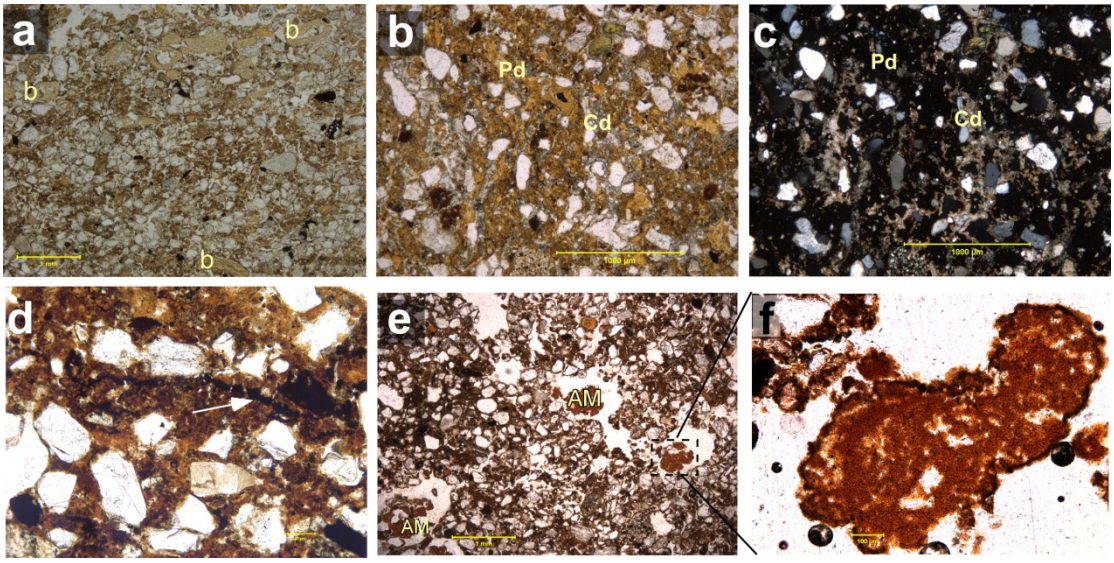

Figure 7: Photomicrograph of Unit C1. (**a**) Detail of one of the rare areas where somewhat bedded altered bones (b) are present in Unit C1 deposits. Note that the remaining silty and sand-size components are, conversely, not bedded, PPL. (**b**) Photomicrograph showing the post-depositional processes that locally affect this archaeological layer, with phosphatized domains of dahllite (Pd) [confirmed by FTIR] followed by micritic cementation (Cd), PPL. (**c**) Same as (b), but in XPL where it is possible to see the bright areas cemented by micrite (Cd) versus the isotropic nature of the phosphatized domains (Pd). (**d**) Domains with accumulation of stringers of manganese (arrow) in a reddish brown groundmass rich in quartz grains, PPL. (**e**) Photomicrograph showing the presence of authigenic red minerals (AM) growing on voids, PPL. (**f**) Enlargement of area marked by square in (e) showing one of the authigenic minerals, PPL. The scale bars in photomicrographs (a – c) and (e) is 1 mm, and 100 µm in (d) and (f).

Unit C2 (samples 09-35b - see Table 1 in supplementary material for sample location):

Unit C2 constitutes a calcareous crust that caps the Unit C deposits and is a stratigraphic marker throughout the CEA, despite the fact that it can be somewhat discontinuous locally and truncated by the overlying Unit D deposits. Micromorphological observations of these sediments show characteristics associated with a calcareous globular calcrete layer that incorporates quartz grains, occasional sand-sized bone fragments and rounded soil aggregates. The deposits show the presence of rhizoliths

(that is, calcareous root replacements) and other types of thin sparitic coatings on voids (Figure 8). Iron staining and phosphatized domains are also present in sample 09-35b, showing that the calcitic crust is being decalcified. As seen in the field, the indurated C2 Unit is locally displaced (Figure 8a) indicating that slumping of the deposits into a putative swallow whole in the areas of G/H5-13 occurred (or continued to occur) after the deposition and cementation of this crust.

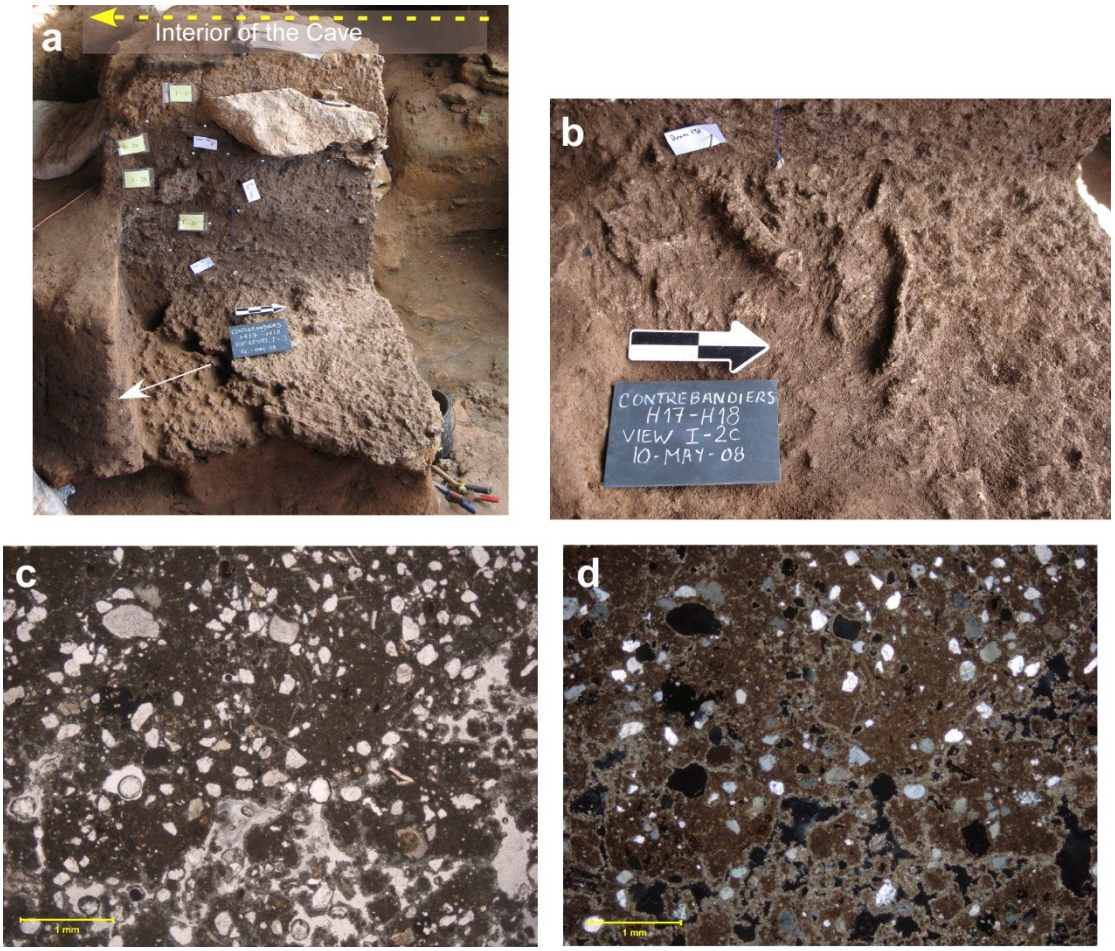

Figure 8: Unit C2 (**a**) Field photograph of the top of the cemented crust Unit C2 in squares H17/H18, where it is possible to see that the cemented deposits are broken and slumping towards the interior of the cave. The approximate direction of slumping is indicated by the white arrow, and the arrow on the top of the photograph shows the direction of the cave's interior (see also Figure 2). The scale is subdivided into 5

cm increments; (**b**) Field photograph of rhizoliths (root casts) just above the cemented Unit C2. The scale is subdivided into 10 cm increments; (**c**) Photomicrograph of Unit C2 deposits with the presence of ubiquitous quartz grains and the globular arrangement of the finer matrix, PPL; (**d**) same as (c) but in XPL. The photomicrograph scale is of 1 mm.

Unit D (AL 5a/b/c, samples 09-2a-b, 09-9, 09-10a-b, 09-35a, 09-43, 10-4, 10-11, 10-12, 10-18 10-22, 10-24 - see figure S2 in supplementary material for sample location):

The darker brown coloration of this Unit seen in the field is associated with an increase in charcoal, burned bones and organic matter. Seen in thin section, the deposits consist mainly of an unbedded, jumbled mixture of anthropogenic inputs: calcitic ash, charred organic matter, shells (some burned), and bone fragments exhibiting various degrees of thermal alteration (Figure 9). Amorphous yellow grains were occasionally observed, probably corresponding to carnivore coprolites. The original structure of the anthropogenic materials, namely the ashes and associated combusted remains, was repeatedly disrupted by abundant syn- and post-depositional bioturbation and possibly also by trampling (the latter expressed by the fragmentation of several components such as shell fragments). Bioturbation is expressed mostly in the form of very frequent channels and chambers, alongside with abundant fecal pellets, wasp cocoons and coalesced aggregation of the matrix due to earthworm activity. In addition, cm-sized rhizoliths were also observed in the field, namely towards the base of subunit D1 (Figure 8b).

Post-depositional features are likewise expressed as secondary calcitic cementation of the matrix, thin calcitic coatings on some of the voids, and calcitic

infillings; these, however, are laterally variable. In fact, in squares located along the central axis of the cave, the sedimentary matrix is decalcified and phosphatized (see Figure 15). It is relevant to note that this localized decalcification occurs in the area where the deposits are dipping. Thus, it is possibly correlated with both a higher input of phosphate (possibly guano) and enhanced water percolation in this location, since the dipping of the deposits resulted in a depressed topography with preferential water circulation.

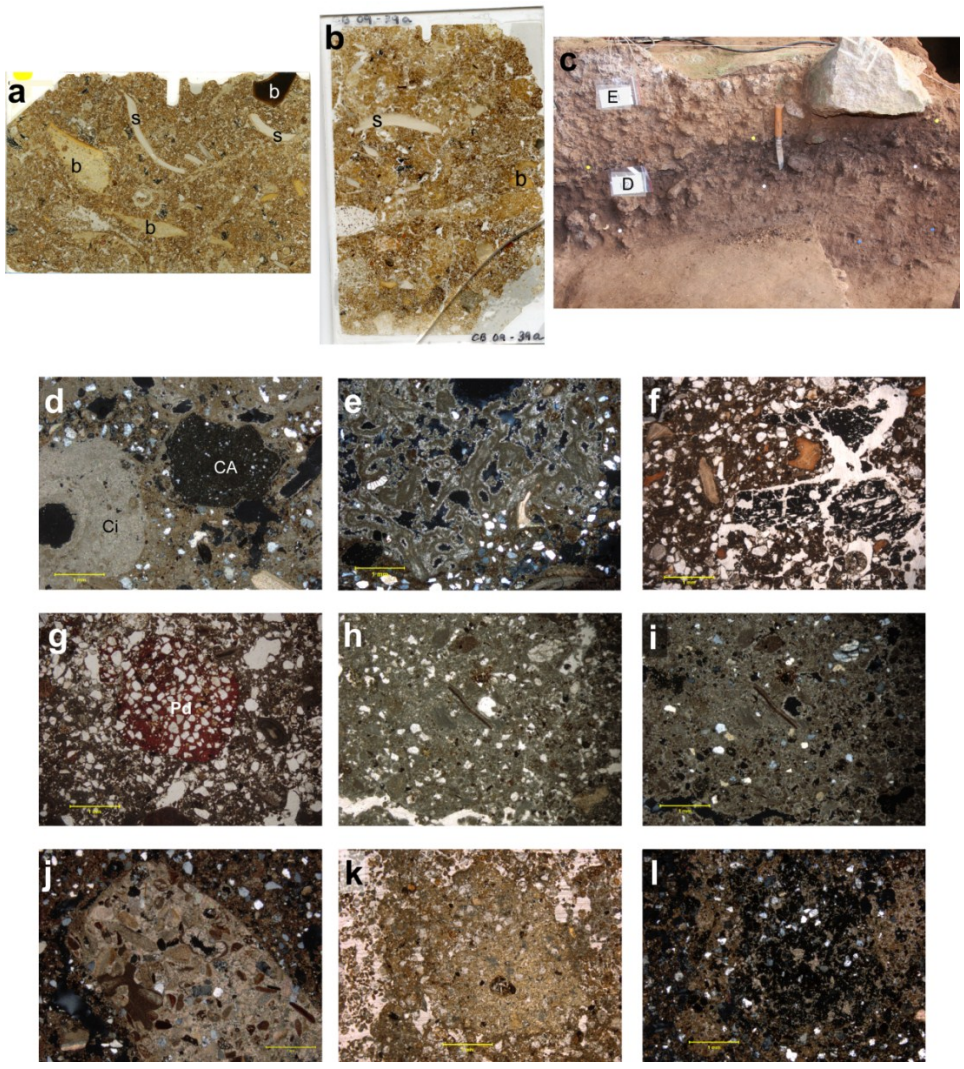

Figure 9: Samples from Unit D: (**a**) Macrophotograph of sample CB07-1a from Unit D showing the coarse, anthropogenic nature of the deposits with chaotic organization of cm-sized bones (b) with several degrees of thermal alteration, and shell fragments (s), PPL; height of view = 50 mm; (**b**) Macrophotograph of sample CB09-39a from Unit D with common bones (b) and shells (s), PPL; height of view = 75 mm; (**c**) Field photograph of the sharp contact between the darker deposits of Unit D and the reddish sediments of Unit E with common dm-sized roof fall in squares G17/18; (**d**) Photomicrograph of Unit D deposits with the presence of reworked calcareous infillings (Ci) corresponding to rhizoliths in a micritic matrix, which includes a sub-rounded clay aggregate (CA), XPL; (**e**) Photomicrograph of calcitic rhizoliths attesting to plant growth in localized areas, XPL. (**f**) Photomicrograph showing the presence of mm-sized charcoal fragments and bone fragments, PPL; (**g**) Photomicrograph of red pedorelicts (Pd = soil aggregates) rich in silt-sized quartz grains in Unit D sediments, PPL; (**h**) massive, secondarily cemented accumulation of calcareous ashes in Unit D incorporating shell fragments and quartz grains, PPL; (**i**) same as (h) but in XPL. Note the calcitic nature of the ash deposits; (**j**) cm-sized calcarenite fragment rich in bioclasts, XPL; (**k**) Photomicrograph of phosphatized domains in sample CB10-22, PPL; (**l**) same as (k) but in XPL. Note the isotropic nature of the phosphatized domains. The scale bar of the photomicrographs is 1 mm.

Unit E and F (AL 4, samples 08-5a-c, 09-30, 09-36, 09-39a-d - see figure S1 in supplementary material for sample location):

Unit E/F truncates the underlying Unit D deposits and is expressed in the field as a sharp contact or with an irregular undulating morphology. However, this contact was not possible to observe in thin section since bioturbation has somewhat masked the limit between these two Units at the micromorphological level. Unit E deposits were sampled in the area of squares G/J 15-14, where they were excavated, and are lithostratigraphically correlated with Unit F sediments present in Roche's trench (squares J/K 22-19), although the latter were not the target of excavations by the current team.

Alongside with the field evidence of a major roof fall episode at the base of Unit E/F, the micromorphological analyses show that mm- to μm-sized calcarenite roof spall fragments are frequent in thin section. On the whole, the deposits reveal similar geogenic components as the underlying Units, but are, however, strikingly different in the decrease of the anthropogenic signal when compared to deposits in Unit D. Nonetheless, scattered bone fragments and shells are still observed throughout. Most relevant is the presence of rare charred remains (specifically charcoal fragments and thermally altered bones) in thin section, since no macroscopic evidence of use of fire was identified during excavation of these layers (e.g., samples CB09-39a and 08-5a). However, direct evidence of ashes in the microscope, was not observed.

Bioturbation is extensive resulting in the local reworking of the sedimentary components. Accordingly, the distinctiveness of the original microstructure might have been obliterated resulting in an apparent homogeneity of these deposits.

2.7.2 Micromorphological observations in Sector V

Unit G (AL IV-2, samples 09-28, 10-16a-b bottom, 10-21 - see Table 1 in supplementary material for sample location):

Unit G was only identified in excavation sector IV and corresponds to the stratigraphically uppermost Aterian occupations with an age of 92 ± 6 ka (Jacobs et al. 2011). The sediments consist of pebbly silty sands with a lateral changes in color and stone abundance, varying from pale brown almost clast-supported with common shells in the southern areas of sector IV to a lighter yellowish brown matrix-supported towards north. Micromorphological observations show a clear contact with the above deposits of Unit F (Figure 10). Common human inputs in the form of cm-size shell fragments and bones are observed and the mineral fraction shows a chitonic to enaulic c/f distribution. Overall the sediments were decalcified in the southern areas and vary laterally towards the north, where the pale color in the field can be associated with an increase in carbonate content. In fact, the deposits in the northern part of sector IV show relatively fewer anthropogenic remains in thin section and are characterized by a crystallitic calcareous b-fabric, with c/f distribution pattern varying from close to loose porphyric (Figure 10d-e).

Unit H (AL IV-1a-b, samples 09-29, 10-6a-b top - see Table 1 in supplementary material for sample location*):*

Unit H corresponds to the Iberomaurusian occupations present only in sector IV and expressed in the field by loose and moderately-sorted deposits. In thin section, the fine matrix is sparse and coats the coarser components (chitonic c/f distribution), namely quartz grains, sand-sized bone fragments, and rare phosphatic grains – probably corresponding to coprolites (Figure 11). The porosity is composed of packing voids, as well as channels and chambers, the last frequently corresponding to wasp cocoons. The micromorphological characteristics make these deposits very distinct from the older sediments of the cave: they are generally finer grained, moderately sorted, and the fine matrix coatings that equally affects the geogenic and the anthropogenic/biogenic components. The fact that the anthropogenic components are also surrounded by partial or complete surrounding coatings suggests that the depositional processes of these inputs are not distinct from those of the mineral (quartz) fraction.

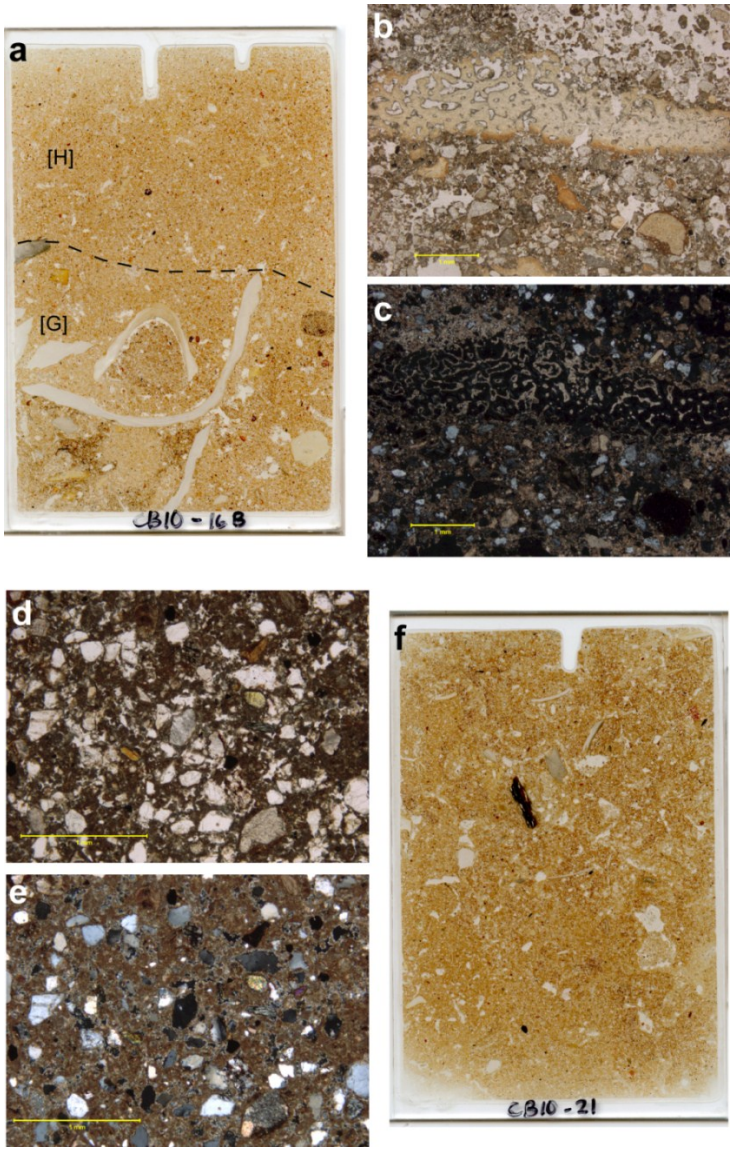

Figure 10: Unit G. (**a**) Macrophotograph of sample showing the contact (dashed line) between Unit H and Unit G in the southern area of excavator sector IV. Note the frequency of cm-size shell fragments in Unit G deposits *vs.* the better sorted sediments from overlying Unit H; the height of view = 75 cm; (**b**) Photomicrograph of Unit G sediments where several bones, including a cm-size spongy bone fragment show signs of burning, PPL. (**c**) Same as (b) but in XPL. Note the presence of calcite cementation associated with some calcareous ash within the bone microfractures; (**d**) Photomicrograph of Unit G deposits toward the northern area of sector IV illustrating the presence of rounded to subrounded quartz grains embedded in a calcitic matrix, PPL; (**e**) Same as (d) but in XPL. Note the calcitic nature of the matrix, and the lack of porosity, when compared to photomicrographs b – c from the southern section; (**f**) Macrophotograph of sample CB 10-21 located toward the northern area of sector IV. This sample displays a somewhat finer nature of the deposits, though small size shell fragments and a burned bone (black) are visible in the upper part of the slide; height of view = 75 cm.

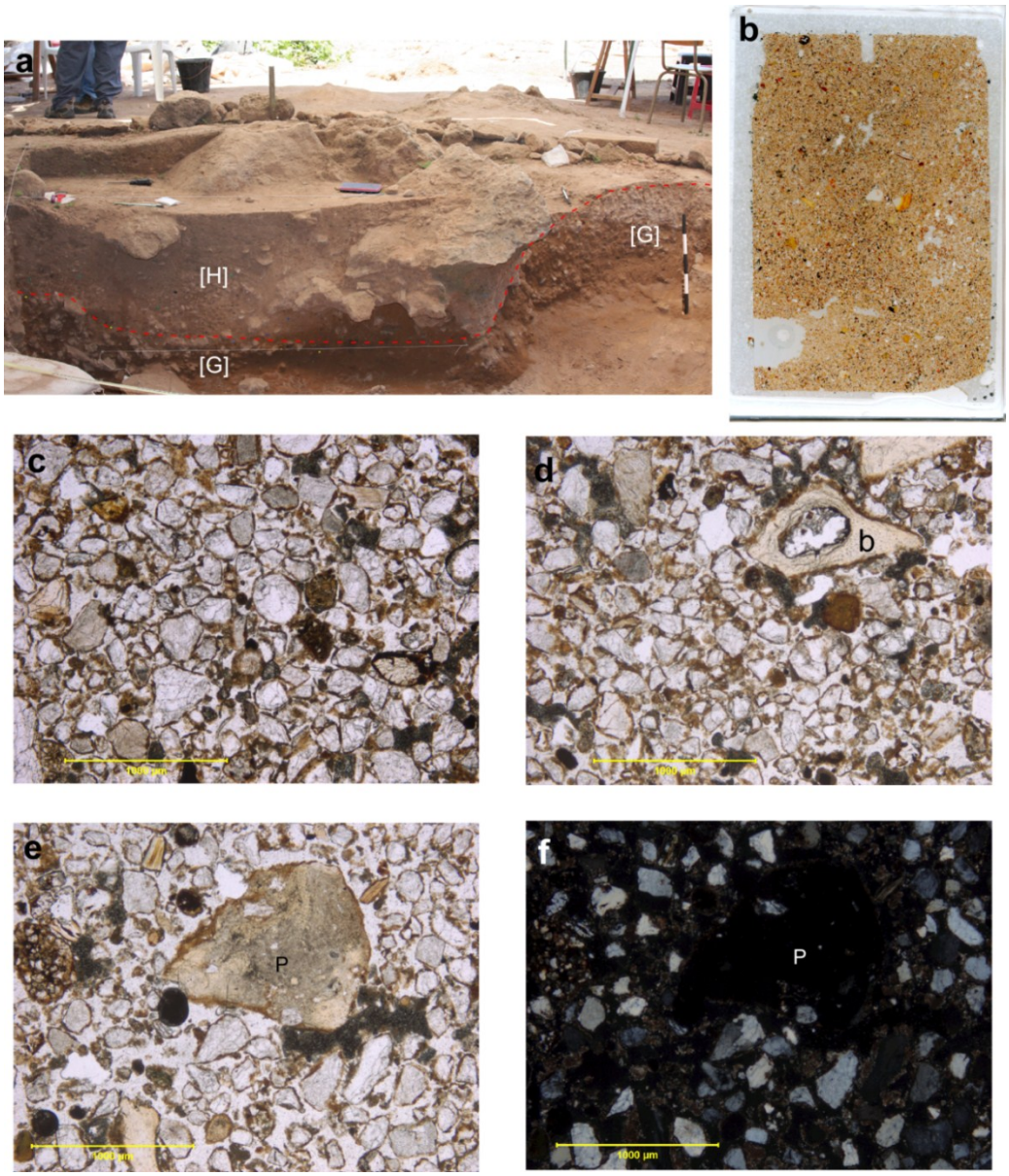

Figure 11: Field Photograph of excavation sector IV where it is possible to see the geometry of Unit G underlying deposits and the Iberomaurusian bearing deposits of Unit H filling the cut/fill type of structure. The dashed line shows the contact between the two Units. Note the presence of abundant roof fall blocks in this area; the scale is subdivided into 10 cm increments; (**b**) Macrophotograph of sample CB09-29 in PPL. Note the well sorted silty nature of the sediments; height of view = 75 mm; (**c**) Photomicrograph of Unit H deposits where it is possible to view the fine matrix coating the mineral sandy quartz fraction (chitonic related distribution) and the abundance of packing voids (white areas), PPL; (**d**) Photomicrograph showing the presence of bones (b) in the deposits with similar coatings as the quartz grains, PPl; (**e**) Photomicrograph illustrating a sub-rounded phosphatic grain (P; coprolite?) and the presence of silt-sized bone fragments in the lower part of the image, PPL; (**f**) same as (e) but in XPL. Note the isotropic nature of the phosphatic grain. The scale of the photomicrographs is of 1000 µm.

2.7.3 Micromorphological observations in Sector V

Unit V-A (AL V-2, samples 10-5, 10-17, 10-20, 10-25 - see Table 1 in supplementary material for sample location):

Unit H is distinguished in the field by a darker color and the presence of combustion remains. In thin section, the deposits show an enaulic to porphyric related distribution with a relatively higher proportion of fines when compared with the sediments from the CEA. Charred remains, namely ashes, charcoal fragments, and burned bones are observed and often scattered in yellowish red groundmass that shows an undifferentiated b-fabric (Figure 12). The original microstructure of the combustion deposits is commonly bioturbated, with abundant channels and wasp borrowings. The anthropogenic ashes are commonly decalcified, but bone fragments are still preserved, some with evidence of weathering. Yellowish phosphatic components are common and expressed as lumps or stringers of apatite or as rounded isotropic grains (Figure 12a-c). Occasional rounded clay aggregates are also present.

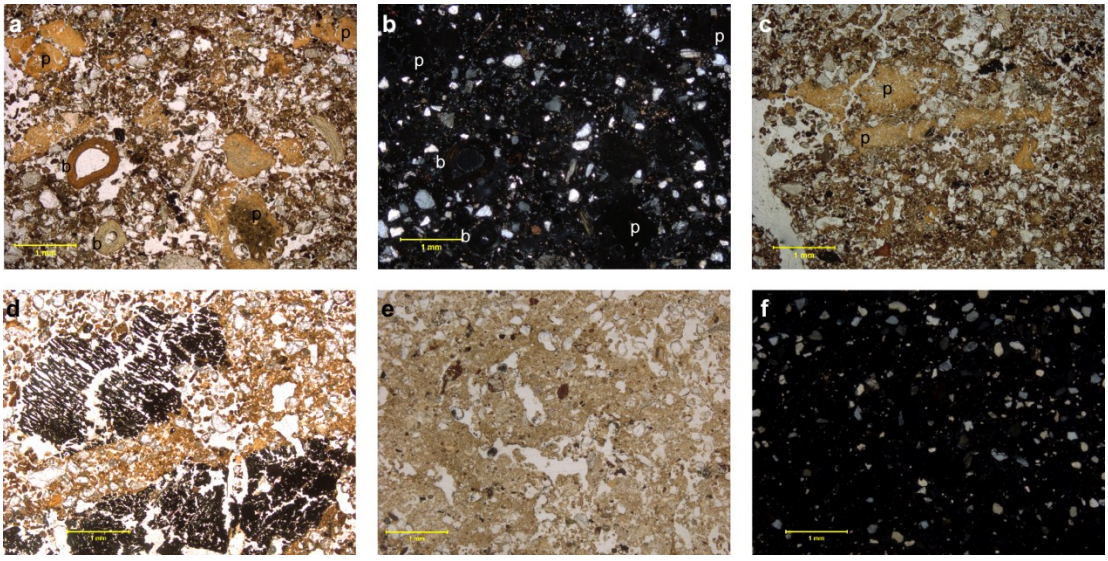

Figure 12: Photomicrographs of Unit V-A deposits. (**a**) presence of scattered rounded bone fragments (b) surrounded by common yellow phosphatic grains (p; coprolites?), PPL; (**b**) same as (a) but in XPL showing the isotropic nature of the phosphatic grains and silty size quartz grains, XPL; (**c**) stringers of amorphous phosphates in Unit V-A, PPL; (**d**) charcoal fragment with disturbed by a passage feature, PPL; (**e**) detail of ash deposits with embedded silt size quartz grains. Note the pale brown coloration and the bioturbated nature of the ashes, PPL; (**f**) same as (e) but in XPL. The ashes are altered by phosphatization and are black in XPL. Scale of the photomicrograph is of 1 mm.

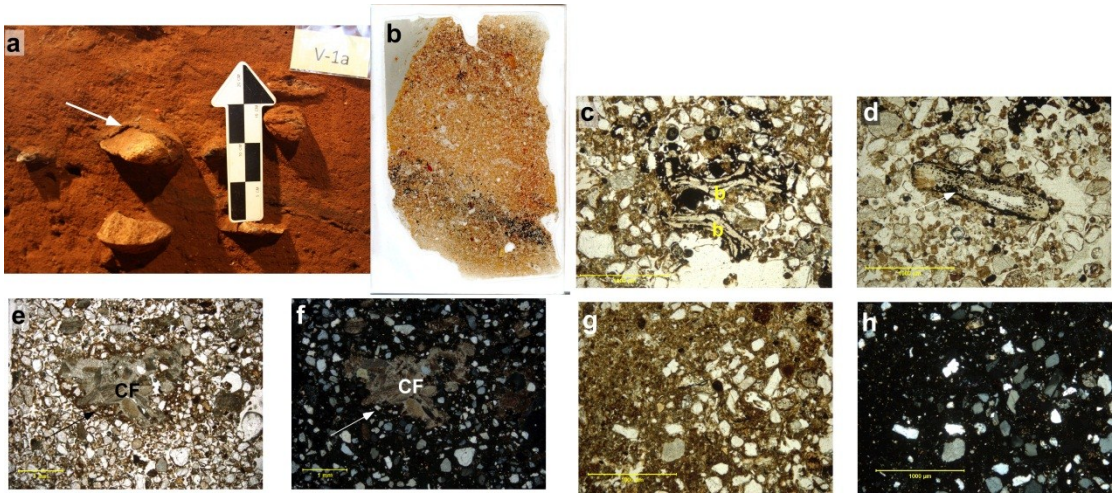

Figure 13: (**a**) Field photograph of profile in Unit V-B, illustrating a phosphatic alteration rim around the roof spall fragments (white arrow). The scale is subdivided into 5 cm increments; (**b**) Macrophotograph of indurated manganese lenses visible toward the bottom of the slide; height of view = 75 cm; (**c**) Photomicrograph view of the manganese lenses staining bone fragments (b), PPL; (**d**) Example of a poorly preserved bone fragment stained by manganese (white arrow), PPL; (**e**) Photomicrograph of roof spall calcarenite fragment (CF) being dissolved and displaying a phosphatic alteration rim (arrow), PPL; (**f**) same as (e) but in XPL where the isotropic nature of the alteration rim is clear, XPL; (**g**) Photomicrograph of

matrix in Unit V-A where the increase in clay fraction (namely when compared with deposits from CEA) is visible. Note also the phosphatized nature of the sediments, PPL; (**h**) same as (g) but in XPL.

Unit V-B (AL V-1a-b, samples 09-37, 09-38, 09-42 - see Table 1 in supplementary material for sample location):

The matrix of the upper part of Unit V-B is reddish brown under the microscope and includes rare, sand-sized rounded bones and common roof spall fragments. The latter are being decalcified (Figure 13e-f), in accordance with field observations of frequent phosphatic reaction rims and calcarenite 'phantoms' in these deposits. Roughly towards the middle of the Unit, stringers and lumps of manganese are present and occasionally coat the coarser components, including bone fragments that exhibit various degrees of weathering (Figure13c-d). Isotropic dusty gray brown grains (possibly coprolites) are scattered throughout in addition to very rare charcoal fragments. On the whole, the deposits are being decalcified, with only localized calcitic domains remaining.

2.8 Discussion of the Site Formation Processes

2.8.1 Sedimentary Sources and Dynamics

The micromorphological analyses shed light into the reconstruction of the sedimentary history at Contrebandiers Cave. The stratigraphic framework varies

according with the location inside the cave and, consequently, the sedimentary sources and dynamics will be discussed individually for each sector of excavation, specifically the CEA, sector V and sector IV.

Central Excavation Area (CEA)

As stated above, the original processes involved in the formation of the lowermost Unit A are related to a marine environment. This is evidenced microscopically by the composition, grain size, textural selection, and sedimentary structures. The same characteristics (e.g., composition and granulometric homogeneity of the sediments), most likely point to an association of this facies with a beach depositional environment and not due to storm surges, for instance, since the latter would impart poorer sorting of the bioclastic sands (Kilfeather et al., 2007). Unit A sediments occur at about 7.5 m above present sea level, in accordance, or slightly above the overall estimates of 5 to 7 m higher sea levels during MIS5e (e.g., Kopp et al., 2009; Rohling et al., 2008). Despite this initial depositional dynamic, micromorphological observations show the incorporation of terrestrial elements into the mineral fraction (bones and coprolites) that would not be compatible with a high energy coastal marine environment, and clearly attest to a local reworking of the deposits after the sea's retreat. Accordingly, the obtained weighted OSL mean age of ~126 ka falls within the lower range of sea-level interval with higher sea level peaks (from ~130 to ~125ka) that precedes the brief fall to near or below present sea level values around 125 ka (Hearty et al., 2007).

Continental sedimentary dynamics prevailed for the succeeding sedimentary sequence. Combined field and micromorphological observations indicate that there was not a substantial change in the *geogenic* sources and style of sedimentation throughout the subsequent sequence (Units B to F). This constancy is expressed by the similar mineral fraction seen in all the Units. In effect, the ubiquitous presence of monocrystalline quartz grains in the silt and sand fraction constitutes a background presence in all the examined slides and can ultimately be associated with two main sources. On one hand, similar shape and size fractions of quartz are observed in the encasing calcareous sandstone (calcarenite). Roof spall is a common process, and it seems to have been a more or less continuous contributor of siliciclastic and carbonated materials into the archaeological deposits. Gravity-driven calcarenite fragments are commonly affected by in situ dissolution of the carbonate content, with the consequent release of the quartz components into the sediments. Thus, this disaggregation encompasses the release of unbleached or partially bleached quartz grains, that is, grains that have not been exposed to sunlight prior to their burial (Jacobs et al. 2011). Since this process is so widespread at Contrebandiers, OSL dating using multi-grain aliquots, with age averaging of quartz grains, results in an overestimation of the sedimentary age, not taking into account the separation of older, unbleached bedrock-driven grains (Schwenninger et al., 2009). In contrast, the single-grain OSL method used at Contrebandiers allows for the separation of bedrock-aged grains and constitutes a cautionary tale for the use of OSL dating aliquots for cave settings where weathering of roof and walls constitutes a significant sedimentary source (Jacobs et al 2011).

Notwithstanding the relevance of roof-spall-derived components, the weathering of the encasing bedrock is insufficient to explain the volume of sediments filling the cave. There is a concomitant contribution of siliciclatic materials derived from allochthonous gravity-driven sources. The presence in thin sections of soil material (pedorelicts), in the shape of rounded to sub-rounded iron and quartz-rich clay aggregates, indicates the reworking of '*Harmri'* soils from areas relatively close to the site. Studies of soil formations in the Témara area confirm the ubiquity of siliciclastic grains in these deposits, interpreted both as aeolian and residual quartz inputs (Bronger and Bruhn-Lobin, 1997). Although the original topography surrounding Contrebandiers Cave has been intensively modified in recent years, one of the few photographic records of the site prior to urbanization shows slope deposits located NW of the cave's entrance (Figure 2a). Thus clay/soil aggregates and quartz grains could have been derived from colluvial processes resulting from erosion of soils around the cave. The constancy of this sedimentary source throughout Units B to F reflects a somewhat continued destabilization of soil profiles during most of MIS 5 (~ 110 to 95 ka), most likely associated with relative retreat of sea level and the onset of changes in vegetation cover and soil formation. Unfortunately, the ubiquitous presence of bioturbation features at Contrebandiers hampers the distinction of the exact gravity-driven process due to obliteration of indicative syn-depositional sedimentary structures (for instance, bedding features and micro scale contacts).

The scarce development of microstructure also denotes a relative continuity in sedimentation processes, related to somewhat rapid accretion rates. A rough estimate of

the sedimentation rate can be attained from the OSL chronology, with a rate of ~2 cm/100 yr obtained for the time span between Units B to E. This fairly rapid sedimentation may have additionally contributed to the relative homogeneity of the deposits. Erosional contacts and periods of relative stabilization are, nonetheless, discernible through micromorphological observations of ephemeral surfaces developed in a temporal scale (e.g., centuries or even decades) that is beyond the scope of the current chronometric dating techniques. In Unit B, mm-thick tabular shaped phosphatic (apatite-rich) weathering crusts are interpreted as byproducts of guano accumulation on short-lived surfaces during periods of non-deposition (Shahack-Gross et al., 2004; Stoops et al., 2010). Micromorphological characteristics of this stratum attest to predominant humid microenvironment, with dripping, clay illuviation and the deposition of manganese rich lenses.

A more widespread period of non-deposition is associated with the cemented calcitic crust of Unit C2. The micromorphological characteristics of these sediments show a stabilization period, with carbonate-rich waters dripping and cementing the silty and sandy substrate. In addition, the colonization by plant vegetation is expressed by common rhizoliths and the globular reworking of the matrix, concomitant with a wet spell calcitic-rich microenvironment in the cavity. The fact that the indurated crust is not formed by pure calcite/flowstone accumulation but contains common quartz grains and bones attests to the fact that this layer formed in an aerated, somewhat open space (Karkanas and Goldberg, 2010). The interpretation of Unit C2 as a short-lived surface stems from the presence of roots, the lack of *lessivage* features in the above Units, and

more importantly, the microstructure of the matrix, which seems to have been transported as aggregates and later cemented. Furthermore, the upper limit of this Unit is subsequently truncated by the deposition of the overlying deposits of Unit D, again implying deposition, cementation, and then erosion. These observations are not in agreement with the interpretation proposed by Niftah (2003).

Unit D has an overall similar geogenic background, with the distinguishable color of these sediments relating to a higher contribution of human organic inputs (discussed below), rather than a substantial change in the geogenic sedimentary dynamics. The OSL chronology established a temporal hiatus of 13 ± 3 Ka between the deposition of Unit D and the beginning of the lowermost Aterian occupations at Contrebandiers (Unit E/F) dated to ~107 ka (Jacobs et al., 2011). This temporal gap is expressed in the field by the sharp, erosional contact between these two lithostratigraphic layers (Figure 9c), with the onset of the Aterian strata in the CEA (Units E/F) associated with a generalized roof fall episode.

Sector V

Thus far, the excavations in sector V have descended only to ~130 cm, and an unknown thickness of deposits is still to be excavated. The exposed sediments were subdivided into two lithostratigraphic Units, both containing stemmed pieces, and, accordingly, associated with Aterian occupations. The presence of combusted materials (burned bones, ashes and charcoals) shows human occupation of this locus of the cave. Under the microscope, the general mineral fraction is similar to that of the deposits in the

CEA described above. However, sector V sediments are distinct in terms of the relatively higher proportion of fine components (increase in the clay fraction), as well as the abundance of roof spall, with the latter being more predominant in Unit V-B. The geogenic sedimentary dynamics in this area of the site continue, thus, to show important contributions from bedrock disaggregation, but are, most importantly, characterized by higher inputs of clay/soil material. These deposits are roughly contemporaneous with the sand-rich Aterian strata from the CEA, with an age of ~107 ± 9 ka. The somewhat concomitant accretion of clayey sediments in sector V and the sandier nature of deposition in the CEA points to distinct sedimentary sources of the geogenic components, with the enrichment of clay/soil material in sector V resulting from sediments directly entering through the roof chimneys located in this area. The lateral variability in grain size is not, consequently, associated with any landscape or climatic change.

Excavation Sector IV

Figure 14 illustrates the connection of the deposits excavated in sector IV and those present in the profile resulting from Roche's excavations. It is clear from this image that the geometry of the Units varies laterally, from the apparently horizontal thicker sediments in the area of Roche's trench to being truncated and eroded in sector IV. It is interesting to note that the profile seen in Roche's trench is often the only profile illustrated in previous publications of Contrebandiers Cave (Bouzouggar, 1997a; Niftah, 2003; Roche and Texier, 1976). The extension of our excavations thus serve as a relevant example of the lateral variability in depositional and postdepositional processes that

characterize cave deposits and serve, in this sense, as a caveat for the necessity of not focusing on a single 'reference' profile but including as much excavations areas as possible.

Understanding the causes of the truncation in sector IV deposits is, however, problematic and not straightforward. There is no bedding evidenced either in the field or at microscopic scales. Although bioturbation by wasps is pervasive here, this alone would not account for the sharp contact or the large (> 2 m wide) depression seen in the geometry of the upper limit of Unit G (Figure 14). The presence of large roof fall blocks can, however, offer some evidence, since the erosion of part of the deposits can potentially be associated with a reconfiguration of the cave's roof in this area. Such reconfiguration would imply that at least part of the roof collapsed, possibly resulting in an opening to the plateau above the cave. This hypothesis could explain the localized erosional environment of already-deposited strata from Unit G, as well as the loss of fines in the southern area with part of these sediments being reworked, at least locally, towards the interior of the cave. The inclination of the top of Unit G towards the back of the cave is in accordance with this possibility, but our excavations were limited and further exposure of these deposits could help to substantiate or disprove this hypothesis. For instance, whereas the environment was mainly erosional in this area, one would expect the presence of higher proportion of fine sediments, possibly showing some bedding, in the unexcavated area just to the east of Roche's trench. In the excavated areas, the deposits vary from extremely cemented in the northern areas of sector IV (~ squares G/H 22-21) to almost clast supported in the concave area towards the south (squares E/F 22-

21). Micromorphological observations show that the sediments in this south concave area are somewhat mixed, with turnover of the deposits (expressed for example by the chitonic to enaulic c/f distribution). This is furthermore shown by the single-grain OSL indeterminate dates obtained for these sediments in the southern area. Jacobs et al. (2011) recorded a wide dispersion of equivalent dose (D_e) rates for sample SC30 taken in square F22, associated with mixing of the grains. Conversely, samples from the Northern area (SC39 and SC37) indicated normal dispersion of grains and dates of 96 ± 8 and 101 ± 9 were, respectively, obtained (Jacobs et al. 2011). We then suggest that the reconfiguration of the cave's roof may have promoted the localized erosion and reworking of Unit G sediments, namely in squares E/F 22-21, through increased water decalcifying the sediments and facilitating their reworking. This evidence indicates that these younger Aterian strata at Contrebandiers are poorly preserved and that an unknown thickness of sediment was eroded. Furthermore, this localized erosion can help explain why no occupations postdating ~95 ka were identified at Contrebandiers thus far, while Aterian occupations dating to ~73 ka are present at nearby sites like El Haroura 2 and El Mnasra (Jacobs et al., 2012b).

The naturally truncated Unit G is unconformably overlain by Upper Paleolithic/Epipaleolithic Iberomaurusian stratum (Unit H), which fills the existent depression. Roche had already noted that the Iberomaurusian occupations at Contrebandiers were present only in localized depressions that he interpreted as anthropic pit structures. However, Roche's observations (see profile drawing in Roche, 1976a) were made in grid rows 20/21, that is, two meters away from our current profiles in

Sector IV where similar features continued to be recorded. If in fact these were pit features, it would encompass strange shapes for human-dug features. In other words, these would constitute at least 3 m elongated pits with asymmetrical limits that change from two adjacent pits in Roche's profile to a large depression in our final profile (Figure 14). In addition to this uncharacteristic geometry, the micromorphological observations not only attest the erosional nature of these features, but also show that the infilling archaeological content associated with Unit H is not in primary position.

Unlike the sand-rich deposits elsewhere in the Cave, Unit H is composed by well sorted, primarily silty deposits with finer matrix present as coatings around the coarser components, as well as abundant calcarenite spall and large roof fall blocks (Figure 14). Such evidence points to a substantial increase of aeolian contributions at this time and fragmentation of the encasing bedrock, presumably related to the onset of drier climatic conditions. It is important to note that both the mineral and the biogenic/anthropic fractions (for example, sand-sized bone fragments and coprolites) have the same type of fine matrix coatings, pointing to similar depositional process for all the distinct inputs. These micromorphological features have been shown to relate to aeolian transport (e.g., Courty et al., 1989; Frébourg et al., 2008), and the fact that these are also present around the anthropic components shows that these have equally been reworked from elsewhere in the cave – most probably, near the cave's entrance toward the north. The Schimdt Equal Area orientation analyses of Unit H clasts shows, in fact, a predominant orientation from North, toward the back of the cave, that is, following the geometry of the underlying depression (Figure 14). This interpretation implies that the Iberomaurusian assemblages

are not here in a primary position, but that this topographic lower area acted as a sedimentary trap during increased aeolian activity. In this regard it is interesting to note that according to Roche the densest concentration of Iberomaurusian remains corresponds to the area where the natural eroded features are present, which would not be expected if these were just refuse pits and the main occupational space was elsewhere in the site. Although chronometric dating of the Iberomaurusian deposits are still ongoing, it is clear that there is a substantial temporal hiatus between the underlying Aterian MSA occupations of Unit G and the deposition of Unit H, with a clear shift in the sedimentary sources and dynamics towards dried climatic conditions observed in association with UP occupations.

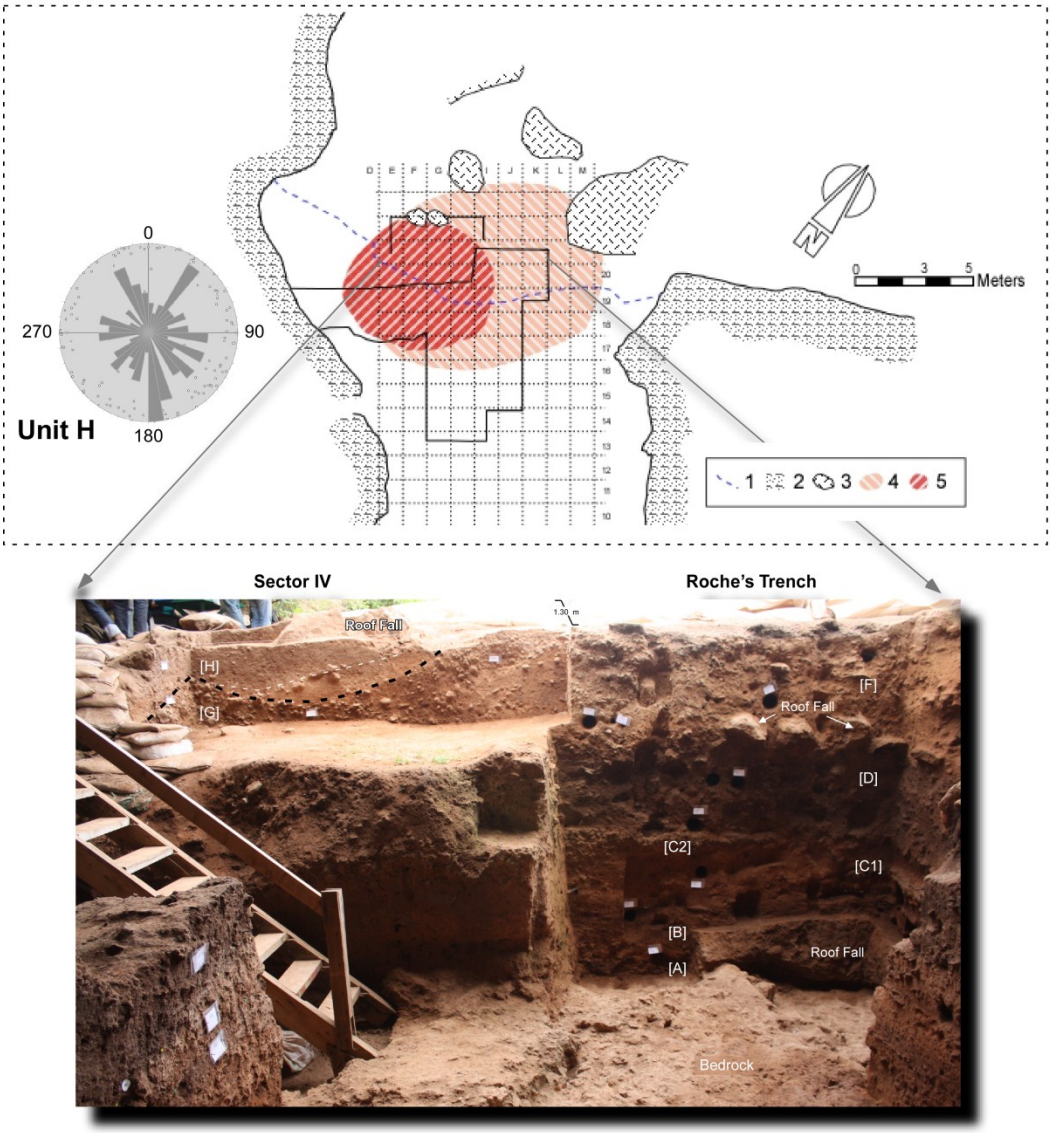

Figure 14: *Top*: Detail of the location of Iberomaurusian in the Contrebandiers Cave grid map. 1: current dripline; 2: Calcarenite bedrock; 3: large roof fall blocks visible in the present surface near the cave's entrance; 4: area with Epipaleolithic (Iberomaurusian) occupations reported by Roche (1976); 5: Area with dense Epipaleolithic occupations reported by Roche (1976). The Schimdt Equal Area diagram (*left*) for Unit H artifacts shows the preferential orientation towards the back of the cave and somewhat less towards North. *Bottom*: Field photograph facing the cave's entrance at the end of field work in 2010. Note the lateral variability between the apparent horizontal stratigraphy in Roche's trench and the truncation visible in our excavation sector IV. The letters in white correspond to the lithostratigraphic Units.

2.8.2 Anthropogenic Formation Processes

Human occupations at the site occur in the deposits just above the marine sands and are expressed by the presence of discrete combustion features, infrequent bone fragments, and lithic artifacts. Nevertheless, a higher contribution of anthropogenic inputs into the sediments is clear only in Unit D, where anthropic remains are more abundant and easily recognizable both in the field and in thin section. The presence of calcitic ashes and charred remains, namely an enrichment of dispersed charcoal microfragments is characteristic of Unit D, and contributed to the darker organic color visible in the field. In thin section, the human inputs of Unit D are often represented by a widespread chaotic jumble of coarse elements, with wood ashes and charcoal fragments constituting a substantial component. The presence of charred material is equally common in Unit V-A in sector V in association with Aterian industries. This is in contrast with the roughly contemporaneous Aterian occupations in the CEA (specifically Units E/F), where no macroscopic or microscopic evidence of ashes was recognizable. However, thin section observations of Unit E show the presence of rare charcoal fragments, and it is interesting to note that data from burned lithics also indicate the presence of similar percentages of burning between Units E and the relatively more anthropic Unit D (see Dibble et al. *Submitted*). Either these charred materials result from reworking from other areas of the site (for instance, from the contemporaneous occupations in the back of the cave), or they encompass the loss of the ash components in this area (e.g., by wind blowing or chemical dissolution). The former is more coherent

with our micromorphological observations, since Unit E has predominantly alkaline conditions conductive to the preservation of wood ashes, and in addition one would expect that even if these conditions were not always predominant, chemically resistant combustion residues (e.g., phytoliths) would still be visible in thin section, which is not the case.

Finally, the presence of unworked pebbles (usually 2 to 10 cm range) of exogenous raw material, namely quartz and quartzite, was noted in most Units at Contrebandiers, both from the renewed excavations as well as from revisiting Roche's collections (Schurmans et al., 2009). The abundance of these materials in association with the fact that they do not present any sign of use (e.g., used as hammer stones) suggests that the incorporation of these pebbles into the archaeological deposits results from natural processes and not due to human action. Their integration in the sediments is an outcome of the weathering of the cave's roof and the intersection of dissolution pockets present in the encasing bedrock, containing these types of clasts (see Figure 1c).

Overall, the density of anthropogenic elements is low in the Contrebandiers sequence, with an average of 109 lithic (objects ≥ 2.5 cm) per cubic meter of excavated sediments, with extremely low densities of 43 lithics per cubic meter in basal Unit B, for instance. These ephemeral densities seen at Contrebandiers seem to correspond to sporadic occupations of the site by human communities, and to a less extent due to high sedimentation rates. Such evidence seems to be in concert with reported feeble archaeological densities in the nearby MSA cave sites in the Témara area (Debénath, 2000; Nespoulet et al., 2008a). Yet the density of lithics computed by Nespoulet et al.

(2008a) for the sites of Dar es-Soltan 1, Dar es-Soltan 2, El Mnasra and El Haroura 2 present even lower numbers, with an average of 36 objects per cubic meter across the sites. While it would be tempting to take such values as representing higher densities of human occupations at Contrebandiers, several caveats must be taken into consideration. The majority of the collections reported by Nespoulet et al., resulted from old excavations that did not employ modern, systematic standards of recording. Selective bias for certain types of stone tools artifacts versus others is also one of the issues of such old excavations. In addition, modern excavation methods – with regular sieving of the exhumed sediments – were not generally applied. These factors disable accurate comparisons from these MSA contexts with Contrebandiers data. Though, the new burst of archaeological research in many of these contexts might enable future extrapolations and comparisons of specific archaeological densities across roughly synchronous occupations. This would allow for a better grasp of human settlement dynamics in this geographical area.

2.8.3 Syn- and Post-depositional Processes

Biogenic syn- and post-depositional processes are frequent at Contrebandiers and are often expressed micromorphologically by the presence of loose aggregated fabric, fecal pellets and increased porosity (in the form of channels and chambers). It is possible to observe that a substantial portion of the bioturbation took place in the past and, at times, it was possibly syn-depositional. This timing is inferred, for example, by the fact

that excremental fabrics and organic matter are commonly assimilated into the mineral fraction and often presenting similar post-depositional cementation as the surrounding sedimentary components. Nonetheless, recent large cm- to dm-sized burrows are abundant in the deposits located in sector V and can be associated with rodents or even larger fauna such as porcupines, which are known for creating extensive holes. In effect, crested porcupine remains have been recovered from this excavation sector (Dibble et al., submitted); among the microfauna assemblages at Contrebandiers, *Gerbillus campestris* is one of the main burrowing rodents identified thus far (Reed and Barr, 2010). In addition, smaller mm- to cm-sized bioturbation by land snails and wasps is pervasive in all Units and wasp cocoons constitute a common feature in many thin sections. These are identifiable in the field and microscopically by the somewhat oval shape with compacted fine matrix along the cocoon walls corresponding to single celled nests (Hasiotis, 2003). Digger wasps (namely *Sphecidae*) built tunnels and shafts that reach variable depths, from shallow 2 – 5 cm to 75 cm deep (O'Neil, 2001). Further bioturbation by earthworms is conversely more accurately identified at micro scales and is expressed by globular reworking of the original sediments under neutral to alkaline pH conditions (Goldberg and Macphail, 2006). At Contrebandiers, earthworm disturbance was identified mainly in Unit D deposits and could have acted syn-depositionally in accordance with the more organic nature of this Unit and the fact that earthworm activity was not observed in the overlying deposits. On the whole, the extensive bioturbation at Contrebandiers contributes significantly to the obliteration of stratigraphic features and/or contacts and played an important role in the fragmentation/scattering of the original sedimentary

constituents. The biogenic mixing does not seem, however, to encompass major reworking from distinct stratigraphic layers. Though it undoubtedly led to a dissociation of the original occupational elements and vertical/horizontal movement of artifacts hampers spatial analysis studies.

In terms of chemical post depositional processes, these are better characterized in thin section. Secondary carbonates were detected in the majority of the observed samples, typically as micritic cementation of the matrix and less commonly as coatings and infillings; the latter are commonly associated with rhizoliths, attesting to plant colonization during periods of accretion stasis (namely during Unit C2 and basal part of Unit D, as discussed above). The main source of carbonates is from water percolation through the calcarenite encasing bedrock. Somewhat continued dripping of carbonate-charged waters produced impregnation and localized cementation of the underlying detrital sediments. In situ dissolution of other carbonate sources in the sediments, such as aragonitic/calcitic mollusks shells or calcareous ashes, played a minor role and these anthropogenic components are generally well-preserved. The lack of substantial speleothem growth or pure travertine accumulations attests to the continued exposure of the cave setting to aerated, open conditions, with continued contributions from exogenous siliciclastic materials entering the site. With the exception of Unit H in sector IV, there is an overarching predominance of carbonate impregnation indicating prevalence of humid, warm climatic conditions during most of the deposition.

Post-depositional dissolution of calcium carbonate results from acid conditions produced by guano accumulations. These resulted in localized alteration of the calcitic

nature of the deposits into phosphatic minerals, namely apatite. This type of diagenesis is more expressive in two areas of the site: on sector V and in restricted areas in the CEA. The stratigraphic units in sector V, namely Unit V-B, express incipient rim alteration of the calcarenite fragments to phosphates. FTIR analyses show that phosphate mineralization pathways are in their primary stages, with the main phosphate being carbonated apatite (dahllite) (Karkanas et al., 2000; Karkanas et al., 2002; Shahack-Gross et al., 2004). Bone dissolution was only rarely observed in thin section. This evidence points to guano, and not the dissolution of bones, as the major source of phosphates, further indicating that pH never reached values below 8.1 (Berna et al., 2004; Shahack-Gross et al., 2004). In the CEA, slumping of the deposits is associated with a putative swallow whole that lead to periodical dislocation of the sediments. The slumping of the deposits in squares G/J 15/14 is also accompanied by localized decalcification of the sediments. This post-depositional process is distinguishable in thin sections from this area (Figure 15) and is related to preferential accumulation of acidic-enriched water along the central axis of the cave. Similarly to the discussed geochemistry in sector V, phosphate mineralization is more incipient in this locus, but equally characterized by phosphate mineralization of dahllite.

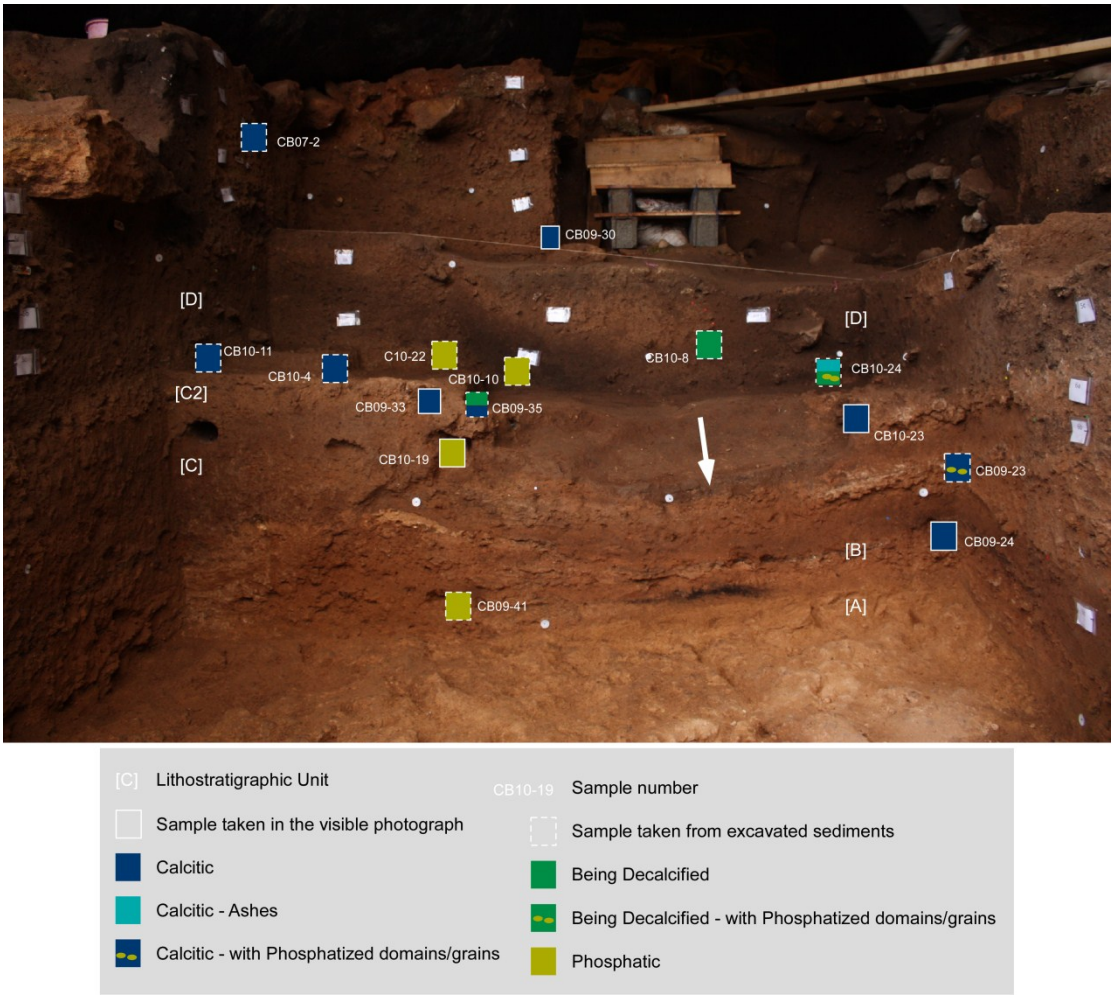

Figure 15: Field photograph of the middle of the CEA at the end of the 2010 excavation season, showing the collected micromorphology samples and their calcitic or phosphatic nature. The arrow (in white) points to dark thin deposits that resulted from modern walking in this area of the site and do not represent in place sediments. Note the calcitic nature of the deposits to the sides and the presence of decalcification in the form of phosphatization in the central area where it is possible to see that the deposits are dipping into.

2. 9 Conclusions

The micromorphology study of site formation processes at Contrebandiers cave sheds light on the sedimentary history of the site and the integrity of the archaeological assemblages. This study shows that most of the MSA sedimentary

deposits at Contrebandiers consist of gravity-derived silts and sands, possibly with some aeolian contributions, mixed with breakdown of the encasing calcarenite bedrock. Anthropogenic inputs are present in the form of bones, shells and lithic artifacts, as well as charred ashes and charcoals, the latter assuming a greater expression in the Mousterian Unit D in the CEA and in the Aterian layers in the back of the cave (sector V). The presence of unworked quartz and quartzite pebbles in all Units is associated with the dissolution and gravity falling of these materials from the calcarenite bedrock, and do not reflect human transport. The lowermost Unit at the site is related to marine deposition. But as discussed above, micromorphological observations show that the sea had already begun to retreat from here and thus these sediments to some extent post-date MIS 5e and are no longer in situ beach deposits. Although there are diagenetic alterations in the form of localized decalcification of the sediments and phosphate accumulations, bone is still preserved and does not seem to have gone through preferential dissolution.

The relevance of establishing the stratigraphic integrity at Contrebandiers Cave is incorporated into the broader discussion on the emergence of anatomical modern humans and modern human behavior in North Africa. At Contrebandiers, the MSA archaeological assemblages are directly connected with *Homo sapiens* remains. Since the archaeological visibility of modern behavioral traits is often associated with the presence or absence of key artifacts (e.g., shell beads, worked bone, or ochre), establishing the stratigraphic provenience and context of such objects is of utmost importance. For the Contrebandiers' MSA assemblages, the sedimentary dynamics did not include major reworking of the deposits, and it is clear that the anthropogenic elements reflect the

occupation inside the cavity and were not reworked from outside contexts (attested, for instance, by the presence of 'fragile' sediments such as ashes, and lack of edge damage in the lithics artifacts). In addition, the relatively high sedimentation rates enable the preservation of the human occupational signatures by rapid burial. However, since biogenic activity is widespread, it is clear that the deposits are not in pristine condition and some degree of vertical and lateral displacement of the artifacts has to be assumed. That such reworking did not include the overall mixing of time-distinct assemblages is indicated by the fact that the contacts between the major lithostratigraphic Units are still discernible and are often sharp. Nonetheless, the slumping of the deposits in the CEA and biogenic reworking has contributed to localize displacing of the original arrangement related to human occupations, making these assemblages unsuitable to spatial analyses studies. Conversely, a higher degree of post-depositional modification is attested in the uppermost Aterian bearing layers in excavation sector IV, which are truncated by natural processes and the infilling Iberomaurusian occupations, are not in place, nor do they seem to represent anthropic dug pits.

Chapter 3: Use of Fire by Modern Humans at Contrebandiers Cave (Morocco): a Micromorphological Perspective

3.1 Abstract

Habitual use of fire is a hallmark of human adaptations and interpreted as a significant technological trait in prehistoric adaptations. Several Middle Stone Age (MSA) contexts show that early modern humans controlled and made extensive use of fire, though the timing of such control or specific related activities remains elusive. Research of North African fire evidence has been sparse. The site of Contrebandiers Cave (Morocco) yields fire-associated sediments and features (e.g., charred remains, ashes and charcoals) that have been the target of recent excavations. The goals of this paper are to provide detailed evidence on aspects relating to pyrotechnology and integrity of the MSA combustion features by combining field observations with micromorphology and FTIR laboratory techniques. Micromorphology observations show that the fires correspond to discrete combustion features incorporating wood and grass ashes, typically resting on charcoal-rich layers. The integrity of the combustion remains is frequently disturbed by burrowing, human actions, and, to a less extent, by weak diagenesis. The microscopic scale of analyses was an essential tool to overcome the bioturbated aspect of the fire remnants and, furthermore, allowed for the identification of features that, macroscopically, could easily be misinterpreted as fire evidence.

3.2 Introduction

Controlled management of fire is a characteristic trait of human behavior, and its use by early humans is often seen as a significant adaptive strategy. Fire may have been exploited for a variety of activities, including heating, illumination, cooking, and protection against predators. Following ethnographic observations, an increased control of fire is often linked with the development of a formal conception of the living space, despite the fact that extracting information on the exact function(s) of fire features has proven to be difficult to attain (Mallol et al., 2007; Sandgathe et al., 2011a; Sandgathe et al., 2011b). Nonetheless, well–preserved hearths most often reflect short-term activities, constituting a valuable insight to behavioral events that are not reachable through the study of artifact assemblages, which often reflect accumulations over hundreds or even thousands of years that were continuously being reworked and subjected to transport (Goldberg, 2008; Goldberg et al., 2009; Wadley et al., 2012).

The recognition of hearths in the archaeological record has been occasionally surrounded by debate (Goldberg et al., 2001; James, 1989; Rolland, 2004). There are several reasons why the contextual interpretation of fire residues (such as charcoal, ash, heat-altered sediments, burned bones, lithics, or shells) is not a straightforward task. On the one hand, combustion episodes in hunter-gatherer communities are often spatially and temporally ephemeral and the sediments associated with them are easily displaced and/or diagenetically altered (Bellomo, 1993, 1994; Cohen-Ofri et al., 2006; Karkanas et al., 2007; Schiegl et al., 1996; Schiegl et al., 2003; Shahack-Gross et al., 1997). For instance, in cave settings the ash components – which in fresh ash are mainly composed of calcite

– can go through several degrees of diagenetic alterations when in contact with guano phosphate-rich waters, and this can ultimately lead to the complete dissolution and loss of the ashes (Courty et al., 1989; Karkanas, 2010; Karkanas et al., 2002; Schiegl et al., 1996; Sergant et al., 2006). Second, there are natural phenomena that superficially resemble burned materials, such as manganese coatings on bones or the natural deposition of apparently rubefied sediments, which may be mistaken as direct evidence of human-made fire (Goldberg et al., 2001; López-González et al., 2006; Marin Arroyo et al., 2008; Shahack-Gross et al., 1997). A further complication is that normal field observations cannot always differentiate preserved hearth versus reworked combusted sediments (Goldberg, 2006; Goldberg et al., 2012; Goldberg et al., 2009; Schiegl et al., 2003; Sergant et al., 2006). In spite of these difficulties, unequivocal identification of anthropogenic fire can be revealed by detailed studies that go beyond the field observations. Such studies can show, for example, the presence of ash or its stable byproducts (e.g., phytoliths); that the embedded or surrounding artifacts and sediments (e.g., bones, lithics, shells or clays) were subject to burning; and whether fire residues are in their primary depositional context or have been reworked. High-resolution soil micromorphology analyses allow an observation of undisturbed sediments at several degrees of magnification and the application of such studies has revealed to be a crucial tool for the understanding of the composition, formation processes and integrity of archaeological fire features (e.g., Goldberg, 2006; Goldberg et al., 2009; Goren-Inbar et al., 2004; Karkanas et al., 2007; Schiegl et al., 1996)

The timing for the emergence of fire use is still controversial, but evidence seems to be present at least by 450 ka in association with *Homo erectus* (e.g., Goldberg et al., 2001; Goren-Inbar et al., 2004; Gowlett, 2006; Rolland, 2004; but see James, 1989), and recently fire remains dating to as far back as 1.0 Ma have been reported for Wonderwerk Cave (South Africa - Berna et al., 2012). Nonetheless, incontrovertible widespread control of fire seems to occur around 300 – 200 ka (James, 1989; Karkanas et al., 2007; Roebroeks and Villa, 2011; Rolland, 2004; but see also Sandgathe et al., 2011a). However, there has not been extensive in-depth investigations on the nature and integrity of fire residues from early North African contexts, unlike research elsewhere, namely in Europe (e.g., Karkanas et al., 2002; Sergant et al., 2006; Théry-Parisot, 2002), or in the Near East (e.g., Berna and Goldberg, 2007; Karkanas et al., 2007; Schiegl et al., 1996). Currently, the evidence for fire use in Morocco has largely been based on brief mentions to the presence of charcoals and burned artifacts in association Middle Stone Age (MSA) occupations in Northern Africa. Such references to use of fire occur, for instance, at the Moroccan sites of Jebel Irhoud, Pigeon Cave (Taforalt), Rhafas, Dar es-Soltan I and II, El Mnasra and Contrebandiers Cave. But clearly more details are needed since North Africa, especially Morocco, has been emerging as one of the crucial areas for understanding early modern humans origins and adaptation strategies before their diaspora out of Africa (e.g., Balter, 2011; Barton et al., 2008; Hublin, 2001). Two types of assemblages, the so-called Mousterian and Aterian, characterize northern Africa MSA.

At Jebel Irhoud (Marrakesh), the Mousterian industries are associated with the presence of apparently well-preserved combustion features from strata dated to at least

160 ka (complete publication of these results is still on-going, McPherron, personal communication, see also Grün and Stringer, 1991; Smith et al., 2007). A bit later in time, and also in association with Mousterian occupations, are fire residues from Rhafas cave (Oujda Mountains) where flat non-structured hearth features have been identified in stratigraphic layers 5 and 6, both interpreted as "living floors" dated to ~85 ka (Mercier et al., 2007; Wengler, 2001). In the area of Témara (south of Rabat), the cave site of Dar es-Soltan I shows a stratigraphic sequence with the presence of several hearth-rich lenses and charcoal associated with Aterian occupations, around 100 – 90 ka (Barton et al., 2009; Debénath, 2000). The nearby site of El Mnasra (Témara, Rabat) equally includes deposits associated with Aterian techno-complexes, and fire residues are expressed in the field as thin lenses of black coloration or whitish-beige, presumably representing charcoal and ash deposits, respectively (Debénath et al., 1986; El Hajraoui, 1993, 2004). However, several thin lenticular features have also been documented in the lower layers at El Mnasra with no direct association to archaeological occupations.

More in-depth study of anthropogenic sediments in Morocco were implemented at Grotte des Pigeons (Taforalt), where soil micromorphological analyses have been applied to the characterization of the composition, types of fuel used and temperatures reached during fire events at the site (Courty et al., 1989). These fire features are mainly in the form of frequent accumulations of light-grey ashy layers associated with Aterian and Upper Paleolithic Iberomaurusian occupations. Combustion residues in the Aterian are characterized by the burning of deciduous, coniferous woods and tree leaves at temperatures averaging 500^{o} C, with a complete combustion of the wooden fuel, as seen

by the paucity of associated charcoals. Courty (1989) also observed that ashes were commonly disorganized and dispersed, possibly due to trampling. Unlike the above Upper Paleolithic evidence - where ash decalcification is common-, the fire residues in the Aterian layers are characterized mainly by calcitic conditions, in layers dated to around ~82 ka (Bouzouggar et al., 2007).

The present paper focuses on in-depth analyses of combustion-associated features from Contrebandiers cave (Témara, Morocco). The site sedimentary sequence yields so-called Mousterian overlain by Aterian occupations, associated with early modern humans fossil remains (Balter, 2011; Roche, 1976b; Roche and Texier, 1976). Fire-derived residues have been exposed from three main stratigraphic layers in distinct areas of the cave, associated with both types of archaeological assemblages. This study focuses on the context, composition and post-depositional processes of combustion related sediments by using an integrative approach that combines field data with laboratory techniques, namely soil micromorphology and Fourier transform infrared spectroscopy (FTIR). These higher-resolution observations allow an understanding of the exact nature of some features initially interpreted as fire residues, as well as the characterization of processes that played a role in the preservation of fire features, their composition and integrity during the occupations at Contrebandiers cave.

3.3 Materials and Methods

3.3.1 The site of Contrebandiers Cave and its stratigraphic framework

Contrebandiers cave is situated 17 km south from Rabat and near the town of Témara in the Atlantic coast of Morocco, in a geographical area where several caves bearing archaeological evidence have been identified (Figure 1). Excavations at Contrebandiers were originally carried out by Roche (from 1955-1957, and from 1967-1976 co-directing with Texier), and subsequently smaller excavations were undertaken by Bouzouggar (Bouzouggar, 1997b). Renewed excavations took place from 2007 – 2010 under the direction of Dibble and Hajraoui (Dibble et al., submitted). The latter excavations have focused on establishing a continuous profile connecting the old excavations trenches dug by Roche in what is now called the Central Excavation Area (designated as CEA from here onwards). In addition, a test pit (Sector V) was located in the back of the cave (Figure 2).

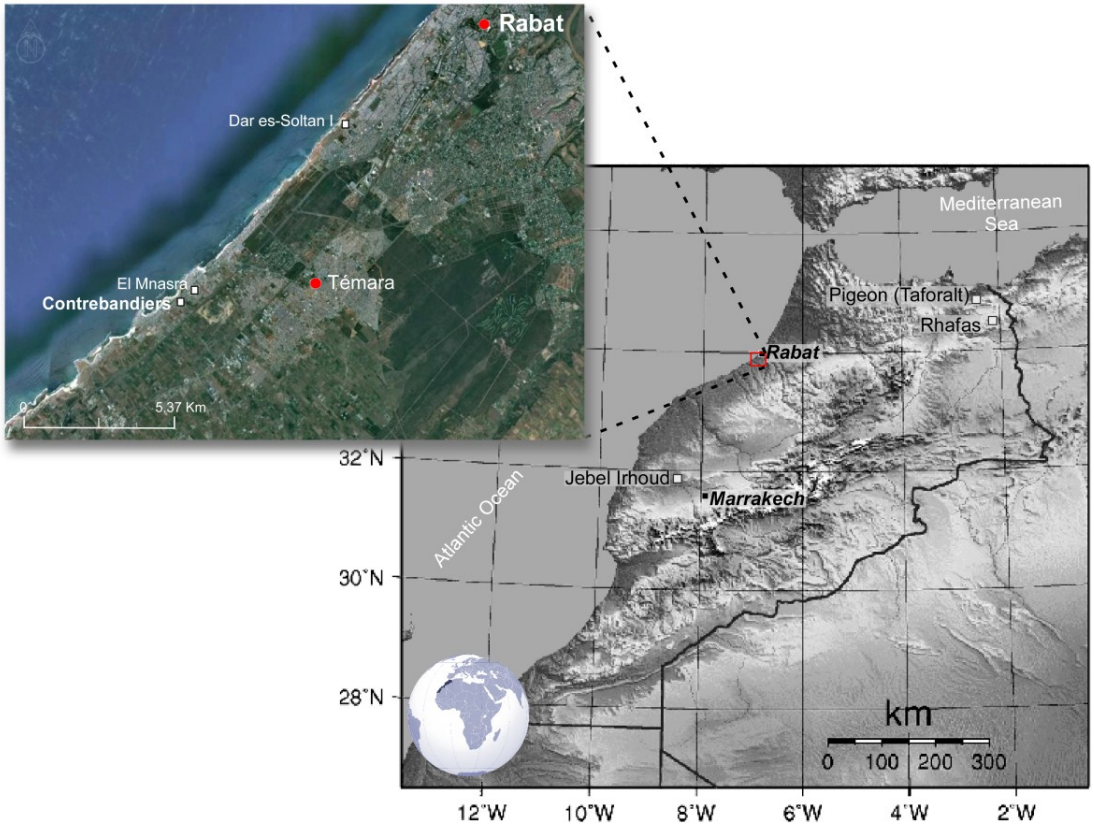

Figure 1: Map of Morocco (*right*) with the location of the archaeological sites mentioned in the text. The map to the top left is an aerial photograph of the area south from the city of Rabat with the location of Contrebandiers Cave and nearby sites.

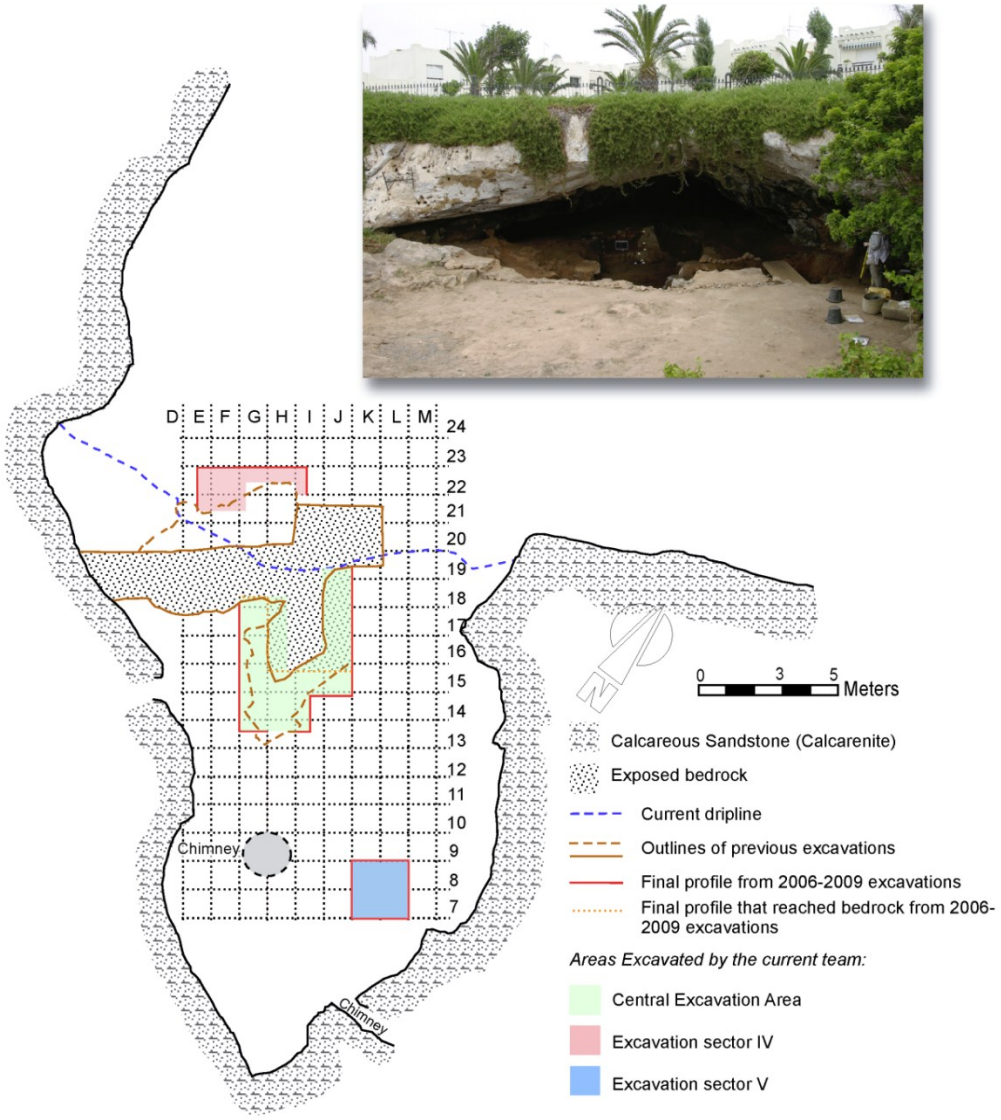

Figure 2: Plan view of Contrebandiers Cave showing the excavation grid and the main sectors of current excavations at the site. On the top right corner is a photograph showing the cave in 2006.

The present-day exposures of Contrebandiers stratigraphic sequence in the CEA show ~3 m thick deposits containing MSA industries, characterized by Aterian overlying Mousterian assemblages. The excavations thus far in sector V have reached roughly 1.30 m in depth, and all the deposits here are associated with Aterian industries. Both the Aterian and Mousterian assemblages are similar in terms of their stone tool types and technology, which is flake based with some use of Levallois technology and a low frequency of retouched tools (Bordes, 1976-77; McBurney, 1975; Wendorf et al., 1993). The main distinguishing elements between these two entities are the presence of stemmed tools and bifacial foliates in the Aterian and their absence in the so-called Mousterian (Caton-Thompson, 1946; Clark, 1993; Debénath, 2000; Hawkins and Kleindienst, 2001; Reygasse, 1921–1922). Nonetheless, the interpretation of these industries as complete separate entities or as part of a single archaeological complex has recently been questioned based on lithic characteristics and chronological overlapping (Dibble et. al. *submitted*). Since this is still an ongoing debate, and for the sake of clarity, in this paper, we maintain the distinction between the layers that contain Aterian versus those with co-called Mousterian industries, although no behavioral interpretation or adaptation shift is necessarily attached to such reference.

Single grain Optical Stimulated Luminescence (OSL) dates of the sediments suggest that the MSA occupations at Contrebandiers started ~122 ka and ended possibly ~96 ka (Jacobs et al., 2011). The CEA sedimentary sequence is divided into six main stratigraphic Units, and these match, for the most part, the sequence identified by Roche (1976). Detailed descriptions of the Lithostratigraphic Units and associated

archaeological context are presented in Dibble et al. (*submitted*). Readers are referred to this source for more details, and a summary description of the Lithostratigraphic Units with their correspondence to the archaeological layers (AL) is available in Figures 3 and 4. The present paper focuses on the Units that are associated with fire remnants, and these constitute Units B and D from the CEA and Unit V-A in sector V.

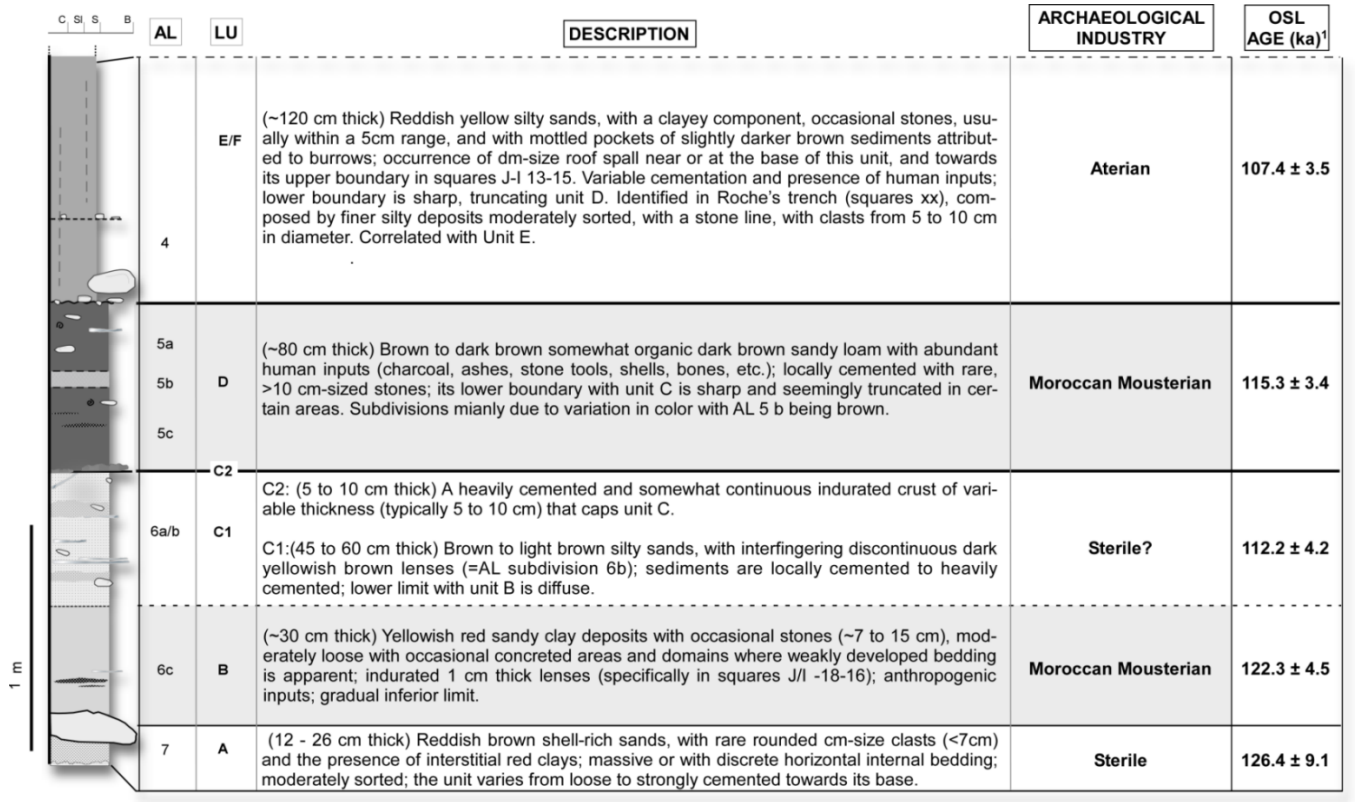

AL	LU	DESCRIPTION	ARCHAEOLOGICAL INDUSTRY	OSL AGE (ka)[1]
4	E/F	(~120 cm thick) Reddish yellow silty sands, with a clayey component, occasional stones, usually within a 5cm range, and with mottled pockets of slightly darker brown sediments attributed to burrows; occurrence of dm-size roof spall near or at the base of this unit, and towards its upper boundary in squares J-I 13-15. Variable cementation and presence of human inputs; lower boundary is sharp, truncating unit D. Identified in Roche's trench (squares xx), composed by finer silty deposits moderately sorted, with a stone line, with clasts from 5 to 10 cm in diameter. Correlated with Unit E.	Aterian	107.4 ± 3.5
5a 5b 5c	D	(~80 cm thick) Brown to dark brown somewhat organic dark brown sandy loam with abundant human inputs (charcoal, ashes, stone tools, shells, bones, etc.); locally cemented with rare, >10 cm-sized stones; its lower boundary with unit C is sharp and seemingly truncated in certain areas. Subdivisions mianly due to variation in color with AL 5 b being brown.	Moroccan Mousterian	115.3 ± 3.4
6a/b	C2 C1	C2: (5 to 10 cm thick) A heavily cemented and somewhat continuous indurated crust of variable thickness (typically 5 to 10 cm) that caps unit C. C1:(45 to 60 cm thick) Brown to light brown silty sands, with interfingering discontinuous dark yellowish brown lenses (=AL subdivision 6b); sediments are locally cemented to heavily cemented; lower limit with unit B is diffuse.	Sterile?	112.2 ± 4.2
6c	B	(~30 cm thick) Yellowish red sandy clay deposits with occasional stones (~7 to 15 cm), moderately loose with occasional concreted areas and domains where weakly developed bedding is apparent; indurated 1 cm thick lenses (specifically in squares J/I -18-16); anthropogenic inputs; gradual inferior limit.	Moroccan Mousterian	122.3 ± 4.5
7	A	(12 - 26 cm thick) Reddish brown shell-rich sands, with rare rounded cm-size clasts (<7cm) and the presence of interstitial red clays; massive or with discrete horizontal internal bedding; moderately sorted; the unit varies from loose to strongly cemented towards its base.	Sterile	126.4 ± 9.1

Figure 3: Stratigraphic description from CEA; (left) schematic stratigraphic column used as reference for the CEA deposits (see Dibble et al., submitted). The width of the columns represents grain size (C clay, SL silt, S sand, and B boulders). The assigned Archaeological Layers (AL), their correspondence with the Lithostratigraphic Units (LU) and single-grain OSL ages are presented alongside with a description of each Unit and the associated archaeological industries. The Units highlighted in grey show the presence of fire residues (charcoal, ashes and/or rubefied sediments) and are the ones being discussed in the present paper. 1 = Weighted mean OSL ages, see Jacobs et al., 2011.

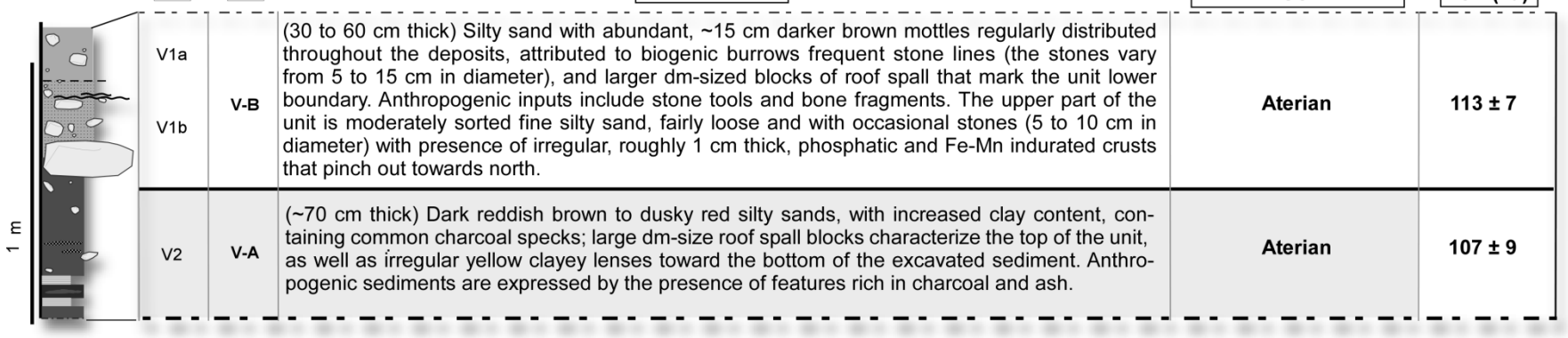

AL	LU	DESCRIPTION	ARCHAEOLOGICAL INDUSTRY	OSL AGE (ka)[1]
V1a V1b	V-B	(30 to 60 cm thick) Silty sand with abundant, ~15 cm darker brown mottles regularly distributed throughout the deposits, attributed to biogenic burrows frequent stone lines (the stones vary from 5 to 15 cm in diameter), and larger dm-sized blocks of roof spall that mark the unit lower boundary. Anthropogenic inputs include stone tools and bone fragments. The upper part of the unit is moderately sorted fine silty sand, fairly loose and with occasional stones (5 to 10 cm in diameter) with presence of irregular, roughly 1 cm thick, phosphatic and Fe-Mn indurated crusts that pinch out towards north.	**Aterian**	**113 ± 7**
V2	V-A	(~70 cm thick) Dark reddish brown to dusky red silty sands, with increased clay content, containing common charcoal specks; large dm-size roof spall blocks characterize the top of the unit, as well as irregular yellow clayey lenses toward the bottom of the excavated sediment. Anthropogenic sediments are expressed by the presence of features rich in charcoal and ash.	**Aterian**	**107 ± 9**

Figure 4: Stratigraphic description from Sector V; (*left)* schematic stratigraphic column used as reference for the CEA deposits (see Dibble et al., submitted) where the width of the columns represents grain size (C clay, SL silt, S sand, and B boulders). The assigned Archaeological Layers (AL), their correspondence with the Lithostratigraphic Units (LU) and single-grain OSL ages are presented alongside with a description of each Unit and the associated archaeological industries. Unit V-A, highlighted in grey, contains fire residues (charcoals, ashes and/or rubefied sediments) and is being discussed in the present paper. [1] = OSL ages, see Jacobs et al., 2011.

3.2.2 Analytical Methods

When combustion related sediments (ashes, charcoal-rich or fire-reddened sediments) were encountered during excavation they were photographed and recorded. In addition, when spatially well-defined fire features were exposed, they were given a unique sequential number in order to keep track of the different combustion residues throughout the sequence. The limits of the combusted residues and all the artifact location were tridimensional recorded using a Total Station (see Dibble et al. *submitted* for details).

Soil micromorphology samples were collected from combustion residues as undisturbed, oriented blocks of sediment from both features visible in the exposed profiles or features encountered during excavation. The integrity and internal arrangement of the deposits was ensured by carefully detaching the blocks or by excavating around the selected sediments, and wrapping them with soft paper or plaster bandages. The blocks were oven-dried in the laboratory at ~60^{o} C for several days and impregnated in a 7:3:1 ratio mixture of unpromoted polyester resin, styrene and catalyzed with Methyl ethyl ketone peroxide (MEKP), respectively. The hardened samples were then cut into thin slabs and prepared into 30 μm thick, 5 x 7.5 cm petrographic thin sections by Spectrum Petrographics (Vancouver, WA, USA). The produced thin sections were examined with a petrographic microscope at several magnifications from 2x to 40x, and described following standardized micromorphological nomenclature (Courty et al., 1989; Stoops, 2003).

Fourier Transform infrared Spectrometry (FTIR) spectra were obtained from samples processed in thin section using a Thermo-Nicolet Continuum IR microscope attached to the spectrometer. Spectra of particles with diameter of about 100 μm were collected either with ATR diamond objective, or with a Reflectocromat 15x objective in Transmission mode. The spectra were collected between 4000 and 450cm-1at 8cm-1 resolution. FTIR spectroscopy is a molecular analytical technique well suited to identify heat-related transformation in materials of different nature such as clay minerals (Berna et al. 2007 and refs. therein) and bone (Berna, 2010). In particular, the structure of kaolinite (FTIR absorption at ca 3695cm-1) is destroyed at ca. 500C while the structure of mica-smectite (FTIR absorption at ca 3620cm-1) at above 700C. Similarly, the bone mineral – namely carbonate-hydroxylapatite – undergoes characteristic recrystallization upon heating. The recrystallization occurs at approximately 500 °C and above, and is appreciable by FTIR spectroscopy via the sharpening of the ν4PO4 (565–630cm−1) and ν3PO4 (1,020–1,100 cm−1) bands. The sharpening caused by high temperature therefore results in the appearance of two characteristic peaks at 630 cm−1 and 1,096 cm−1 that are absent in fresh, archaeological, and fossil bone (Berna, 2010).

These analyses were complemented by powder X-Ray Diffraction (XRD) studies of loose samples. The samples were dried and grinded into a fine powder. This powdered sample was then mounted into a sample holder and analyzed in the laboratory at Earth & Environmental Science (University of Pennsylvania), scanning continuously from 3 °2Θ to 75 °2Θ.

3.4 Results

As mentioned previously, the presence of combustion residues is most abundant in lithostratigraphic units B and D in the CEA and with unit V-A in excavation sector V. The main results will be discussed in stratigraphical order within each excavation area, integrating the observations made in the field with the micromorphological observations and FTIR results when available. A summary of the selected samples, their micromorphological observations, and interpretation is provided in Table 1.

Unit B (= Archaeological Layer 6c) in the CEA

Unit B is characterized by a low visibility of the human occupations, with density of lithics and fauna being relatively sparse throughout the excavated areas. Roche (1976) had already mentioned the presence of combustion residues (‘foyers’) in this layer, but a detailed description of such features was not given. Combustion-associated sediments are visible in the exposed profiles from Roche’s excavations (see Figure 2), expressed by scattered charcoal fragments (typically in the mm-size range) and as laterally discontinuous, discrete, lenses. These lenses often have a stratigraphic arrangement with white sediments (presumably ash) superimposing black deposits and, less frequently, followed by rubefication (fire-reddening) of the underlying sedimentary matrix in features that assume a typical thickness of ≤ 5 cm (Figures 5 and 6a-b, and Table 1). The renewed excavations at the site only exposed sediments of Unit B in squares G–J 19/16, and somewhat discrete combustion features were specifically encountered during excavations of squares J19 and H17 (Figure 6c-d).

Figure 5: Photographs of combustion residues in unit B visible in the exposed profiles dug by Roche in squares K/L 21/19. The central photograph shows the profile and the location of the collected micromorphology samples (depicted in yellow squares). The white numbers in brackets correspond to the lithostratigraphic units. The photos to the right and left are close up of the sampled sediments. 1: Sample CB 09-21, where (1a) corresponds to the photograph in the profile before sampling and (1b) shows the deposits after the sample was detached. Note in both images the presence of bioturbation, namely in (1b) where the brown irregular patches of sediments correspond to burrows (possibly made by wasps); 2: Sample CB 09-25, representing two apparent superimposing hearths; 3: Area of sample CB 09-27 showing the lateral discontinuity of two sampled features.

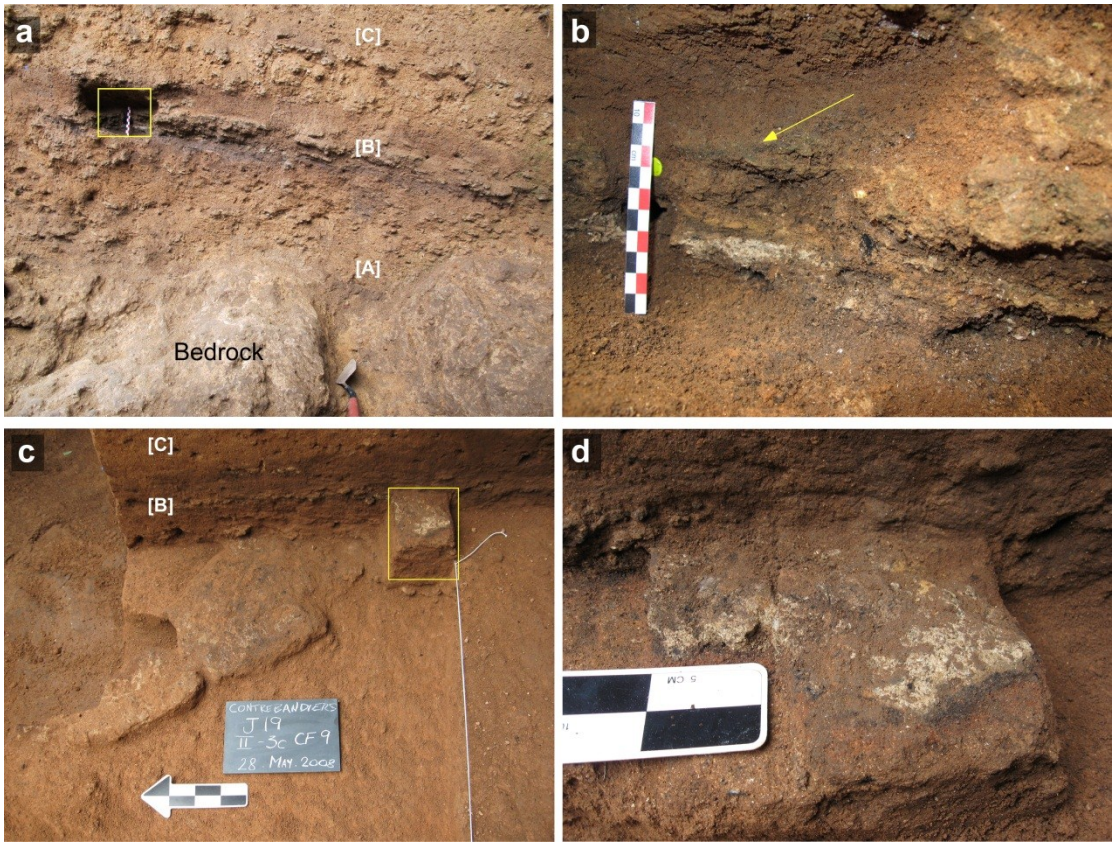

Figure 6: Field photographs of combusting residues in unit B. (a) Photograph showing the darker lenses of sediments within unit B in the exposed profile in square G18. (b) Close up of the area marked with a square in (a) from which sample CB10-2 was collected. Note the combusted remains, namely the white lens of the ashes and its lateral discontinuity. The arrow points to a Fe-Mg rich indurated lens. The scale bars in photographs (a-b) is divided into 1 cm increments. (c) Field photograph of combustion features exposed during excavation in square J19 where it is possible to see the dispersed natures of charcoals (black) and white ashy sediments in the lower feature. To the right is a column left for micromorphology sample CB 08-1. The arrow bar is divided into 5 cm increments and points to the cave's entrance. (d) Detail of area marked by yellow square in (c), showing the microstratigraphic arrangement of burrowed white ashy sediments superimposing black, charcoal-rich lens resting on a rubefied substrate. The scale corresponds to 5 cm subdivisions. The numbers in brackets in (a) and (c) correspond to the lithostratigraphic units.

Micromorphological samples were collected from Roche's trench in squares K/L 21/19 (samples CB09-21, CB09-27, CB09-25), from square G18 (sample CB10-2) and from excavation square J19 (sample CB08-1) in Unit B, targeting areas where combustion residues were apparent. Macroscopically, the sampled deposits frequently seem to represent a series of at least two superimposed hearth remnants, with a somewhat repeated sequence of thin 1 – 2 cm thick whitish sediments, occasionally cemented, overlying darker brown presumably charcoal-rich lenses in an overall lenticular shape that is difficult to trace horizontally over more than a few centimeters. These microstratigraphic combustion sequences are separated by a varying thickness (although usually not thicker than 3 cm) of non-combusted sediments. Biogenic activity is pervasive (namely by insect burrowing), regularly disrupting the integrity of the deposits and contributing to the blurring of the original microstructure and bedding. In effect, the presence of bioturbation results in difficulty in analyzing the samples even under the microscope, since the undisturbed original sediments can correspond to small, even mm-thick, domains surrounded by loosely arranged microfabrics composed by a disorganized burrowed mixture of geogenic (mostly silt- and sand-sized quartz grains) and anthropogenic sediments (mostly scattered charcoals and bones). Such post-depositional disturbance makes microscopic analyzes somewhat challenging and forces one to keep track of the area under analysis in order to ensure that bioturbated areas are not taken as the indicative anthropogenic driven deposits.

Despite this fact, it is still possible to discern microscopically the remnants of fires from Unit B. The ashes are normally calcitic in nature and exhibit some cementation. Although burrowed, the ash component has not been significantly displaced (that is, more than a few centimeters) in samples CB10-2, CB08-1 and in the top feature identified in sample CB09-21 (Figures 7, 9 and 10 a-c). These ashes often incorporate quartz grains, some wooden plant relicts and, more rarely, burned shells and calcined bones (Figures 7 and 10). Underlying charcoal-rich microfacies are also observed in samples CB10-2, CB08-1, and CB09-21a. These three features are interpreted as poorly preserved hearth remnants, with the post-depositional disturbance not resulting in a significant displacement of the fire's microstructure (that is, no more than a few centimeters or less).

Conversely, the cemented ash deposits in sample CB09-27 suffered a more substantial post-depositional reworking (likely after its cementation). Such reworking is expressed by the truncated lower limit of the ash component and its lack of association with burned remains (Figure 8). This microfacies in sample CB 09-27 represents a displaced feature and not remnants of an *in situ* hearth.

Additionally, it was also possible to observe in the thin sections that some remnants that resembled fire residues in the field, correspond in fact to laminated, sometimes finely bedded, stringers of organic matter that resemble a peat type of microfacies (Figures 9 and 10). They do not, however, extend more than a few centimeters in diameter (~ 10 cm), corresponding to spatially restricted lenses intercepted in samples CB09-21b and CB09-27. FTIR results have additionally confirmed that these

sediments do not show signs of burning and have not been subject to high temperatures related to a direct contact with fire (see Supplementary Material). Typically, the observed stringers of organic matter are embedded in a non-calcareous groundmass and are not associated with root penetration or rhizoliths (root castings). The microarrangement of these deposits is typically horizontally bedded, therefore, not expressing vertical growing of plants in the underlying sediments. Instead, based on their fine thickness and lamination, they seem to be associated with grasses or algae showing different degrees of humification or oxidation. The origin of these deposits can tentatively be associated with small puddles forming on the cave's floor at this time.

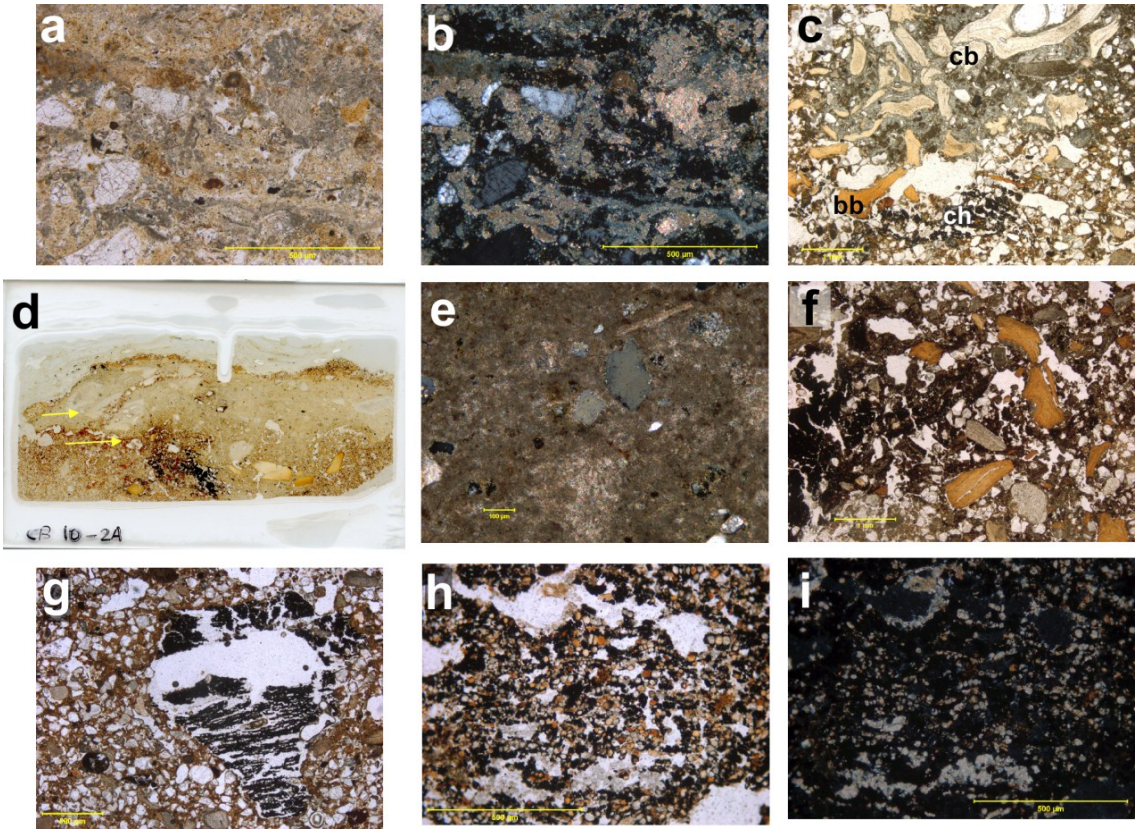

Figure 7: Unit B samples from fire residues; (a) Photomicrograph of ashes from sample CB08-1 (see Figure 6d), PPl; (b) same as (a) but in XPL. Note the fine micritic composition of the ashes and their decalcification in certain domains (expressed in black); (c) Detail of sample fragmented calcined bone (cb), burned bone fragments (bb) and charcoal fragment (ch) in sample CB8-1, PPL; (d) Macrophotograph of sample CB10-2a (see figure 6a-b) where it is visible the white ash sediments, which include calcined bone fragments (arrows), overlying burrowed black charcoal-rich layer (center bottom); (e) Detail of calcareous nature of the ashes in sample CB10-2a, XPL; (f) Photomicrograph of charcoal-rich layer of sample CB10-2, showing charcoal fragments and burned bone fragments, PPL; (g) Photomicrograph of charcoal fragment (partially ground away during manufacturing of the thin section), PPL; (h) Photomicrograph of plant remain in sample CB10-2a, PPL; (i) same as (g) but in XPL.

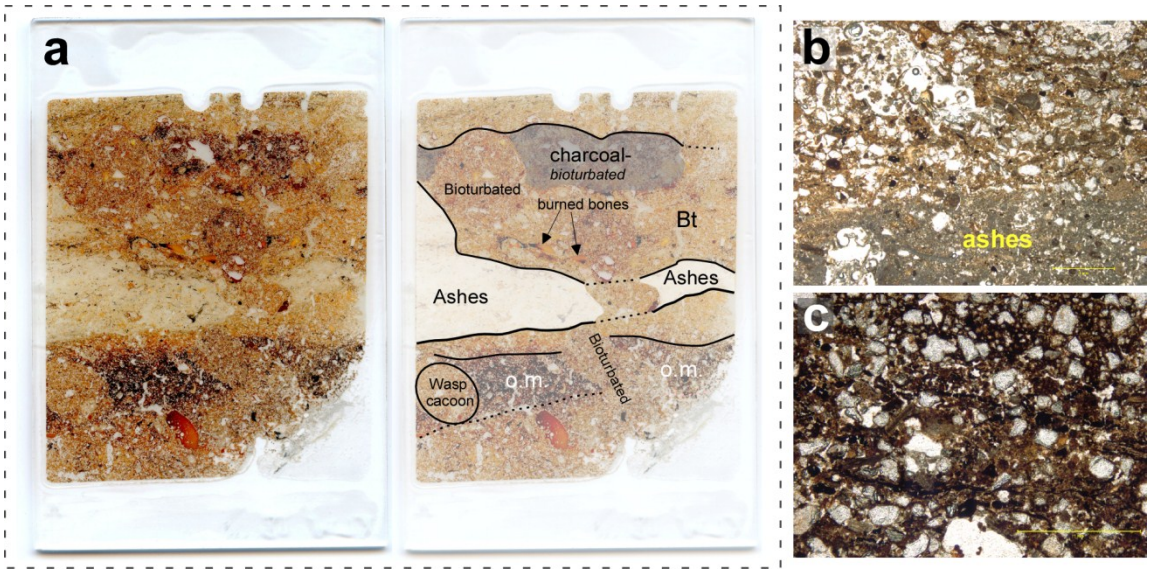

Figure 8: (a) Macrophotograph of sample CB09-27b and to the right is the interpretation of the microfacies. Note the abrupt contact of the ashes. These are not in place and there are not "genetically" associated with the underlying layer that is composed mainly by somewhat bedded stringers of organic matter. The bioturbation of the sediments by wasps is evident and greatly disturbs the deposits. (b) Photomicrograph of the grey sediments associated with calcareous ashes, PPL; (c) Photomicrograph of the stringers of organic matter underlying the ash layers, PPL. The scale in the photomicrographs is of 1 mm.

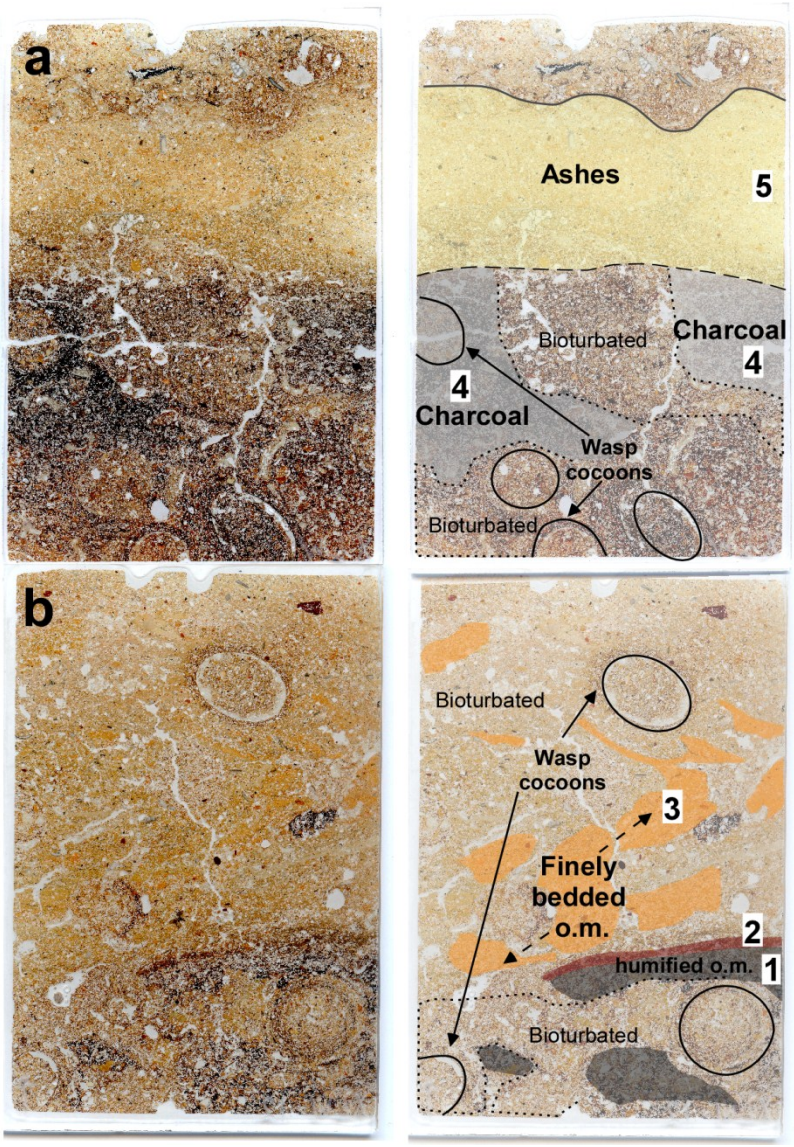

Figure 9: Macrophotographs of thin sections of sample CB09-21. To the right is the correspondent interpretation of the microfacies. The height of view = 7 cm. Overall, these microfabrics correspond to intensively burrowed deposits (mainly by wasps) that corresponds to remnants of a hearth on top (a; microfabrics 5–4) resting on similarly burrowed ~7cm accumulation of finely bedded stringers organic matter. The latter microfrabrics (1–3) vary mainly in terms of the humification or hematite rich organic matter and are uncharred. These are laterally discontinuous in the field (see Figure 5 – 1a and 1b, for field photograph). Microfabrics: [1] finely bedded quartz grains with humified stringers of organic matter; [2] the red clay-rich kaolinite clays (confirmed by FTIR) embedding laminated stringers of organic matter; [3] hematite stained stringer of fine organic matter; [4] charcoal-rich layer; [5] calcareous ashes which incorporate burned remains (bones and shells) and silt- and sand-sized quartz grains.

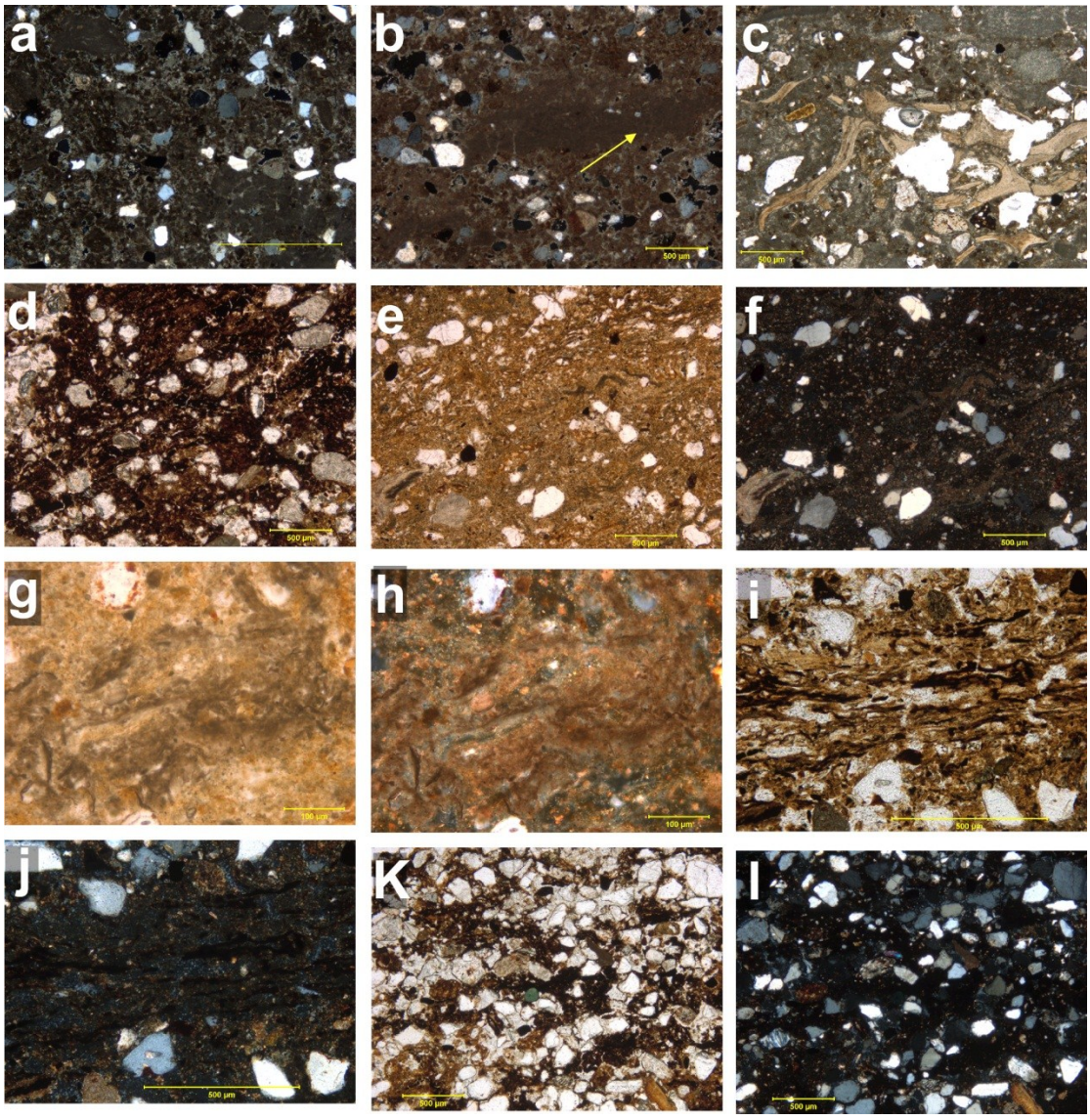

Figure 10: Photomicrographs of samples Cb09-21; (a) View of the calcitic nature of the ashes (microfabric 5) in cross-polarized light (XPL); (b) Detail of the ashes with the preservation in certain domains of plant pseudomorphs (arrow), XPL; (c) Fragmented calcined bone embedded in the ashes, plane-polarized light (PPL); (d) View of the charcoal-rich layer underlying the ashes and corresponding to microfabric 4; FTIR results showed that these deposits have been burned to temperatures above 500^{o} C; PPL (e) View of microfabric 3 where it is visible somewhat dispersed stringers of organic matter with hematite staining (confirmed by FTIR), PPL; (f) same as (e) but in XPL; (g) Detail of stringer of organic matter in microfabric 3 sediments where the cells of the plant material are visible; (h) same as (g) but in XPL; (i) view of microfabric 2 that corresponds to a red lens in thin section composed of finely bedded stringers of plant material and clays, PPL; (j) same as in (i) but in XPL. Note the fine clays embedding the organic matter in this thin lens; (k) View of microfabric 1 corresponding to bedded humified stringers of organic matter and moderately bedding of the quartz grains, PPL; (l) same as (k) but in XPL.

Unit D (AL 5) in the Central Excavation Area (CEA)

Unit D is easily distinguished due to its darker brown sandy silt deposits and the relatively higher frequency of anthropogenic inputs, expressed by lithics, bone fragments, marine shells, ashes and charcoals. The latter are a common anthropogenic component and, in fact, charcoal fragments of cm- and, more frequently, mm-size are regularly scattered throughout, contributing greatly to the darker coloration of this Unit (Figures 3 and 5). Grey-white cemented ashes are commonly dispersed with dimensions that vary from ~ 20 to 5 cm in diameter (Figure 11). Unlike the combustion features present in unit B, the features exposed in unit D do not display a microstratigraphy with identifiable organic-rich lenses underlying the ash component, notwithstanding the fact that charcoals, burned bones or shells are usually present as isolated fragments and scattered throughout. It was possible to observe some variations in terms of the composition, nature, and spatial arrangements of the combusted residues from Unit D both in the field and under the microscope. These can be divided into two main types: (1) *ashy accumulations* and (2) *dispersed fire residues*.

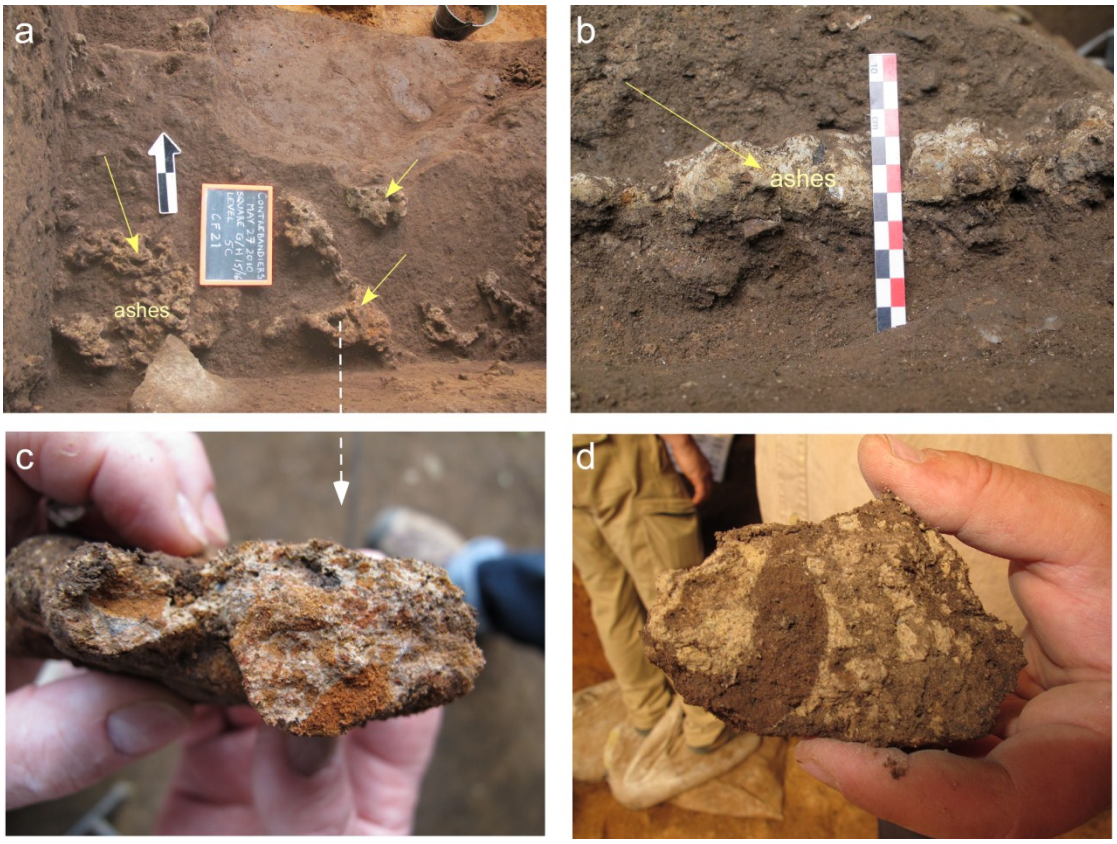

Figure 11: Examples of *Ashy Accumulations* in unit D squares H/I 16. (a) Field photograph showing the dispersed nature of the fire residues (yellow arrows). Note the irregular surfaces of the ashes. The arrows point to the ash chunks; the scale bar is divided into 5 cm increments. (b) Photograph of a combustion feature in profile, where the white layers corresponds to heavily cemented ashes. Scale bar is divided into 1 cm increments; (c) Detail of a piece of ashes with common reddish soil aggregates embedded in the ashes. This piece is a part of one of the ash accumulations seen in (a) and indicated by the white arrow; (d) Detailed photograph showing the degree of bioturbation of some ashes. Note the passage feature with strong brown sediments and the rounded aggregation of the whitish ashy sediments due to biological reworking of the deposits.

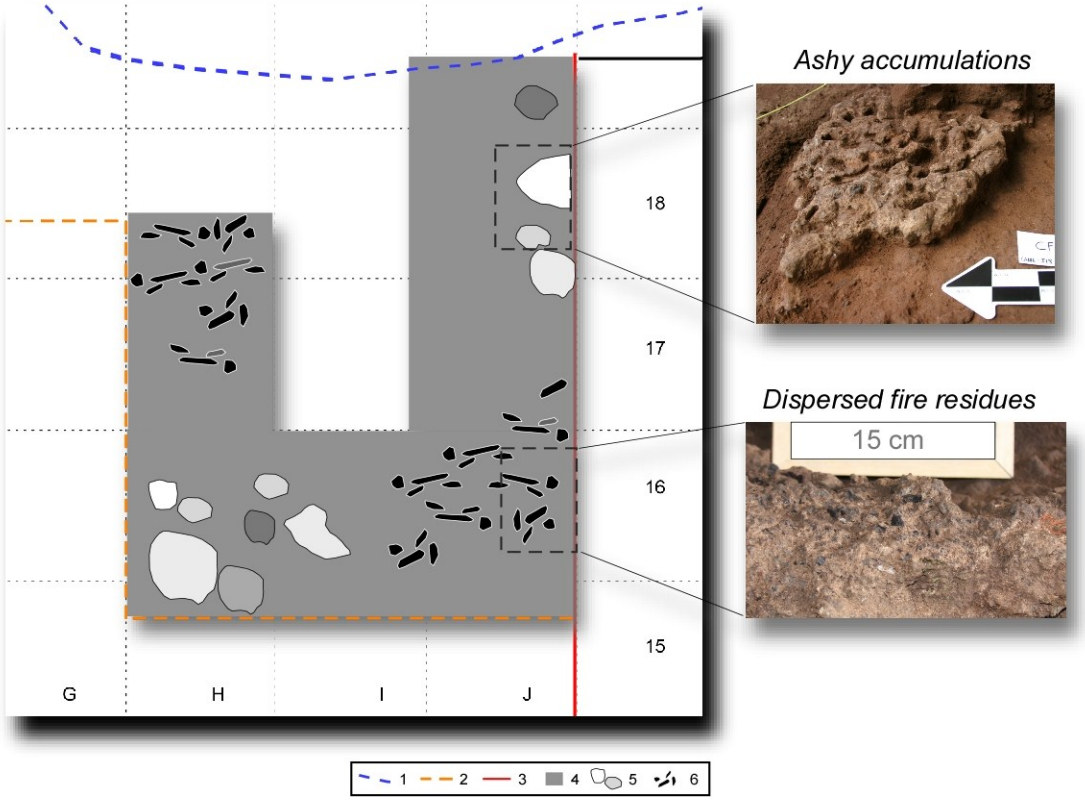

Figure 12: Sketch of the distribution of the two types of combustion residues in unit D within the Contrebandiers site grid. LEGEND 1: current dripline; 2: profile of current excavations that reached bedrock; 3: above profile from recent excavations; 4: rough areas where unit D where excavated; 5: areas where *ashy accumulations* type of residues are found; 6: areas with the *dispersed fire residues*.

Ashy accumulations (*representative samples CB10-18, CB10-12)*: in the excavated areas, ashy accumulations are mainly concentrated in squares H-I 15-16 and J18-19, and are expressed by grey-white usually ~ 2-5 cm thick ashy chunks whose dimensions vary, but are normally ≤ 15 cm in diameter and around 5 cm thick. As seen under the microscope, the main component is micritic calcite, which embeds rare burned remains (usually mm-sized shells and bones) and silt- to sand-sized quartz grains – the

latter are ubiquitous in all the stratigraphic units at Contrebandiers. Microscopically it is possible to observe that the thick ash components have occasional relict calcitic cellular pseudomorphs of wood fragments (Figure 13). These cell pseudomorphs derive from the replacement of wood material by calcite due to burning at temperatures not substantially higher than 500^{o} C (Courty et al., 1989), attesting the use of wood as fuel. The calcitic nature of the ashes indicates minimal chemical diagenesis and that the geochemistry of the sediments did not change substantially (Karkanas, 2010; Schiegl et al., 1996).

In addition, some of the ash accumulations also incorporate common reddish sub-angular sediment aggregates that can reach 2 to 3 cm in diameter and include silt-sized quartz grains (Figures 11 and 13). FTIR results show that these rubefied aggregates have been burned to temperatures above 500^{o} C, as indicated by the absence of Kaolinite clays (see Supplementary Material). The presence of these cm-large baked soil aggregates is somewhat intriguing since they represent the rubefication of sediments that typically underlie fire features and are not a natural component of ashes. The interpretation of these embedded soil aggregates will be discussed in more detail further later in this paper, but overall these ashy accumulations do not seem to represent combustion features preserved in place. The irregular and bioturbated nature of the ashes is also evident not only in the field but microscopically, in the form of passage channels and domains with increased porosity (e.g., Figure 13b), with the degree of bioturbation varing between some features (that is, it is more or less intense in certain domains). It seems clear that a substantial part of the biogenic activity occurred before the cementation of the ashes, as

evidenced by the calcareous cementation of biogenic channels and the irregular surface of these ashy features, implying that these were bioturbated and latter cemented.

It is also important to note that Unit D contains abundant, laterally discontinuous, indurated yellow-grey lenses that originated from geogenic processes: either due to localized dripping of carbonate rich waters on an exposed surface or due to postdepositional cementation with detrital calcite. In some aspects, these natural occurring lenses are similar to the anthropic cemented ashes (e.g., heavy calcitic cementation and lateral discontinuity), but they are distinguishable from the latter in terms of color, composition and by the absence of any associated burned remains (bones, shells, or soil aggregates).

Dispersed fire residues (representative samples CB07-1, CB10-11): consist of areas where remains of charcoals, bones and shells are scattered throughout without a discernible microstratigrahic arrangement. These artifacts often show several degrees of thermal alteration, from burned to non-burned remains (Figure 14c) and are intermixed with thin mm- or smaller size lenses of white sediments that pinch out laterally (Figure 14b and 14e). In thin section, it is possible to observe that these lenses correspond to ashes that have been partially dissolved and recrystallized (Figure 15), with secondary calcium carbonate precipitation within the underlying groundmass and along channels. The original arrangement of the ashes is no longer discernible. The presence of biogenic activity is well expressed, namely the perforation of the sediments by plant roots (Figure 15f), which have contributed to the recrystallization and cementation of the deposits and

suggest that these areas of the site were exposed to sunlight. The dispersed nature of the fire residues is explained by the combined action of biogenic activity and the association of these areas with localized driplines from the cave's roof, which, in turn, facilitating plant growth .

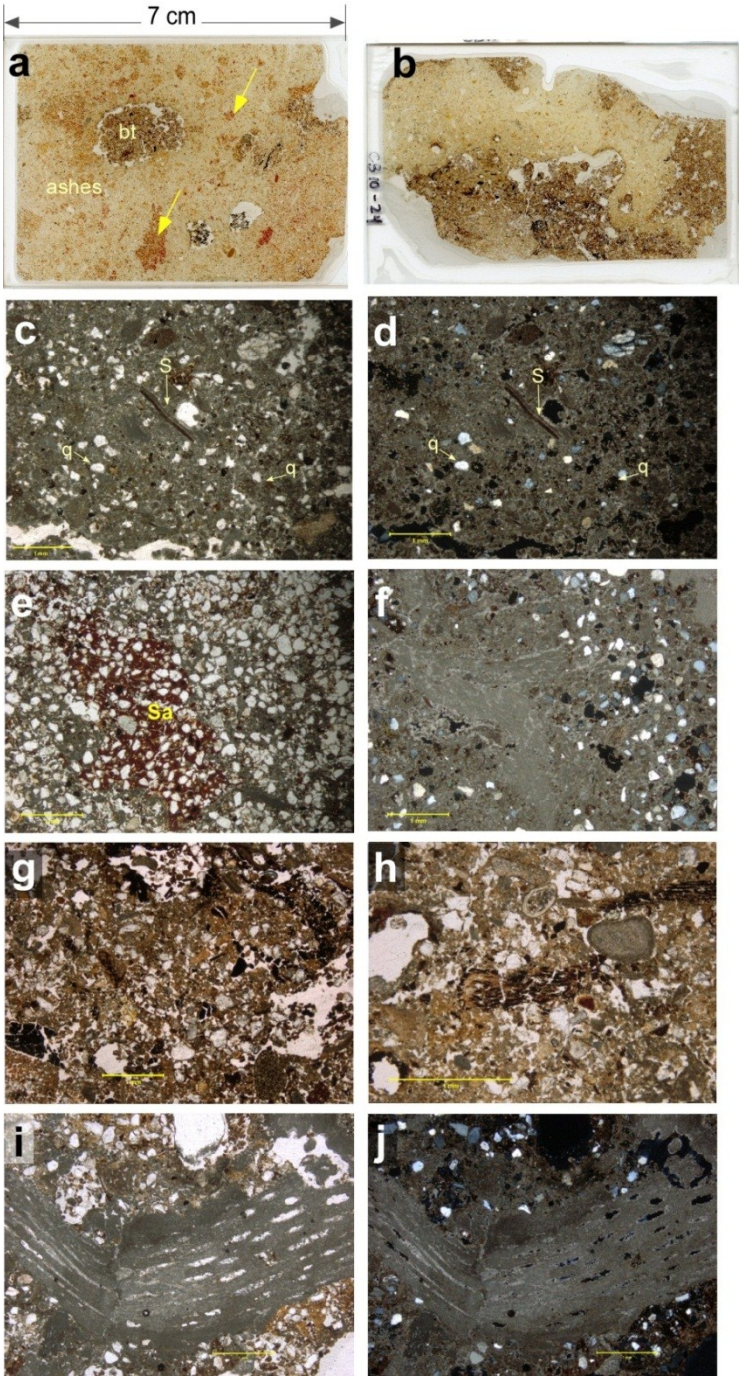

Figure 13: Samples of ashy accumulations in Unit D. (a) Macrophotograph of sample CB10-12, showing thick accumulation of ashes (a) with bioturbated areas (bt) and the incorporation of reddish soil aggregates (arrow), which have been exposed to temperatures ≥500^{o} C; (b) Macrophotograph of sample CB10-24, showing the presence of bioturbated white ashes (top) overlying sediments that are somewhat richer in charcoal fragments; height of view = 5 cm; (c) Photomicrograph of the ash component in sample CB 10-12. Note the presence of quartz grains (q) and burned shell fragments, PPL; (d) Same as (c) but in XPL. Note

the calcitic nature of the ashes; (e) Microphotograph of the inclusion of mm-sized angular red soil aggregate (Sa) within the ashes, PPL; (f) Detail of the preservation of the original laminated nature of the ashes in sample CB 10-12, XPL; (g) Macrophotograph of sediments underlying the ashes in sample CB10-24 where dispersed charcoal fragments are visible. Note the bioturbated nature of the deposits with common porosity, PPL; (h) Detail of charred plant remains in sample CB10-24, PPL; (i) Photomicrograph of cellular calcitic pseudomorphs of a fragmented wood fragment, PPL; (j) same as (i) but in XPL. Note the calcitic nature of the wood cell pseudomorphs derived from the calcitic replacement of the wood material caused by burning. Scale of the photomicrographs is of 1 mm.

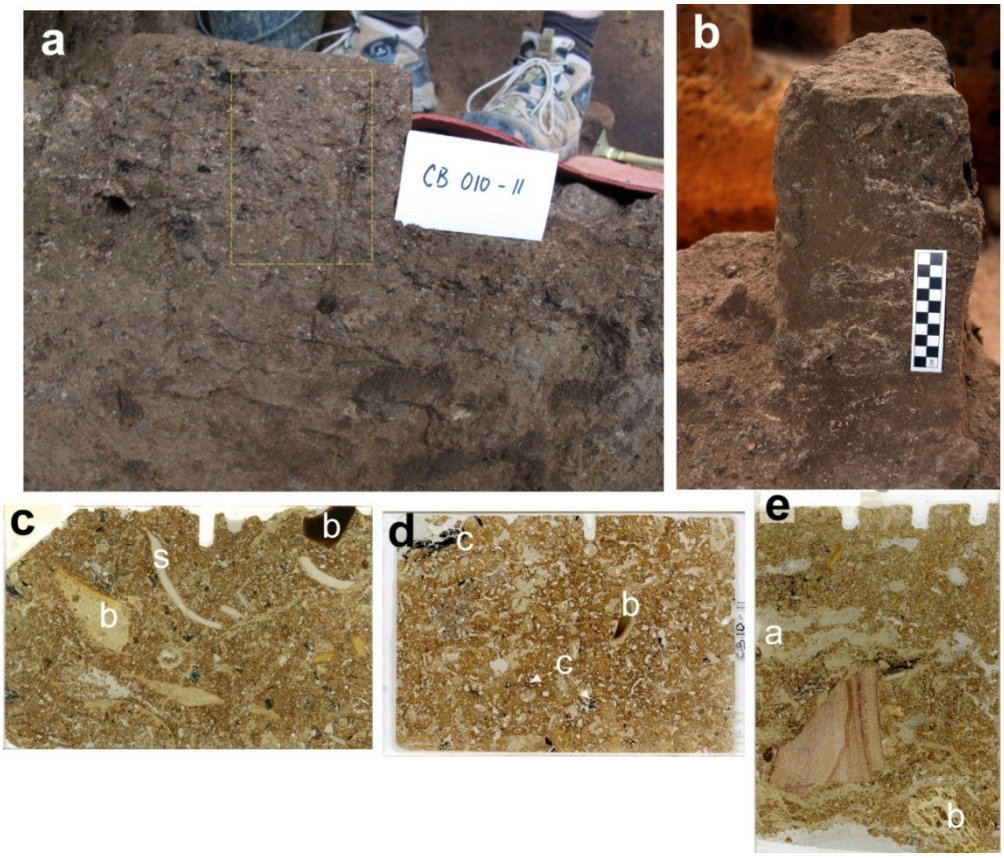

Figure 14: Examples of dispersed fire residues in Unit D. (a) Profile photograph of deposits in square J16 where it is possible to see the dispersion and abundance of black charcoals specks; the white card has a height of 5 cm, and the squared area marks the outlines of sample CB10-11. (b) area of sample CB07-1 in square H18 where combusted deposits are scattered and spread throughout in the form of thin lenses of whitish ash mixed with charcoal fragments; the scale is subdivided into 1 mm increments. (c) Macrophotograph of sample CB07-1a where it is possible to see the presence of cm-sized bones (b) with different degrees of thermal alteration, and shell fragments (s). Note the lack of a distribution or orientation pattern of the anthropic inputs; scale of view is of 5 cm. (d) Macrophotograph of sample CB10-11 with the presence of mainly mm-thick charcoal specks (c) and bones in a cemented matrix; height of view is of 5 cm; (e) Macrophotograph of sample CB07-1c showing the white lenses of ahs (a), bone (b) and an angular fragment of siltstone; height of view = 7 cm.

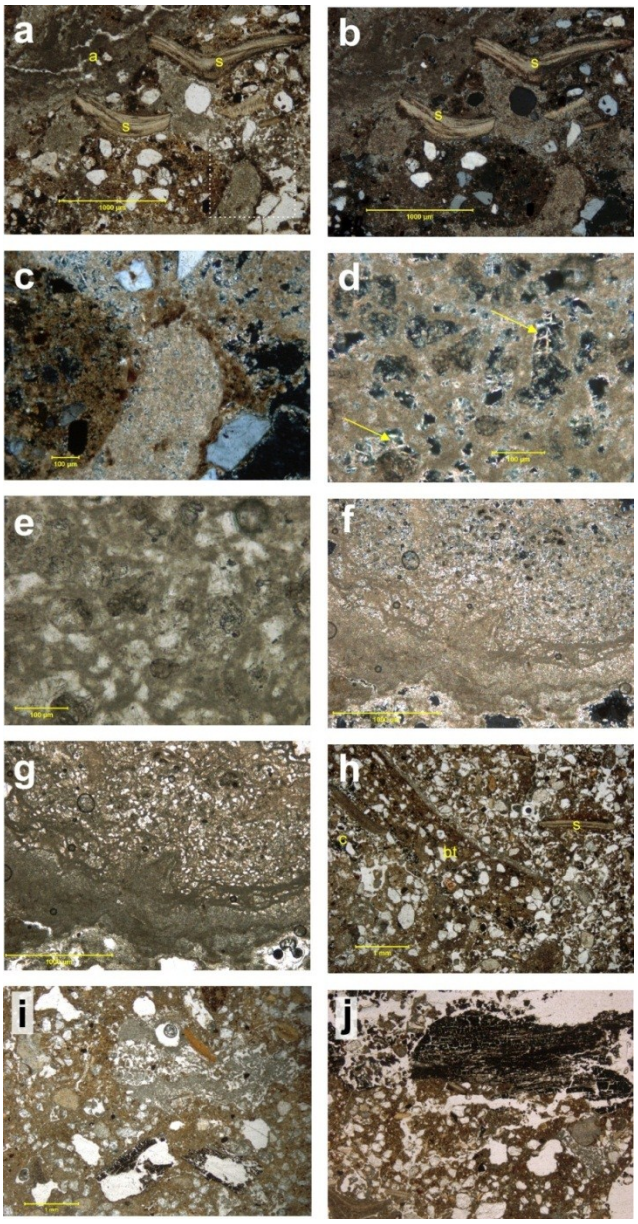

Figure 15: Photomicrographs of dispersed fire residues in Unit D samples CB07-1 and CB10-11. (a) View of ashy lenses (a) in sample CB07-1a with brownish grey color shell fragments (s) that have been altered due to heating, PPL; (b) Same as (a) but in XPL. Note the calcitic nature of the ashes and the secondary calcium carbonate precipitation into the underlying matrix; (c) Detail view of area marked with dotted square in (a) where it is visible the secondary calcitic precipitation into a channel feature, XPL; (d) High magnification view of secondary calcite, showing the recrystallization with needle shape calcite crystals, XPL; (e) Same as (d) but in PPL; (f) Photomicrograph of sample CB07-1c with alveolar structure indicative of a cacified root mat, PPL; (g) Same as (f) but in XPL; (h) View of the matrix in sample CB07-1b with the presence of a reworked wall of a wasp cocoon (bt) and the scaterring of shell (s) and charcoal (c) fragments, PPL; (i) Photomicrograph of ample CB10-11 with calcitic infillings and scattered mm-size

charcoal (partially ground away during manufacturing of the thin section), PPL; (j) Detail of charcoal fragments in sample CB10-11. Note the abundance of porous space (in white) due to biogenic activity, PPL.

Unit V-A (AL V-2) in excavation sector V

In sector V, fire residues occur in the red brown Unit V-A (Figure 4). The base of this unit has not been reached and the sediments excavated thus far contain lithic artifacts (representing an Aterian assemblage), along with bone fragments and other cultural remains that attest to the occupation of this locus of the cave by humans around 110 ka (Jacobs et al., 2011).

In plan view the fire remnants are composed of non-cemented yellowish white lenses of ash superimposing dark brown charcoal-rich layers. Unlike the fire residues from the CEA, which cannot be traced during excavation over more than a few cm (usually 10 or 20 cm), the features exposed in sector V are somewhat more expressive with features reaching 30 to 40 cm in diameter (Figure 16a). Microscopically, the ash component is pale yellow beige in plane-polarized light and mainly black (isotropic) when observed with crossed nickels. The ashes incorporate common silt-sized quartz grains, burned bones, some of which are calcined, that is exposed to temperatures >700^{o} C (Figure 16). In addition, phytoliths, consisting of almost pure amporphous siliceous plant remains, were also observed in association with the ashes. Phytoliths derive mainly from grasses and are present to a less extent in some wodden species (Albert et al., 2000; Courty et al., 1989; Piperno et al., 1999). These plant materials are highly insoluble at neutral to acidic pH values (around 8 or below) and can go through complete or partial

dissolution in prolonged high alkaline conditions (Albert et al., 2003; Cabanes et al., 2011). FTIR and powder XRD analyses from Unit V-A sediments attest to the non-calcarous nature of this lithostratigraphic unit. The deposits are mainly characterized by a phosphatic microenvironment marked by the common presence of dallite in the form of isotropic yellow brown phosphatic matrix and rounded aggregates of pale yellow grains. Such conditions allow for a good preservation of ash-derived phytoliths, and reflect minor diagenesis where the bone component is still expected to be well preserved. Typically underlying the ashy deposits is a darker brown layer composed by common charcoal fragments and bones showing several degrees of burning, but usually below 500^{o} C (Figure 16b). From these microscopic observations, it seems that a substantial part of the fuel used in the features from Sector V represents the burning of grasses, though a more thorough analyses of the type of phytoliths present is still necessary in order to identify these remnants to the species level.

Overall, the fire features of layer V-A are mechanical disturbed by biogenic activity (mainly wasps), which resulted in some mixing of the orignal microstratigraphy. Such burrowing is expressed microscopically by the presence of fecal pellets, passage features and common wasp coccons (Figure 16). In addition, there is a moderate chemical weathering in the form of phosphatization that contributed to the yellowish non-calcitic nature of the ash component. The diagenetic aleration is, however, mild and did not encompass the loss of the organic components.

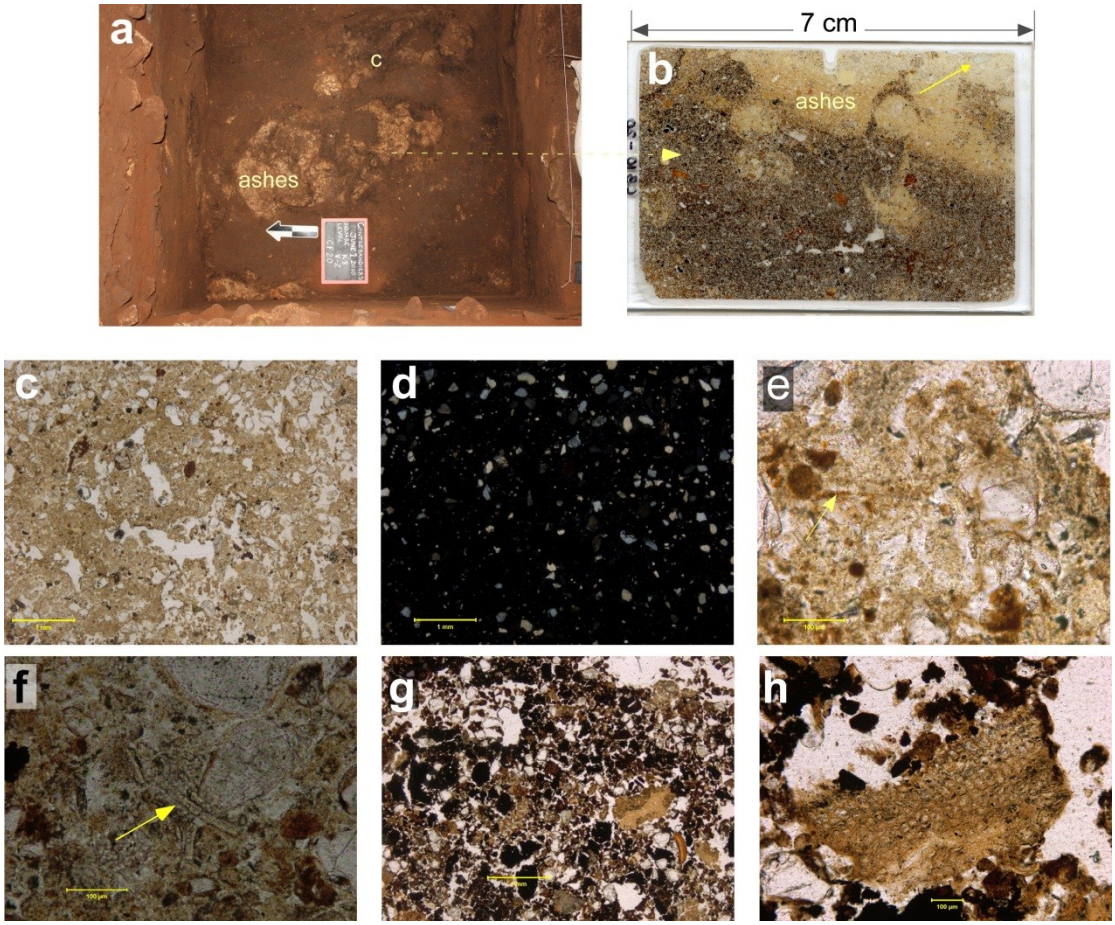

Figure 16: Fire residues from the Aterian Unit V-A. a) Field photograph showing a combustion feature, note the presence of ashes and darker, black charcoal-rich domains [marked c in photograph]; the scale bar is divided into 5 cm increments; b) thin section scan from combustion feature where the whitish ashy layer is visible on the top of the slide; c) microphotograph of the ashes of sample shown in (b) that incorporate silt-size quartz grains, in plane-polarized light (PPL); e) same as (c) but in cross-polarized light (XPL), note the phosphatic nature of the ashes; f) detail of the ashy layer where the presence of phytoliths [p] is visible, in PPL. The scale bars in microphotographs (c) and (e) are 1 mm in length and 100 μm in (f).

3.5 Discussion and Conclusions

Observations at both the macroscopic and microscopic scales allows for a better understanding of fire evidence from Contrebandiers Cave. An underlying characteristic is the burrowed nature of the fire-associated sediments. Bioturbation features are visible in the field and expressive under the microscope, with pervasive traces of biogenic activity linked to insect burrowing (namely wasps) and plant growth observed in the analyzes samples. Insect activity is observed microscopically by increased porosity, passage features, and abundant wasp cocoons, which commonly truncate fire-associated sediments. Post-depositional breakage of bones and shells, as well as the lateral discontinuity of the fire features, are commonly observed as a result. Rhizoliths (calcitic root casts) are visible in the lower sections of Unit D and attest to this area of the cave being colonized by plants and exposed to sunlight. Rooting resulted in the dispersion and mixing seen in the fire residues (ashes, charcoals, and burned remains), and contributed to the secondary precipitation of ash-driven calcium carbonate within the underlying sediments. Other post-depositional modifications visible microscopically are related to moderate diagenetic alteration of the ashes in sector V in the form of phosphatization. In this locus of the cave, micromorphological samples additionally showed the presence of phosphatic minerals (mainly dahllite) and the almost complete decalcification of the sediments associated with Unit V-A (Figure 16). The presence of dahllite attests to mild diagenesis and, as seen in thin section, small cm- and mm-sized bone component are preserved.

Despite the less than ideal degree of preservation, microscopic analysis made it possible to analyze domains of undisturbed fire residues, and this showed that most of the fire-associated features identified in Units B and V-A still preserved a microstratigraphic arrangement with charcoal-rich bases overlain by lenticular ash deposits. Rubefied substrates are less common, though still present as discrete, discontinuous lenses (see samples CB08-1 and CB10-6). This evidence constitutes an indication that there was not a complete reworking of the original sediments and that the degree of movement due to bioturbation was probably in the order of cm or smaller scales of displacement.

When viewed in terms of the overall compositional and internal organization, the fire remnants from Units B and D integrate an ash component that is calcitic in nature, indicating minimal chemical diagenesis and implies that the paleo-chemistry of the associated sediments did not change substantially over time (Courty et al., 1989; Karkanas, 2010). These alkaline conditions are conductive to the preservation of organic components, such as bones, and calcitic wood ashes. Moreover, the preservation of wood pseudomorphs within the calcareous ashes in the CEA attests to the use of wood as the main fuel source. The abundance of charcoal fragments shows that fire-oxidizing conditions were not sufficient for a complete burning of the wooden remains. FTIR analyzes indicate that the majority of the fires reached moderate combustion temperatures around 500^{o} C. Micromorphological observations of combustion features identified in Unit V-A show somewhat significant portions of phytoliths within the decalcified ashes. While a complete study of the species present is still necessary, it seems that some portion of grasses was used as fuel in these fires located in the back of the cave. Different

thermal alterations of coarser components, such as shell and bones fragments, were observed and bones vary from partially charred to, more rarely, completely calcined fragments as attested by FTIR analyses.

Essentially, the fire evidence from Contrebandiers in Units B and V-A consist of ephemeral non-structured, flat combustion features. No type of preparation of the surface prior to the construction of the fires was observed, e.g., creation of depressions to contain the fires or stone arrangements. The alteration of the combustion features is mainly due to mechanical disturbance by soil-associated fauna in these stratigraphic units, with mild diagenesis in Unit V-A. As seen in thin section, the degree of alteration did not completely obliterate the original stratification, and the majority of the observed features reflect in place construction of fire features, though frequently poorly preserved. Conversely, there is a regular dispersion of the combustion remains in Unit D. When preserved, there is a calcareous cementation of the ash components, though dissolution and plant-mitigated alteration of ashes is common in the *dispersed fire residues* seen in this Unit.

One distinctive line of evidence is the presence in Unit D of thick *ashy accumulations*, showing an absence of layering and expressed as somewhat massive accumulations of cemented calcareous ashes containing common burned soil aggregates. Such evidence raises the question of how the usually underlying rubefied matrix comes to integrate the ash component. Bioturbation cannot be the process involved in the incorporation of rubefied soil aggregates into the ashes, as one would expect that other fire remnants (such as charcoals and burned bones or shells) would equally be reworked.

As seen in thin section, this is not the case. The ashes almost exclusively include rubefied soil aggregates that are not integrated in bioturbated domains – for instance, they are not associated with channels or increased porosity. In this sense, the burned soil elements do not seem to result from biological processes or trampling by humans or animals, and FTIR analyses show that these aggregates have been burned to temperatures above 500^{o} C. Another possibility to consider is that these features represent some type of raking out activity by past human populations. The raking out of hearth-associated sediments implies the removal of the material from its original location and its dumping in another locus or loci of the site. Similar activities have been identified in the archaeological record, for instance at Kebara Cave in Israel (Bar-Yosef and Meignen, 2007). Nonetheless, at Kebara cleaning activities resulted in a substantial accumulation of dumped ashes, reaching about 90 cm thick in the back of the cave. This is not the case at Contrebandiers Cave, although it can be argued that the sporadic and ephemeral construction of fires at Contrebandiers substantially differs from the intensive use of fire seen in Kebara (Albert et al., 2000; Bar-Yosef and Meignen, 2007; Meignen et al., 1989). In other words, there were not enough ashes to be remobilized in the first place. Experimental studies on the transformation of hearths by human-related activities have shown that pieces of rubefied material may be incorporated into the ashes resulting from dumping actions (Miller et al., 2010). Since no natural process seems to explain the somewhat thick, massive ashes embedding rubefied soil aggregates visible in Unit D, our working hypothesis is that these accumulation resulted from some type of human action, such as the clearing out of previously constructed hearths, remobilizing the ash and

rubefied substrate with it (see also Binford, 1078). In fact, although combusted remains are common in Unit D, none of the analyzed features represents intact hearths, and some degree of displacement may be due to human actions.

Finally, micromorphological observations also allowed for the differentiation of sediments that initially appeared to correspond to fire features in Unit B. Microscopically it is clear that these laterally discontinuous deposits do not correspond to byproducts of combustion episodes, reflecting instead natural deposition of stringers of more or less humified organic matter in low-energy features. The genesis of these features points to the effect of dripping from the cave's roof and formation of spatially restricted puddles. Effects of runoff were not discernible, but several lines of evidence attest to humid conditions at the site during the deposition of Unit D. It is expected that such features are not unique to the sampled areas, and similar sediments may be present in the unexcavated deposits. This underlines the difficulty of interpreting potential fire features based solely on field observations and stresses the necessity for higher degrees of analyses, such as those attainable through soil micromorphology techniques.

Overall, the evidence at Contrebandiers Cave show that fires were present in the cave during the Mousterian occupations around 122 and 115 ka (Units B and D, respectively), and in association with Aterian assemblages at ~107 ka (Unit V-A). Albeit not being rare features, combustion-driven residues do not contribute substantially to the bulk of the sedimentation at the site. In some archaeological contexts, the ash components can be quite substantial (Goldberg et al., 2009; Meignen et al., 1989; Schiegl et al., 1996). For instance, at the MSA site of Sibudu (South Africa) deposition is largely anthropogenic,

and micromorphological studies have shown an array of activities developed by the human occupants, including construction of fires, bedding, and possible use of cemented ashes as work surfaces for manipulation of ochre (Goldberg et al., 2009; Wadley, 2010; Wadley et al., 2012). Fire manipulation for heat treatment of silcrete stone tools has also been attested at Pinnacle point (South Africa) as early as ~164 ka, and it has been argued that such treatment would demand a sophisticated control of pyrotechnology by early modern human populations (Brown et al., 2009). It is somewhat incontrovertible that early modern humans used fire as part of their adaptation repertoire. Yet, the lack of in-depth studies has somewhat hampered our interpretations on the extent and ways in which fire may have been relevant to modern human adaptations in North Africa, and Morocco in particular. For the moment, there is no evidence of preparation, structuring of hearths or burning of bedding for North African contexts. From a standpoint of stone tools (e.g., McBrearty and Brooks, 2000; Nespoulet et al., 2008b), human fossil record (Hublin, 1993; Hublin, 2001), and use of adornments (Bouzouggar et al., 2007; d'Errico et al., 2009), Morocco has been emerging as one of the crucial areas for understanding early modern human behaviors and innovative adaptation strategies. Consequently, a new burst of research is today visible in Moroccan contexts, though additional research is still required if we want to capture variability in behaviors in H. sapiens throughout Africa.

We have shown here that Contrebandiers Cave has evidence attesting to habitual use of fire in association with the main MSA occupations at the site. However, these occupations seem to be relatively ephemeral with the analyzed hearths consisting of non-structured discrete features. The degree of post-depositional modification, namely by

biogenic activity, hampers the study of potential structuring of activities around such features, namely from the perspective of the distribution of artifactual remains. The employed of a microscopic scale of analyzes was, however, fundamental for circumventing the bioturbated nature of fire remnants, as well as for characterizing the composition and integrity of combustion features at Contrebandiers. In order to achieve a better grasp of the role of fire and associated-activities in early modern human contexts throughout North African, similar systematic micromorphological analysis from well-preserved stratigraphic contexts will be necessary.

Chapter 4: Evidence for Neandertal use of fire at Roc de Marsal (France)

Published in Journal of Archaeological Science (in press)

Vera Aldeias [a*], Paul Goldberg [b,c], Dennis Sandgathe [d,e], Francesco Berna [b], Harold L. Dibble [e,f,g], Shannon P. McPherron [f], Alain Turq [h], and Zeljko Rezek [e]

[a] *Department of Earth and Environmental Sciences, University of Pennsylvania, Hayden Hall 240 South 33rd Street, Philadelphia, PA 19104, USA*
[b] *Department of Archaeology, 675 Commonwealth Ave., Boston University, Boston, MA 02215, USA*
[c] Institute for Archaeological Sciences, Universität Tübingen,, Rümelinstrasse 23, 72070 Tübingen, Germany
[d] Department of Archaeology and Human Evolutionary Studies Program, 8888 University Drive, Simon Fraser University, Burnaby, BC V5A-1S6, Canada
[e] *Department of Anthropology, University of Pennsylvania, 3260 South Street, Philadelphia, PA 19104, USA*
[f] *Department of Human Evolution, Max Planck Institute for Evolutionary Studies, Deutscher Platz 6, Leipzig D-04103, Germany*
[g] *Institute of Human Origins, School of Human Evolution and Social Change, Arizona State University, Box 874101, Tempe, AZ 85282-4101, USA*
[h] Museé National de Préhistoire, Les Eyzies 24200, France

* Corresponding author.

E-mail address: valdeias@sas.upenn.edu (V. Aldeias).

Highlights

>We present data on hearths from the Middle Paleolithic site of Roc de Marsal >We applied field observations, soil micromorphology and GIS techniques >We demonstrate the well-preserved and in place nature of the hearths >No spatial organization pattern was detected > The contemporaneity between features and/or artifacts is difficult to establish

4.1 Abstract

The association of Neandertal occupations with fire has been reported for several European late Middle Paleolithic sites. Renewed excavations at the French site of Roc de Marsal (Dordogne) have exposed a series of well-preserved fire features associated with artifact-rich Neandertal occupations. This paper provides detailed descriptions of the combustion sediments and associated archaeological assemblages, using field observations and laboratory methods, including soil micromorphology, FTIR, and GIS techniques. From an integrity point of view, the available data demonstrate the excellent preservation of the hearths at Roc de Marsal, which display minimal or no post-depositional movement. However, our results suggest that it is often impossible to access the level of contemporaneity between different combustion events, the absence of association between burned objects and the hearths, and that it is often very difficult to distinguish distinct fire events based solely on macroscopic observations. These problems have significant implications for how such features are excavated and analyzed.

KEYWORDS: Roc de Marsal, Mousterian, Combustion Features, Micromorphology, Spatial analyzes, Geographical Information Systems, Fire

4.2 Introduction

The development of controlled use of fire must be seen as one of the most important developments in prehistory. Currently there is significant debate over what constitutes the earliest evidence for controlled use of fire, although there appears to be incontrovertible evidence by at least 250 ka (e.g., Mercier et al., 2007; Roebroeks and Villa, 2011). However, even after 250 ka fire-use appears to have remained intermittent, at least in Europe, until perhaps the Upper Paleolithic (Sandgathe et al., 2011a; Sandgathe et al., 2011b). And while fire presents a range of potential functions (e.g., cooking food, providing light, providing warmth, heat treatment of lithics, etc.), it has proven difficult to determine exactly its applications during the Paleolithic (Sandgathe et al., 2011a). It is true, however, that detailed studies of fire residues are rare, though more recently several examples illustrate where they have been studied more closely with regard to spatial organization (e.g., Galanidou, 2000; Henry et al., 2012; Henry et al., 2004;Vallverdú et al., 2012; Vaquero and Pastó, 2001) and internal composition and structure (e.g., Baquedano et al., 2004; Berna and Goldberg, 2008; Dibble et al., 2009; Goldberg et al., in press; Goldberg et al., 2009; Gómez et al., 2010; Schiegl et al., 1996; Schiegl et al., 2004; Texier et al., 2010). The aim of this paper is to provide detailed data on combustion features uncovered during recent excavations at the French Neandertal site Roc de Marsal. These include (1) high resolution micromorphological data on the nature and variation in composition of combustion features and on their internal organization and structure; (2) basic data on their vertical and spatial distribution, and variation in size and shape. The high-resolution micromorphological data can be evaluated in order to understand some aspects of Neandertal pyrotechnology: types of combustibles used,

hearth integrity, or temperatures attained. In addition, data are presented on the spatial distribution of these features and associated artifacts in an attempt to reconstruct patterns of site use.

4.3. The Site of Roc de Marsal

Roc de Marsal is a small cave that developed along a fissure in Cenonian limestone. The south-facing cave is situated 80 m above a small tributary valley of the Vézère River, approximately 5 km southwest of Les Eyzies (Figure 1). Early excavations at the site were carried out by amateur archaeologist, Jean Lafille, from 1953 until 1971 (Bordes and Lafille, 1962; Sandgathe et al., 2011c; Turq, 1979). New excavations by the authors took place from 2004 through 2010 (Turq et al., 2008).

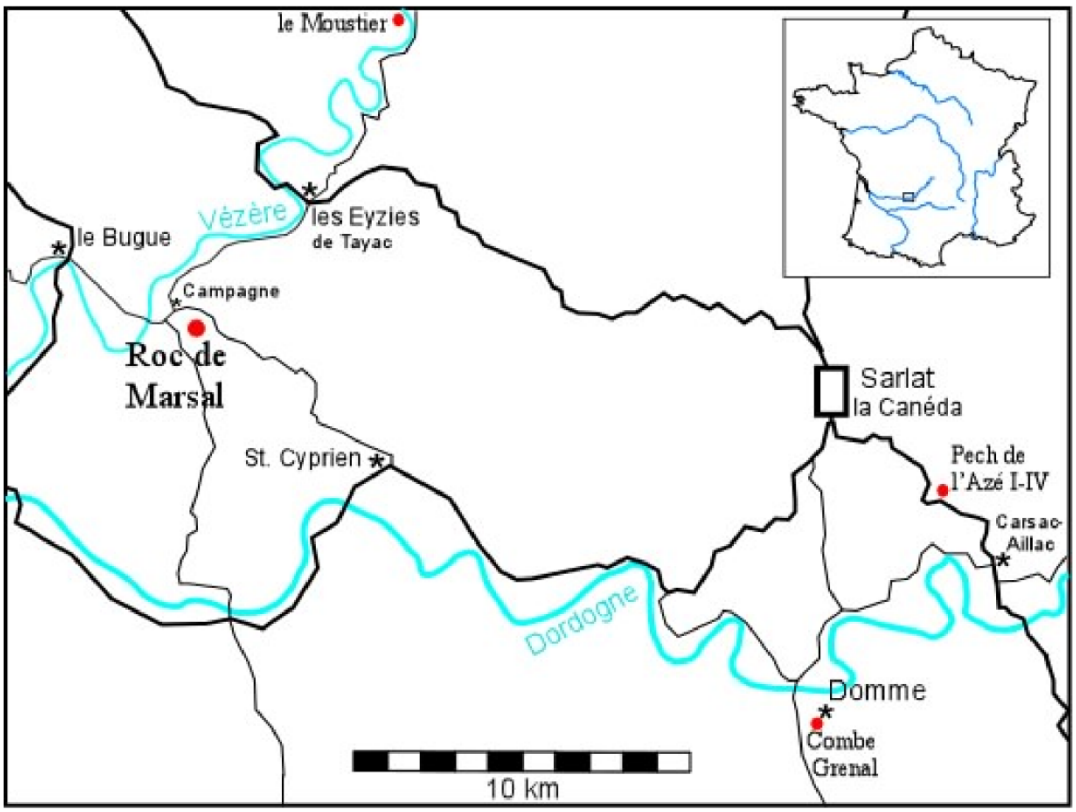

Figure 1: Map showing the location of Roc de Marsal in relation to other Middle Paleolithic sites in the vicinity.

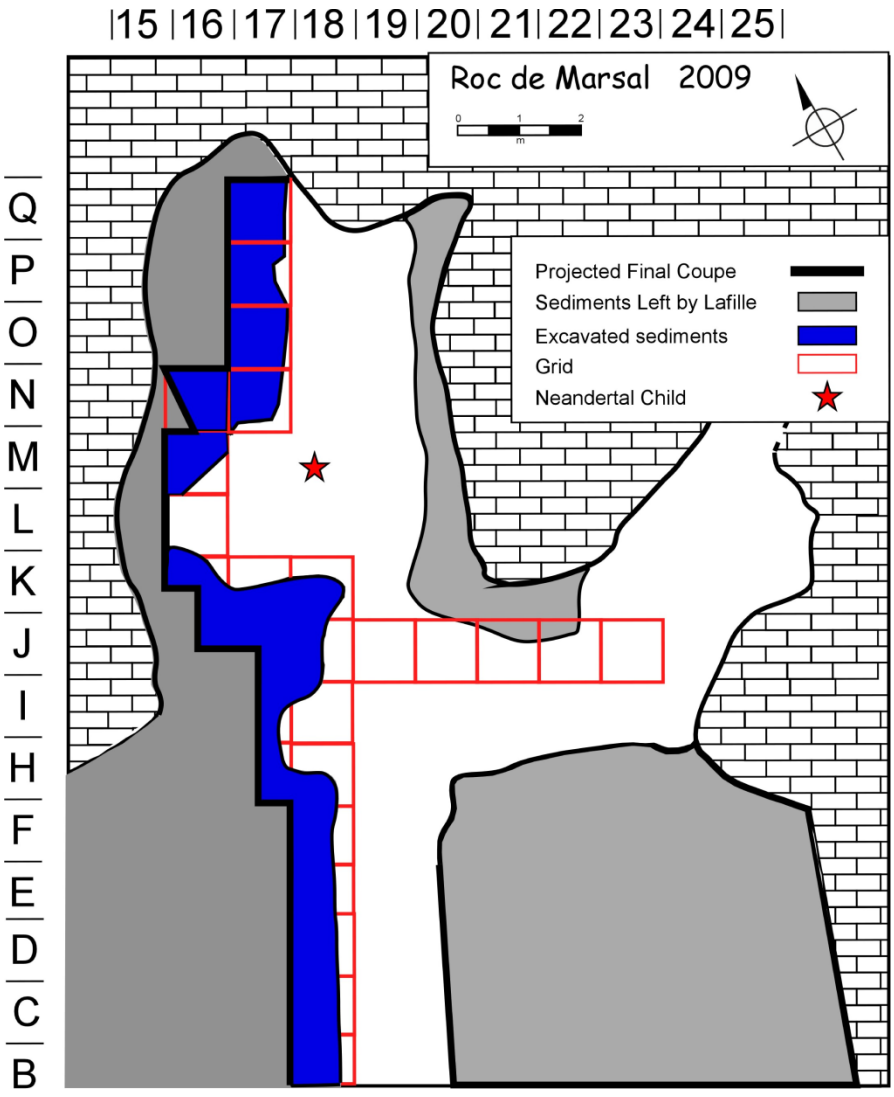

Figure 2: The general plan of Roc de Marsal showing shape of cave, grid, and areas left by Lafille, as well as those excavated recently by the current team.

The area of occupation at Roc de Marsal is about 50 m^2 and consists of a main elongated area trending approximately N-S (principally squares B-N, 16-19); another, more open area, still unexcavated, is located in the front part of the cave (Figure 2).

Briefly, the principal aspects of the stratigraphic succession are as follows. Overall, the deposits consist of sands and silts, with abundant lithic and bone remains. In the basal layers, these components are interbedded with intact and partly remobilized combustion features (CF) principally comprised of charcoal and organic matter, burned bone, and ashes. Seven geological lithostratigraphic units (*GU*, numbered from bottom to top) were identified based on color, composition, and texture. Within these geological units several archaeological layers (AL) were recognized using these and other criteria; these are numbered from top to bottom. GU 1, 2, 3 are of particular focus here and include AL 13 through 4. The main features of each of the GU and AL are illustrated in Figure 3 and summarized in Table 1.

The dating of the site is still on going. A series of preliminary TL dates from burned sediments at the very base of the sequence have yielded ages spanning from 72 to 91 kya (Guibert et al in Sandgathe et al., 2008), suggesting that the initial occupations at Roc de Marsal began in Marine Isotopic Stage (MIS) 5a. A mean ESR date for AL2 (the final Mousterian layer) of 43,600 ±2600 (Blackwell et al. in Sandgathe et al., 2008) suggests the final Mousterian occupations occurred during late mid-MIS 3.

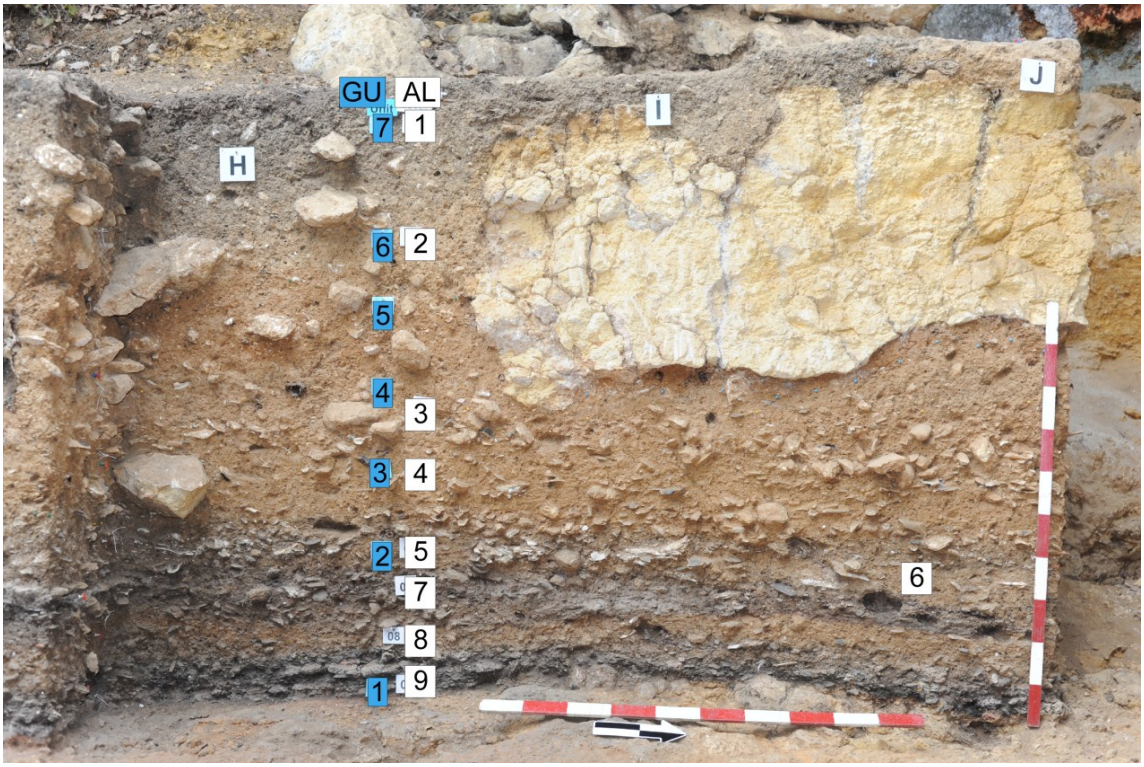

Figure 3: West Section of profile at Roc de Marsal at end of 2009 season showing stratigraphic layers described in Table 1. The blue tags represent Geological Units (GU), whereas the white ones refer to Archaeological Layers (AL). The meter stick is lying on bedrock, which slopes gradually to the north and south from the center of the photo. The arrow points north and is 20 cm long

Geol. Lithostrat. Unit (GU)	Arch. Layer (AL)	Field Description
7	1	Layer with high organic content, especially outside the cave, but is highly disturbed. This is due to both bioturbation and later Medieval occupants who excavated into this AL to create storage pits. The archaeological material reflects this disturbance, including historic materials (metal, pottery) as well as a small number of lithic items that may be Middle and/or Upper Palaeolithic, but which are not particularly diagnostic. 10 to 30 centimeters thick.
6	2	Yellow to light brown clayey-silt, very similar in composition to AL 4; predominantly Aeolian in origin. It includes a large number of limestone blocks (roof fall) ranging from centimeter to meter size. In fact, inside the cave, AL2 is capped by a layer of roof collapse approximately three quarters of a meter thick. The finer sediments are approximately 45-50 centimeters thick.
5		
4	3	Is a very thin lens that is not found throughout the site. Similar in composition to AL4, but is notably darker. Thickest (c. 1-2 cm) near the cave mouth.
3	4	Resembles AL5 in general composition except it is light yellow-brown color and is less consolidated. Rich in lithics, but most notable for the high concentration of faunal remains. 20 to 30 cm thick.
2	5	Composed of light grey clayey-silts that are finer in texture than the lower deposits. It includes small to medium sized pieces of limestone roof fall and a high concentration of archaeological materials. The lithic component is assigned to the Typical Mousterian industry with a significant Levallois component. 10-15 cm thick.
	6	Similar to AL8, it is discontinuous across the site and thickest (c. 3-5 cm) just inside the cave mouth. It is composed of brown clayey-silts.
	7	Similar in color and basic composition to AL8, although darker (due to a higher content of charcoal and burned bone); has slightly decreased concentration of archaeological materials. As in AL9, it contains numerous intact and discrete combustion features. 5-8 cm thick.
	8	Occurs mainly just inside the cave mouth and is discontinuous across the site. It is composed of grey-brown clayey-silts with abundant archaeological materials. c. 8-10 cm thick.
	9	Clayey-silts with a very marked anthropogenic component of combustion features consisting of ash, burned bone, and charcoal; these components occur in both localized lenses and as more massive accumulations. AL9 contains the most abundant combustion features and very high concentrations of archaeological materials. 5 to 10 cm thick
1	10	Very thin (c. 1-5 cm) orange clayey-silt, with some small fragments of roof fall. Very little archaeological material, but lens of rubefied AL10 sediments separated from AL9 by thin lens of unrubefied AL10 sediments indicate that the initial occupations were associated with uppermost AL10.
	13-11	Brown to orange clayey-sand that rests directly on bedrock and fills in locally undulating karstic mini-topography. 1-2 cm to 20-30 cm thick; archaeologically sterile.

Table 1: Summary of principal Geological Units (GU) and Archaeological Layers (AL) from Roc de Marsal. (Read from bottom up)

The upper part of the Roc de Marsal sequence, that is ALs 4 through 2, contains Quina Mousterian industries characterized by high frequencies of scrapers made on thick blanks, few cores, and almost no Levallois components. These levels also contain very high concentrations of heavily butchered faunal remains dominated almost entirely by reindeer (*Rangifer tarandus*), but with small percentages of bos/bison and *Equus* sp. The combustion features, however, are associated with ALs 10, 9, and 7, which contain Mousterian industries characterized by lower frequencies of retouched pieces overall, more cores and clearer evidence that core reduction took place on the site, significant presence of Levallois technique, and many so-called Asinipodian elements (Bordes, 1975; Dibble and McPherron, 2006), including diminutive Levallois cores, truncated-faceted pieces, and Kombewa cores and flakes. ALs 9 through 5 contain lower concentrations of faunal remains compared to the upper layers, although they are still rich in fauna that were also heavily exploited. There is also a wider range of species represented, including red deer (*Cervus elephus*), roe deer (*capreolus capreolus*), wild pig (*sus scrofa*), horse (*Equus* sp.), and beaver (*Castor* sp.); reindeer, while rare in ALs 9 and 8, steadily increase in frequency throughout the sequence.

4.4. Methods

4.4.1 Excavation Methods

The methods of excavation employed at Roc de Marsal follow the concepts used in other archaeological sites and described elsewhere (see Dibble et al., 1997; Dibble and Lenoir, 1995; McPherron and Dibble, 2002). The location of all artifacts (stone tools, bones, charcoal fragments, etc) with dimensions greater than 2.5 cm was recorded using a total station and integrated into the local coordinate system developed for the site. All non-artifact features, including hearth-related sediments, were recorded in the same manner, with the limits of these sediments taken as sequential points. This method of point proveniencing all individual artifacts and features allowed the recording of spatial information in three dimensions.

In addition, once the hearth-rich anthropogenic layers (namely AL7 and 9) were reached during excavation, the methodology was modified to expose "*décapage*" surfaces. This excavation method has been widely used in archaeology, particularly in French archaeological contexts (see, for example the excavation at the site of Pincevent: Leroi-Gourhan, 1984). The basic concept of *décapage* is to expose the features and archaeological materials and to associate these objects with a specific *décapage* surface number. Consequently, the criteria to define each décapage surface is somewhat flexible and inherently dependent on factors such as the concentration of artifacts and/or features exposed while excavating thin slices of sediments over a somewhat horizontal surface.

The *décapage* method we used, however, still involves the separation of different natural and anthropic layers. Consequently, since the combustion features are often composed of the superposition of distinct types of sediments (for instance, an ash layer overlying charcoal-rich sediments): each of these deposits was excavated separately and associated with distinct *décapage* surface numbers.

The result of these procedures is the slicing of a stratigraphic unit into several sub-surfaces (often of varying thickness, but generally within a range of 2 to 4 cm) that - at least theoretically - should associate artifacts and bones that are penecontemporaneous. As each *décapage* surface was exposed, it was then photographed, and its associated bones and artifacts were provenienced and removed, with each object or sample linked to the *décapage* surface on which it was found and also linked to particular combustion features. It should be emphasized that there is no claim that these *décapage* surfaces represent "living floors." In fact, as the discussion below will make clear, our own experience has led us to be skeptical that such surfaces can be identified or followed across a specific horizon, at least in a sedimentary environment such as that which exists at Roc de Marsal.

The individual combustion features were studied first in the field during excavation and then sampled for micromorphological and other analyses. Field observations were made both in plan and section view where possible, and include diameter, thickness, color, shape of the features, and basic composition. Commonly, however, it was not always possible to determine these parameters because many of the features were intercalated and overlapped. Similarly, several extended into the

unexcavated section walls, and several more had been wholly or partially removed during the previous excavation by Lafille.

In almost all cases at Roc de Marsal individual combustion features were easily recognized when encountered during the excavation process, both in profile section and in plan (*décapage*) view. In profile section, combustion features generally occurred as thin lenses of either strongly black sediments, strongly white sediments, and/or superimposed lens of both black and white sediments, all with clearly observable horizontal spatial limits. Only one of the combustion features was associated with a depression and this depression was completely natural. When exposed in plan view, with few exceptions, features were easily distinguished from surrounding sediments by the spatial limits of the black and/or white sediments associated with each feature; very little lateral displacement of residues appears to have occurred, which contributed to the very good preservation of individual combustion features. Very few of the combustion features have undergone varying degrees of post-depositional movement or loss of residues; CF 27, for example, is comprised solely of a spatially discrete lens of fire-reddened (rubefied) sediments. As each combustion feature was encountered and its limits defined, it was assigned its own combustion feature ('CF') number in a simple sequence applied to the whole site. Although 27 combustion features were initially recognized and thus numbered, the total eventually decreased to 22, as some were eventually rejected either as excavation proceeded or because of subsequent laboratory analyses. In some cases, while it was clear that multiple features had been encountered because of spatial overlapping and limited vertical separation, the individual limits of the

features were unclear, and this was reflected by adding letter suffixes to their identification numbers (e.g., CF18a and CF18b).

4.4.2 Analytical Methods

Micromorphology

The combustion features were studied primarily using micromorphology and Fourier Transform Infrared Spectrometry (FTIR). Micromorphology has proven to be an effective means to evaluate both the components of combustion features but also their internal organization and degree of integrity (Berna and Goldberg, 2008; Cabanes et al., 2010; Goldberg and Berna, 2010; Goldberg et al., in press; Goldberg et al., 2009; Mallol et al., 2010; Mallol et al., 2007). Similarly, it is possible to recognize whether a particular combustion feature is intact or whether it has been modified by certain post-depositional and syn-depositional effects such as trampling (Miller et al., 2010).

Micromorphological samples were collected from combustion features during the excavation as intact blocks that, in certain places in the cave, commonly spanned more than one recognized combustion feature. These blocks (varying in size but typically being ~20 cm long by ~12-15 cm wide and deep), were oven dried for several days at ~60°C and then impregnated with unpromoted polyester resin diluted with styrene at a ratio of 7 parts resin to 3 parts styrene. Methyl ethyl ketone peroxide (MEKP) was added as a catalyst at about 7 ml MEKP to 1 liter resin/styrene mixture. After gelling, the blocks were heated overnight at ~60°C and then sliced with a diamond rock saw to fit the 50x75

mm dimension of the thin section. These trimmed chips were sent to Spectrum Petrographics (Vancouver, Washington, USA), where they were processed into petrographic thin sections (30 µm thick).

FTIR spectra were obtained from both micro bulk samples using K-BR pellets and from direct measurements of bone, clay, and ashes within the thin sections. Samples processed in thin section were analyzed by FTIR microspectroscopy using a Thermo-Nicolet Continuum IR microscope attached to the spectrometer. Spectra of particles with diameter of about 100µm were collected either with ATR diamond objective, or with a Reflectocromat 15x objective in Transmission mode. The spectra were collected between 4000 and 450cm-1at 8cm-1 resolution.

Spatial analyses of Combustion Feature horizons

Geographical Information Systems (GIS) are optimal tools for both visualizing the distribution underlying the scattering of archaeological artifacts and to analyze diachronic changes of the assemblages. It is often the case that such studies are done using a stratigraphic layer as the primary unit of analysis (e.g., Alperson-Afil et al., 2009; Anderson and Burke, 2008). However, geological units potentially incorporate numerous occupations during hundreds or even several thousands of years. One of the major analytical problems we face is, therefore, how to achieve meaningful units of analyses

with greater control on the temporal relationship between distinct occupations (e.g., Vaquero, 2008; Vaquero and Pastó, 2001).

Since there are several combustion features recognized in both AL7 and 9 of Roc de Marsal, our goal was to examine the distribution of artifacts and other materials associated with each of these fire-events. Although AL7 and 9 were excavated using the *décapage* approach, several problems were encountered when individual *décapage* layers were used as units of analysis. These problems include: (1) some combustion features were sufficiently thick that they spanned more than one *décapage* surface, and therefore their association with the surrounding artifacts was difficult to establish with certainty; (2) the thickness of each *décapage* surface can be defined only loosely (excavation proceeds until artifacts are exposed across a surface), and therefore any particular *décapage* surface varies in part due to individual excavators as well as the abundance of artifacts encountered; (3) the excavation of each *décapage* was done over approximately horizontal surfaces, but these somewhat flat surfaces might not have been the original occupational floor at each time of occupation since circumstances such as an inclination of the bedrock might dictate non-horizontal tilt of the cave sediments. Overall, and to be honest, we just did not know which artifacts were associated with each combustion feature while excavating. In order to try to establish the degree of patterning of burned lithics and association of archaeological artifacts within and around each combustion feature (but still within the same stratigraphic layer) a methodology was developed for reaching thin meaningful slices of strata associated with each feature/fire event. Our approach was designed to define unbiased units based on paleosurface markers present

within the stratigraphic layers. One of these markers is obviously the presence of a combustion feature itself, since its construction and use was done at a time when this was the level of the cave´s floor. These features thus offer the potential to serve as indicators of "paleosurfaces" that can be used in defining horizons of analyses.

Distinct combustion feature horizons were obtained by plotting the limits of each combustion feature in ArcMap. The center for each combustion event was then computed using the Mean Center tool available in Arctoolbox. In order to assign the surface level, a shape file was created outlining the bottom of the stratigraphic layer, taken as our base line. The bottom of the stratigraphic layer constitutes a surface into which sediments are added, and, consequently, a more accurate assumption of a paleosurface's altimetric mean throughout the thickness of the stratigraphic layer rather than its top limit. This line was then copied and manually juxtaposed to the elevation of each mean center of combustion features. In order to assign the artifacts to their horizons, all burned artifacts larger than 2.5cm in maximum dimension were joined spatially with the nearest combustion feature horizon. ArcMap software was used to examine the manner burned artifacts are spatially distributed within each of the produced combustion horizons, their association with one another and with the location of identified combustion features. Due to inherent finite nature of the type of data we have, Kernel density estimations were chosen as an analytical technique to identify overall patterns, following similar approaches done in other archaeological contexts (Alperson-Afil et al., 2009). The search radius was maintained constant (with a value of 0.3) whenever the produced maps were

analyzing the same type of artifacts over distinct horizons. The density values from the different horizons were then standardized to values ranging from 0 to 100.

For AL7, where the seven individual combustion events were at clearly distinct elevations, the produced horizons are associated with only one combustion feature. In AL9, however, several of the combustion features identified were at the same elevations in different areas of the cave. Whenever this was the case it became impossible to separate one event and/or feature from another based on elevation, and thus some of the horizons defined in this way reflect the presence of one or more combustion features.

4.5. Results

Below we present the results of field and laboratory analyses of the combustion features at Roc de Marsal. Some results are based on the combined data of all 22 features recognized in the field, but limitations of space preclude a detailed treatment of all 22 combustion features. Consequently, some results are based primarily on the analysis of a selected sample of features, namely CFs 10, 15, 16, 18a, 20, 23, 24, and 27 (see Figures S1, S2 and S3). This sample includes features that represent the range of variation recognized among the total. (A summary of field observations and soil micromorphology analysis results for all identified features is presented in the supplementary material table S1).

When viewed in terms of the basic overall structure and internal organization of the components, basically two ‘types’ of combustion features were noted: those

composed of a lower, dark (mainly charcoal) unit coupled with an upper ash unit, and those that include only an ash-rich-component with jumbled orientations of all materials (bone, *éboulis*, charcoal, lithics). We interpret the former as typical (and, in most cases, intact) hearths in which, after being extinguished, the associated materials were not – or were minimally – displaced from their original positions. The second type, with internally mixed components and no evident structure, appear to represent secondarily reworked combustion features, such as those found in ash 'dumps' that may reflect hearth cleaning activity events.

Examples of intact and in place combustion features (hearths) include:

CF3 and 7 (in AL 7).

CF1, 4, 5, 10, 11, 13, 14, 18a, 18b, 20, 21, 22, 23, 24, 26 (in AL 9).

Features interpreted as ash dumps with no internal organization include:

CF15 (AL 7), where it is clear from the density maps that a considerable percentage of burned lithics were dumped alongside with ashes (Figure S1).

CF12 (AL 9), where the higher percentage of burned lithics is not associated with this feature but located, instead, towards the inside of the cave.

There are also several features that are neither intact nor in their original position, and thus cannot readily be placed in either of these categories:

CF2 is a small concentration of loose charcoal in a shallow depression. Its size and composition may represent either the remnants of an in-place hearth or, more likely, redeposited eroded hearth residues. Its small size could indicate that partial erosion of the

material took place in the past or that a specific activity might have been associated with it.

CF16, with its mixture of materials, is clearly composed of reworked fire residues (mainly burned bone, burned lithics, and charcoal - Figure S1).

CF27 is a zone of rubefied sediments that clearly marks the original location of a combustion feature. However, as none of the actual fire residues remain, nothing can be said of the nature of the original feature (size, components, or internal organization) - see Figure S3.

4.5.1 Combustion Feature Morphology

Few complete combustion features were uncovered during the recent excavations (due to previous excavations and our own limits of excavation) and so spatial limits are not known for all of the hearths. For some of the combustion features that might have been complete, the limits were not distinct enough to be confident of the feature's actual extent. Several other combustion features, however, are either complete or complete enough so that an idea of their original dimensions can be determined with some degree of confidence (see Table 2). It is most likely that the range in sizes reflects a continuum of variability, and there is no evidence at this point that the different sizes reflect either duration of use and/or group size.

CF	AL	dimensions (cm)		thickness (cm)			Fauna (counts)	Lithics (counts)	% Burned Lithics
		length	width	dark layer	ash layer	Total			
3	7	120	-	0.5	1	1.5	145	193	33.7
7	7	45	40	1	1	2	41	44	9.1
1	9	100	90	12	0.5	12	135	511	17.6
4	9	100	-	1	1	2	20	208	71.2
5	9	130	-	0.5	1	1.5	-	-	-
18a	9	125	-	0.5	1	1.5	71	162	54.9
10	9	55	-	1	1	2	20	37	73.0
20	9	50	50	0.5	1	1.5	87	136	12.5
22	9	30	-	0.5	1	1.5	24	39	15.4
24	9	115	75	0.5	1	1.5	9	93	16.1
26	9	30	20	1	1	2	38	29	3.4

Table 2: Descriptive parameters of combustion features and artifact contents - values are not included if the feature was not complete in that dimension. CF= Combustion Feature; AL= Archaeological Layer.

The majority of in-place and intact hearths (complete and incomplete) are 1 to 2 cm thick (see Table 2), although typically the ash component is slightly thicker than the dark component. There are some exceptions: CF20 has an ash layer that is 3 cm thick. As revealed in thin section, CF20 is actually associated with a second, smaller combustion feature (left unnumbered since it was only visible in thin section). Micromorphological observations (see supplementary material and Figure S7) show that both features represent intact combustion deposits. The uppermost feature is composed of a thick ash layer with common calcined bones overlying a charred plant-rich layer and rubefied soil

material. The second feature identified microscopically presents a thinner ash component and is overall less well preserved.

CF1 stands out in that at its center the lower dark component is 12 cm thick and pinches out at its limits. However, CF1 is also the only combustion feature associated with a significant depression, which may have acted as a sediment trap that tended to concentrate fire residues, especially burned bone and burned lithics. It should be noted that the depression containing CF1 is entirely natural and reflects the rough, karstic nature of the cave floor. In no case are there indications (from either field observation or thin section analyses) that any intentional modification of the ground surface (for example the creation of depressions) was carried out in order to accommodate combustion features. Of the two features identified as ash dumps, CF12 has a thickness similar to that of the majority of the combustion features, but CF15 is significantly thicker: in profile section it is 7 to 8 cm thick at the center and looks very much like ash that has been piled there. This interpretation is further confirmed by micromorphological observations, where the deposits associated with CF15 are expressed by a scattered mixture of bones (some burned), charcoal, coprolites, chert, and limestone fragments, including reworked clumps of ash. The sediments lack any structured sequence (see supplementary material). All the combustion features that are complete enough to provide some idea of their shape can generally be described as sub-circular. Some (for example CF18a) are more irregular, but there is no apparent patterning. There are also no indications of any intentional arrangements of stones or other materials associated with any combustion features.

4.5.2 Contents of the Combustion Features

The artifactu content (materials ≥ 2.5cm in maximum dimension) directly associated with combustion sediments tends to mimic the overall types of archaeological materials found elsewhere in the stratigraphic layers. Lithic artifacts characterize the majority of the assemblages in both AL7 and 9, with a total of 4024 lithics versus 3599 bone fragments in AL7, and 8101 lithics versus 3632 bones in AL9. Similarly, there is a higher proportion of lithics relative to faunal remains in the sediments associated with CFs 1, 10, 16, 18a, 20, 23, and 24. An exception is combustion feature 15, in which bone fragments make up 58% of the artifactual content. In the majority of the combustion features, there is actually a higher percentage of unburned lithics directly associated with the combustion sediments; exceptions to this are CF10 and 18a, where the percentage of burned lithics is higher than 50% (see table 2). There is also no distinction in terms of the altimetric distribution (i.e., in term of depth, Z) between unburned versus burned lithics inside the features. The presence of unburned lithics within the infilling of hearths most probably indicates that some of the artifacts were deposited after the fire was extinguished. Micromorphological observations, expressed by the presence of *in situ* crushed and broken bones (Figure S7-g), for instance, suggest that trampling may have played a role in mixing these unburned lithics with other artifacts that were directly associated with the combustion event (Miller et al., 2010).

4.5.3 Spatial Distribution of the Combustion Features and Associated Objects

A number of general observations can be made regarding the spatial distribution of individual combustion features at various levels of resolution, from intra-layer observations, to inter-layer observations, and finally to inter-feature observations.

In terms of the distribution of combustion features within AL7 and AL9, there is no apparent patterning either horizontally or vertically, other than some localized concentrations of combustion features (discussed in further detail below). The lack of any apparent horizontal patterning could potentially be due to a lack of complete site data. Many of the deposits immediately adjacent to our own excavations were removed during the original excavations and a significant portion of the basal layer deposits still remains on the terrace of the cave (units F to H, 20 to 24; Figure 2). Perhaps with a more complete sample across the entire site some patterning in the horizontal distribution of combustion features would be detectable.

Kernel Density Estimations

If we take into account the overall concentration of burned lithics (Figures 4a, and 5a), the Kernel density maps show higher concentrations of burned lithics located inside the cave during the occupations associated with AL9, whereas in AL7 higher density percentages tend to be present towards the cave's entrance in squares H-F 17-18. This patterning, however, seems to be related more to the bedrock topography at Roc de Marsal than to a deliberate placement of hearths by the Neandertals. In the area of

squares J-L 16-18, the bedrock dips into the interior of the cave in a basin shaped morphology, a topographic feature that would have been prominent at the time of the first occupations of the base of layer 9. Subsequent sedimentation of the remaining deposits of AL9 and ultimately AL8 eventually filled in the micro-relief and essentially flattened this area; by the time of the AL7 occupations, the topographic of the occupied surface was roughly level.

The Kernel Density Estimations for individual combustion feature horizons on both AL7 and AL9 indicate very limited patterning in the horizontal spatial relationship between hearths and the distribution of burned lithics (Figures 4 and 5). Within each AL there are concentrations of burned lithics that seem to be associated with individual combustion features (e.g., CF horizon 4 in AL9). There are others, however, that have no association with any preserved, observable combustion features.

Both AL7 and AL9 have localized concentrations of combustion features. In both layers these concentrations are the result of subsequent occupants of the site constructing their fires directly (or almost directly) on top of previously abandoned combustion features. That these stacked sequences of features represent multiple occupations and/or significant temporal hiatuses between events is indicated by several facts. The first is that in both AL7 and AL9 such sequences span the whole thickness of the archaeological layer; even if rates of deposition were relatively high, the deposition of either of these layers must represent many years. Second, in most cases very thin layers (< 1 cm) of non-anthropogenic sediments cover the previous combustion feature.

Micromorphological evidence also indicates mm-thick phosphatic weathering crusts that commonly occur on top of combustion features, again indicating some passage of time between the stacked combustion events. In some cases, however, the individual combustion features within the stacked sequence were not separated by intervening sediments.

The stacking of some of the hearths, especially when the previous one was already covered with sediment and therefore not visible, implies some degree of consistent placement of these features. The location of such stacked features differs between AL7 and AL9.

In AL7, a stacked series of combustion features (which, based on field observations, included at least CFs 3,5 and 11) was located beyond the dripline of the cave mouth, even if we estimate that the roof may have extended out another meter at the time of occupation (Figure 6). The stacked combustion features in AL9 (CFs 24, 23, 21, and 18a/18b) was situated midway between the cave walls and spans the current dripline of the cave mouth; most likely these hearths would have been inside of the dripline when they were active (Figure 7).

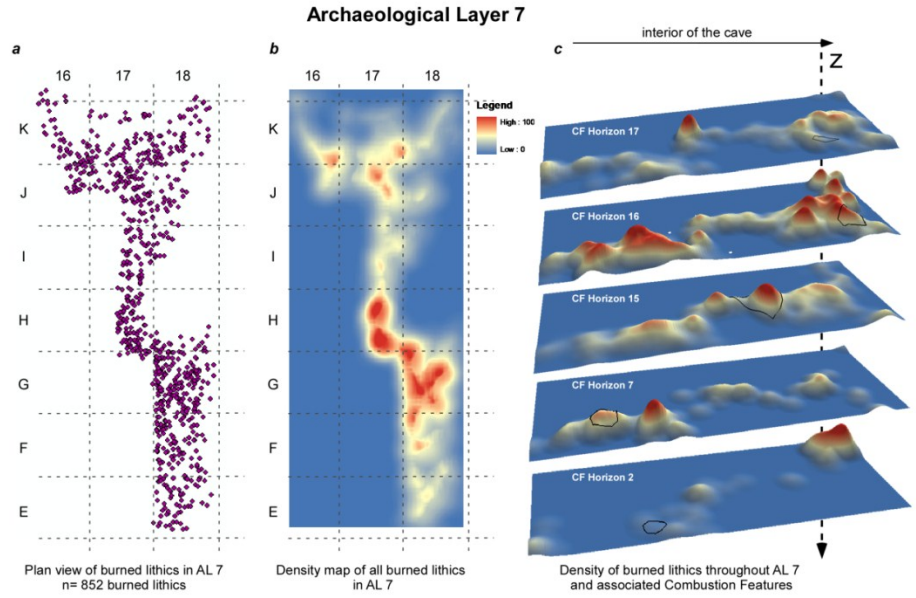

Figure 4: Spatial distribution of burned lithics (≥ 2.5cm) in AL7. (a) Plan view plot of all burned lithics and their location on the site's grid system; (b) Plan view of Kernel density map of burning if all lithics of AL7 are taken into account; (c) density maps showing the main subdivisions into combustion feature horizons throughout AL7, where elevated topographies corresponds to the location of higher densities of burned lithics and the circles (depicted in black) correspond to the limits of each combustion feature. CF= Combustion Feature; AL= Archaeological Layer.

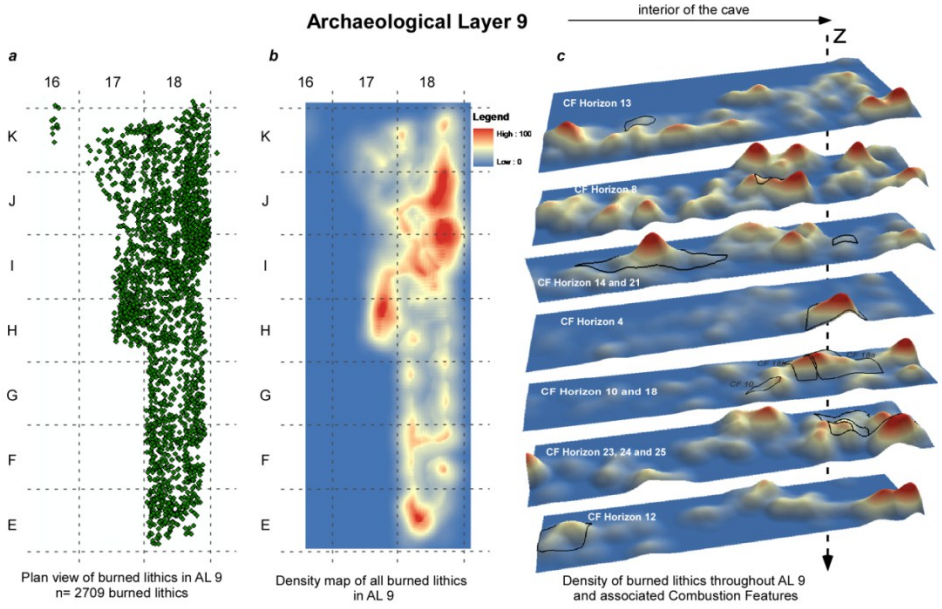

Figure 5: Spatial distribution of burned lithics (≥ 2.5cm) in AL 9. (a) Plan view plot of all burned lithics and their location on the site's grid system; (b) Plan view of Kernel density map of burning if all lithics of AL9 are taken into account; (c) density maps showing the main subdivisions into combustion feature

horizons throughout AL9, where elevated topographies corresponds to the location of higher densities of burned lithics and the circles (depicted in black) correspond to the limits of each combustion feature. CF= Combustion Feature; AL= Archaeological Layer.

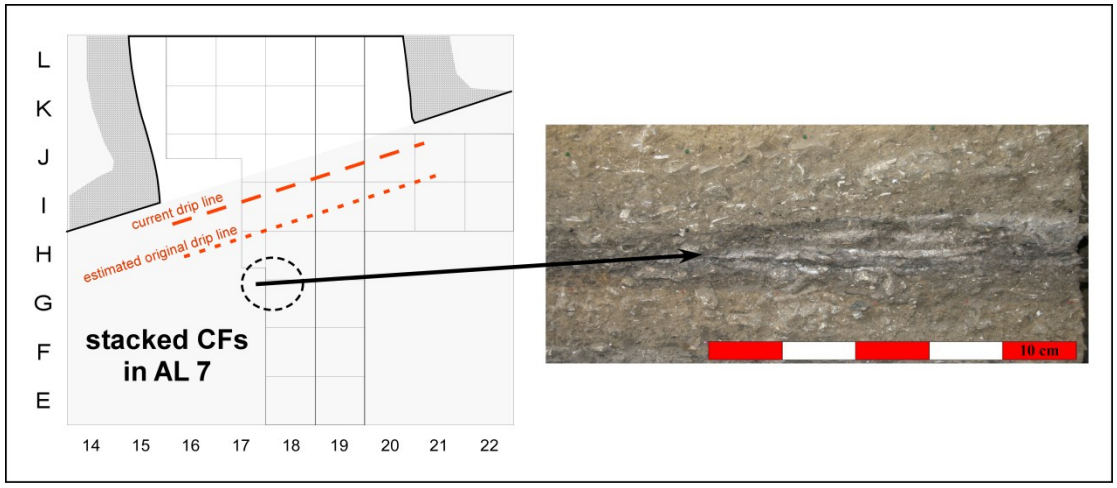

Figure 6: Location of the stacked combustion features in AL7 on the site grid (left) and profile photograph of these features in the field (right).

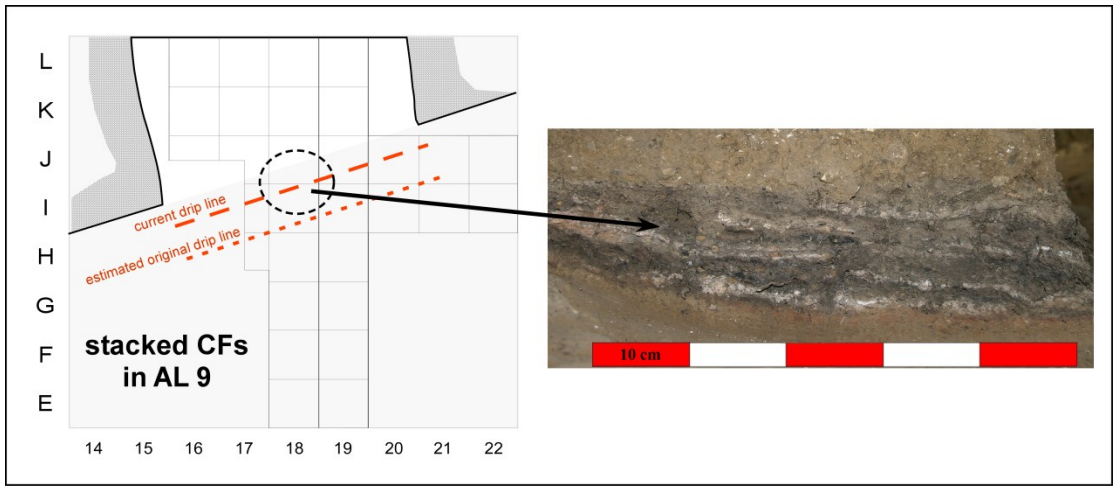

Figure 7: Location of the stacked combustion features in AL9 on the site grid (left) and profile photograph of these features in the field (right).

4.6. Discussion and Conclusions

Both field and microstratigraphic observations attest to the well-preserved nature of fire residues in AL7 and AL9 at Roc de Marsal. From a field *macro*stratigraphic perspective, the combustion features are, for the most part, easily distinguishable and horizontally delimited from the surrounding deposits. This occurrence contrasts with what the authors encountered during excavations at Pech de l'Azé IV, another cave site in the region, which also contains significant concentrations of slightly older fire residues. At Pech de l'Azé IV, individual combustion features were apparent in section, and in plan-view their horizontal limits were blurred due to lateral 'bleeding' of combustion residues, the result of natural and/or anthropogenic processes (Goldberg et al., 2012; Dibble et al,. 2009). At Roc de Marsal, on the other hand, the majority of the fire features seem to have been constructed, used, and abandoned without major reworking or displacement of the residues by subsequent occupations of the site and/or by natural processes.

The high-resolution *micro*stratigraphic analyses have proven to be extremely useful. For example, views of the fire-associated sediments in thin section allowed for the identification of several independent, mm-thick, superimposed combustion events that are virtually undistinguishable during excavation (e.g., CF10, CF18a and CF20 - see Supplementary Materials, and Goldberg et al., 2012). These analyses also allowed for the high-resolution characterization of the nature and the degree of integrity of individual fire events. Overall, the evidence shows that the majority of the identified combustion

features in AL7 and 9 represent intact, in-place features, that is, with minimum or no displacement from their original position. There are a couple of exceptions. CFs 12 and 15 were interpreted as ash dumps and, therefore, do not represent in-place burning. CF 27, located in AL10 and one of the first identifiable fire events at the site, is the only example of a feature without an ash component and is characterized instead by the presence of a fire-reddened substrate.This rubefication indicates erosion of part of the original deposits (namely ashes and charcoal components). Other visible post-depositional alterations are related to trampling, diagenetic alteration of the ashes (namely in the areas of squares K16-18) and phosphate accumulation on an exposed surface, indicating a periodic abandonment of the site.

The results of our spatial analyses show that there is no striking patterning of the Roc de Marsal combustion features, with the exception of minor differences in the location of stacked hearths and a difference in the concentration of combustion features primordially inside the cave during AL9 times and more towards the cave mouth during AL7. The data from the intra-layer analyses demonstrate that, for the majority of the features, there is no association between the distribution of burned lithics and the location of the combustion features. In fact, concentrations of burned lithics are dispersed throughout a surface, even though combustion features are often well preserved and in place.

It is too early to say that the lack of evidence for any structured spatial organization reflects the lack of such behaviors of the hominins who occupied the site, since this could be due to several factors. There is no question, for example, that the area

exposed during our own excavations was quite limited, and for the most part was only 1m wide. Furthermore, trampling and other kinds of bioturbation may have resulted in some lateral movement, but evidence for such effects on any kind of significant scale is lacking. Examples of concentrations of burned artifacts *not* in association with an identifiable combustion feature may reflect a natural loss of preservation of the features, though this is difficult to prove if no evidence remains. Finally, actions taken by the hominins themselves – such as the purposeful raking out of hearth deposits and subsequent dumping of the contents elsewhere (as in CF15; see supplementary material) and/or the recycling of previously deposited lithic artifacts, can significantly alter original distributional patterns.

It was originally hoped that particular excavation and analytical techniques, such as those developed for other sites (e.g., Abric Romaní, Spain (Vaquero and Pastó, 2001, Vallverdú et al., 2012; Courty et al., 2012)], El Mirón, Spain (Marín Arroyo, 2009)], Mandrin, France (Yvorra, 2003)], Gesher Benot Ya'aqov, Israel [(Alperson-Afil et al., 2009)], or at Tor Faraj, Jordan (Henry et al., 2004; Henry 2012)]) would help to expose any spatial patterning on the assemblages. Unfortunately, such techniques were not successful, perhaps due to several reasons. For example, one of the main methodological constraints on looking for spatial patterning is defining the scales of analyses to use (see for e.g., Vaquero, 2008). Quite simply, if the goal is to investigate how Neandertals were using the space available to them, including where they decided to put their combustion features, then the first step is to decide how best to define an 'occupational surface'. In the case of Roc de Marsal, as at most sites of this age, there are archaeological layers that

are obviously deposited over a geological time scale (i.e., over hundreds and probably even thousands of years), and therefore these layers clearly incorporate many distinct occupations with potentially different occupational strategies. At the other end of our resolution are the thin sections taken for micromorphological analysis, where it is possible to recognize micro-strata of much more limited duration, including superimposed combustion features that are not recognizable in the field (see Goldberg et al., 2009). Although these micro-strata may be clearly visible under a microscope, it is impossible to trace them out beyond the sample itself and thereby define penecontemporaneous occupation surfaces. This, then, makes it impossible to extrapolate the original occupation surface at the time that a combustion feature is being used.

Unfortunately, this was the case even though every attempt was made to expose surfaces using a *décapage* excavation technique. In fact, our experience at both Roc de Marsal and Pech de l'Azé IV has shown that such an excavation technique is too dependent on the abundance of artifacts and decisions made by individual excavators. Furthermore, the use of this technique will result in "surfaces" even if artifacts are both horizontally and vertically randomly distributed, and there is no way to confirm or deny that such surfaces represent true occupational surfaces. Even from a theoretical perspective, any surface occupied in the past undoubtedly included a relatively thick "active zone" of several centimeters into which artifacts were pushed and from which artifacts were incidentally dislodged or actively selected for further use. In sum, it is our

conclusion that these approaches are not particularly useful, and that the surfaces thus exposed are essentially an artifact of the method itself.

In conclusion, it is clear that the basal AL7 and AL9 of Roc de Marsal contain several combustion features – hearths – that are exceptionally well preserved. This observation alone is ample evidence that European Neandertals of MIS 5-4 were able to control fires – if not able to start them – and that at certain times they used it to a considerable degree (Sandgathe et al 2011a). What we have shown here is that considerable information can be gleaned from these features through the application of high-resolution techniques such as micromorphology and FTIR analysis (see supplementary material for details). However, in spite of their almost "pristine" state of preservation, the difficulty of using such features as anchors for understanding Neanderthal behavioral activities has shown to be challenging, both because of the intrinsic nature of archaeological sediments and the inherent difficulty to assess the degree of contemporaneity of archaeological features and associated assemblages.

It is clear that by the time of the Middle Paleolithic, evidence for controlled fire occurs more frequently than before (Roebroeks and Villa, 2011), though there is still much more to be learned about Neandertal use of fire, especially concerning its functions and the role it may have played in Mousterian adaptations to particular conditions. Simply documenting the presence of burning does little to inform us on these questions. Thus, there is still a clear need for more systematic publication of detailed analyses and descriptions of such features from a variety of sites.

CHAPTER 5: Conclusions

The primary line of research in this thesis is the application of soil micromorphology techniques to evaluate the archaeological record. This geoarchaeological approach builds upon major scientific endeavors seen in recent years to achieve a higher degree of resolution in the study of cultural occupational sites and sedimentation. It is becoming increasingly clear that reconstructing past human behaviors and activities is achievable not only through studying the manufactured artifacts themselves, but also that substantial information can be gleaned from analyzing the embedding sediments. Moreover, while substantial information is detectable at the site- or even landscape-scale of analyses, there are several, discrete events pertaining to site formation and anthropic sedimentation which are preferentially recorded at a microscopic level (Courty, 2001; Courty et al., 1989; Goldberg, 1983).

Chapter 2 focuses on reconstructing the processes involved in site formation at Contrebandiers Cave, Morocco. Although the site has been known for several years, questions relating to sedimentary sources, post-depositional processes, and the degree of preservation of the archaeological assemblages remained unanswered. The study presented here allows for a detailed characterization of the sedimentary history of the site; considered the predominant paleoclimatic conditions of deposition; and attests to the degree of integrity of the embedded archaeological assemblages. The results demonstrate the necessity of considering geological constraints and processes in the characterization of the archaeological record. Although studies on the emergence of anatomically and behaviorally modern humans have identified North Africa, and Morocco in particular, as one of the crucial areas for investigating this stage in human evolution, there is still a

striking lack of research on the integrity and context of the archaeological assemblages. This study, then, constitutes one of the first applications of in-depth micromorphological and geoarchaeological analyses for Moroccan Middle Stone Age (MSA) contexts. The deposits from Contrebandiers Cave show the predominance of sedimentation during Marine Isotopic Stage (MIS) 5, and systematic research of the sedimentary history of nearby archaeological sites can, in the future, contribute greatly to the characterization of the geological evolution of this coastal area, as well as patterns of Paleolithic human adaptations that took place there (discussed in the Introduction).

The control of fire is commonly seen as an important technological achievement and its use as carrying relevant adaptive strengths for ancient human communities. Widespread, controlled use of fire is associated with several traits in human behavior, namely the emergence of a formal organization of the living space visible in virtually all human societies today. As such, hearths are thought as one of the traits that allow archaeologist to decipher the timing (or timings) linked to the emergence of modern behavior in early *Homo sapiens* communities in Africa (McBrearty and Brooks, 2000). Chapters 3 and 4 apply soil micromorphology to the study of anthropogenic derived sediments, specifically fire-associated deposits. **Chapter 3** investigates the nature and integrity of combustion features related to the MSA occupations at Contrebandiers Cave. The micromorphological methodology employed here, complemented by FTIR analyses, was an essential tool to overcome the disturbed, burrowed nature of combustion-associated sediments. This micro-scale view provides relevant windows of analyses that attest to the discrete, ephemeral nature of the hearths, and the characterization of the main pyrotechnological features employed by early modern human habitants at the site. It is

possible to ascertain the modification of the original microstratigraphic arrangement of the combustion features due, in this case, to both human and predominantly biogenic actions. Moreover, the microscopic resolution allows for the discrimination between hearth remnants and natural deposits that, superficially, resemble anthropogenic features. Deciphering the nature of combustion remains is not a straightforward task and it is best achieved at high-resolution microscopic scales that incorporate a geological and sedimentological approach. With the notable exception of South African contexts (e.g., Goldberg et al., 2009; Wadley et al., 2012), micromorphology research, or similar in-depth studies of fire residues, remain poorly developed in African contexts, but particularly in North Africa. We argue that if one is to make inferences about structuralization of the living space and putative associated distributions of Paleolithic activities, first and foremost the nature and integrity of the fire remains has to be fully understood.

Similar research, presented in **Chapter 4,** is conducted on the combustion features found at the Neandertal site of Roc de Marsal (France). Here, micromorphological approaches attest to the extremely well-preserved nature of the hearths located in the basal stratigraphic layers of the site, embedded in artifact-rich Neandertal occupations. Superimposed (mm-thick of smaller) discrete, in-place succession of fire events were easily recognizable in thin section, even though they were virtually undistinguishable in the field. Considering the almost 'pristine' state of preservation of the combustion episodes seen microscopically, this study then tests the distribution of hearth associated assemblages. The study is based on Geographical Information Systems (GIS) techniques to detect patterns of spatial distribution of the

archaeological assemblages, namely burned and unburned lithics. Our results show that traditional, and widely used, "*décapage* technique" of excavation – that is, exposing features and archaeological materials over a theoretical penecontemporaneous surface – is inappropriate for accessing any type of potential spatial organization. Moreover, in many cases it can lead to false impressions, simply because a reliance on macroscopic field observations alone is insufficient to document the complexity of the archaeological record. Thus, in spite of the fact that the hearths at Roc de Marsal were minimally affected by post-depositional disturbances, the problem remains of how to separate distinct occupational events around them. This research highlights the complexity of studying hearth related features and the necessity of developing more in-depth geoarchaeological levels of analysis to address questions about prehistoric spatial patterning related to past human behaviors.

Concluding Remarks

In addition to the chapters presented in this thesis, I have also contributed to three other papers, namely:

1) *"New Excavations at the Site of Contrebandiers Cave, Morocco",* submitted to Paleoanthropology journal. Authors: Harold L. Dibble, Vera Aldeias, Esteban Alvarez-Fernández, Bonnie Blackwell, Emily Hallett-Desguez, Zenobia Jacobs, Paul Goldberg, André Morala, Michael C. Meyer, Deborah I. Olzsewski, Kaye Reed, Denne Reed, Teresa E. Steele, Daniel Richter, Richard G. Roberts, Dennis Sandgathe, Utsav Schurmans, Anne Skinner, Mohamed El-Hajraoui.

This publication reports on the combined study developed by the multidisciplinary team of research at Contrebandiers Cave, presenting the main results obtained from several lines of evidence, namely an overview of the excavations, the stratigraphic sequence of the site, detailed data on lithic and fauna assemblages and preliminary results from chronometric dating of the deposits. From the geoarchaeological point of view, the goal of developing a site-wide description of the stratigraphic succession of the cave site was achieved. The various stratigraphic units were isolated and identified on the basis of basic principles of lithostratigraphy, taking into account sedimentological criteria (color, grain-size, texture, sorting, compaction, sedimentary structures, thickness, etc.), as well as the presence of unconformities and/or erosional

boundaries. This work allows for the correlation of the stratigraphic framework across the several exposed profiles at the site and its correspondence with previous, succinctly published stratigraphic descriptions (Bouzouggar, 1997; Niftah, 2003; Roche, 1976; Roche and Texier, 1976). Thus, these results provide the basic contextual framework and relative stratigraphic chronology of the site, on which the study of the archaeological content and features can be built.

2) *"Single-grain OSL dating at La Grotte des Contrebandiers ('Smugglers' Cave'), Morocco: Improved age constraints for the Middle Paleolithic levels"*. Authors: Jacobs, Z., Meyer, M.C., Roberts, R.G., Aldeias, V., Dibble, H., El Hajraoui, M.A.; published in (2011) Journal of Archaeological Science 38, 3631-3643.

This paper presents the results of chronometric dating of Contrebandiers Cave sequence developed using single-grain Optically Stimulated Luminescence (OSL). The obtained ages suggest that the time span of deposition was between ~126 and 95 ka ago, with the MSA occupations being restricted to the interval from 120 to 90 ka (MIS 5d to 5b). OSL dates for the bedrock in which the cave was formed suggest that the deposition of the calcareous sandstone falls within MIS 11 limits (~400 – 350 ka). The developed collaborative work allowed for the integration of aspects related to site formation to the dating methodology. Specifically, some of the major geological and biogenic post-depositional processes were considered, such as: (1) the frequent incorporation of older

bedrock-driven grains into the cave's sedimentation; and (2) intrusion of younger grains by vertical movement due to the pervasive bioturbation affecting the deposits. These geoarchaeological-driven processes, in combination with the single-grain technique employed by Jacobs et al. (2011), allow for the rejection of individual grains that, if used, would have resulted in an overestimation (roof fall contamination) or underestimation (bioturbation) of the sedimentary ages.

3) "*On the industrial attributions of the Aterian and Mousterian of the Maghreb*", submitted to Journal of Human Evolution. Authors: Harold L. Dibble, Vera Aldeias, Zenobia Jacobs, Deborah I. Olzsewski, Zeljko Rezek, Sam C. Lin, Esteban Alvarez-Fernández, Carolyn C. Barshay-Szmidt, Emily Hallet-Desguez, Kaye Reed, Denne Reed, Daniel Richter, Teresa E. Steele, Anne Skinner, Bonnie Blackwell, Ekaterina Doronicheva, Mohamed El-Hajraoui.

This study deals with the interpretation and nature of North African Late Pleistocene industries. This research stems from our work at Contrebandiers Cave and leads to the questioning if there is, in fact, justification for continuing to distinguish between the two stone tool industries identified in North Africa – the Aterian and the Mousterian –, and their broader affiliation with either the Late Pleistocene African industries (MSA) or the Middle Paleolithic of western Eurasia. We argue, based on overlapping of stone tool characteristics and absolute ages of sites across North Africa,

that Aterian and Mousterian assemblages are simple variants of the same archaeological entity. We additionally propose that their traditional attribution to the Eurasian Middle Paleolithic is related to historical research bias, and that, conversely, these are in fact closely affiliated with the broadly pan-African MSA-type of industries. This research is significant in trying to understand the overall context in which modern humans developed before their diaspora out of Africa, and it lays out testable hypothesis for future archaeological research.

APPENDIX I: CHAPTER TWO SUPPLEMENTARY MATERIALS

The Stratigraphic Sequence at Contrebandiers Cave

The correspondence between our lithostratigraphic nomenclature and previous published stratigraphic descriptions by Roche and Texier (e.g., 1976) is presented in Table S1. Industrial attributions, with both Aterian and the so-called "Mousterian" considered as Moroccan variants of the pan-African Middle Stone Age, are based on results published in Dibble et al (submitted).

Central Excavation Area

Six major lithostratigraphic units are distinguished in the CEA. These units are, with minor exceptions, comparable to the archaeological layers. From bottom to top, the units are as follows:

Unit A (Archaeological Layer 7): 12 to 26 cm thick. Tabular lithostratigraphic unit characterized by reddish brown (5YR 5/4) with brownish yellow mottles (10YR 6/6) shell-rich sands that vary from loose to strongly cemented towards the base. This cementation of Unit A makes its distinction from the cave's floor difficult to establish in certain areas. Overall, the deposits are massive or with discrete horizontal internal bedding, moderately sorted, with rare well-rounded cm-size calcarenite clasts (<7 cm); interstitial red clays and foraminifera were observed. A large (>1m) calcarenite block is visible in the profile of squares K 21/22. These deposits constitute the basal sediments in

the cave and have an apparent dip towards the entrance of the cave, following the natural inclination of the bedrock. Localized bioturbation is visible (typically with diameter of roughly 1.5 cm, with some of which likely due to wasps), which may be responsible for the gradual contact with the overlying deposits, and common incorporation of the coarse grains in the above strata. No archaeological material was observed within this unit in the field, although mm-size bones and coprolites were identified in thin section.

Unit B (Archaeological Layer 6c): ~30 cm thick. Moderately loose yellowish red (5YR 4/6) with reddish brown areas (5YR 3/4) sandy clay, with occasional concreted areas and domains where weakly developed bedding is apparent. Presence of occasional calcarenite clasts (~ 7 to 15 cm), along with mm-size charcoal fragments. Lenticular indurated Fe/Mn-rich crusts roughly 1 cm thick were identified (specifically in squares J/I 18-16), as well as local phosphatization of the sediments. Anthropogenic inputs are present as discrete combustion areas, identified by ash and carbonaceous accumulations in association with artifacts (Moroccan MSA without tanged pieces), which is less frequent than in the above Unit D. Biological activity is represented by channels and mm-size plant roots. The lower contact is somewhat gradual with unit A.

Unit C (Archaeological Layers 6a/b*)*: can be subdivided into two subunits. *Subunit C1* is 45 to 60 cm thick, light brown (7.5YR 5.5/4) silty sands with interfingering darker yellowish brown (10YR 4/4) sediments that are laterally and vertically discontinuous. The presence of lenticular carbonate-cemented crusts is common throughout the unit (typically 3 to 5 cm thick), as are areas that are more phosphatic in nature. As in unit B, lenticular indurated Fe/Mn-rich crusts were identified, as for example in squares H17-18.

Overall, this unit has extremely rare human inputs in the excavated areas. *Subunit C2* is comprised of a heavily cemented and somewhat continuous indurated calcareous crust of variable thickness (typically 5 to 10 cm) that caps Unit C. Above Unit C the deposits dip more markedly in different directions. Its lower limit with unit B is diffuse. Similar industry as in Unit B.

Unit D (Archaeological Layers 5a, 5b, 5c, and 5d): is on average 80 cm thick. Its lower boundary with Unit C is sharply inclined, and Unit D seems to truncate Unit C in some areas. The unit is generally characterized as reddish brown silty sand, which can be subdivided into three main facies based on composition and color. Throughout Unit D the archaeological industry continues as Moroccan MSA without tanged pieces.

Subunit D1 (~45 cm thick) is a dark brown (10 YR 4/3) more organic deposit with abundant human inputs, namely charcoal specks, ashes, stone tools, shells, and bones. Human fossil remains were identified in this unit during the 2009 field season. The deposits are locally cemented, and cm to dm-size bioturbation is common, reflecting a clear increase in earthworm and wasp activity. The irregular nature of several of the cemented lenses shows that bioturbation occurred prior to the cementation of the deposits. Rock fragments >10 cm are rare, and when present, are mainly calcarenite.

Subunit D2 (~16 cm thick) is brown/dark brown (7.5YR 4/4), lighter than subunit D1, with rarer ash accumulations; the charcoal specks are smaller and scattered. These deposits are locally cemented by calcium carbonate.

Subunit D3 (~20 cm thick) is comprised of dark brownish deposits similar both in color and in composition to those in Subunit D1, although they lack ashy deposits, at

least in the excavated areas; human inputs continue to be frequent. Several dip directions can be recorded in Unit D: a general inclination towards the cave's entrance in squares J/K 19-16, and flattening in the area of K/L 20-22. In squares H18-15 and G18-16, Unit D seems to be dipping in the opposite direction, roughly towards the interior of the cave. The dips appear to be controlled by the presence of a swallow hole that was active in the area of squares G-H 15/13.

Unit E (Archaeological Layer 4): (thickness unknown because sediments were removed by previous excavations –the more extensively preserved deposits are 110 cm thick, e.g., squares J14-I14). The description of this unit throughout the site is hampered by the widespread excavations in the past, in addition to the presence of Neolithic pits that disrupt the deposits. The associated archaeological industry is Moroccan MSA with tanged pieces (Aterian).

Unit E is composed by reddish yellow (7.5YR 6/6) silty sands, which are overall extremely bioturbated. Mottled pockets consisting of slightly darker brown clayey silts are attributed to burrows. Dm-size roof spall occurs in several profiles throughout the site at the base of this unit, and towards its upper boundary in squares J-I 13-15. Besides these roof fall accumulations, clasts about ~5 cm in diameter occur locally in the Unit. Common human inputs (bones, shells, lithics) are present, as well as cm-size grass roots and localized calcite-cemented areas. The lower boundary with unit D is sharp, and Unit E seems to truncate the underlying deposits, at least in squares H-J/15-16.

Unit F (no archaeological equivalent): ~120 cm thick in squares K/L21 and K/L22. This unit consists of well-sorted orangey yellow fine silt with reddish domains, and exhibiting a stone line with clasts from 5 to 10 cm in diameter.

Excavation Sector IV

Excavation in this Sector, which is located on the northern side of Roche's main trench and thus independent from the other excavation areas, has descended only slightly more than a meter below the present surface. Only two main stratigraphic units have been identified there so far. From bottom to top, the units are as follows:

Unit G (Archaeological Layer IV-2). The unit has a wavy, somewhat concave geometry, with a sharp, truncated upper limit. Although the excavated area is limited, at least locally the upper limit is inclined toward the interior of the cave in squares E/F 22-21. Due to its geometry, Unit G varies in thickness from ~20 cm to ~80 cm, although its lower boundary was not reached during excavations. Overall, the deposits of *subunit G2* are crumbly pebbly silty sands characterized by a lateral variability in color - from light yellowish brown (10YR 6/4) to pale brown (10YR 6/3) - and stone abundance. The unit gradually varies from almost clast-supported (with stones typically in the 3 to 15 cm range) and ubiquitous shells in its concave area, to extensively cemented matrix-supported deposits towards North. Anthropogenic inputs are common, characterized by an Aterian stone tool assemblage, with abundant complete shells that occur locally in darker brown sediments within its concavity. Finally, slightly darker, well-indurated brown sediments, with rare ~5 cm stones occur towards the base of this Unit in squares

H21/20. These deposits are designated as *subunit G1* and have been only partially excavated; the contact and differentiation with G2 is not clear at present.

Unit H (Archaeological Layers IV-1a and IV-1b*)*, which is ~ 60 cm thick, unconformably overlies the sediments of Unit G in a cut/fill type of structure. The deposits are loose and moderately sorted; based on color and composition; they can be subdivided into two subunits. The color varies from yellowish brown (10YR 5/6, Subunit H2, Layer IV-1a, identified as Iberomaurusian pits by Roche 1976) to orange-brown silty sands (Subunit H1, Layer IV-1b*)*. Extensive fist-size roof spall is present in both subunits, and there is an increase of stones (usually smaller than 20 cm) in Subunit H1. The distinction between Subunits H1 and H2 is gradual and hampered by bioturbation, principally wasp cocoons. The origin of the 'pockets' that characterize subunit H2, and the overall erosional contact with unit G are still unclear at present. These are the only layers that contained Iberomaurusian, along with numerous bone fragments, and marine shells. The top of this unit was truncated by previous excavations.

Excavation Sector V

Sector V is a 2-m square test pit in the interior of the cave. Although only ~130 cm was excavated here, two main lithostratigraphic units were defined. Combined with somewhat distinct lithological characteristics, the roughly 5 m that separates this excavation sector from the central area of the cave precludes for the moment any attempt at direct correlation between the deposits. Consequently, the lithostratigraphic

nomenclature for this sector remains independent. Both units contain archaeological industries with tanged pieces (Aterian).

*Unit V-A (*Archaeological Layer V-2*)*: the lower limit of this unit was not reached during excavation. Currently, the unit is ~70 cm thick in the deepest areas. The deposits are loose dark reddish brown (2.5YR 3/4) to dusky red (10R3/3) silty sands with common charcoal specks; large dm-size roof spall blocks characterize the top of the unit. Anthropogenic sediments are expressed by the presence of features rich in charcoal and ash, the latter being diagenetically altered. Bioturbation is visible, including wasp cocoons. This unit is also distinguished by irregular yellow (2.5Y 7/6) clayey lenses that are discontinuous throughout the deposits, and there is a clear decrease in stones throughout in comparison with unit V-B.

*Unit V-B (*Archaeological Layers V-1a and V-1b*)*: varies in thickness from ~30 cm to 60 cm and overall dips towards the west. Based on color and composition differences, this unit was subdivided into two subunits, from bottom to top. *Subunit V-B1* (Archaeological Layer V-1b) is reddish brown (2.5YR 4/4) silty sand with abundant, ~15 cm darker brown mottles regularly distributed throughout the deposits. These darker mottles can largely be attributed to animal burrows, namely wasps and rodent burrowing, some of which are clearly recent. In addition, modern cm-size roots were also observed, providing further evidence of bioturbation in this area of the cave. This subunit is characterized by frequent stone lines (the stones vary from 5 to 15 cm in diameter), and by larger dm-sized blocks of roof spall that mark its lower boundary. The sediments are clearly phosphatic, often favoring the decalcification of the calcarenite stones, although

mm-size size shell fragments (probably from both marine mollusks and terrestrial snails) are observed. Anthropogenic inputs include stone tools and bone fragments. *Subunit V-B2* (Archaeological Layer V-1a) is dark reddish brown (2.5YR 3/4) moderately sorted fine silty sand, fairly loose and with occasional stones (5 to 10 cm in diameter) and mottles with darker coloration. These darker mottles are mainly due to reworking of the sediments by bioturbation, although some can also be attributed to phosphatization and local disaggregation of the roof spall. This subunit is better expressed in the grid south areas of squares K-L 7. The presence of irregular, roughly 1 cm thick, phosphatic and Fe-Mn indurated crusts is observed. These crusts pinch out towards north.

Archaeological Layers	Lithostratigraphic Unit	Roche (1976) Stratigraphy	Archaeological Industries
4a	F2	8?	Moroccan MSA with tanged pieces (Aterian)
4b			
4c			
4d	F1	9/10	
4e			
5a	D3	11a	Moroccan MSA without tanged pieces ("Mousterian")
5b	D2	11b	
5c	D1	11c	
5d			
6a/b	C2 (crust)	12	
	C1	13a/13b/13c	
6c	B	13d/14/15?	
7	A	16	Sterile

Table S1. Synthesis of the main stratigraphic sequence in the central excavation area of Contrebandiers cave with the correlation with previous published stratigraphy from Roche (1976). Terminology of the archaeological industries follows Dibble et al (submitted), in which it was proposed to drop the distinction between the Moroccan Aterian and Mousterian assemblages at Contrebandiers Cave and to consider them as a Moroccan variant of the pan-African MSA rather than as part of the western Eurasian Middle Paleolithic.

Sample No.	LU	AL	Sq.	ID	X	Y	Zctr	Zup	Zlow
010-6	H	IV1a and IV1b	F22	1215	6.498	22.817		-1.344	-1.472
09-29	H/G	IV1a and IV1b	E22	28	5.947	22.786		-1.374	-1.535
010-16	H/G	IV1b and IV2	F22	1304	6.736	22.832		-1.654	-1.794
09-28	G	IV2	I22	27	9.122	22.525		-1.336	
010-21	G	IV2b	I22	178	9.198	22.906	-1.493		
09-36	F	NA	L21	33	12.239	21.405		-1.800	-1.952
09-39	E/D3	4 and 5a	F17	17	6.970	17.331		-1.639	-1.788
08-5	E/D3	4 and 5a	E18	1	5.819	18.364	-2.263		
09-9	D3/D2	5a and 5b	G16	141	7.378	16.442		-1.879	-1.944
09-1	D3/D2	5a and 5b	K19	4	11.467	19.769		-2.433	-2.54
CB07-4	D2	5b	J18	407	10.784	18.43	-2.152		
CB07-2	D1	4c	J16	105	10.876	16.132	-1.1		
09-30	D1	4d	I15	26	9.509	15.017		-1.765	
010-4	D1	5c	J16	449	10.414	16.999		-2.258	-2.368
010-7	D1	5c	H16	85	8.221	16.264	-2.455		
010-11	D1	5c	J16	558	10.641	16.9944	-2.366		
010-12	D1	5c	H15	56	8.641	15.91	-2.534		
010-18	D1	5c	H16	168	8.153	16.265	-2.705		
010-24	D1	5c	H15	73	8.724	15.997	-2.695		
CB07-1	D1	5c	H18	147	8.643	18.43	-2.062		
CB07-3	D1	5c	J18	442	10.874	18.95	-2.545		
CB07-5	D1	5c	J19	38	10.917	19.014	-2.6		
09-2	D1	5c	K19	5	11.532	19.76		-2.668	-2.798
09-10	D1	5c	I16	232	9.822	16.332		-2.313	-2.414
09-33	D1	5c	I16	23	9.958	16.954		-2.481	
09-43	D1	5c	I16	237	9.415	16.735		-2.537	
010-22	D1	5c	I15	497	9.905	15.795	-2.559		
09-35	D1/C	5c and 6	I16	24	9.856	16.914		-2.497	-2.605
09-22	D1/C	5c and 6	K20	36	11.999	20.086		-2.903	-3.114
010-19	C	6a	I16	550	9.833	16.93	-2.812		
010-23	C	6a	H16	179	8.167	16.968	-2.686		
08-4	C	6a and	J17	907	9.965	17.446	-2.819		

		6b							
09-4	C	6a and 6b	J19	306	10.969	19.696		-3.145	-3.360
08-2	C	6b	J18	507	10.361	18.875	-2.971		
08-3	C	6b	J18	530	10.282	18.721	-3.171		
010-13	B/A	6c and 7	H17	393	8.812	17.144	-3.489	-3.363	
09-24	B/A	6c and 7	G17	19	7.961	17.645		-3.278	-3.484
09-41	B/A	6c and 7	J17	25	10.380	17.994		-3.342	-3.505
08-1	B	6c	J19	273	10.821	19.091	-3.45		
010-2a	B	6c	G18	39	7.103	18.275	-3.211		
010-2b	B	6c	G18	38	7.103	18.263	-3.144		
010-9	B	6c	J17	1126	g	17.681	-3.133		
010-10	B	6c	I15	480	9.725	15.802	-2.504		
09-21	B	6c	J21	16	11.866	21.361		-3.525	-3.711
09-25	B	6c	K20	35	12.018	20.685		-3.568	-3.792
09-27	B	6c	J21	34	11.851	21.626		-3.284	-3.467
09-5	B	6c	J19	307	10.957	19.742		-3.415	-3.524
09-27bis	B	6c	K21	34b	11.851	21.626		-3.284	-3.467
09-42	V-B	V1a	L6	21	12.211	6.991		-1.073	
09-37	V-B	V1a and V1b	L7	30	12.224	7.005	-1.269		
09-38	V-B	V1b	L7	29	12.180	7.119		-1.276	-1.394
010-5	V-A	V2	L8	555	12.434	8.825	-1.946		
010-17	V-A	V2	L7	506	12.531	7.789	-2.029		
010-20	V-A	V2	K8	742	11.665	8.104	-2.297		
010-25	V-A	V2	L8	781	12.047	8.121	-2.29		

Table S2: List of samples collected for soil micromorphology. LU = Lithostratigraphic Unit; AL = Archaeological Layer; Sq = Square; Zctr = z value taken in central part of samples; Zlow = Z value taken lower part of sample; Zup = Z value taken upper part of sample.

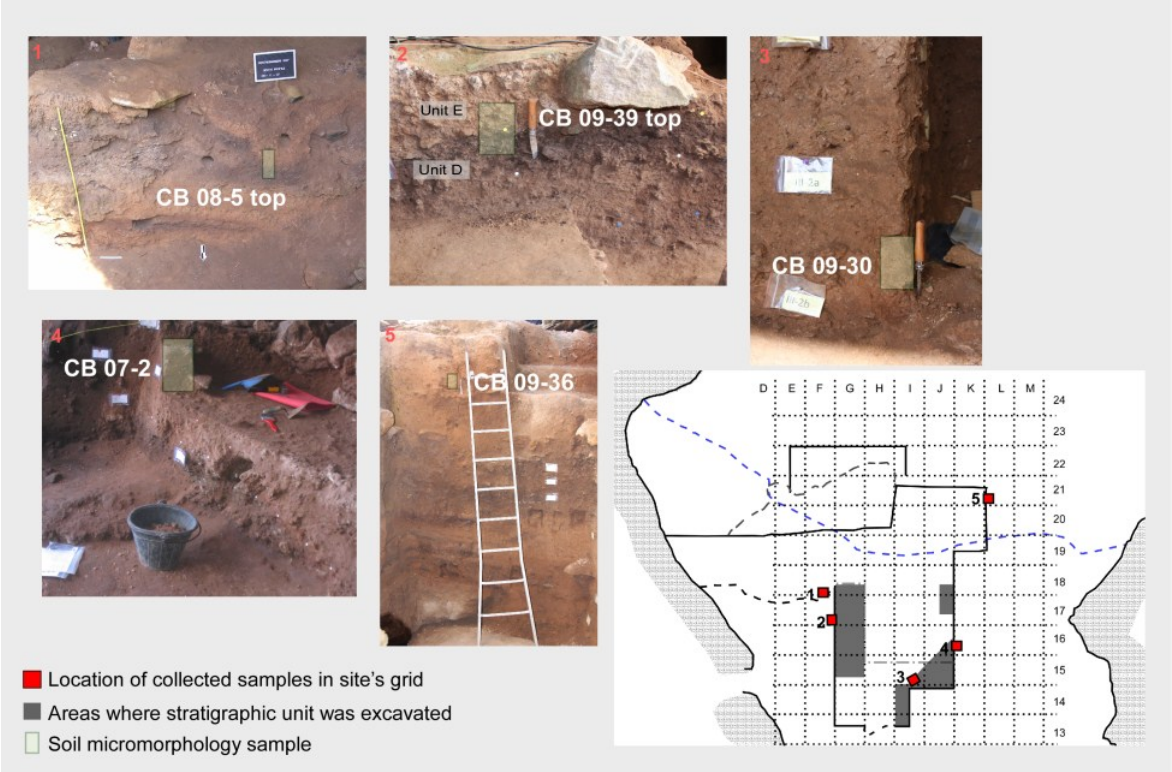

Figure S1: Location os samples collected from Unit E/F

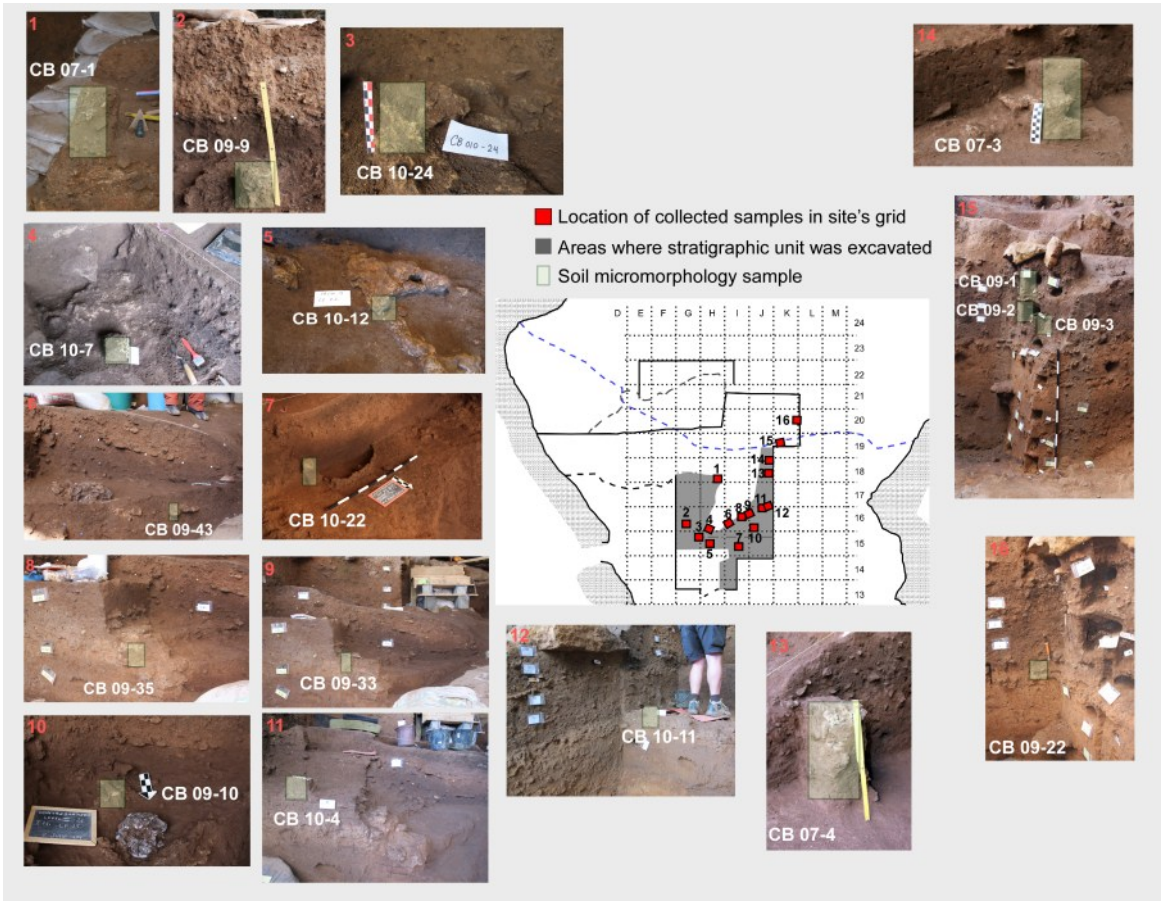

Figure S2: Location of samples collected for soil micromorphology from Unit D.

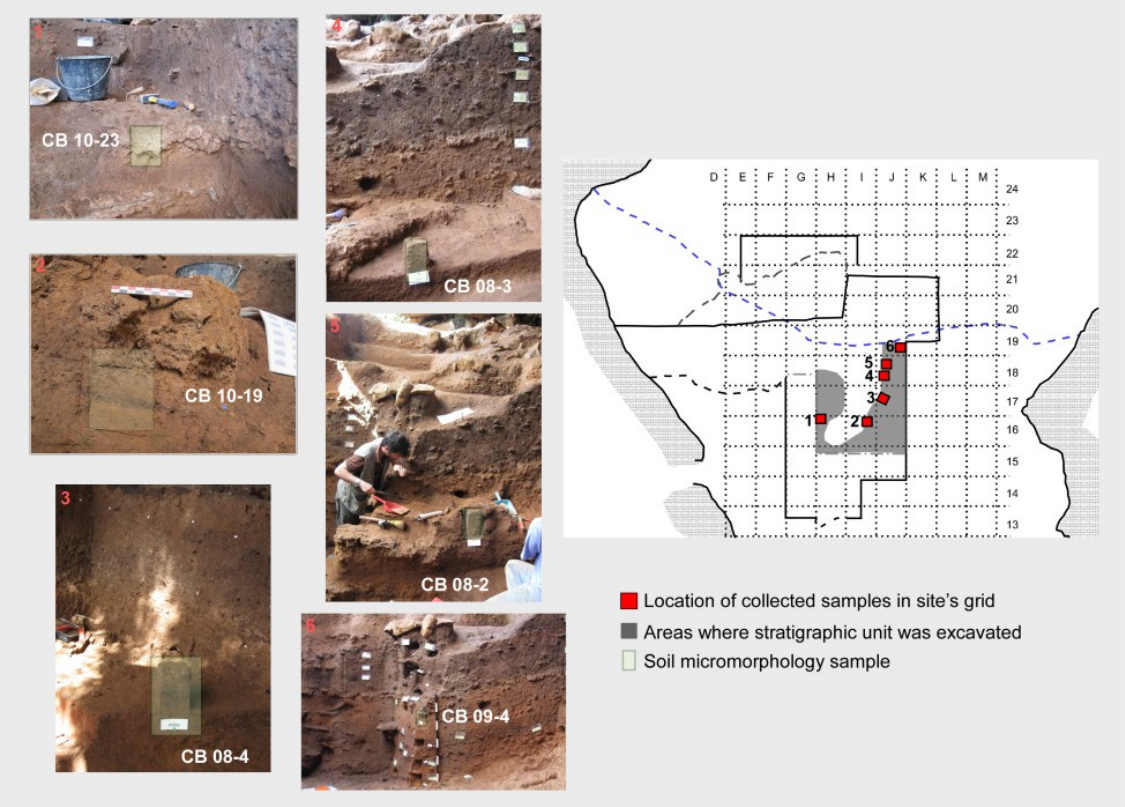

Figure S3: Location of samples collected for soil micromorphology from Unit C.

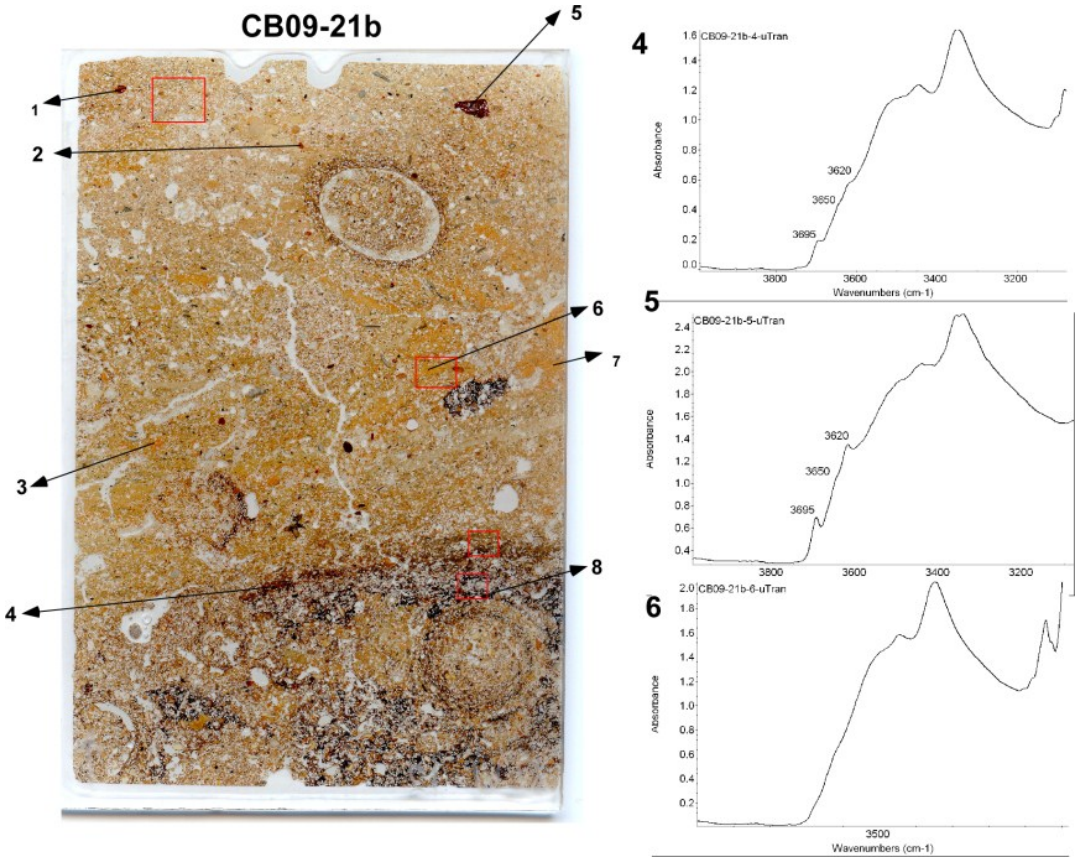

Figure S4: (left) Macrophotograph of Sample 09-21b with the arrows and number showing the location of FTIR spectra taken. (Right) Examples of the FTIR spectra taken – the numbers (4-6) correspond to the locations in the macrophotograph.

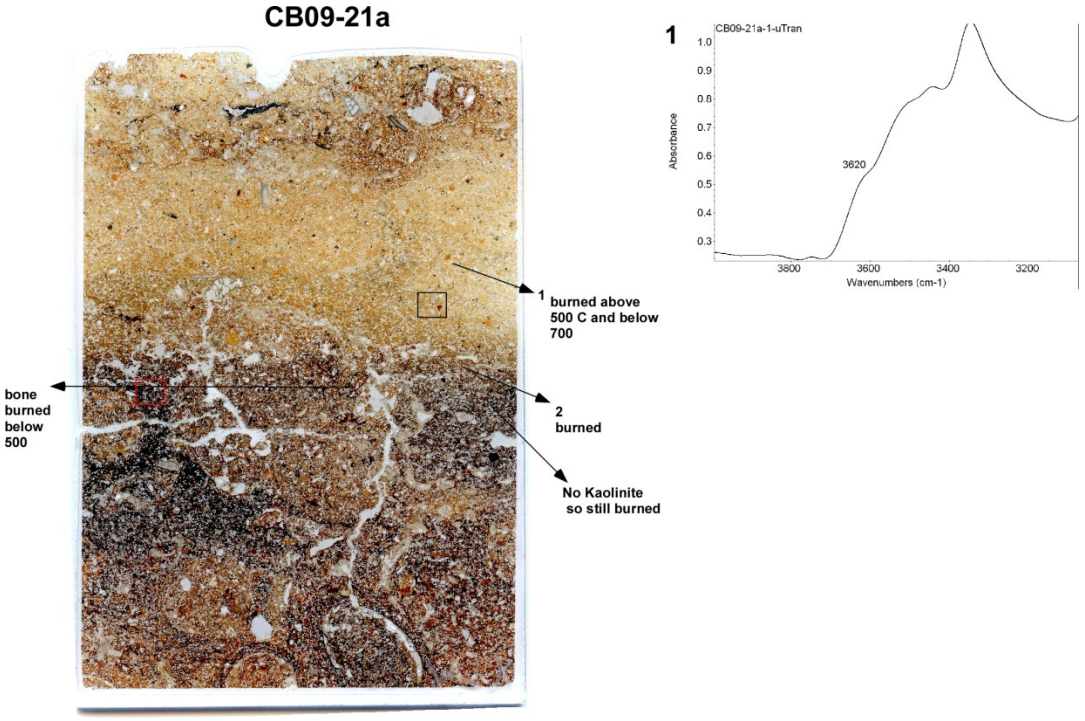

Figure S5: (left) Macrophotograph of Sample 09-21a with the arrows and number showing the location of FTIR spectra taken. (Right) Example of the FTIR spectra taken – the number correspond to the locations in the macrophotograph.

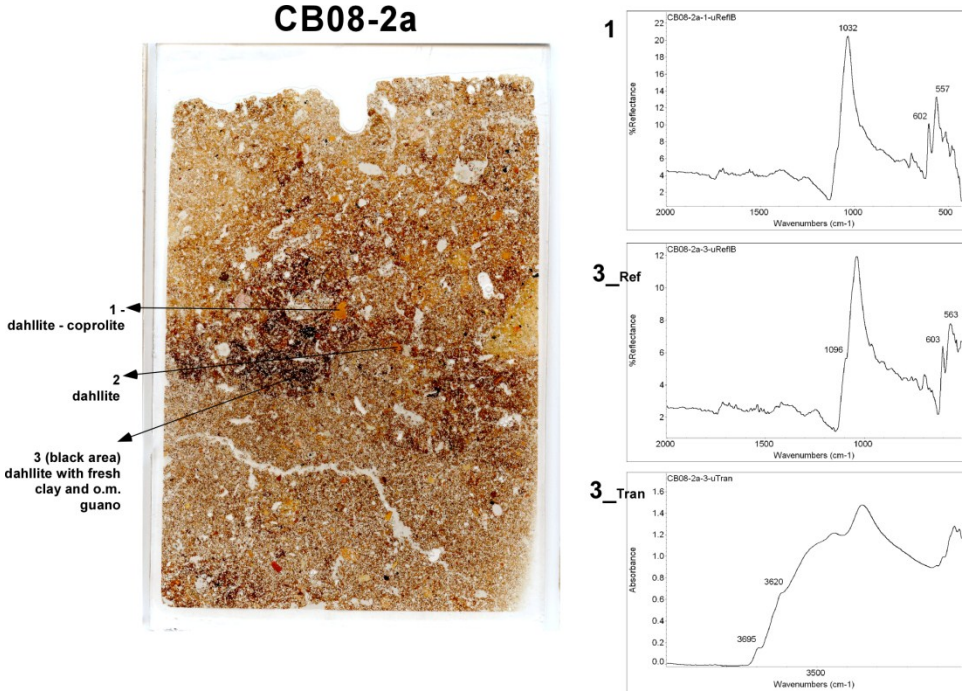

Figure S6: (left) Macrophotograph of Sample 08-2a with the arrows and number showing the location of FTIR spectra taken. (Right) Example of the FTIR spectra taken – the number correspond to the locations in the macrophotograph and Reflective (Ref) or Transmitted light (tran).

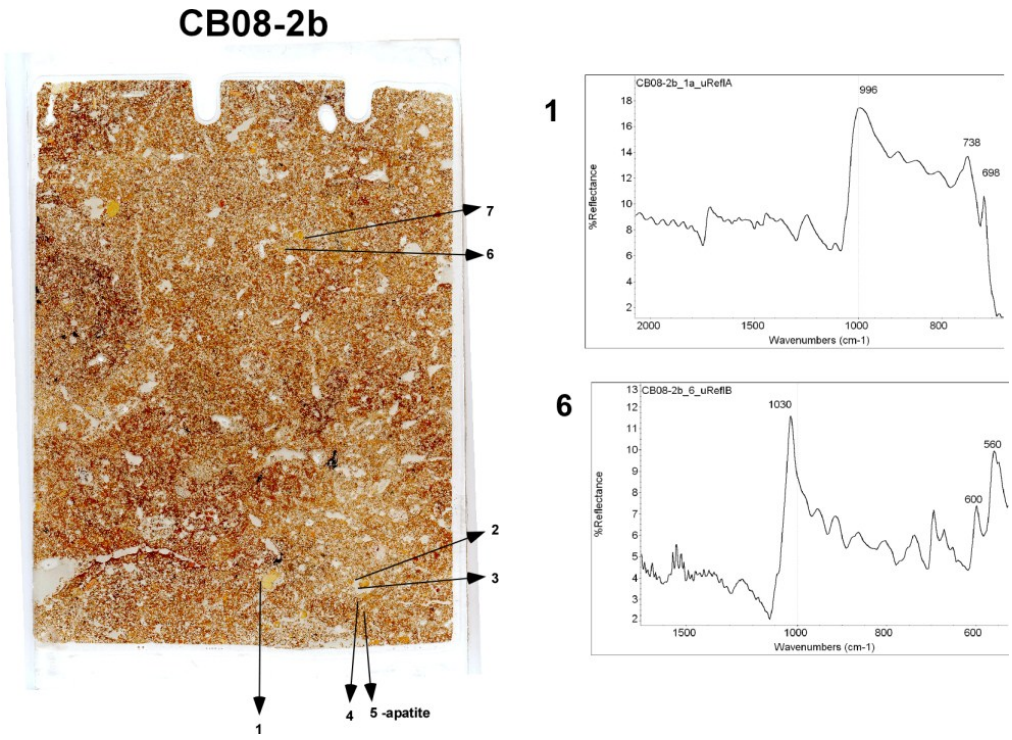

Figure S7: (left) Macrophotograph of Sample 08-2b with the arrows and number showing the location of FTIR spectra taken. (Right) Example of the FTIR spectra taken – the number correspond to the locations in the macrophotograph.

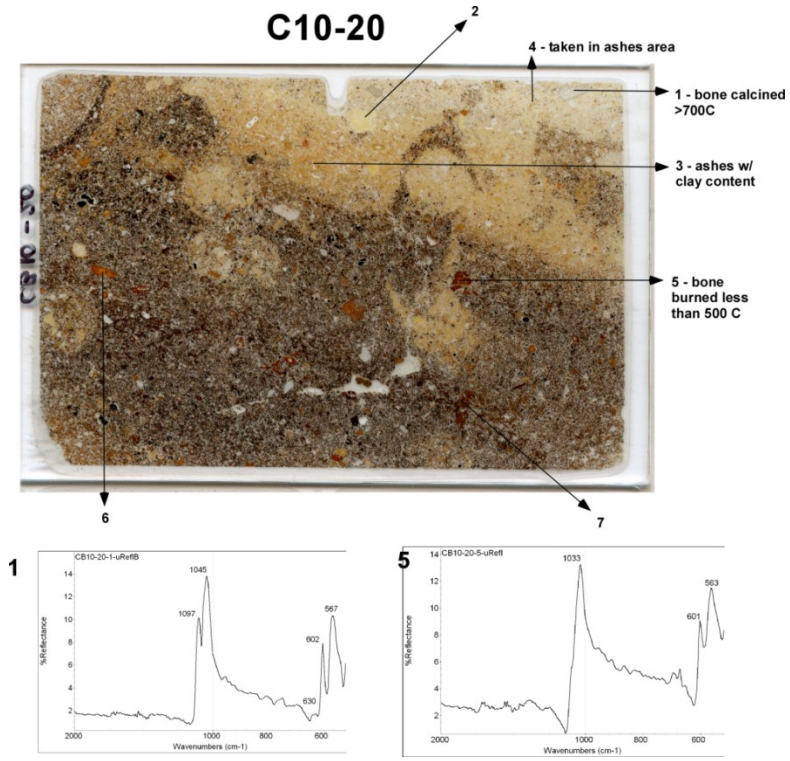

Figure S8: (top) Macrophotograph of Sample 10-20 with the arrows and number showing the location of FTIR spectra taken. (bottom) Example of the FTIR spectra taken – the number correspond to the locations in the macrophotograph.

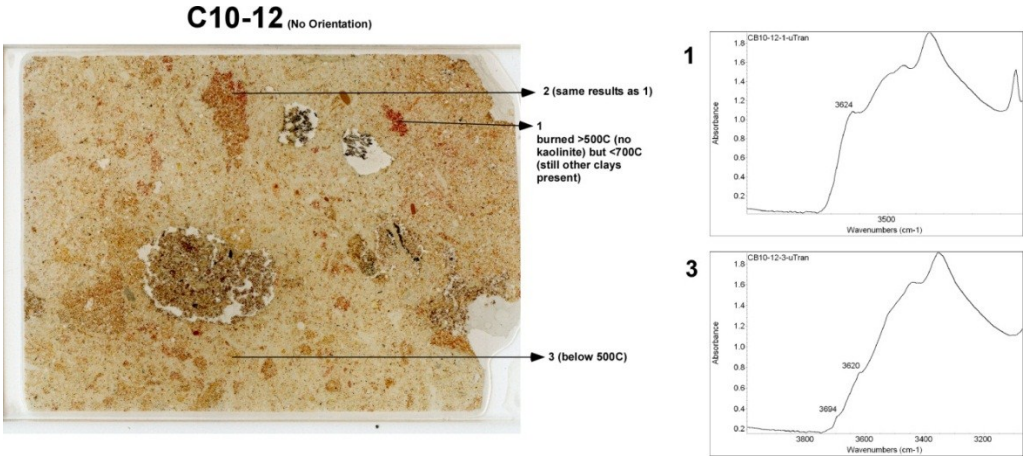

Figure S9: (left) Macrophotograph of Sample 10-12 with the arrows and number showing the location of FTIR spectra taken. (Right) Example of the FTIR spectra taken – the number correspond to the locations in the macrophotograph.

APPENDIX II: CHAPTER FOUR SUPPLEMENTARY MATERIALS

Detailed Description of Selected Combustion Features

As outlined in the text, limitations on space make it impossible to include the analysis of all 22 combustion features here, and therefore a small sample was selected for which more detailed analysis was carried out and is presented below. The sample was selected so that the apparent variability among all combustion features was represented, including those from both AL7 and AL9. The location of each combustion feature in the site is provided in figures S1, S2, and S3. In addition to field descriptions, we add both micromorphological and FTIR data when available.

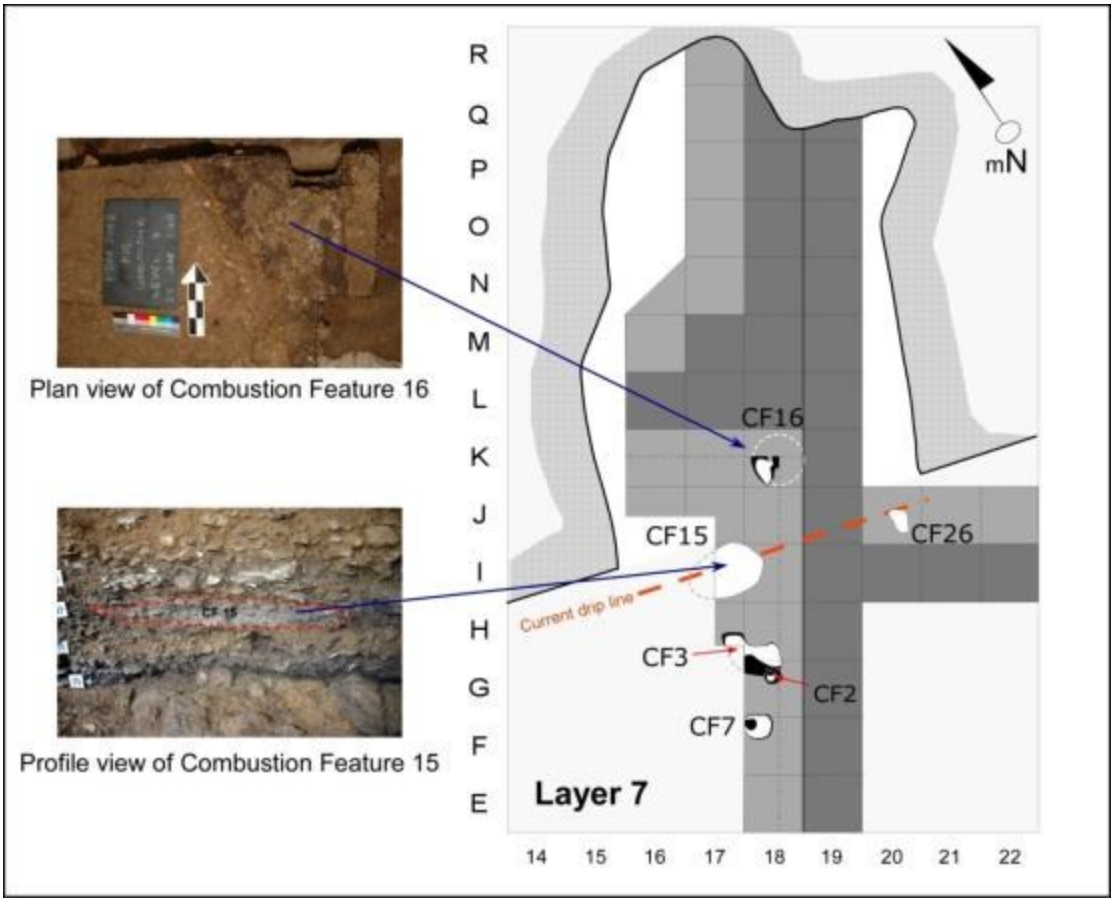

Figure S1: Map showing the location of CFs 15 and 16 in archaeological layer 7 (right), and field photographs of these CFs (left). CF 15 is comprised by a thick lens of cemented ash, better visible in profile and has been interpreted as a ash dump. CF 16 is characterized by the presence of several trampled and burned bones and flint artifacts, but lacks an ash component.

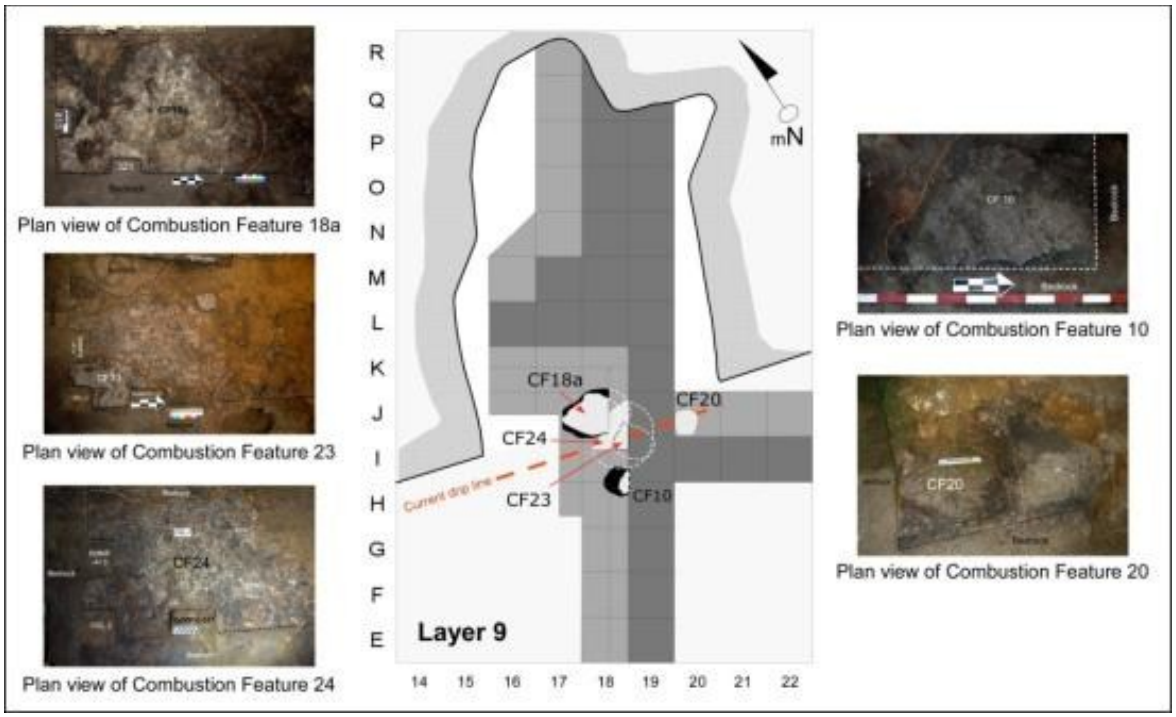

Figure S2: Map showing the location of CFs in archaeological layer 9 (center), and field photographs of each CF (left and right). As visible in the photographs, all the CFs are easily distinguishable by a white ash component. Note the abundance of burned artifacts, for e.g. in CF 24. The superimposition of combustions in the site is visible in the cave's map.

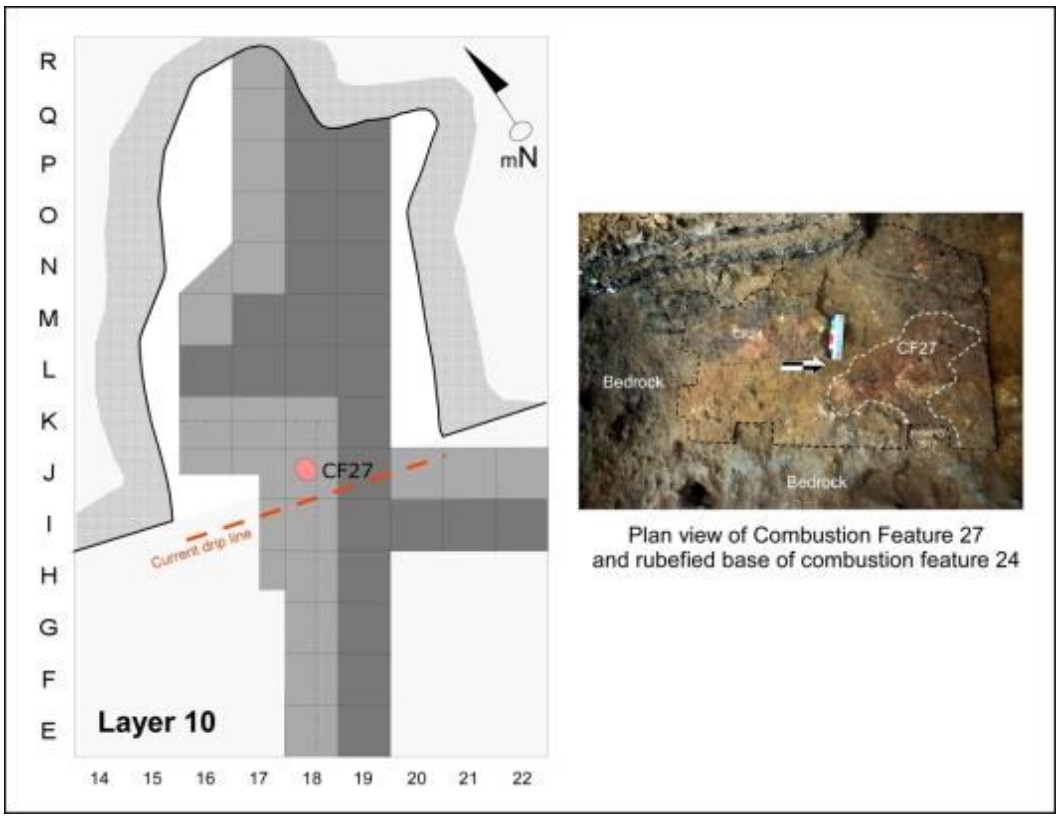

Figure S3: Map showing the location of CF 27 in archaeological layer 10 (left), and field photographs (right) showing the rubified sediments associated with this feature. The lack of ash and charcoal lenses on CF 27 attests to post-depositional loss of these components.

Intact, In-Place Combustion Features

Combustion Feature 10 (AL9)

CF10 represents an intact combustion feature lying on a base of rubefied sediments. A particularly clear view of the feature is shown in micromorphology **sample 218** (Figure S4; see also Goldberg et al. in press) which comes from square H18 along the entrance section within AL9. In the field, this is a large well-preserved discrete cemented ash lens and charcoal lens that sits just above bedrock; a semi-circular limit was defined on the basis of the cemented ash on top of the zone. This combustion zone is

adjacent to and in between combustion feature 5 and combustion feature 4. Below the main horizon of ash and charcoal is a second, smaller area of ash, which suggests this zone preserves two independent superimposed combustion events. As a whole, CF10 included both unburned (n=10) and burned lithics (n=27).

A much more nuanced and detailed view of these deposits can be seen in thin section (Figure S4) where it is possible to divide the feature into a number of subunits:

Subunit 6 – Brown partially dissolved calcitic ashes with brown Fe-Mn staining, fragments of yellow and charred bones (IR shows some are partially calcined), and elongated domains of isotropic phosphate and dissolved bones.

Subunit 5 – Compact, bedded whitish calcitic ashes mixed with bone fragments (FTIR shows both calcined and non-calcined bone, but with completely calcined bone at the top), flint, yellow isotropic nodules (FTIR peak at 1070 cm^{-1}), and a few rubefied soil inclusions (IR shows no kaolinite or smectite/illite). The ashes exhibit organic and Fe-Mn staining.

Subunit 4 – Calcitic ashes mixed with charred organic matter and yellow bone fragments (IR shows no calcined bone).

Subunit 3 – Calcitic ashes mixed with sand and rubefied soil aggregates (FTIR shows no kaolinite or smectite/illite; temperature >700° C), yellow bone (not calcined - FTIR) and pale yellow (calcined - FTIR) bone.

Subunit 2 – Bright reddish brown, with fine fraction composed of dispersed calcite aggregates (ashes?) impregnated with fine bright reddish brown clay (FTIR shows kaolinite + smectite/illite and calcite). The coarse fraction is composed of quartz sand,

bone fragments (FTIR = most are not calcined), limestone (some dissolved), and rubefied nodules/soil aggregates (FTIR shows no kaolinite and some only with smectite/illite).

Subunit 1 – Dark reddish brown, with fine fraction composed of fine sand mixed with yellow to reddish orange silty clay (FTIR= kaolinite + smectite/illite and calcite). The coarse fraction is composed of quartz sand, yellow bone fragments (most not calcined), and limestone, some of which are dissolved and phosphatized.

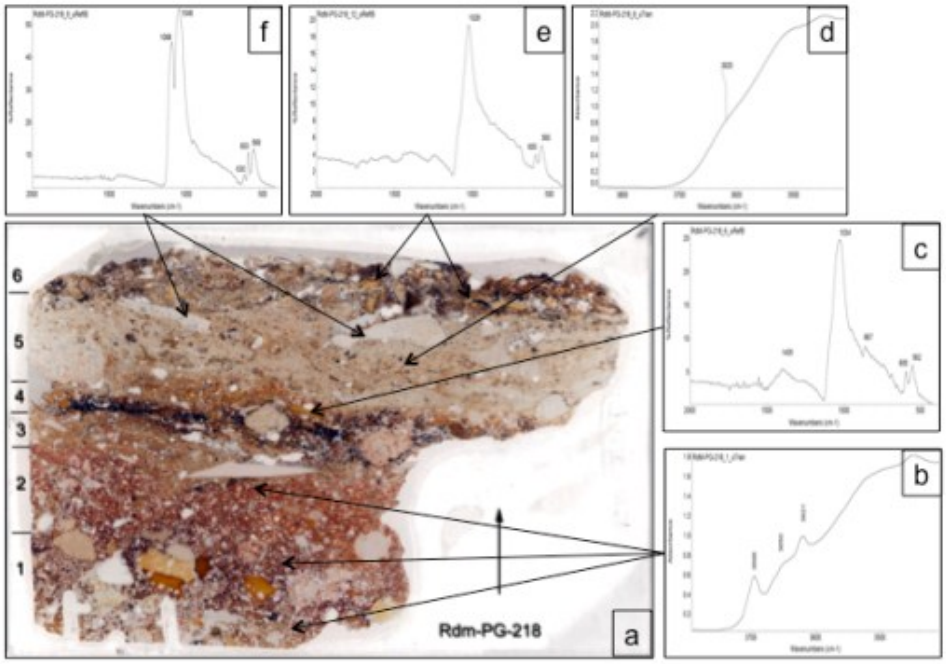

Figure S4: Sample 218 from Roc de Marsal (modified from Goldberg et al., in press). (a) Scan of thin section (50 x75 mm) showing several subunits expressed by change in color and composition. PPL. The surrounding boxes are FTIR spectra of bone and other materials with arrows pointing to their position in the slide. (b) IR spectrum of fine soil material showing IR absorption of kaolinite and smectite/illite at 3695, 3650, and 3620 cm^{-1}; (c) IR spectrum of charred bone which is composed of slightly recrystallized dahllite, thus indicating that it was heated a temperature below 500 °C; (d) IR spectrum of rubefied soil particles in calcitic ash layer (unit 5) indicating the absence of kaolinite peak at 3695 cm^{-1} and a weak absorption at 3620 cm^{-1}; it fits with soil having been burned between ca. 420° and 700 °C; (e) IR spectrum of isotropic yellow material from bone dissolution with characteristic IR absorptions of dahllite; (f) Characteristic IR spectrum of bone fragments in calcitic ashes of unit 5; shown here are strong OH absorptions at 630 and 1095 cm^{-1}, which indicate that large portions of the bone have been transformed from dahllite into hydroxyl apatite; thus the bone fragments are extensively calcined.

The above demonstrates that this sample represents at least one major structured intact combustion feature and the remains of another (shown by the ashes in subunit 3). A darker brown basal sandy clay (subunit 1), constitutes the remains of karstic infilling in the cave, and grades into a brighter red clay (subunit 2), which appears reddened from burning. The thin ashy layer of subunit 3 separates it from the overlying organic-rich layer of subunit 4. Thus is appears that the fire event that produced the rubefication is associated with the thin ashes of subunit 3 and not the subsequent burning episode that is represented by subunits 4 and 5, which would appear to represent an in situ hearth. If this scenario is correct, it suggests that the upper part of subunit 3 is truncated and some of it is missing. Subunits 4 and 5 appear to represent a major burning event that not only resulted in the accumulation of ashes (subunit 5) but also the calcined bone at the top of the subunit. Interestingly, subunit 6 rests on phosphatized subunit 5, which is partially dissolved and exhibits limited replacement of calcareous ashes by apatite. In consequence it is evident that after the combustion event associated with the ashes of subunit 5, this ashy combustion feature was exposed for some period of unknown duration and was diagenetically altered during this period. Thus, the contact between subunits 5 and 6 is an unconformable one, representing a certain gap in time and abandonment of the cave. The significance of subunit 6 is difficult to evaluate, as it is so thin.

Combustion Feature 18a (AL 9)

CF18a was one of the most complete features within the area excavated during the recent project (although the extreme western and eastern edges were not within the

current excavation area it was apparent that over 90% of the feature was present). It was also one of the largest features, spanning 125cm north-south and likely around 125-150 cm east-west. In the field it was difficult to identify the exact southern limit of CF18a relative to CF18b due to some spatial overlap at their extremities. Together, these two features were recognized as being among a series of more-or-less intact, in-place combustion features that had been constructed in the same location over time and thus occurred in the deposits as a series a superimposed (stacked) charcoal/ash lenses. Visually, this series included at least CF18a/18b, CF23, and CF24.

CF18a included an upper ash component with very fragmented, burned and calcined bone, most of which were trampled and clearly broken in situ. Beneath the ash was a black (charcoal, burned bone) component that. Both components included burned (n=99) and unburned lithics (n=67).

Micromorphology [Samples 517, 517bis and upper 518]

Examination in thin section (**Samples 517 and 517bis**) indicates that, in fact, CF18a is composed of two distinct, centimetric, superposed combustion features. The upper one [(I) in Figure S5] was exposed on the surface during the excavation and consists of interspersed burned bone, charcoal, and reddish brown charred organic remains; burned bone is relatively rare. The remains of phosphatized ash occur localized only in one small area of the slide in the upper left (they were ground off the slide during manufacture). This feature, and in fact much of the sediments, including the underlying feature II, were modified by significant localized bioturbation, presumably by earthworms. Such activity hinders the recognition of the original aspects of the combustion features.

The lower combustion feature [(II) in Figure S5] has isolated mm diameter clumps of ash that rest on relatively intact mm-thick layer of bone and charcoal. In turn, the latter overlies a discontinuous layer of largely rubefied silty sand locally enriched in clay. Traces of phosphatic (e.g., hyaena?) coprolites were observed. Here, too, bioturbation has effaced much of the original structure of the combustion feature.

Combustion feature 18a also occurs in **Sample 518**, which is overall similar, particular with regard to bioturbation. However, charcoal is more abundant and larger (mm-size). The uppermost part is rich in bone (exhibiting various degrees of burning) with isotropic yellow brown (phosphatic?) matrix. This coarser layer overlies a slightly more compact one with finer bone and charcoal fragments, as well as yellow brown organic matter. This latter layer rests on bioturbated, rubefied silty sand mixed with bone and some charcoal fragments.

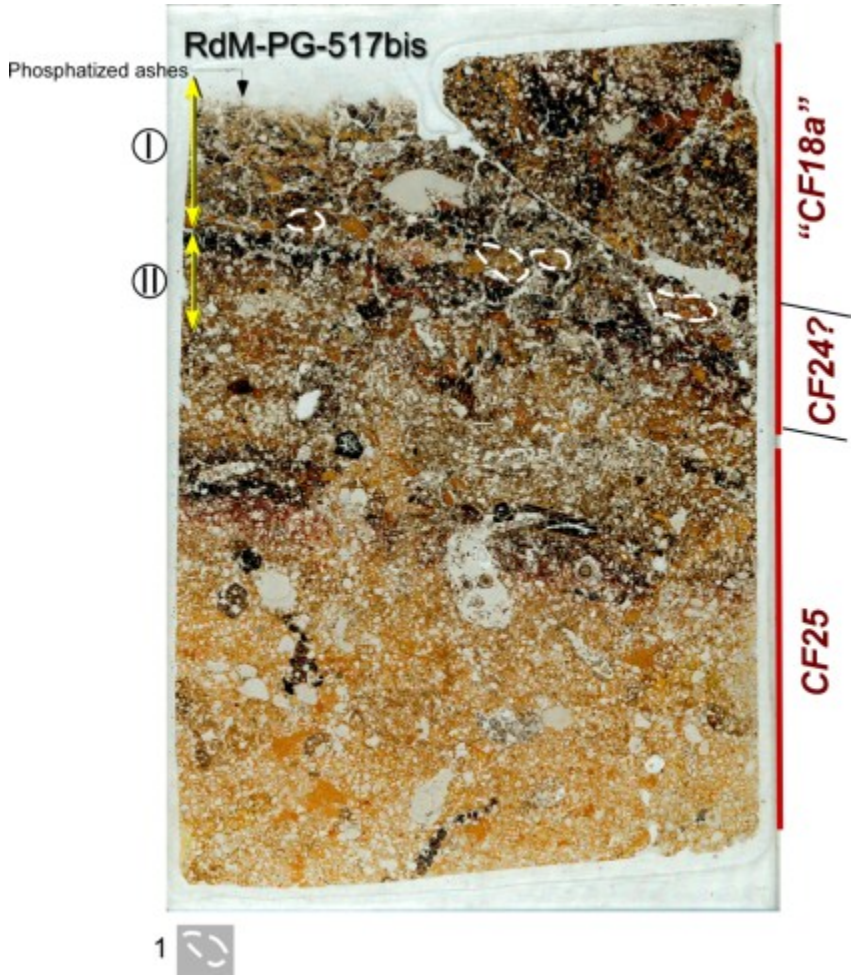

Figure S5: Thin section scan of sample 517bis showing the centimetric superimposition of at least three distinct combustion events. CF 18a, in the upper part of the photograph [designated as (I)], is composed by phosphatized ash superimposing burned bone, charcoal and charred organic remains. In turn, these sediments are superimposed on another combustion feature [designated as (II)] charachterized by isolated clumps of ash overlying layer with bone, charcoal and discontinuous rubified silty sands. Based on field observations, these latter sediments are possibly associated with CF 24. The original structure of the fires is locally modified by bioturbation, which may have contributed to the disrupted nature of ashes in layer (II), for example. PPL; 1= clumps of ash; length of thin section = 75 mm.

Combustion Feature 23 (AL 9)

Combustion Feature 23 is second from bottom of the series of stacked features in basal AL9 in units I18, I19, J18 and J19. It is situated stratigraphically below CF18a/18b (and spatially to the south of 18a) and above CF24. Only a small portion of CF23

occurred within the current excavation area so determining its size is not possible (most of the feature extended east into squares I18 and J18 and was removed during Lafille's excavation). Based on the radius of the remaining portion it was likely a smaller feature than CF18a and CF24.

It included an upper ash component with very fragmented, burned and calcined bone, most of which were trampled and clearly broken in situ. Beneath the ash was a black (charcoal, burned bone) component that. Both included burned (n=7) and unburned lithics (n=17).

The vertical limits of CF23 were easily distinguished in the field from 18a and 24 because the components of each feature (a lower black lens and an upper white lens) were in such contrast to each other. During the excavation of each feature, as the lower black component was removed it clearly exposed the white ash component of the feature below it.

Combustion Feature 24 (AL 9)

Combustion Feature 24 is an almost complete (in terms of spatial limits), intact, and in place feature. It is the bottom (below CF18a at its western side and below CF23 at its southeastern edge) in a clearly defined series of stacked features in squares I17/I18/J17/J18. Spatial limits are clearer than some upper features that were much less complete, and vertically it was also clearly a discrete feature.

It includes an upper ash component with very fragmented, burned/calcined bone, much of which is trampled and broken in situ. Beneath the ash is a black (charcoal, burned bone) component. Both included burned (n=20) and unburned lithics (n=14).

Below the black layer is a clear zone of rubefied substrate in AL10, but clearly associated with CF24 in AL9 (i.e., CF24 was constructed directly on top of AL10. The rubefied sediments occur as zones of varying degrees of reddening; with a striking, bright orange patch (beneath the central area of CF24) surrounded by a weaker reddish zone, which is surrounded by weakly orange-grey sediments (see Figure S3). Presumably these zones reflect decreasing intensity of heat away from the centre of the fire feature.

Micromorphology [Samples 413B; 518 lower, 520]

Sample 413B is the lower half of a sampled block that includes CF 24 and AL 10 at the bottom of the profile. Overall, this appears to be an intact combustion feature consisting of bioturbated phosphatized ash at the top overlying a rubefied substrate consisting of bone-rich sand. Specifically, the basal half of the slide is composed of a massive, generally unbedded mixture of coarse quartz sand, charcoal, bone, rounded aggregates of pale yellow, mostly isotropic and diagenetically altered (phosphatized, deferrified?) yellow and greenish silty clay. At the very base is a thin (<1 mm) lens of black and reddish brown organic matter (plant tissue). The uppermost ~1 cm is noticeably rubefied. The upper half consists of a mixture of phosphatic ash with common charcoal fragments, large bones, and cm-size angular chert. Some of the bones are definitely burned. Charcoal is very fragmented and tends to be coarser in the upper right hand part of the slide. Burrowing obscures much of the original structure and organization of the ash but the rubefication and ash association points to a generally intact combustion feature.

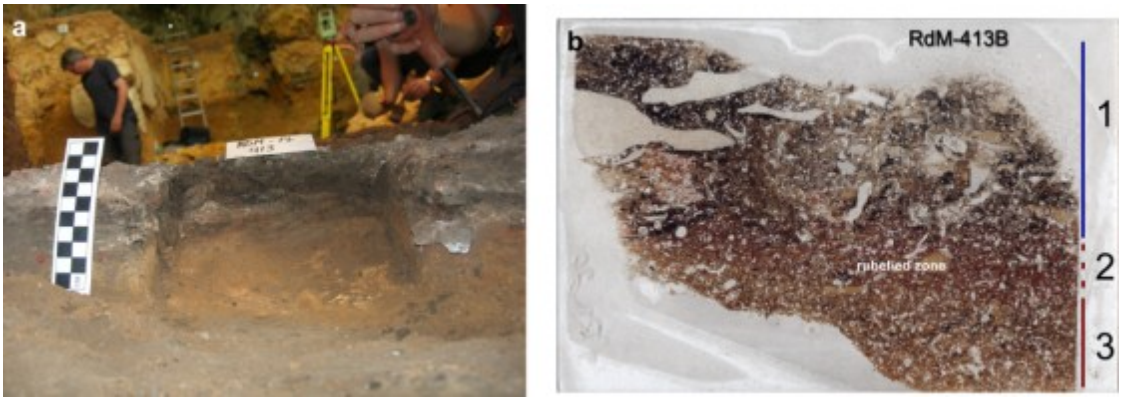

Figure S6: a) Field photograph of area of sample 413; scale = 10 cm; b) thin section scan of sample 413b showing the original structure of CF 24: 1= mixture of phosphatic ash with common charcoal fragments, large bones, and cm-sized angular chert. Some of the bones are definitely burned. Charcoal is very fragmented and tends to be coarser in the upper right hand part of the slide. Burrowing obscures much of the original structure and organization of the ash; 2 = rubefied zone; 3 = Massive, generally unbedded mixture of coarse quartz sand, charcoal, bone, rounded aggregates of pale yellow, mostly isotropic and diagenetically altered yellow and greenish silty clay. PPL; length of thin section = 75 mm.

The bottom half of **sample 518**, contains combustion feature 24, which is about 2.5 cm thick. The topmost part is disturbed by bioturbation. No ash is present but the sediments are composed of abundant bone fragments and charcoal. The bones are highly fragmented and some are both burned and unburned. In addition, there are rounded aggregates of pale yellow, mostly isotropic and diagenetically altered (phosphatized, deferrified?) yellow and greenish silty clay.

Combustion Feature 20 (AL9)

Combustion feature 20 is somewhat isolated from the others presented here, occurring in unit J21, east of the main area of excavation. It rests on bedrock and represents among the first fires in the cave. It is one of several combustion features (along with CF 22 and CF 26) constructed on irregular and inclined bedrock in squares I20, J19,

and J20. Preservation is very good, due in part at least to post-depositional cementing of the ash component. Original construction on the inclined bedrock here may have been to take advantage of the bedrock as a reflective background for the fire.

The feature included clear upper ash and lower black (charcoal/burned bone) components. These are cemented to the underlying bedrock in places. They both included burned (n=28) and unburned lithics (n=29).

Micromorphology [sample 501]

Sample 501, in fact, records two intact combustion features: the remains of a small (cm thick) feature at the base (Unit II), overlain by a much thicker intact feature exhibiting rubefication and extensive calcification of the bone (Unit I). The base, Unit *Id*, grades up to *Ic*, and is organic rich, with common burned bones, charcoal and black and brown plant fragments. Unit *Ic* contains mm-size bone, charcoal fragments, and rubefied silty clay aggregates. It is predominantly calcareous, but domains appear decalcified. In Unit *Ib,* charred plant remains occur at the base, along with smaller (mm-) sized burnt bone, as well as rubefied, rounded aggregates of silty clay soil material (these are more abundant in *Ic*). Ash is present as fine recemented aggregates, implying ash formation, disaggregation and recementation. Unit *Ia* at the top is comprised of rounded grains of cemented calcareous ashes, with common, cm-size calcined bone, angular fragments of chert, and partially silicified limestone.

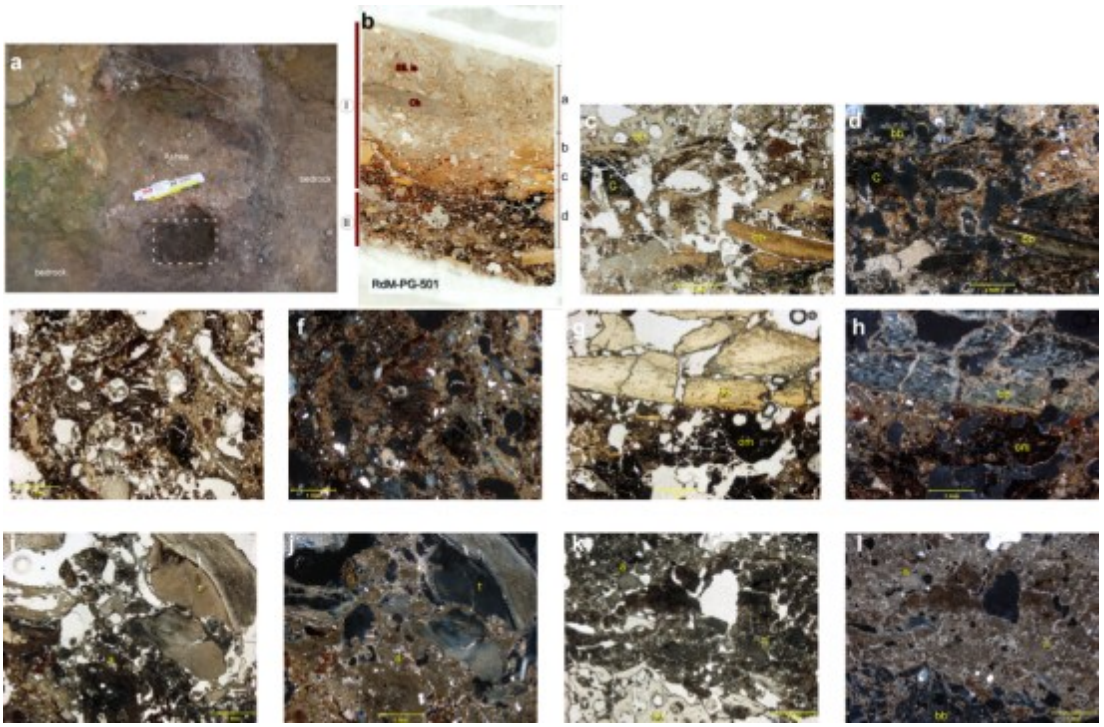

Figure S7: a) field view of location of sample 501 within CF20 (photograph taken after removal of sample); b) macrophotgraph of sample 501 showing that CF 20 incorporates two distinct superimposed combustion events that were undistinguishable in the filed (see text for details). Note the tilt of the deposits derived from the fact that this feature rests on top of steeply sloping bedrock; PPL; Sil. ls = siliceous limestone, Ch = chert grain; length of thin section = 75 mm; c) Photomicrograph from base of thin section, Unit II of Figure S7b. Shown here is a compacted mass of burned bone [bb], charcoal [c], and ashes; the latter are locally recemented. PPL; d) Same as c but in XPL; e) Base of unit Id in Figure S7b. Overall, this is similar to the materials shown in Unit II above. PPL; f) Same as at left but in XPL. Note how the calcareous ashes, though concentrated at the right-hand part of the photograph, can be seen dispersed throughout the area of the photograph; g) Crushed calcined bone (unit Ic [bb]) overlying ashes and organic matter (Unit Id [om]) at the contact between Unit I c/d in Figure S7b. PPL; h) Same as at left but in XPL. Note the secondary calcite cementation in the fissures of the bone in the upper part of the photograph; i) Unit Ib, consisting of burnt and calcined teeth [t] and bone, mixed with cemented ashes [a], particularly in the lower part. PPL; j) This view of the photo at left in XPL shows more clearly the cemented nature of the calcareous ashes; k) Unit Ia from the top of the slide, with rounded grains of cemented calcareous ashes at the top [a], and cm-size calcined bone [bb] at the base of the photo here. PPL; l) The aggregated nature of the ashes is somewhat clearer in this XPL of the photo at the left. All photomicrographs with 1 mm scale.

The lower part of 501 exhibits another combustion feature (II), which was not recognized in the field. At the top is a mm-thick discontinuous, bioturbated lens of calcitic ashes with phosphatic domains. The ash contains angular bones with different degrees of burning, charred organic remains, and yellow brown organic matrix. Much of

the material is partially disaggregated, probably due to the fact that it rests on a knob of irregularly and steeply sloping bedrock.

Redeposited Combustion Feature Contents

Combustion Feature 16 (AL7)

Combustion Feature 16 is characterized by a concentration of burned bone, burned flint, and charcoal (no ash) with better defined horizontal and vertical limits in the northeast corner of the décapage area. Any structure to this feature is unclear and it lacks the clear laminar stratigraphy of other combustion features. The feature was cut by a burrow along its eastern edge, but preservation of the remaining components is striking with clear examples of in situ trampled bone.

Micromorphology [Sample 221]

CF16 is most visible and striking along the south face of K18 when it was sampled in 2006. It is characterized by abundant quartz sand, very fragmented predominantly burned bones, which are finely fractured and dispersed among charcoal fragments. Some of the groundmass is comprised of locally rubefied silty clay, as well as brownish silty clay; a few angular grains of chert were observed. Most of the groundmass is non calcareous and iron rich; only some traces of calcite are preserved in what appear to be remains of hypocoatings. The lower part of the combustion feature is more aggregated and porous than the upper part due to bioturbation.

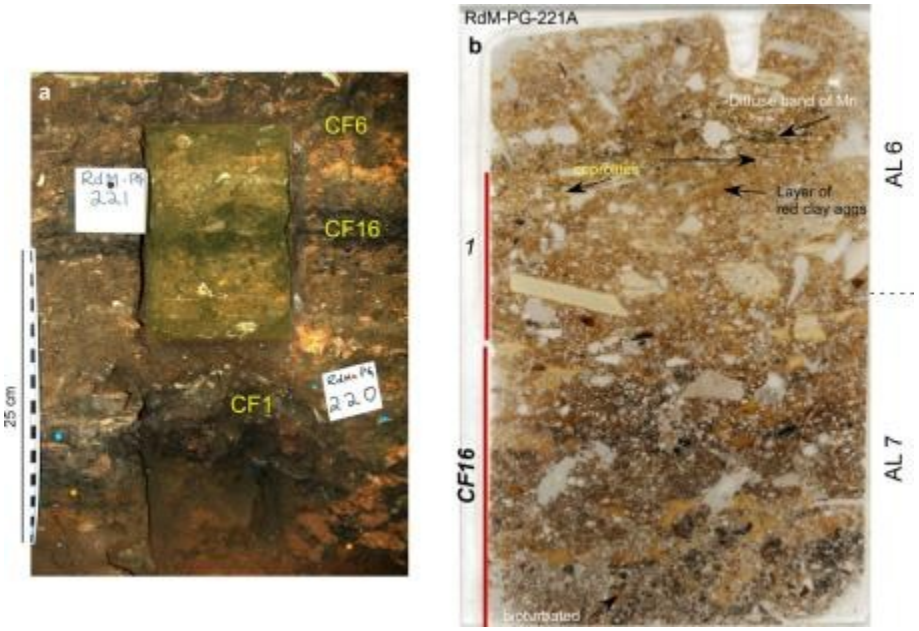

Figure S8: a) Profile fiew of sample 221 in the field and associated CFs, scale = 25 cm; b) thin section scan of sample 221a showing the transition between ALs 6 and 7; 1 = area with abundant coprolites, angular rounded bone (some burnt), with micaceous clay aggregates (aggs) and calcite dusting around the bones; CF16 associated sediments are present in the lower part of the slide and are show a mixed association of very fragmented burned bones and dispersed charocal fragments that have been interpreted as redeposited combustion feature(s) remains.

This feature does not appear to be intact or in place and is interpreted here as the contents of one or more combustion features that were displaced and redeposited. Whether this has any association to rodent burrowing activity is difficult to determine, but is certainly possible.

Ash Dumps

Combustion Feature 15 (AL7)

In the field, Combustion Feature 15 was not very distinct or well delineated and exhibited little structure. However, the subsequent profile section shows a clear lens of cemented ash within the generally burned sediments of AL7 (see Figure S1). This lens is quite thick compared to most features; c. 8 cm at the centre. The upper and lower surfaces show relief, and the ash very much has the appearance of being secondarily cemented after being reworked.

Although this feature included burned and fragmented bone, this did not include examples of clear in situ trampling of individual fragments as were noted within most other features. It did include burned lithics (n=10) as well as unburned lithics (n=40).

Micromorphology [Sample 402B]

In thin section, **sample 402B** overall is a loose mixture of angular bone, some chert and extensively dissolved limestone, mixed with brownish red phosphatic clay. Larger bones are angular, whereas those <1cm tend to be rounded, and some appear to be burned. Scattered throughout are sand-size rounded coprolite grains and charcoal; the latter are relatively rare. Phosphatization is quite widespread, although some domains have not been decalcified. These include reworked ashes that are in the form of localized unbedded clumps. Manganese appears to occur as localized clots and sand-size clumps. Bioturbation occurs as rare worm casts, but more typically as chambers filled with subrounded silt-sized pellets (likely insect in origin). Components like charcoal/organic matter, ashes and rubefied sediments are completely mixed and do not exhibit a distinct structured sequence. In sum, CF15 more likely represents a heavy trampled and bioturbated area of former combusted products.

The presence of coprolites (presumably hyaena) is in line with the degree of bioturbation and mixing of the deposits in this feature.

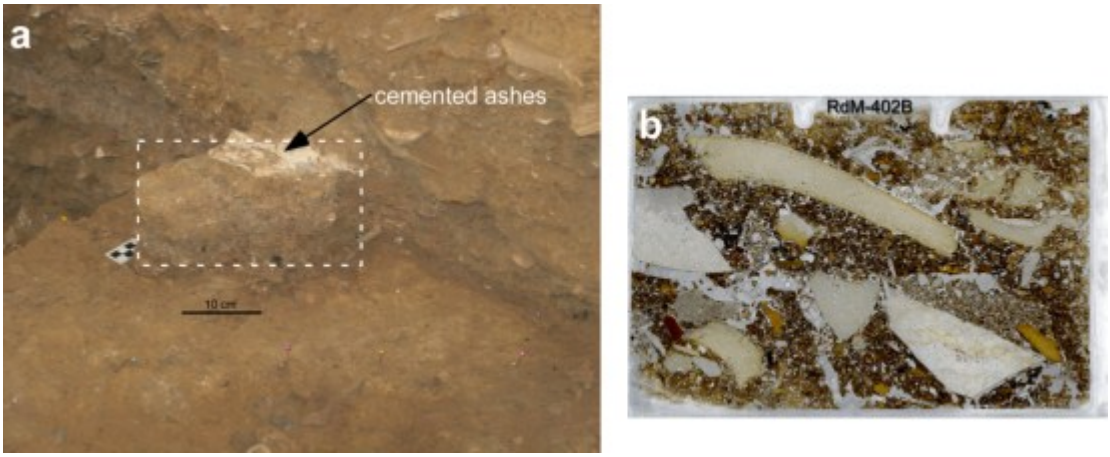

Figure S9: a) Field view of CF 15 and location of soil micromorphology sample (marked by square); note the presence of white cemented ashes on the top of the sampled area; b) thin section scan of sample 402b associated with CF15 where cm-sized angular bones and limestone fragments are ubiquitous. Overall, this thin section shows a jumble of unorganized reworked bones, ashes, and charcoal fragments that are in line with the interpretation of this feature as a ash dump.

Isolated Rubified Sediments

Combustion Feature 27 (AL10)

Combustion Feature 27 is a relatively large area of rubified sediments (with no associated ash or charcoal components) at the top of AL10, but separated from the base of AL9 by a thin (<0.5 cm) lens of AL10 sediments: i.e., this feature is in AL10. However, archaeological residues in AL10 are very sparse (125 lithics compared to 8100 for AL9) and occur at the very top of the AL10 sediments - these must mainly represent post-depositional movement from AL9. While definitely in AL10, this feature must be associated with initial occupations of the site; being more or less coeval with the base of AL9. In any case, the ash and charcoal residues from this feature were removed post-

event. No micromorphological samples were taken that included sediments from CF27 so no thin section analysis is available.

Bibliography

Aberkan, M., 1986. Le Quaternaire littoral de la bordure meridionale du Rharb (Maroc nord-occidental). Aspects sedimentologique, pedologique et neotectonique. Bulletin - Institut de Geologie du Bassin d'Aquitaine 39, 185-190.

Aberkan, M., 2000. Précisions sur la chronostratigraphie des formations littorales quaternaires au Nord-Est de Rabat (Maroc). Apport de la thermoluminescence. Géologie Méditerranéenne 27, 27-31.

Aboumaria, K., Gigliuto, L.G., Puglisi, D., Zaghloul, M.N., Aberkan, M., Di Staso, A., 2006. Quaternary marine terraces on the southern side of the Gibraltar strait and on the Northern Atlantic Coast of Morocco: Lithostratigraphy, provenance and drainage patterns. Bollettino della Societa Geologica Italiana 125, 93-104.

Ait Brahim, L., Chotin, P., Hinaj, S., Abdelouafi, A., El Adraoui, A., Nakcha, C., Dhont, D., Charroud, M., Sossey Alaoui, F., Amrhar, M., Bouaza, A., Tabyaoui, H., Chaouni, A., 2002. Paleostress evolution in the Moroccan African margin from Triassic to Present. Tectonophysics 357, 187-205.

Akil, M., Gayet, J., 1984. Processus de lithification des calcarenites eoliennes quaternaires de la region de Rabat (Maroc). Bull. Inst. Géol. Bassin d'Aquitaine 35, 45-51.

Albert, R.M., Bar-Yosef, O., Meignen, L., Weiner, S., 2003. Quantitative phytolith study of hearths from the Natufian and Middle Palaeolithic levels of Hayonim Cave (Galilee, Israel). Journal of Archaeological Science 30, 461-480.

Albert, R.M., Weiner, S., Bar-Yosef, O., Meignen, L., 2000. Phytoliths in the middle palaeolithic deposits of Kebara Cave, Mt Carmel, Israel: Study of the plant materials used for fuel and other purposes. Journal of Archaeological Science 27, 931-947.

Andersen, M.B., Stirling, C.H., Potter, E.K., Halliday, A.N., Blake, S.G., McCulloch, M.T., Ayling, B.F., O'Leary, M.J., 2010. The timing of sea-level high-stands during Marine Isotope Stages 7.5 and 9: Constraints from the uranium-series dating of fossil corals from Henderson Island. Geochimica et Cosmochimica Acta 74, 3598-3620.

Andre, A., Beaudet, G., 1981. Formations marines et tectonique plio-quaternaires du Nord-Ouest atlantique marocain., Actes du Colloque Niveaux Marins et Tectonique Quaternaire dans l'aire Mediterraneenne. CNRS, Paris, 29 Novembre 1980, pp. 449-476.

Angelucci, D.E., 2003. Geoarchaeology and micromorphology of Abric de la Cativera (Catalonia, Spain). Catena 54, 573-601.

Antonioli, F., Bard, E., Potter, E.K., Silenzi, S., Improta, S., 2004. 215-ka history of sea-level oscillations from marine and continental layers in Argentarola Cave speleothems (Italy). Global and Planetary Change 43, 57-78.

Arboleya, M.L., Babault, J., Owen, L.A., Teixell, A., Finkel, R.C., 2008. Timing and nature of Quaternary fluvial incision in the Ouarzazate foreland basin, Morocco. Journal of the Geological Society 165, 1059-1073.

Bailey, G., 2007. Time perspectives, palimpsests and the archaeology of time. Journal of Anthropological Archaeology 26, 198-223.

Balek, C.L., 2002. Buried Artifacts in Stable Upland Sites and the Role of Bioturbation: A Review. Geoarchaeology - An International Journal 17, 41-51.

Balter, M., 2011. Was North Africa the launch pad for modern human migration? . Science 331, 20-23.

Banks, W.E., d'Errico, F., Dibble, H.L., Krishtalka, L., West, D., Olszewski, D.I., Peterson, A.T., Anderson, D.G., Gillam, J.C., Montet-White, A., Crucifix, M., Marean, C.W., Sánchez-Goñi, M.-F., Wohlfarth, B., Vanhaeran, M., 2006. Eco-Cultural Niche Modeling: New Tools for Reconstructing the Geography and Ecology of Past Human Populations. PaleoAnthropology, 68−83.

Bar-Yosef, O., Meignen, L., 2007. Kebara Cave, Mt. Carmel, Israel: the Middle and Upper Palaeolithic archaeology. Part I. Peabody Museum of Archaeology and Ethnology, Harvard University, Cambridge.

Bardají, T., Goy, J.L., Zazo, C., Hillaire-Marcel, C., Dabrio, C.J., Cabero, A., Ghaleb, B., Silva, P.G., Lario, J., 2009. Sea level and climate changes during OIS 5e in the Western Mediterranean. Geomorphology 104, 22-37.

Barton, N., Bouzouggar, A., Lubell, D., 2008. Modern human dispersals, environments and cultural change in the late pleistocene of Northwest Africa. African Archaeological Review 25, 1-2.

Barton, R.N.E., Bouzouggar, A., Collcutt, S.N., Schwenninger, J.L., Clark-Balzan, L., 2009. OSL dating of the Aterian levels at Dar es-Soltan I (Rabat, Morocco) and implications for the dispersal of modern Homo sapiens. Quaternary Science Reviews 28, 1914-1931.

Bateman, M.D., Carr, A.S., Dunajko, A.C., Holmes, P.J., Roberts, D.L., McLaren, S.J., Bryant, R.G., Marker, M.E., Murray-Wallace, C.V., 2011. The evolution of coastal barrier systems: A case study of the Middle-Late Pleistocene Wilderness barriers, South Africa. Quaternary Science Reviews 30, 63-81.

Bateman, M.D., Holmes, P.J., Carr, A.S., Horton, B.P., Jaiswal, M.K., 2004. Aeolianite and barrier dune construction spanning the last two glacial-interglacial cycles from the southern Cape coast, South Africa. Quaternary Science Reviews 23, 1681-1698.

Bellomo, R.V., 1993. A Methodological Approach for Identifying Archaeological Evidence of Fire Resulting from Human Activities. Journal of Archaeological Science 20, 525-553.

Bellomo, R.V., 1994. Methods of determining early hominid behavioral activities associated with the controlled use of fire at FxJj 20 Main, Koobi Fora, Kenva. Journal of Human Evolution 27, 173-195.

Berna, F., 2010. Bone alteration and diagenesis, in: Artioli, G. (Ed.), Scientific Methods and Cultural Heritage. An Introduction to the Application of Materials Science to Archaeometry and Conservation Science. Oxford University Press, Oxford, pp. 364-367.

Berna, F., Behar, A., Shahack-Gross, R., Berg., J., Zorn, J., Boaretto, E., Gilboa, A., Sharon, I., Shalev, S., Silshtein, S., Weiner, S., 2007. Sediments exposed to high temperatures: reconstructing pyrotechnological processes in Late Bronze and Iron Age Strata at Tel Dor (Israel). Journal of Archaeological Science 34, 358-373.

Berna, F., Goldberg, P., 2007. Assessing Paleolithic pyrotechnology and associated hominin behavior in Israel. Israel Journal of Earth Sciences 56, 107-121.

Berna, F., Goldberg, P., Horwitz, L.K., Brink, J., Holt, S., Bamford, M., Chazan, M., 2012. Microstratigraphic evidence of in situ fire in the Acheulean strata of Wonderwerk Cave, Northern Cape province, South Africa. PNAS early edition.

Berna, F., Matthews, A., Weiner, S., 2004. Solubilities of bone mineral from archaeological sites: The recrystallization window. Journal of Archaeological Science 31, 867-882.

Biberson, P., 1961. Le cadre paléogéographique de la Préhistoire du Maroc Atlantique. Publ. Serv. Antiq. Maroc 16, 1-235.

Binford, L., 1078. Dimensional analysis of behavior and site structure: learning from an Eskimo hunting stand. American Antiquity 43, 330-361.

Boggs, S., 2001. Principles of Sedimentology and Stratigraphy, 3rd ed. Prentice Hall, New Jersey.

Bordes, F., 1976-77. Moustérien et Atérien. Quaternaria 19, 19-34.

Bouzouggar, A., 1997a. Économie des matières premières et du débitage dans la séquence Atérienne de la Grotte d'El Mnasra I (Ancienne grotte des Contrebandiers - Maroc). Préhistoire Anthropologie Méditerranéennes T. 6, 35-52.

Bouzouggar, A., 1997b. Matieres premieres et processus de fabrication et de gestion des supports dóutils dans la sequence aterienne de la grotte des Contrebandiers a Temara. Universite de Bordeaux, Bordeaux.

Bouzouggar, A., Barton, N., Vanhaeren, M., D'Errico, F., Collcutt, S., Higham, T., Hodge, E., Parfitt, S., Rhodes, E., Schweninger, J.L., Stringer, C., Turner, E., Ward, S., Moutmir, A., Stambouli, A., 2007. 82,000-Year-old shell beads from North Africa and implications for the origins of modern human behavior. Proceedings of the National Academy of Sciences of the United States of America 104, 9964-9969.

Brebion, P., Raynal, J.P., Texier, J.P., Alouane, M., 1986. Nouvelles donnees sur le Quaternaire littoral du Maroc atlantique a Casablanca et Cap Achakar. Comptes Rendus - Academie des Sciences, Serie II: 302, 901-904.

Brewer, R., 1972. The basis of interpretation of soil micromorphological data. Geoderma 8, 81-94.

Bronger, A., Bruhn-Lobin, N., 1997. Paleopedology of Terrae rossae-Rhodoxeralfs from quaternary calcarenites in NW Morocco. Catena 28, 279-295.

Bronger, A., Sedov, S.N., 2003. Vetusols and paleosols: Natural versus man-induced environmental change in the Atlantic coastal region of Morocco. Quaternary International 106-107, 33-60.

Brooke, B., 2001. The distribution of carbonate eolianite. Earth-Science Reviews 55, 135-164.

Brown, K.S., Marean, C.W., Herries, A.I.R., Jacobs, Z., Tribolo, C., Braun, D., Roberts, D.L., Meyer, M.C., Bernatchez, J., 2009. Fire As an Engineering Tool of Early Modern Humans. Science VOL 325 859-862.

Butzer, E.K., 1982. Archaeology as Human Ecology. Cambridge University Press, Cambridge.

Butzer, K.W., 1977. Geoarchaeology in practice. Rev. Anthropology 4, 125-131.

Butzer, K.W., 2008. Challenges for a cross-disciplinary geoarchaeology: The intersection between environmental history and geomorphology. Geomorphology 101, 402–411.

Cabanes, D., Weiner, S., Shahack-Gross, R., 2011. Stability of phytoliths in the archaeological record: A dissolution study of modern and fossil phytoliths. Journal of Archaeological Science 38, 2480-2490.

Campy, M., Chaline, J., 1993. Missing Records and Depositional Breaks in French Late Pleistocene Cave Sediments. Quaternary Research 40, 318-331.

Canti, M.G., 2003a. Aspects of the chemical and microscopic characteristics of plant ashes found in archaeological soils. Catena 54, 339-361.

Canti, M.G., 2003b. Earthworm Activity and Archaeological Stratigraphy: A Review of Products and Processes. Journal of Archaeological Science 30, 135-148.

Carr, A.S., Bateman, M.D., Roberts, D.L., Murray-Wallace, C.V., Jacobs, Z., Holmes, P.J., 2010. The last interglacial sea-level high stand on the southern Cape coastline of South Africa. Quaternary Research 73, 351-363.

Carrancho, Á., Villalaín, J.J., Angelucci, D.E., Dekkers, M.J., Vallverdú, J., Vergès, J.M., 2009. Rock-magnetic analyses as a tool to investigate archaeological fired sediments: A case study of mirador cave (Sierra de Atapuerca, Spain). Geophysical Journal International 179, 79-96.

Castañeda, I.S., Mulitza, S., Schefuß, E., Dos Santos, R.A.L., Damsté, J.S.S., Schouten, S., 2009. Wet phases in the Sahara/Sahel region and human migration patterns in North Africa. Proceedings of the National Academy of Sciences of the United States of America 106, 20159-20163.

Caton-Thompson, G., 1946. The Aterian Industry: its Place and Significance in the Palaeolithic World. . Royal Anthropological Institute of Great Britain and Ireland 76, 87-130.

Clark, J.D., 1993. The Aterian of the Central Sahara, in: L. Krzyzaniak, M.K., and J. Alexander (Ed.), Environmental Change and Human Culture in the Nile Basin and Northern Africa until the Second Millennium B.C. Poznan Archaeological Museum, Poznan, pp. 49-68.

Cohen-Ofri, I., Weiner, L., Boaretto, E., Mintz, G., Weiner, S., 2006. Modern and fossil charcoal: Aspects of structure and diagenesis. Journal of Archaeological Science 33, 428-439.

Courty, M.A., 2001. Microfacies analysis assisting archaeological stratigraphy, in: Goldberg, P., Holliday, V.T., Ferring, C.R. (Eds.), Earth Sciences and Archaeology. Kluwer Academic / Plenum Publishers, New York, pp. 205-240.

Courty, M.A., Goldberg, P., Macphail, R., 1989. Soils and micromorphology in archaeology. Cambridge University Press, Cambridge.

Courty, M.A., Vallverdú, J., 2001. The Microstratigraphic Record of Abrupt Climate Changes in Cave Sediments of the Western Mediterranean. Geoarchaeology - An International Journal 16, 467-500.

d'Errico, F., Vanhaeren, M., Barton, N., Bouzouggar, A., Mienis, H., Richter, D., Hublin, J.J., McPherron, S.P., Lozouet, P., 2009. Additional evidence on the use of personal ornaments in the Middle Paleolithic of North Africa. Proceedings of the National Academy of Sciences of the United States of America 106, 16051-16056.

Davidson, D.A., Shackley, M., 1976. Geoarchaeology: Earth Science and the Past. Duckworth, London.

Debénath, A., 1976. Le site de Dar Es Soltane 2, a Rabat (Maroc). Bulletins et Mémoires de la Société d'anthropologie de Paris 13 III, 181-182.

Debénath, A., 2000. Le peuplement préhistorique du Maroc : Données récentes et problèmes. Anthropologie 104, 131-145.

Debénath, A., Raynal, J.P., Texier, J., Roche, J., Ferembach, D., 1986. Stratigraphie, habitat, typology et devenir de l'Atérien marocain: donées récentes. L'Anthropologie 90, 233-246.

deMenocal, P., 1995. Plio-Pleistocene African climate. Science 270, 53-59.

Dibble, H., Aldeias, V., Alvarez-Fernández, E., Blackwell, B., Hallet-Desguez, E., Jacobs, Z., Goldberg, P., Morala, A., Meyer, M.C., Olzsewski, D., Reed, K., Reed, D., Steele, T.E., Richter, D., Roberts, R.G., Sandgathe, D., Schurmans, U., Skinner, A., El-Hajraoui, M., submitted. New Excavations at the Site of Contrebandiers Cave, Morocco. PaleoAnthropology.

Dibble, H.L., Chase, P.G., McPherron, S.P., Tuffreau, A., 1997. Testing the reality of a "living floor" with archaeological data. American Antiquity 62, 629-651.

Donald, A.D., Stephen, P.C., Timothy, A.Q., 1992. An evaluation of micromorphology as an aid to archaeological interpretation. Geoarchaeology 7, 55-65.

El Hajraoui, M.A., 1993. Nouvelles découvertes néolithiques et atériennes dans la région de Rabat "Grotte d'Elmnasra". Mediterrâneo, 105-121.

El Hajraoui, M.A., 1994. L'industrie osseuse atérienne de la grotte d'El Mnasra (Région de Témara,Maroc). Préhistoire Anthropologie Méditerranéennes 3, 91-94.

El Hajraoui, M.A., 2004. Le Paléolithique du domaine mésetien septentrional. Données récentes sur le littoral: Rabat, Témara et la Mamora. Université Mohamed V Rabat.

Ellwood, B.B., Harrold, F.B., Benoist, S.L., Straus, L.G., Morales, M.G., Petruso, K., Bicho, N.F., Zilhão, J., Soler, N., 2001. Paleoclimate and Intersite Correlations from Late Pleistocene/Holocene Cave Sites: Results from Southern Europe. Geoarchaeology - An International Journal 16, 433-463.

Evans, C., Pollard, J., Knight, M., 1998. Life in the Woods: Tree-throws, 'Settlement' and Forest Cognition. Oxford Journal of Archaeology 18, 241-254.

Farrand, W.R., 1985. Rockshelter and cave sediments. Archaeological sediments in context, 21-39.

Farrand, W.R., 2001. Sediments and Stratigraphy in Rockshelters and Caves: A Personal Perspective on Principles and Pragmatics. Geoarchaeology - An International Journal 16, 537-557.

Feller, C., Brown, G.G., Blanchart, E., Deleporte, P., Chernyanskii, S.S., 2003. Charles Darwin, earthworms and the natural sciences: Various lessons from past to future. Agriculture, Ecosystems and Environment 99, 29-49.

Ferembach, D., 1976. Les restes humain Atériens de Témara (Campagne 975). Bulletin Mémoires de la Société d'Anthropologie de Paria 13 III, 175-180.

Ferembach, D., 1998. Le crâne Atérien de Témara (Maroc Atlantique). Bulletin D'Archeologie Marocaine 18, 19-66.

Ferring, C.R., 1986. Rate of fluvial sedimentation: Implications for archaeological variability. Geoarchaeology 1, 259-274.

Fisher, E.C., Bar-Matthews, M., Jerardino, A., Marean, C.W., 2010. Middle and Late Pleistocene paleoscape modeling along the southern coast of South Africa. Quaternary Science Reviews.

Fornós, J.J., Clemmensen, L.B., Gómez-Pujol, L., Murray, A.S., 2009. Late Pleistocene carbonate aeolianites on Mallorca, Western Mediterranean: a luminescence chronology. Quaternary Science Reviews 28, 2697-2709.

Frébourg, G., Hasler, C.A., Le Guern, P., Davaud, E., 2008. Facies characteristics and diversity in carbonate eolianites. Facies 54, 175-191.

Gigout, M., 1957. Recherches sur le Pliocène et le Quaternaire atlantiques marocains, Trav. Inst. Sci. Chérif, Rabat, p. 77.

Gladfelter, B., 1977. Geoarchaeology: the geomorphologist and archaeology American Antiquity 42, 519-538.

Goldberg, P., 1983. Applications of micromorphology in archaeology. Soil micromorphology. Vol. 1, 139-150.

Goldberg, P., 2000. Micromorphology and site formation at Die Kelders Cave I, South Africa. Journal of Human Evolution 38, 43-90.

Goldberg, P., 2006. Palaeolithic Pyrotechnology, High Resolution Behavioral Events, and the Neanderthal/Modern Human Question. National Science Foundation
BCS - ARCHAEOLOGY

Goldberg, P., 2008. Raising the bar, in: Sullivan, A.P. (Ed.), Archaeological Concepts for the Study of the cultural Past. University of Utah Press, Salt Lake City, pp. 27-.

Goldberg, P., Berna, F., 2010. Micromorphology and context. Quaternary International 214, 56-62

Goldberg, P., Dibble, H., Berna, F., Sandgathe, D., McPherron, S.J.P., Turq, A., 2012. New evidence on Neandertal use of fire: Examples from Roc de Marsal and Pech de l'Azé IV. Quaternary International 247, 325-340.

Goldberg, P., Macphail, R., 2006. Practical and Theorectical Geoarchaeology. Blackwell publishing.

Goldberg, P., Macphail, R.I., 2003. Short contribution: Strategies and techniques in collecting micromorphology samples. Geoarchaeology 18, 571-578.

Goldberg, P., Miller, C.E., Schiegl, S., Ligouis, B., Berna, F., Conard, N.J., Wadley, L., 2009. Bedding, hearths, and site maintenance in the Middle Stone Age of Sibudu Cave, KwaZulu-Natal, South Africa. Archaeological and Anthropological Sciences Volume 1, Number 2 95-122.

Goldberg, P., Nash, D.T., Petraglia, M.D., 1993. Formation Processes in Archaeological Context. Prehistoy Press., Madinson.

Goldberg, P., Sherwood, S.C., 1994. Micromorphology of Dust Cave Sediments: some preliminary results. Journal of Alabama Archaeology 40, 57-65.

Goldberg, P., Sherwood, S.C., 2006. Deciphering human prehistory through the geoarcheological study of cave sediments. Evolutionary Anthropology 15, 20-36.

Goldberg, P., Weiner, S., Bar-Yosef, O., Xu, Q., Liu, J., 2001. Site formation processes at Zhoukoudian, China. Journal of Human Evolution 41, 483-530.

Goren-Inbar, N., Alperson, N., Kislev, M.E., Simchoni, O., Melamed, Y., Ben-Nun, A., Werker, E., 2004. Evidence of Hominin Control of Fire at Gesher Benot Ya'aqov, Israel. Science 304, 725-727.

Grün, R., Stringer, C.B., 1991. Electron spin resonance dating and the evolution of modern humans. Archaeometry 33, 153–199.

Hasiotis, S.T., 2003. Complex ichnofossils of solitary and social soil organisms: Understanding their evolution and roles in terrestrial paleoecosystems. Palaeogeography, Palaeoclimatology, Palaeoecology 192, 259-320.

Hawkins, A.L., Kleindienst, M.R., 2001. Aterian in: Melvin, P.N.P.a.E. (Ed.), Encyclopedia of Prehistory. Kluwer Academic/Plenum Publishers., New York, pp. 23-45.
.

Hearty, P.J., Hollin, J.T., Neumann, A.C., O'Leary, M.J., McCulloch, M., 2007. Global sea-level fluctuations during the Last Interglaciation (MIS 5e). Quaternary Science Reviews 26, 2090-2112.

Hearty, P.J., Kindler, P., Cheng, H., Edwards, R.L., 1999. A +20 m middle Pleistocene sea-level highstand (Bermuda and the Bahamas) due to partial collapse of Antarctic ice. Geology 27, 375-378.

Hublin, J.-J., 1992. Recent human evolution in northwestern Africa. Philosophical Transactions - Royal Society of London, B 337, 185-191.

Hublin, J.-J., 1993. Recent Human Evolution in Northwestern Africa, in: M. Aitken, C.S., and P. Mellars (Ed.), The Origin of Modern Humans and the Impact of Chronometric Dating. Princeton University Press, Princeton, pp. 118–131.

Hublin, J.-J., 2001. Northwestern African Middle Pleistocene hominids and their bearing on the emergence of Homo sapiens, in: Barham, L., Robson-Brown, K. (Eds.), Human roots: Africa and Asia in the Middle Pleistocene. Western Academic & Specialist Press, pp. 99-122.

Hublin, J.-J., Tillier, A.-M., 1981. The Mousterian Juvenile Mandible from Jebel Irhoud (Morocco): A Phylogenetic Interpretation, in: Stringer, C.B. (Ed.), Aspects of Human Evolution. Taylor and Francis, London, pp. 167–185.

Imbrie, J., Hays, J.D., Martinson, D.G., McIntyre, A., Mix, A.C., Morley, J.J., Pisias, N.G., Prell, W.L., Shackleton, N.J., 1984. The orbital theory of Pleistocene climate: support from a revised chronology of the marine d18O record, in: Berger, A.L., et al., (Ed.), Milankovitch and Climate, Reidel, pp. 269– 305.

Jacobs, Z., Meyer, M.C., Roberts, R.G., Aldeias, V., Dibble, H., El Hajraoui, M.A., 2011. Single-grain OSL dating at La Grotte des Contrebandiers ('Smugglers' Cave'), Morocco: Improved age constraints for the Middle Paleolithic levels. Journal of Archaeological Science 38, 3631-3643.

Jacobs, Z., Roberts, R.G., Nespoulet, R., El Hajraoui, M.A., Debénath, A., 2012a. Single-grain OSL chronologies for Middle Palaeolithic deposits at El Mnasra and El Harhoura 2, Morocco: Implications for Late Pleistocene human-environment interactions along the Atlantic coast of northwest Africa. Journal of Human Evolution.

Jacobs, Z., Roberts, R.G., Nespoulet, R., El Hajraoui, M.A., Debénath, A., 2012b. Single-grain OSL chronologies for Middle Palaeolithic deposits at El Mnasra and El Harhoura 2, Morocco: Implications for Late Pleistocene human-environment interactions along the Atlantic coast of northwest Africa. Journal of Human Evolution 62, 377-394.

James, S., 1989. Hominid use fo fire in the lower and middle pleistocene. Current Ahtropology 30.

Karkanas, P., 2002. Micromorphological Studies of Greek Prehistoric Sites: new insights in the interpretation of the archaeological record. Geoarchaeology 17, 237-259.

Karkanas, P., 2010. Preservation of anthropogenic materials under different geochemical processes: A mineralogical approach. Quaternary International 214, 63-69.

Karkanas, P., Bar-Yosef, O., Goldberg, P., Weiner, S., 2000. Diagenesis in prehistoric caves: The use of minerals that form in situ to assess the completeness of the archaeological record. Journal of Archaeological Science 27, 915-929.

Karkanas, P., Goldberg, P., 2007. Micromorphology of sediments: Deciphering archaeological context. Israel Journal of Earth Sciences 56, 63-71.

Karkanas, P., Goldberg, P., 2008. Micromorphology of sediments: Decipheirng archaeological context. Israel Journal of Earth Sciences 56, 63-71.

Karkanas, P., Goldberg, P., 2010. Site formation processes at Pinnacle Point Cave 13B (Mossel Bay, Western Cape Province, South Africa): Resolving stratigraphic and depositional complexities with micromorphology. Journal of Human Evolution 59, 256-273.

Karkanas, P., Rigaud, J.P., Simek, J.F., Albert, R.M., Weiner, S., 2002. Ash bones and guano: A study of the minerals and phytoliths in the sediments of Grotte XVI, Dordogne, France. Journal of Archaeological Science 29, 721-732.

Karkanas, P., Shahack-Gross, R., Ayalon, A., Bar-Matthews, M., Barkai, R., Frumkin, A., Gopher, A., Stiner, M.C., 2007. Evidence for habitual use of fire at the end of the

Lower Paleolithic: Site-formation processes at Qesem Cave, Israel. Journal of Human Evolution 53, 197-212.

Kilfeather, A.A., Blackford, J.J., van der Meer, J.J.M., 2007. Micromorphological analysis of coastal sediments from Willapa Bay, Washington, USA: A technique for analysing inferred tsunami deposits. Pure and Applied Geophysics 164, 509-525.

Kopp, R.E., Simons, F.J., Mitrovica, J.X., Maloof, A.C., Oppenheimer, M., 2009. Probabilistic assessment of sea level during the last interglacial stage. Nature 462, 863-867.

Lefévre, D., Raynal, J.P., 2002. Les formations plio-pléistocènes de Casablanca et la chronostratigraphie du quaternaire marin du Maroc revisitées. Quaternaire 13, 9-21.

Leroi-Gourhan, A., 1984. Pincevent: campement magdalenien de chasseurs de rennes, Guides archaeologiques de la France. Ministere de la culture Direction du Patrimoine Sous-directon de l'archeologie, Paris.

Leroi-Gourhan, A., Brezillon, M.N., 1972. Fouilles de Pincevent. Essai d;analyse ethnographique d'un habitat magdalenien. Centre National de la Recherche Scientifique Paris.

López-González, F., Grandal-d'Anglade, A., Vidal-Romani, J.R., 2006. Deciphering bone depositional sequences in caves through the study of manganese coatings. Journal of Archaeological Science 33, 707-717.

Macphail, R.I., Cruise, G.M., Allen, M.J., Linderholm, J., 2006. A rebuttal of the views expressed in "Problems of unscientific method and approach in Archaeological soil and pollen analysis of experimental floor deposits; with special reference to Butser Ancient Farm, Hampshire, UK by R.I. Macphail, G.M. Cruise, M. Allen, J. Linderholm and P. Reynolds"; by Matthew Canti, Stephen Carter, Donald Davidson and Susan Limbrey [2]. Journal of Archaeological Science 33, 299-305.

Mallol, C., Marlowe, F.W., Wood, B.M., Porter, C.C., 2007. Earth, wind, and fire: ethnoarchaeological signals of Hadza fires. Journal of Archaeological Science 34, 2035-2052.

March, R.J., 1992. L'utilisation du bois dans les foyers préhistoriques: une approche expérimentale. Bulletin de la Societé Botanique Française 139, 1-12.

Marin Arroyo, A.B., Landete Ruiz, M.D., Vidal Bernabeu, G., Seva Román, R., González Morales, M.R., Straus, L.G., 2008. Archaeological implications of human-derived manganese coatings: a study of blackened bones in El Mirón Cave, Cantabrian Spain. Journal of Archaeological Science 35, 801-813.

McBrearty, S., 1990. Consider the humble termite: Termites as agents of post-depositional disturbance at african archaeological sites. Journal of Archaeological Science 17, 111-143.

McBrearty, S., Brooks, A.S., 2000. The revolution that wasn't: A new interpretation of the origin of modern human behavior. Journal of Human Evolution 39, 453-563.

McBurney, C.B.M., 1975. Current status of the Lower and Middle Palaeolithic of the entire region from the Levant through North Africa, in: Marks, F.W.a.A.E. (Ed.), Problems in Prehistory: North Africa and the Levant. Southern Methodist University Press, Dallas, pp. 411-423.

McLaren, S., 2007. Aeolinite, in: Nash, D.J., McLaren, S. (Eds.), Geochemical Sediments & Landscapes. Blackwell Publishing, Oxford, pp. 144-172.

Meignen, L., Bar-Yosef, O., Goldberg, P., 1989. Les structures de combustion mousteriennes de la grotte de Kebara (Mont Carmel, Israel), in: Olive, M., Taborin, Y. (Eds.), Nature et Funtion des Foyers Prehistoriques. Memoires du Musee de Prehistorire d;Ile de France, pp. 141-146.

Meignen, L., Goldberg, P., Bar-Yosef, O., 2007. The Hearths at Kebara Cave and Their Role in Site Formaiton Processes, in: Bar-Yosef, O., Meignen, L. (Eds.), Kebara Cave Mt. Carmel, Israel. The Middle and Upper Paleolithic Archaeology. Part I. Peadbody Museum of Archaeology and Ethnology Harvard University, Cambridge, Massachusetts, pp. 91-122.

Mercier, N., Wengler, L., Valladas, H., Joron, J.L., Froget, L., Reyss, J.L., 2007. The Rhafas Cave (Morocco): Chronology of the mousterian and aterian archaeological occupations and their implications for Quaternary geochronology based on luminescence (TL/OSL) age determinations. Quaternary Geochronology 2, 309-313.

Mhammdi, N., Medina, F., Kelletat, D., Ahmamou, M., Aloussi, L., 2008. Large boulders along the Rabat coast (Morocco); possible emplacement by the November, 1sr, 1755 A.D. tsunami. Science of Tsunami Hazards 27, 17.

Miller, C.E., Conard, N., Goldberg, P., Berna, F., 2010. Dumping, sweeping and trampling: experimental micromorphological analysis of anthropogenically modifies combustion features, in: Théry-Parisot, I., Chabal, L., Costamagno, S. (Eds.), The raphonomy of burned organix residues and combustion features in archaeological contexts. Palethnologie, Proceedings od the round table, Valbonne, May 27-29, pp. 25-37.

Millies-Lacroix, A., 1874. Carte Géotechnique de la région de Rabat, Notes et Mémoires 128 ed. Editions du Service Géologique du Maroc, Rabat.

Morin, E., 2006. Beyond stratigraphic noise: Unraveling the evolution of stratified assemblages in faunalturbated sites. Geoarchaeology 21, 541-565.

Murray-Wallace, C.V., 2002. Pleistocene coastal stratigraphy, sea-level highstands and neotectonism of the southern Australian passive continental margin - A review. Journal of Quaternary Science 17, 469-489.

Murray-Wallace, C.V., Schnack, E.J., Orford, J., 2003. Special Issue: Coastal Environmental Change During Sea-Level Highstands (IGCP Project 437): Introduction. Marine Geology 194, 1-2.

Mylroie, J., Sasowsky, I.D., 2007. Lithofacies and transport of clastic sediments in karstic aquifers. Studies of cave sediments. Physical and chemical records of paleoclimate. Springer, New York.

Nahid, A., 2001 Six décennes d'évolution des idées su les méthodes et concepts en chronostigraphie du Quaternaire continental marrocain: entre les difficultés, les incertitudes des te le
progrès. Rev. C. & G. 15 135-160

Nami, M., Moser, J., 2010. La Grotte D'Ifri n'Ammar. Reichert Verlag, Deutsches Archaologisches Institut, Wiesbaden.

Nespoulet, R., Debenath, A., El Hajraoui , M.A., Michel, P., Campmas, E., Oujaa, A., Ben-Ncer, A., Lacombe, J.P., Amani, F., Stoetzel, E., Boudad, L., 2008a. Le contexte archéologique des restes humains atériens de la région de Rabat-Témara (Maroc): apport des fouilles des grottes d'El Mnasra and El Harhoura 2 caves, Actes RQM4, Oujda, pp. 356-375.

Nespoulet, R., El Hajraoui, M.A., Amani, F., Ben Ncer, A., Debénath, A., Idrissi, A., Lacombe, J.P., Michel, P., Oujaa, A., Stoetzel, E., 2008b. Palaeolithic and neolithic occupations in the Témara region (Rabat, Morocco): Recent data on hominin contexts and behavior. African Archaeological Review 25, 21-39.

Nest, J.V., 2002. The Good Earthworm: How Natural Processes Preserve Upland Archaic Archaeological Sites in Western Illinois. Geoarchaeology 17, 53-90.

Nielsen, K.A., Clemmensen, L.B., Fornós, J.J., 2004. Middle Pleistocene magnetostratigraphy and susceptibility stratigraphy: Data from a carbonate aeolian system, Mallorca, Western Mediterranean. Quaternary Science Reviews 23, 1733-1756.

Niftah, S., 2003. Étude géologique des grottes du littoral atlantique marocain: El Harhoura 2, El Mnasra et grotte des Contrebandiers à Témara. Université de Perpignan, Perpignan.

Niftah, S., Debenath, A., Miskovsky, J.C., 2005. Origine du remplissage sedimentaire des grottes de Temara (Maroc) d'apres l'etude des mineraux lourds et l'etude exoscopique des grains de quartz
Quaternaire 16, 73-83.

O'Leary, M.J., Hearty, P.J., McCulloch, M.T., 2008. Geomorphic evidence of major sea-level fluctuations during marine isotope substage-5e, Cape Cuvier, Western Australia. Geomorphology 102, 595-602.

O'Neil, K.M., 2001. Solitary Wasps. Behavior and Natural History. Comstock Pubishing Associates, Ithaca and London.

Olson, S.L., Hearty, P.J., 2009. A sustained +21 m sea-level highstand during MIS 11 (400 ka): direct fossil and sedimentary evidence from Bermuda. Quaternary Science Reviews 28, 271-285.

Olszewski, D.I., Schurmans, U.A., Schmidt, B.A., 2011. The Epipaleolithic (Iberomaurusian) from Grotte des Contrebandiers, Morocco. African Archaeological Review 28, 97-123.

Piperno, D.R., Pearsall, D.M., Benfer R.A, Jr., Kealhofer, L., Zhao, Z., Jiang, Q., 1999. Phytolith morphology [2]. Science 283, 1265-1266.

Plaziat, J.C., Aberkan, M., Ahmamou, M., Choukri, A., 2008. The quaternary deposits of Morocco, in: Michard, A., Saddiqi, O., Chalouan, A., Frizon de Lamott, D. (Eds.), Lecture Notes in Earth Sciences, pp. 359-376.

Plaziat, J.C., Aberkan, M., Reyss, J.L., 2006. New late Pleistocene seismites in a shoreline series including eolianites, north of Rabat (Morocco). Bulletin de la Societe Geologique de France 177, 323-332.

Potter, E.K., Esat, T.M., Schellmann, G., Radtke, U., Lambeck, K., McCulloch, M.T., 2004. Suborbital-period sea-level oscillations during marine isotope substages 5a and 5c. Earth and Planetary Science Letters 225, 191-204.

Rapp, G.J., 1987. Geoarchaeology. Ann_ Rev_ Earth Planet_ ScL 15, 97-113.

Rapp Jr, G., Hill, C.L., 1998. Geoarchaeology. The Earth-Science Approach to Archaeological Interpretation. Yale University Press, New Haven and London.

Raynal, J.P., Texier, J.P., Lefevre, D., 1986. An attempt at land-sea correlation of the Quaternary in Morocco. Essai de correlation de l'ocean au continent pour le Quaternaire du Maroc. 27, 141-147.

Reed, D.N., Barr, W.A., 2010. A preliminary account of the rodents from Pleistocene levels at Grotte des Contrebandiers (Smuggler's Cave), Morocco. Historical Biology 22, 286-294.

Renfrew, C., 1976. Archaeology and the Earth Sciences, in: Davidson, D.A., Shacley, M.L. (Eds.), Geoarchaeology: Earth Science and the Past. Duckworth, London, pp. 1-5.

Reygasse, M., 1921–1922. Etudes de Palethnologie Maghrébine (deuxième série). . Recueil des Notices et Mémoires de la Société Archéologique Historique et Géographique de Constantine 53, 159–204.

Rhodes, E.J., Singarayer, J.S., Raynal, J.P., Westaway, K.E., Sbihi-Alaoui, F.Z., 2006. New age estimates for the Palaeolithic assemblages and Pleistocene succession of Casablanca, Morocco. Quaternary Science Reviews 25, 2569-2585.

Roche, J., 1958-1959. L'Epipaléolithique Marocain. Libyca 6-7, 159-192.

Roche, J., 1963. L'Épipaléolithique Marocain. Fondation Calouste Gulbenkian, Lisbon.

Roche, J., 1969. Fouilles de la grotte des Contrebandiers, Paleoecology of Africa & of the surrounding islands & antarctica, Cape Town, pp. 120-121.

Roche, J., 1976a. Cadre Chronologique de L'Épipaléolithique Marocain, in: Camps, G. (Ed.), IX Congrés. Colloque II: Chronologie er Synchronisme dans la Préhistoire Circum-Méditerranéenne. Union Internationale des Sciences Préhistoriques et Protohistoriques, Nice, pp. 153-167.

Roche, J., 1976b. Chronostratigraphie des restes Atériens de la Grotte des Contrebandiers a Témara (Province de Rabat). Bull, et Mém. de la Soc. d'Anthrop. de Paris t. 3, séries XIII, 165-173.

Roche, J., Texier, J.-P., 1976. Paléontologie Humaine. Découverte de restes humains dans un niveau atérien supérieur de la grotte des Contrebandiers, á Témara (Maroc). C. R. Acad. Sc. Paris t. 282, 45-47.

Roebroeks, W., Villa, P., 2011. On the earliest evidence for habitual use of fire in Europe. Proceedings of the National Academy of Sciences of the United States of America 108, 5209-5214.

Rohling, E.J., Grant, K., Hemleben, C., Siddall, M., Hoogakker, B.A.A., Bolshaw, M., Kucera, M., 2008. High rates of sea-level rise during the last interglacial period. Nature Geoscience 1, 38-42.

Rolland, N., 2004. Was the emergence of home bases and domestic fire a punctuated event? A review of the Middle Pleistocene record in Eurasia. Asian Perspectives: the Journal of Archaeology for Asia and the Pacific 43, 248-281.

Ruhlmann, A., 1951. La grotte préhistorique de Dar es-Soltan, Institut des Hautes Études Marocaines. Larose, Paris, p. 210.

Sandgathe, D.M., Dibble, H.L., Goldberg, P., McPherron, S.P., Turq, A., Niven, L., Hodgkins, J., 2011a. On the Role of Fire in Neandertal Adaptations in Western Europe: Evidence from Pech de l'Azé and Roc de Marsal, France. PaleoAnthropology, 216-242.

Sandgathe, D.M., Dibble, H.L., Goldberg, P., McPherron, S.P., Turq, A., Niven, L., Hodgkins, J., 2011b. Timing of the appearance of habitual fire use. Proceedings of the National Academy of Sciences of the United States of America 108.

Schellmann, G., Radtke, U., Potter, E.K., Esat, T.M., McCulloch, M.T., 2004. Comparison of ESR and TIMS U/Th dating of marine isotope stage (MIS) 5e, 5c, and 5a coral from Barbados-implications for palaeo sea-level changes in the Caribbean. Quaternary International 120, 41-50.

Schiegl, S., Goldberg, P., Bar-Yosef, O., Weiner, S., 1996. Ash deposits in Hayonim and Kebara caves, Israel: Macroscopic, microscopic and mineralogical observations, and their archaeological implications. Journal of Archaeological Science 23, 763-781.

Schiegl, S., Goldberg, P., Pfretzschner, H.U., Conard, N.J., 2003. Paleolithic burnt bone horizons from the Swabian Jura: Distinguishing between in situ fireplaces and dumping areas. Geoarchaeology 18, 541-565.

Schiegl, S., Stockhammer, P., Scott, C., Wadley, L., 2004. A mineralogical and phytolith study of the Middle Stone Age hearths in Sibudu Cave, KwaZulu-Natal, South Africa. South African journal of science 100, 185-194.

Schiffer, M.B., 1985. Is there a ‘‘Pompeii premise’’ in archaeology? Journal of Anthropological Archaeology 41, 18–41.

Schiffer, M.B., 1987. Formation Processes of the Archaeological Record. University of New Mexico Press, Albuquerque.

Schurmans, U., Dibble, H.L., El Hajraoui, M.A., 2009. Archaeological excavations of Smugglers Cave‘, Temara. Report of the 2008 Excavation Season. , Interim Field Report University of Pennsylvania. Philadelphia & Ministre de la Culture, Rabat.

Schwenninger, J.-L., Colcutt, S.N., Barton, R.N.E., Bouzouggar, A., El Hajraoui, M.A., Nespoulet, R., Debénath, A., 2009. Luminescence chronology for Aterian cave sites on

the Atlantic coast of Morocco, in: Garcea, E.E.A. (Ed.), South-Eastern Mediterranean Peoples between 130,000 and 10,000 years ago. Oxbow Books,, Oxford, pp. 19-37.

Sergant, J., Crombé, P., Perdaen, Y., 2006. The 'invisible' hearths: A contribution to the discernment of Mesolithic non-structured surface hearths. Journal of Archaeological Science 33, 999-1007.

Shackley, M.L., 1974. Stream abrasion of flint implements. Nature 248, 501-502.

Shackley, M.L., 1978. The behaviour of artifacts as sedimentary particles in a fluviatile environment. Archaeometry 20, 55-61.

Shahack-Gross, R., Bar-Yosef, O., Weiner, S., 1997. Black-coloured bones in Hayonim Cave, Israel: Differentiating between burning and oxide staining. Journal of Archaeological Science 24, 439-446.

Shahack-Gross, R., Berna, F., Karkanas, P., Weiner, S., 2004. Bat guano and preservation of archaeological remains in cave sites. Journal of Archaeological Science 31, 1259-1272.

Siddall, M., Chappell, J., Potter, E.K., 2007. 7. Eustatic sea level during past interglacials, pp. 75-92.

Smith, T.M., Tafforeau, P., Reid, D.J., Grün, R., Eggins, S., Boutakiout, M., Hublin, J.J., 2007. Earliest evidence of modern human life history in North African early Homo sapiens. Proceedings of the National Academy of Sciences of the United States of America 104, 6128-6133.

Stearns, C.E., 1978. Pliocene-Pleistocene Emergence of Moroccan Meseta Geological Society of America Bulletin 89, 1630-1644.

Stearns, C.E., 1981. Mediterranean shorelines from a Moroccan point of view. Actes du colloque: niveaux marins et tectonique quaternaires dans l'aire mediteraneenne, Paris, 1980, (CNRS & Universite de Paris I), 439-447.

Stein, J.K., 1993. Scale in archaeology, geosciences, and geoarchaeology. Effects of scale on archaeological and geoscientific perspectives, 1-10.

Stein, J.K., 2001. A Review of site formation process and their relevance to geoarchaeology in: Goldberg, P., Holliday, V.T., Ferring, C.R. (Eds.), Earth Sciences and Archaeology. Kluwer Academic / Plenum Publishers, New York, Boston, Dordrecht, London, Moscow, pp. 37-51.

Stoops, G., 2003. Guidelines for analysis and description of soil and regolith thin sections. Soil Science Society of America, Madison, WI:.

Stoops, G., Marcelino, V., Mees, F., 2010. Interpretation of Micromorphological Features of Soils and Regoliths. Elsevier.

Texier, J.-P., Raynal, J.-P., Lefevre, D., 1985. Nouvelles propositions pour un cadre chronologique raisonné du Quaternaire marocain, Comptes Rendus de l'Académie des Sciences Paris, pp. 183-188.

Texier, J.P., Lefevre, D., Raynal, J.P., 1992. La Formation de la Mamora. Le point sur la question du Moulouyen et du Saletien du Maroc Nord-Occidental. Quaternaire 3, 63-73.

Texier, J.P., Lefevre, D., Raynal, J.P., 1994. Contribution pour un nouveau cadre stratigraphique des formations littorales quaternaires de la region de Casablanca (Maroc). Comptes Rendus - Academie des Sciences, Serie II: Sciences de la Terre et des Planetes 318, 1247-1253.

Texier, J.P., Lefévre, D., Raynal, J.P., El Graoui, M., 2002. Lithostratigraphy of the littoral deposits of the last one million years in the Casablanca region (Morocco). Quaternaire 13, 23-41.

Texier, J.P., Raynal, J.P., Lefevre, D., 1985-1986. Essai de Chronologie du Quaternaire Marocain. Bulletin D'Archeologie Marocaine Tome XVI, 11-25.

Théry-Parisot, I., 2002. Fuel management (bone and wood) during the lower Aurignacian in the Pataud rock shelter (Lower Palaeolithic, Les Eyzies de Tayac, Dordogne, France). Contribution of experimentation. Journal of Archaeological Science 29, 1415-1421.

Tjallingii, R., Claussen, M., Stuut, J.B.W., Fohlmeister, J., Jahn, A., Bickert, T., Lamy, F., Rohl, U., 2008. Coherent high- and low-latitude control of the northwest African hydrological balance. Nature Geoscience 1, 670-675.

Wadley, L., 2010. Cemented ash as a receptacle or work surface for ochre powder production at Sibudu, South Africa, 58,000 years ago. Journal of Archaeological Science 37, 2397-2406.

Wadley, L., Sievers, C., Bamford, M., Goldberg, P., Berna, F., Miller, C., 2012. Middle Stone Age bedding construction and settlement patterns at Sibudu, South Africa. Science 334, 1388-1391.

Waelbroeck, C., Labeyrie, L., Michel, E., Duplessy, J.C., McManus, J.F., Lambeck, K., Balbon, E., Labracherie, M., 2002. Sea-level and deep water temperature changes derived from benthic foraminifera isotopic records. Quaternary Science Reviews 21, 295-305.

Waters, M.R., 1992. Principles of Geoarchaeology: a North American Perspective. University of Arizona Press, Tuckson.

Weiner, S., 2010. Microarchaeology Beyond the Visible Archaeological Record. Cambridge, Cambridge.

Weiner, S., Goldberg, P., Bar-Yosef, O., 1993. Bone Preservation in Kebara Cave, Israel using On-Site Fourier Transform Infrared Spectrometry. Journal of Archaeological Science 20, 613-627.

Weiner, S., Goldberg, P., Bar-Yosef, O., 2002. Three-dimensional distribution of minerals in the sediments of Hayonim Cave, Israel: Diagenetic processes and archaeological implications. Journal of Archaeological Science 29, 1289-1308.

Weisrock, A., Occhietti, S., Hoang, C.T., Lauriatrage, A., Brebion, P., Pichet, P., 1999. Les sequences littorales Pleistocenes de l'Atlas Atlantique entre cap Rhir et Agadir, Maroc. Quaternaire 10, 227-244.

Wendorf, F., R. Schild, A. Close, 1993. Egypt During the Last Interglacial: The Middle Paleolithic of Bir Tarfawi and Bir Sahara East. Plenum Press., New York.

Wengler, L., 2001. Settlements during the Middle Paleolithic of the Maghreb, in: Conard, N. (Ed.), Settlement dynamics of the Middle Paleolithic and Middle Stone Age. . Kerns Verlag, Tubingen, Allemagne, pp. 65–89.

Woodward, J.C., Goldberg, P., 2001. The Sedimentary Records in Mediterranean Rockshelters and Caves: Archives of Environmental Change. Geoarchaeology - An International Journal 16, 327-354.

Zazo, C., Silva, P.G., Goy, J.L., Hillaire-Marcel, C., Ghaleb, B., Lario, J., Bardají, T., González, A., 1999. Coastal uplift in continental collision plate boundaries: Data from the Last Interglacial marine terraces of the Gibraltar Strait area (south Spain). Tectonophysics 301, 95-109.

INDEX

A

B

C

F

G

H

L

M

R

S